Heparan Sulphate, Angiogenesis and the Regulation of Endostatin

A thesis submitted to the University of Manchester for the Degree of Doctor of Philosophy in the Faculty of Medicine, Dentistry, Nursing, and Pharmacy.

2001

Fiona Helen Blackhall

CRC Department of Medical Oncology

University of Manchester

ProQuest LLC.
789 East Eisenhower Parkway
P.O. Box 1346
Ann Arbor, MI 48106 – 1346

Contents

Abstract

It is now well established that angiogenesis, the formation of new blood vessels from existing ones, is essential for sustained tumour growth. Many pro- and anti-angiogenic proteins bind heparin *in vitro* signifying a functional interaction with heparan sulphate proteoglycans (HSPGs) on mammalian cells and in the extracellular matrix, *in vivo*. Endostatin is a heparin binding protein released by proteolytic cleavage of the C terminal domain of collagen XVIII. It is a potent inhibitor of angiogenesis and tumour growth in animal models, and is currently undergoing evaluation in clinical trials, but its mechanism of action is not known.

This study investigates the molecular interaction between endostatin and HS from microvessel and macrovessel endothelial cells. The sulphated (S-) domains of HS were excised using heparinase III and subjected to high resolution gel filtration and SAX-HPLC. This revealed striking similarities in overall design with conservation of structure in the short S-domains (dp4-6), but with differences in fine structural characteristics due to the positions and proportions of 6-O-sulphate groups in the longer S-domains (dp≥8). The affinity of endostatin for excised HS S-domains was associated with the presence of 6-O-sulphation in oligosaccharides of ≥dp6 as determined by a sensitive filter binding assay. Using HS synthesised by an *Hs2st*$^{-/-}$ mutant, it was demonstrated that 2-O-sulphation was not essential for the interaction. An artificial dimeric form of endostatin more closely approximates the arrangement of endostatin in collagen XVIII and has enhanced affinity for HS that could be significant in relation to its distinct biological activity as a promoter of cell migration (Kuo *et al.*,2001. *J Cell Biol.*,152:1233-1246). In order to study the molecular association of heparin/HS and endostatin (monomer/dimer) a zero-length cross-linking procedure was used. This revealed that a heparin dodecasaccharide can act as a template to 'dimerise' endostatin monomers in contrast to preformed dimer in which only one subunit appeared to crosslink the saccharide. Models of the possible molecular assemblies that may form between HS and endostatin (monomer/dimer) in the pericellular environment are proposed. Preliminary data, presented in the appendix, also provide the first direct evidence that the bioactivity of dimeric endostatin is dependent on cell surface HS.

Abbreviations

aMan	Anhydromannose
aFGF	Acidic fibroblast growth factor (FGF-1)
bFGF	Basic fibroblast growth factor (FGF-2)
BSA	Bovine serum albumin
CL	Crosslinked
CS	Chondroitin sulphate
DMEM	Dulbecco's modified essential medium
dp	Degree of polymerisation, or number of monosaccharide units, e.g. dp6=hexasaccharide
DS	Dermatan sulphate
EC	Endothelial cell
ECM	Extracellular matrix
EOMA	Haemangioendothelioma cell line
FBA	Filter binding assay
GAG	Glycosaminoglycan
Gal	Galactose
GlcA	Glucuronic acid
GlcNAc	N-acetylglucosamine
GlcNS	N-sulphated glucosamine
HED	Human recombinant endostatin dimer
HEM	Human recombinant endostatin monomer
HGF	Hepatocyte growth factor/scatter factor
HME	Hereditary Multiple Exostoses
HS	Heparan sulphate
HSPG	Heparan sulphate proteoglycan
IdoA	Iduronic acid
MAb	Monoclonal antibody
NDST	de-N-acetylase/N-sulphotransferase
OST	O-sulphotransferase
NC	Non-collagenous
PAGE	Polyacrylamide gel electrophoresis
PAPS	3'-phosphoadenosine-5'-phosphosulphate
PBS	Phosphate buffered saline

PIM	Porcine intestinal mucosal
PG	Proteoglycan
SAX-HPLC	Strong anion exchange high performance liquid chromatography
SGBS	Simpson-Golabi-Behmel Syndrome
TCA	Trichloracetic acid
TK	Tyrosine kinase
UA	Uronic acid
VEGF	Vascular endothelial cell growth factor
Xyl	Xylose

2S	2-O-sulphate
6S	6-O-sulphate

Declaration

No portion of the work referred to in this thesis has been submitted in support of an application for another degree or qualification of this or any other university or other institute of learning.

Acknowledgements

I thank Professor Judah Folkman and Dr Kashi Javaherian, Harvard Medical School, Boston for the opportunity to collaborate on endostatin. All the staff in the Department of Medical Oncology have contributed to this thesis through their discussions and advice. I acknowledge Professor Robert Hawkins and Dr Gordon Jayson for their support and thank Dr Malcolm Lyon, Mr Graham Rushton, Miss Pat Hyde, Mr Jon Deakin and Mrs Nijole Gasiunas for sharing their expertise. Special thanks to Miss Audrey Henrioud who worked hard over recent months on the matrigel tube forming/morphogenesis assays for her final year undergraduate degree project. I am grateful to Professor John Gallagher for his unerring encouragement and indebted to Dr Catherine Merry for her invaluable instruction and enthusiasm. This work was funded by the Cancer Research Campaign.

Dedication

For Bill, Angus and Emily.

The author

Fiona Blackhall commenced her medical degree in 1985 at St Andrew's University. In 1988 she was awarded a Scottish Home Office Summer Vacation Research Award to study growth factor production in the developing chick embryo with Dr J McLaughlin, St Andrew's University. In 1989 she obtained an intercalated BSc II(I) (hons) in Anatomy and Experimental Pathology which included an 8 month project in the laboratory of Dr Peter Bryant entitled 'The micronucleus-cytochalasin B technique in the measurement of X-ray induced cytogenetic damage in Ataxia Telangiectasia fibroblasts compared to their normal cellular counterparts'. She went on to graduate MBChB(hons) with distinction in Medicine in 1992 from the University of Manchester and was awarded membership of the Royal College of Physicians in 1995. She commenced specialist training in Medical Oncology in 1995 and was awarded a Cancer Research Campaign Fellowship for a Clinician to study for a PhD under the supervision of Professor John Gallagher in 1997.

1. INTRODUCTION

1.1 Overview

Angiogenesis is the formation of new blood vessels from existing ones. It is a complex, multistage process that involves proteolytic degradation of basement membranes, loss of endothelial cell adhesion, proliferation and migration of endothelial cells into the surrounding stroma, and finally, re-adhesion of endothelial cells to form new capillary tubes. This is highly regulated during embryonic development and essential for tissue renewal and repair in adulthood, but aberrant in various pathological conditions that include diabetic proliferative retinopathy, rheumatoid arthritis and cancer (Carmeliet & Jain, 2000).

An association between new vessel growth and malignant tumours was first described 100 years ago (Goldman, 1907) and for many years considered to be a reaction, akin to an inflammatory response to a foreign body (Algire & Chalkley, 1945). However, Judah Folkman, in 1971, proposed that angiogenesis was in fact mandatory for tumour growth. Experimental data suggested that cancer cells produced a diffusible message that activated nearby endothelial cells from a resting, non-regenerating state to a rapidly dividing phenotype, capable of forming new capillary sprouts. Without the message, tumours would remain dormant, about 2-3mm in size but with the message, tumours that had reached the diffusion limit for oxygen and nutrients (~ 100μM) could recruit a blood supply and accelerate growth (Folkman, 1971).

The first diffusible factor identified in human and animal tissues was named tumour angiogenesis factor (Folkman, 1971). This was later found to be identical to basic fibroblast growth factor (bFGF), an 18kDa monomeric protein isolated in 1974 from pituitary tissue, and named due to its ability to stimulate fibroblast cell division (Shing *et al.*, 1984). Many stimulators of angiogenesis have subsequently been identified. Soluble factors stimulate proliferation and migration of endothelial cells and are exemplified by bFGF, acidic FGF (aFGF) and vascular endothelial cell growth factor (VEGF), that signal through tyrosine kinase receptors. Endothelial cell activation is also associated with alteration in the expression of cell-cell and cell-matrix adhesion proteins such as the integrins. In addition, the release and actions of extracellular proteases, such as the matrix metalloproteases, are believed to be essential for the

invasive capability of angiogenic endothelial cells (see Carmeliet & Jain, 2000; Hanahan & Weinberg, 2000 for reviews).

As observed in other biological systems such as anticoagulation, the activity of angiogenic stimulators is balanced by that of an equally heterogeneous family of inhibitors. The concept of naturally occuring antagonists originated in part from rare clinical observations where surgical removal of a primary tumour was associated with rapid growth of metastases (Chen *et al.*, 1995). This suggested secretion of a humoral factor by the primary tumour that held distant metastases in a dormant state. Isolation of a plasminogen cleavage fragment, angiostatin, from the urine of mice carrying low-metastatic Lewis lung carcinomas provided the first confirmation of this theory (O'Reilly *et al*, 1994). A screen of cell lines for similar suppressive factors ensued and in 1997, a potent antiangiogenic activity was identified from the medium of a murine haemangioendothelioma (EOMA) cell line (O'Reilly *et al.*, 1997). This protein, named endostatin, attracted widespread attention from the scientific and lay press. Endostatin induced dramatic inhibition of highly resistant Lewis lung carcinoma in experimental models and suggested that an anti-endothelial cell approach could overcome the drug resistance frequently encountered in standard anticancer therapy (Boehm *et al.*, 1997; Kerbel, 1997).

Cancer is essentially a genetic disease and develops in a manner analogous to Darwinian evolution, in which a succession of mutations, each conferring one or another type of growth advantage, leads to the progressive conversion of normal human cells into cancer cells. There are at least 100 distinct types of cancer but the majority of genotypes are manifest as six essential alterations in cellular physiology. These are progressive cell growth, evasion of apoptosis, limitless replicative potential, sustained angiogenesis, tissue invasion and metastasis (Hanahan & Weinberg, 2000). The vast literature on angiogenesis relates mainly to the early stages in the process for which it is possible to use cell culture and animal models. A consensus view is that initially, small, 2-3mm tumours lack angiogenic ability but exposure to environmental factors such as hypoxia and hypoglycaemia combined with genetic instability eventually promotes an angiogenic phenotype (Carmeliet & Jain, 2000; Harris, 1997). This so-called angiogenic 'switch' results in upregulation of genes that stimulate angiogenesis with downregulation of those suppressing angiogenesis, and can arise via different genetic

mechanisms. For example, p53 mutations, that enable cells to escape programmed cell death by apoptosis, are associated with downregulation of the angiogenesis inhibitor, thrombospondin-1 (TSP-1). Alternatively, the angiogenic stimulator VEGF is under complex transcriptional control and is upregulated by either activation of the ras oncogene, hypoxia-induced factor 1, or loss of the Von Hippel Lindau tumour suppressor gene (see Harris, 1997 for review, and references therein). Although different genetic mechanisms may be implicated depending on the tumour type, angiogenesis is now thought to be an early to midstage event in tumourigenesis and a prerequisite for the rapid clonal expansion associated with macroscopic tumours. Over the last decade experimental strategies to modulate angiogenesis have confirmed that tumour cell growth can be controlled by the vasculature (Hanahan & Weinberg, 2000). Importantly, of the six acquired capabilities that characterise malignant disease, angiogenesis offers a uniquely attractive therapeutic target because it relies on the genetic integrity of the host endothelial cell. In contrast, the genetic instability of cancer cells equips them with a mechanism for development of drug resistance (Harris, 1997; Kerbel, 1997).

At least 20 antiangiogenic drugs are currently in clinical trial (Carmeliet & Jain, 2000) but the exact mechanisms by which the naturally occuring regulators of angiogenesis interact to affect vascular structure and function are not well understood. One common feature, that has been exploited in the purification of many of these proteins, is affinity for the glycosaminoglycan (GAG) heparin (Conrad, 1998) (Tables 1.1 and 1.2). This may be of fundamental biological significance since the ability of a protein to bind heparin can signify a physiological interaction with a chemically related GAG, heparan sulphate (HS) (Bernfield *et al.*, 1999). In contrast to the restricted distribution of heparin, HS is widely expressed, covalently attached to protein in the form of heparan sulphate proteoglycans (HSPGs), on almost all mammalian cell surfaces, including endothelial cells, and in the extracellular matrix (ECM) (Kjellen & Lindahl, 1991).

An early clue to a role of heparin in angiogenesis came from the observation that heparin-producing mast cells often accumulate at points of angiogenesis before capillary ingrowth (Azizkhan *et al.*, 1980). Conditioned medium from mast cells can induce angiogenesis *in vitro,* and this activity is abolished by the heparin antagonist

Angiogenic Factors	Molecular Weight	Heparin binding	Endothelial mitogen
Vascular endothelial growth factors (VEGF)	45000	Yes ($VEGF_{165,189}$)	Yes
Fibroblast growth factors (FGF) FGF-1 (acidic FGF), FGF-2 (basic FGF), FGF-3 (int-2), FGF-4 (KGF)	18000 (bFGF) 16400 (aFGF)	Yes	Yes
Tumour nectrosis factor-α (TNF-α)	17000	Yes	No
Transforming growth factor-β (TGF-β)	25000	Yes	No
Thymidine phosphorylase (platelet derived endothelial cell growth factor)	45000	No	Causes DNA synthesis
Platelet derived growth factor (PDGF)	20000	Yes	Yes
Hepatocyte growth factor (HGF / scatter factor)	92000	Yes	Yes
Interleukin 8 (IL8)	40000	Yes	Yes
Transforming growth factor-α (TGF-α)	5500	No	Yes
Granulocyte colony-stimulating factor	17000	No	Yes
Angiogenin	14100	Yes	No
Proliferin	35000	No	Yes
Midkine	13000	Yes	Yes
HIV-tat protein	10-14000	Yes	Yes

Table 1.1
Properties of angiogenic factors *in vitro* (an incomplete list)
(adapted from Folkman, 1995, Harris, 1997, Bernfield, 1999, Conrad, 1998)

Endogenous Inhibitors of angiogenesis	Molecular weight	Heparin binding	Mechanism of action
Angiostatin	38000	No	↓EC proliferation ↑EC apoptosis
Endostatin	20000	Yes	↓EC proliferation ↑EC apoptosis
Interferon (IFN) -α -β - γ	20-25000	Yes (IFN γ)	↓EC proliferation
Interleukin 12	75000	Yes	↑ IFN γ, IP-10
Platelet factor 4	28000	Yes	
Thrombospondin 1	450000	Yes	↓EC proliferation, migration ↑EC apoptosis ↓ collagen synthesis
Tissue inhibitor of metalloproteinase (TIMP)1,2,3	8.5-21000	Yes	↓ collagenase
Transforming growth factor β	25000	Yes	↓EC motility
Fibronectin	260000	Yes	Role in EC adhesion
Tumour necrosis factor-α (high concentrations	17000	Yes	↓bFGF
Retinoic acid	300	No	Transcriptional regulator
16K prolactin fragment	16000	Yes	↓EC DNA synthesis
Restin	20	No	↓EC proliferation
Arresten*	30	Yes	↓EC proliferation, migration

Table 1.2
Properties of endogenous inhibitors of Angiogenesis *in vitro* (an incomplete list) (adapted from Folkman, 1995, Harris, 1997, Bernfield, 1999, Gasparini 1999. *Colorado et al.,2000). EC = endothelial cell

protamine and heparin degrading enzymes (Azizkhan *et al.*, 1980). More recently, enzymes known to degrade HS (bacterial heparinases and mammalian heparanase) have been shown to modulate angiogenesis (Sasisekharan *et al.*, 1994; Vlodavsky *et al.*, 1999) . Notably, mammalian heparanase(s) is overexpressed in many tumours, its activity correlates with enhanced angiogenesis, tumour invasion and metastasis and it has been associated with an adverse prognosis in clinical studies of cancer (Vlodavsky *et al.*, 1999).

Over the last decade it has become clear that HSPGs play crucial roles in the modulation of many heparin binding proteins (Bernfield *et al.*, 1999; Conrad, 1998; Lyon & Gallagher, 1998). Biochemical and cell culture studies first demonstrated that HSPGs participate as co-receptors in tyrosine kinase mediated signalling of growth factors such as bFGF, aFGF, HGF and VEGF, and integrin mediated signalling of matrix proteins such as fibronectin (see Gallagher, 2000 for review). More recently, genetic studies in *Drosophila* and mice (Selleck, 2000) and identification of the genes responsible for two inherited diseases in man, the Simpson Golabi Behmel syndrome (SGBS) (Pilia *et al.*, 1996) and hereditary multiple exostoses (HME) (Hennekam, 1991), have demonstrated that alterations in HSPG synthesis lead to phenotypic changes indicative of aberrant control of cell growth, differentiation, organogenesis, and bone formation (Lind *et al.*, 1998; McCormick *et al.*, 1998). These effects are generally attributed to disruption of signalling pathways regulated by specific proteins that rely on HSPGs for their activity (Selleck, 2000).

Various roles of HSPGs have been proposed for the heparin-binding regulators of angiogenesis (Table 1.3). In addition to acting as co-receptors, HSPGs can protect these proteins from proteolytic degradation, localise and concentrate cytokines such as IL12, IL8, PF4, act as chaperones during internalisation of proteins as demonstrated for TSP-1, and restore functions of proteins, such as VEGF, when damaged by oxidation (see Bernfield *et al.*,1999 and references therein). Endostatin is one of the newest additions to the heparin-binding family of angiogenic regulators but the role of HS in its mechanism of action is unclear. Indeed, a major question is whether the ability of pro- and anti-angiogenic proteins to bind heparin *in vitro* also translates to a pivotal role of HS *in vivo*. If so, HS may be regarded as a common denominator in angiogenesis and represent a key target for therapeutic control.

ANGIOGENIC REGULATOR	PROPOSED ROLE(S) OF HEPARIN/HEPARAN SULPHATE INTERACTION
ANGIOGENIC FACTORS	
aFGF	Enhances aFGF activation
bFGF	Activation of tyrosine kinase signaling receptors
$VEGF_{165}$	Enhances binding of VEGF to tyrosine kinase signaling receptors
HGF	Activation of met signaling receptor
TNFα	?
TGFβ	Protection from proteolysis and localisation of TGFβ activity
PDGF	Secretion and localisation of PDGF
IL8	Protection from proteolysis and localisation of IL8 activity
HIV-tat protein	*Enhances angiogenic response to HIV-tat (Albini, 1996)
Angiogenin	Protection from proteolysis, angiogenin mediated adhesion
Midkine	Essential for bioactivity, promotes dimerisation
ENDOGENOUS INHIBITORS OF ANGIOGENESIS	
Endostatin	Inhibition of bFGF induced angiogenesis
IFN γ	Concentration and dimerisation of cytokine, protection from proteolysis
IL 12	Tissue localisation of cytokine
PF 4	Tissue localisation of cytokine
TNF α	?
16K prolactin	?
Arresten	?
TSP-1	Receptor function in binding, uptake and degradation of TSP-1
TIMP3	?
TGF β	Protection from proteolysis and localisation of TGFβ activity
Fibronectin	Co-receptor in integrin signalling

Table 1.3
Physiological role(s) of heparin/heparan sulphate proposed for regulators of angiogenesis. Other, as yet unidentified, mechanisms may exist. ? = not known (Adapted from Conrad, 1998, Bernfield *et al.*, 1999, Gallagher &Lyon, 2000)

1.2 Heparan sulphate – a conserved extracellular code ?

It is over 50 years since commercial preparations of the anticoagulant heparin manufactured from extracts of lung and liver were found to contain a 'less sulphated heparin' (Jorpes & Gardell, 1948). Although initially thought to represent an intermediate in heparin biosynthesis, this product was detected in mammalian cell cultures in the 1970's. Subsequent research revealed the HS polysaccharides were chemically related to heparin, but distinct in location, structure and activity (Gallagher & Lyon, 1989).

The GAG group of complex carbohydrates also includes chondroitin sulphate (CS), dermatan sulphate (DS), keratan sulphate (KS) and hyaluronic acid (HA). GAGs are polymers of repeating disaccharide units; an amino sugar and a uronic acid, in all but KS where galactose replaces the uronose residue. The amino sugar is glucosamine in heparin/HS and galactosamine in CS/DS. With the exception of HA, all GAGs are sulphated and covalently linked to a protein core to form proteoglycans (PG), of which the HSPGs are the commonest on cell surfaces (Kjellen & Lindahl, 1991).

PGs sequester proteins within secretory vesicles, link proteins together within the extracellular matrix (ECM), and bind proteins to the cell surface (Bernfield *et al.*, 1999). Serglycin is the single core protein constituent of heparin and its production is confined to mast cell granules, whereas a variety of proteins provide protein core structures of HSPGs (Salmivirta *et al.*, 1996). Most ECM-associated HS is on the basement membrane PGs, perlecan and agrin (Iozzo *et al.*, 1994; Noonan *et al.*, 1991; Tsen *et al.*, 1995). It is also present on type XVIII collagen, that is the first identified collagen to carry HS chains and the precursor of endostatin (Halfter *et al.*, 1998).

At the cell surface, the major families of HSPG are the syndecans (1-4) and glypicans (1-6) (Bernfield *et al.*, 1999; David *et al.*, 1990; Veugelers *et al.*, 1999). Other membrane proteins that may be glycosylated with HS are an isoform of CD44 that incorporates the V3 exon (Jackson *et al.*, 1995), betaglycan (a single HS chain PG) (Andres *et al.*, 1992), and a variant of the high affinity FGF-receptor 2 (Stringer & Gallagher, 1997a). Syndecans and betaglycan are transmembrane proteins that may carry CS chains in addition to HS whereas glypicans are globular proteins, exclusively

substituted with HS, and anchored to the cell membrane via glycosylphosphatidylinositol (GPI).

The HS chains attached to the core proteins provide cells with a mechanism to snare a wide variety of extracellular effectors without requiring multiple novel binding proteins (Bernfield *et al.*, 1999). The biosynthetic scheme for HS is thought to have arisen in the pre- and early Cambrian period concurrent with the emergence of the basic aspects of epithelial sheets in concert with various proteins involved in organising the basic body plan such as *dpp* (bone morphogenetic proteins 2-4) , *wg* (Wnt-1), and *sog* (chordin) (WooPark *et al.*, 2000). Such proteins have retained their affinity for heparin and bind, mainly through ionic interactions, to heparin/HS via basic amino acids on their surfaces that comprise distinct protein domains. There is no single consensus sequence which in itself suggests that many of the HS-binding domains in these proteins are ancient (Bernfield *et al.*, 1999).

Analysis of protein domains that bind HS have revealed linear sequences such as XBBBXXBX, XBBXBX, and a critical 20Å spacing of basic residues (B) in some proteins. This spacing conforms to the helical rotation of heparin that disposes clusters of sulphate groups at regular intervals on either side of the helical axis (Najjam *et al.*, 1998). Less is known about the physical properties of HS but it is likely that the S-domains will form a similar helical structure to heparin. A tertiary motif has also been described, TXXBXXTBXXXTBB, where turns (T) bring basic interacting amino acid residues into proximity (Hileman *et al.*, 1998).

Thus, the heparin-binding domains of the proteins are almost as varied as the proteins themselves and neither the number of basic residues or surface orientation can predict the strength of heparin/HS binding or recognition sequence within heparin/HS (Gallagher & Lyon, 2000). Although contentious, evidence has emerged in support of sequence specific saccharide motifs for proteins within heparin/HS (Lindahl *et al.*, 1998; Perrimon & Bernfield, 2000). However, until recently progress in characterising the recognition epitopes within HS for proteins has been hampered by the structural diversity of HS and cumbersome sequencing technology.

Heparan sulphate synthesis and structure

HS encompasses a range of species with common characteristics but also with fine structural variations that are believed to impart selectivity and/or specificity to HS-protein interactions (Gallagher & Lyon, 2000). An important concept is that HS varies in structure depending on its cellular origin and the core protein does not direct the synthesis of its own unique HS species. For example, syndecan-1 expressed on two different cell types bears structurally different HS (Kato *et al.*, 1994; Sanderson *et al.*, 1994). The structure and functions of the HSPG core proteins will be discussed later but in general, it is not clear how the protein constituents of HSPGs cooperate in the ligand binding properties of the HS chains. Thus, HS design is principally a function of cell type-specific repertoires of biosynthetic enzymes rather than the core protein to which it is attached (Bernfield *et al.*, 1999; Lindahl *et al.*, 1998; WooPark *et al.*, 2000).

The biosynthetic process involves :

1. formation of a region linking the HS chain to protein
2. generation of the polysaccharide chain
3. enzymatic modification of the chain to yield the specific saccharide sequences and structural organisation that are responsible for protein binding

Chain initiation

PG core proteins are synthesised on ribosomes attached to the endoplasmic reticulum (ER) and are translocated into the ER lumen. The biosynthetic enzymes for heparin/HS reside in the Golgi (Humphries *et al.*, 1997) where GAG chain initiation starts with transfer of xylose from UDP-xylose to the hydroxyl group of specific serine residues in consensus sequences of Ser-Gly repeats (Zhang *et al.*, 1995) to form a linkage tetrasaccharide : Ser-O-Xyl-Gal-Gal-GlcA- that is identical for CS and HS (Esko, 1991). A recently cloned enzyme that is related to the EXT genes implicated in HME (GlcNAct1/EXTL2) then determines and initiates HS chain biosynthesis on the common tetrasaccharide linkage sequence with the transfer of N-acetyl glucosamine (GlcNAc) (Kitagawa *et al.*, 1999). Although controversial, this enzyme may also initiate CS chain synthesis with the transfer of N-acetylated galactosamine, depending on the specific peptide sequence around the GAG attachment site (Esko & Zhang, 1996; Kitagawa *et al.*, 1999).

Chain modification

The HS polymerases are the EXT1 and EXT2 gene products that act in concert to catalyse alternating addition of N-acetyl glucosamine (GlcNAc) and glucuronic acid (GlcA), joined by α and β1-4 linkages respectively, to form the precursor polysaccharide 'heparan' (Lind *et al.*, 1998; McCormick *et al.*, 1998). Mutation of either EXT 1 or EXT2 causes the dominant inherited skeletal dysplasia, HME that is characterised by benign bone tumours (exostoses) with a predisposition for malignant transformation (Hennekam, 1991).

Heparan ranges from 50 to 200 GlcNAc α1-4 GlcA repeating disaccharide units (Salmivirta *et al.*, 1996). The mechanisms controlling chain length are largely unknown but tend to be conserved for HS species (Lyon *et al.*, 1994; Turnbull & Gallagher, 1990). The disaccharide units are then subjected to a series of sequential enzyme modifications concomitantly, or lagging slightly behind chain elongation, in which the products of one reaction form the substrates for the next. These reactions are not template driven (Lindahl *et al.*, 1998) and apparently do not convert all of the available substrate, resulting in substantial sequence diversity in the final chain. Initially N-deacetylase/N-sulphotransferase (NDST) enzymes catalyse the conversion of around 50% of GlcNAc to N-sulphated glucosamine (GlcNS), the amino sugar that is unique to HS and heparin. This modification may rarely lead to N-unsubstituted glucosamine intermediates ($GlcNH_2$) if sulphation does not occur following N-deacetylation (Salmivirta *et al.*, 1996). Then GlcA adjacent to GlcNS is C-5 epimerised into iduronic acid (IdoA) by glucuronyl C-5 epimerase (Li *et al.*, 1997). These modified disaccharides (IdoA-GlcNS) are the main target for further modifications by the O-sulphotransferases (OSTs) that, like the NDSTs, use 3′-phosphoadenosine 5′-phosphosulphate as a sulphate donor (Bernfield *et al.*, 1999) .

IdoA may be 2-O-sulphated by iduronosyl 2-O-sulphotransferase (2-OST) and $GlcNSO_3$ may be 6-O-sulphated by glucosaminyl 6-O-sulphotransferases (6-OST). Rarer modifications include 3-O-sulphation of $GlcNSO_3$ by glucosaminyl 3-O-sulphotransferases (3-OST), 2-O-sulphated GlcA and 6-O-sulphated GlcNAc (Salmivirta *et al.*, 1996) (Figure 1.1).

Biosynthesis of Heparan Sulphate

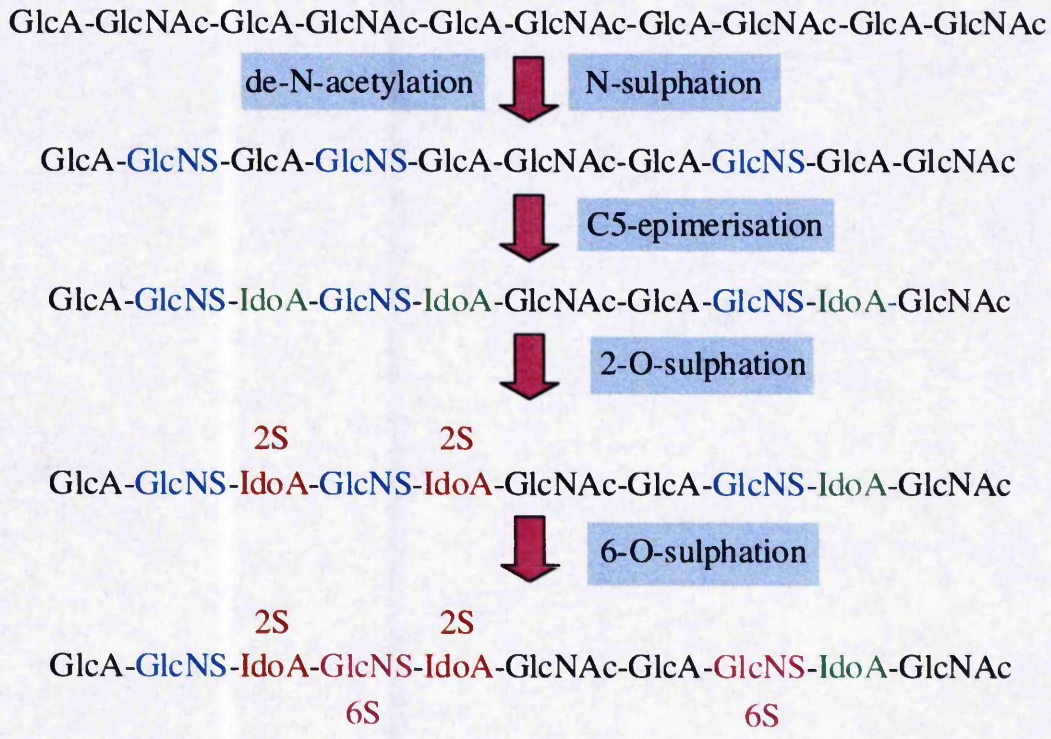

Seven disaccharide units are the principal constituents of Heparan Sulphate

Non-sulphated	Mono-sulphated	Di-sulphated	Tri-sulphated
UA-GlcNAc	UA-GlcNS	UA(2S)-GlcNS	UA(2S)-GlcNS(6S)
	UA-GlcNAc(6S)	UA-GlcNS(6S)	
	UA(2S)-GlcNAc		

Figure 1.1: Heparan sulphate synthesis. Heparan polymers comprise 50-200 N-acetylglucosamine – glucuronic acid (GlcNAc α1,4 GlcA) repeats attached to core proteins at Ser-Gly repeat sequences. Transformation of heparan to HS is initiated by the N-deacetylase/N-sulphotransferase (NDST) enzymes, that modify a proportion (usually 40-50%) of GlcNAc to N-sulphoglucosamine (GlcNS). This, and the following modifications are non-random, interdependent and quantitatively incomplete. Uronate epimerase converts GlcA adjacent to GlcNS to the C-5 epimer, iduronate (IdoA). O-sulphotransferases act on resulting GlcNS/IdoA rich domains, beginning with HS-2OST which transfers sulphate to C-2 of the IdoA residues (and rarely, to GlcA). Subsequently, 6-O and 3-O sulphotransferases (6- and 3-OSTs) complete the heparan-HS transition by transferring sulphate groups to C-6 or C-3 of the amino sugars. Members of the gene families recognise subtly different disaccharide substrates to create microstructurally heterogeneous sulphated (S) domains.

Domain structure

The structural diversity of HS is created by the fractional conversion of potential substrate by the HS modifying enzymes. There is enormous potential for structural permutations but there are constraints. IdoA residues are only found attached to C-1 of GlcNS (GlcNS α1-4IdoA), and 6-O-sulphation mainly occurs on these residues. IdoA is the principal target of 2-O-sulphation whereas GlcA is rarely 2-O-sulphated and 6-O-sulphation of GlcNAc only occurs adjacent to a GlcNS containing disaccharide. These modifications are incomplete and their clustering around the GlcNS – containing disaccharides, creates a domain structure of hypervariable sulphated domains (S-domains) separated by sequences composed largely of unmodified GlcA β1-4 GlcNAc repeats (NAc-domains) (Gallagher *et al.*, 1992; Salmivirta *et al.*, 1996). The boundary between these regions is not sharp and consists of transition zones comprising short, mixed sequences where N-acetylated and N-sulphated disaccharides, alternate (Maccarana *et al.*, 1996). The domain structure of HS discriminates it from its relative, heparin although the biosynthetic machinery is essentially the same. Heparin is enriched with fully modified (trisulphated) disaccharides [IdoA(2S)-GlcNS(6S)] whereas these disaccharides are less prevalent in HS (Gallagher & Walker, 1985) (Figure 1.2).

Polymer sulphation is essential for protein recognition and the S-domains, along with the transition zones, are the regions of hypervariability that give the distinctive characteristics to HS species from different cells. For example HS extracted from rat liver has a relatively small chain (Mr~22000) with a high proportion of N-sulphated glucosamine (~ 60%) and O-sulphate (73/100disaccharides) due to enrichment in IdoA(2S) (Lyon *et al.*, 1994). In contrast, skin fibroblast HS has a longer chain (Mr ~45000) with a lower proportion of N-sulphated glucosamine (~ 47%) and O-sulphate (26/100 disaccharide units)(Turnbull & Gallagher, 1990). The highly conserved domain structure of HS and the consistent structural variations between HS from different cellular sources strongly suggests a predetermination of structure despite the absence of a template driven biosynthesis.

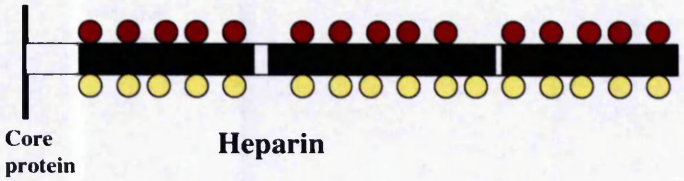

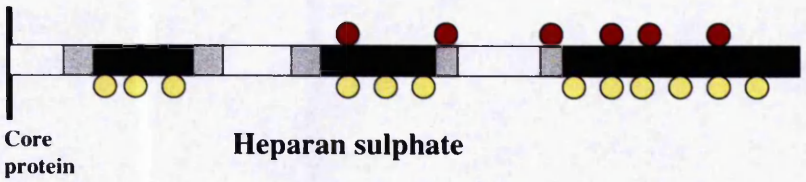

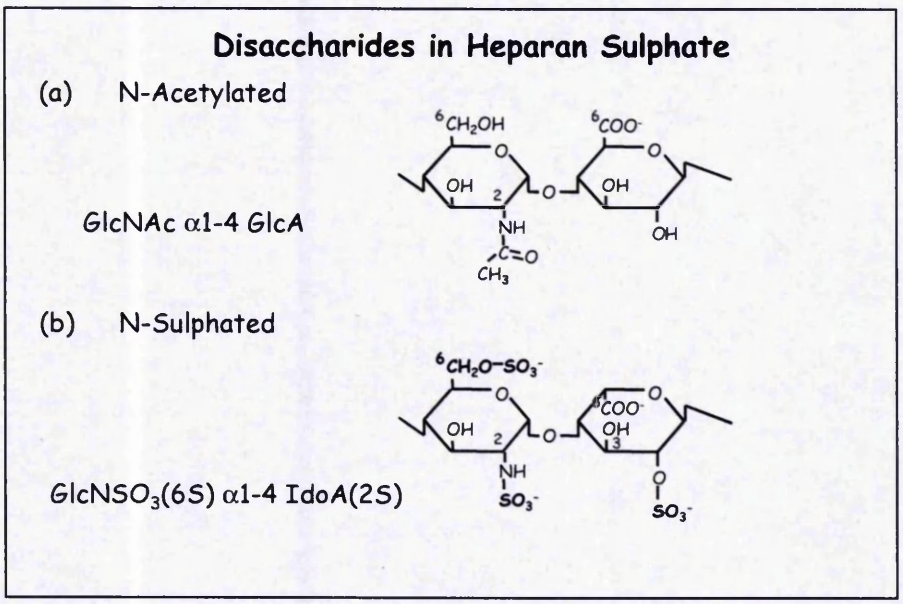

Figure 1.2 : Structural distinctions between heparin and heparan sulphate. Heparin is more highly sulphated than heparan sulphate (HS). There is near equivalence in the frequency of N- ,2-O-,(yellow circles) and 6-O-sulphates (red circles) in heparin, with ≥90% occupancy at each position. In HS, sulphate groups are localised to the S-domains (black rectangles), in which 2-O-sulphate groups may occur on IdoA residues and GlcNS may be 6-O-sulphated. In the transition zones (grey rectangles) of alternating GlcNAc/GlcNS containing disaccharides, 6-O-sulphate may substitute GlcNAc residues. The S-domains differ in length and in contrast to heparin, a significant proportion of the chain is composed of unmodified N-acetylated disaccharides. The structure of an N-acetylated disaccharide and a fully modified, trisulphated disaccharide are shown.

It is not known how such controlled variability of HS biosynthesis is achieved but the recent cloning of HS biosynthetic enzymes has started to provide some clues. The NDSTs, 6-OSTs and 3-OSTs belong to multigene families (Aikawa & Esko, 1999; Habuchi *et al.*, 2000; Shworak *et al.*, 1999) and at least four distinct mammalian isoforms of NDST, three 6OSTs and seven 3OSTs have been identified that exhibit tissue specific expression patterns. Preliminary studies have demonstrated a correlation between HS structure and isoform expression. For example, 6-OST1 is expressed in liver and acts preferentially on IdoA(±2S)GlcNS (Habuchi *et al.*, 2000) to form the highly sulphated disaccharide IdoA(±2S)GlcNS(6S) that is abundant in liver HS (Lyon *et al.*, 1994). Similarly, the enrichment of GlcA-GlcNS(6S) in the brain correlates with expression of 6-OST2 in this location (Habuchi *et al.*, 2000). However, the mechanisms by which the enzymes act interdependently during the modifying steps of HS synthesis remain elusive. In addition, several isoforms of one enzyme may exist in the same cell. As demonstrated for NDST-1 deficient cells, the HS synthesised by these cells is still sulphated, but to a lesser extent than control cells (Aikawa & Esko, 1999; Ringvall *et al.*, 2000).

It has been known for many years that the structure of HS expressed by a single cell may be altered during development (Nurcombe *et al.*, 1993), differentiation (Salmivirta *et al.*, 1998), in cells that have undergone malignant transformation (Jayson *et al.*, 1998; Winterbourne & Mora, 1981) and in ageing (Feyzi *et al.*, 1998). In general, these changes have been assumed to affect ligand binding with consequent alterations in cellular function. More recently, the HME story in humans (Lind *et al.*, 1998; McCormick *et al.*, 1998), and genetic studies in mice and *Drosophila* have revealed direct evidence that HS is essential for the coordination of signalling mediated by multiple growth factors.

Genetic studies of HS biosynthetic enzymes

Over recent years, screens for mutations that affect patterning in *Drosophila* have uncovered genes involved in GAG biosynthesis (Selleck, 2000). *Drosophila* is a reasonable model for vertebrate development because of the evolutionary conservation of mechanisms of cell growth, adhesion, and signal transduction. The first gene identified was named *sugarless (sgl)* (Binari *et al.*, 1997). It is related to vertebrate UDP-glucose dehydrogenase that is required for synthesis of glucuronate-containing

polymers and essential for normal patterning of the embryonic epidermis. Mutations in *sgl* cause defects in signalling of the heparan sulphate binding growth factors wingless (Wg)(Binari *et al.*, 1997) and decapentaplegic (Dpp) (Haerry *et al.*, 1997). In addition, *sgl* is required for FGFR signalling mediated by *heartless* and *breathless* (Lin *et al.*, 1999).

FGFR, Hedgehog (Hh) and Wg signalling are also affected by *sulfateless*, the Drosophila counterpart of the mammalian NDST gene family (Lin *et al.*, 1999; Lin & Perrimon, 1999; The *et al.*, 1999). A Drosophila gene *tout-velu* (*ttv*) that is related to EXT1, the HS co-polymerase, also causes a selective defect in Hh signalling and distribution (The *et al.*, 1999). This is particularly interesting since *ttv* would be expected to have a profound effect on HS synthesis and therefore other HS dependent signalling pathways as outlined above. Since there are other EXT-related genes in Drosophila it is possible that these may be responsible for HS synthesis on some core proteins or tissues, reinforcing the idea that much of the tissue-specificity of HS structure and function may be due to the combination of biosynthetic enzymes present (Selleck, 2000). The tissue-specificity of HS function is particularly evident in the 2-OST knockout mouse that exhibits renal agenesis, eye and skeletal abnormalities (Bullock *et al.*, 1998). These studies have strengthened the view that HS-ligand interactions are specific, tightly regulated and dependent on HS to provide the necessary recognition epitopes for proteins (Perrimon & Bernfield, 2000; Selleck, 2000).

HSPG Degradation

Within 12-15 minutes of completion of synthesis, HSPGs are guided by their core protein to different sites, such as intracellular storage vesicles, the ECM, or the cell surface (Yanagishita & Hascall, 1992). HSPGs typically have a half life of 3-8 hours at the cell surface and their metabolic turnover follows different routes. Transmembrane intercalated forms are either internalised by endocytosis and degraded stepwise in endosomes or lysosomes, or cleaved proteolytically and shed into the extracellular space (Bernfield *et al.*, 1999; Yanagishita & Hascall, 1992). Glypicans can, in addition, be cleaved at the phosphate-inositol bond by phosphatidylinositol-specific phospholipase C resulting in release of the PG from its lipid-anchor (David *et al.*, 1993). Recycling of glypican via endosomes to the trans-Golgi compartment has also been demonstrated and this is accompanied by partial degradation and re-synthesis of HS chains. HS chains are

degraded enzymatically by the action of endoglucuronidases (heparanases) and in transformed human umbilical vein endothelial cells (HUVEC), this may be coupled with nitric oxide mediated, non-enzymatic degradation. Interestingly, nitric oxide derived nitrite cleaves the HS chains at rare, internally located N-unsubstituted glucosamine residues (Mani *et al.*, 2000).

Just as early observations of mast cell heparin implicated a role for GAGs in neovascularisation, the heparanase enzymes that degrade HS chains provide more recent confirmation. By co-operating with proteases such as the matrix metalloproteases (MMPs), heparanase(s) contribute to the breakdown of ECM and basement membranes. They cleave HS chains at specific intrachain sites and the fragments of HS that are released can activate GFs such as bFGF (Kato *et al.*, 1994). Growth factors that are sequestered by HS may also be liberated (Marchetti, 1997). As a consequence these enzymes are believed to be key mediators of angiogenesis, tumour invasion and metastasis (Vlodavsky *et al.*, 1999) and are present in multiple normal and malignant cell types, but have proved particularly difficult to characterise. A range of molecular weights for heparanase has been reported, suggesting a family of distinct enzymes (Bame *et al.*, 1998). This theory was challenged by the recent cloning of a single heparanase gene (HPA1) encoding identical enzymes in human hepatoma, placenta and platelets (Hulett *et al.*, 1999; Vlodavsky *et al.*, 1999). However, a second gene (HPA2) with significant homology to HPA1, that gives rise to 3 proteins by alternative splicing has subsequently been reported (McKenzie *et al.*, 2000). Their functions have not been fully characterised but the tissue distribution and cellular localisation of HPA2 appears distinct from HPA1 suggesting different potential roles in HS catabolism.

Methods for investigating HS structure

Most information about HS structure has been obtained using a combination of enzymatic and chemical methods known to depolymerise HS and heparin at specific glycosidic linkages (see Conrad 1998 for review, and references therein) (Table 1.4). Oligosaccharides generated by these methods can be separated by a variety of chromatographic and electrophoretic techniques to reveal the numbers and spatial arrangements of the glycosidic linkages susceptible to the degradative reagent used.

REAGENT	SUSCEPTIBLE LINKAGE	DOMAINS DISRUPTED
Heparinase I	GlcNS(±6S)α1-4IdoA(2S)	S-domains
Heparinase II	GlcNR(±6S)α1-4UA(±2S)	All domains
Heparinase III	GlcNR(±6S)α1-4UA	NAc-domains
Low-pH nitrous acid	GlcNS(±6S)α1-4UA(±2S)	S-domains

Table 1.4 : Susceptible glycosidic linkages for reagents used to depolymerise heparan sulphate. R=NAc or NSO_3, UA=glucuronic or iduronic acid, S = sulphated, NAc = unmodified (GlcA-GlcNAc)n, IdoA=iduronic acid.

Nitrous acid depolymerisation

Nitrous acid used at pH1.5 effects deaminative scission of glycosidic linkages of GlcNS and converts the amino sugar to anhydromannose (aMan). Non sulphated amino sugars, GlcNAc or GlcN are not susceptible so this enables N-sulphated GAGs (HS and heparin) to be distinguished from other GAGs (eg CS and DS). In addition, the content and positioning of N-sulphate residues can be detailed within a chain (Conrad, 1998) (Figure 1.3).

The heparinases

The bacterium *Flavobacterium heparinum* was discovered as a soil isolate, that produces a range of lyases, glucuronidases, sulphoesterases and sulphamidases to obtain carbon and nitrogen from heparin or HS (Galliher *et al.*, 1981). The lyases (termed heparinases) were used from the earliest days of HS/heparin investigation but it was not possible to clarify their relative specificities with any degree of confidence until recently (Desai *et al.*, 1993; Linhardt *et al.*, 1990) due to difficulties in obtaining preparations free from impurities such as sulphatases. Heparinase I was purified to homogeneity in 1985 (Yang *et al.*, 1985) and heparinases II and III in 1992 (Lohse & Linhardt, 1992). The accepted substrate specificities for these enzymes are shown in table 1.4 and a scheme of characteristic products from an HS chain of typical domain structure in Figure 1.3.

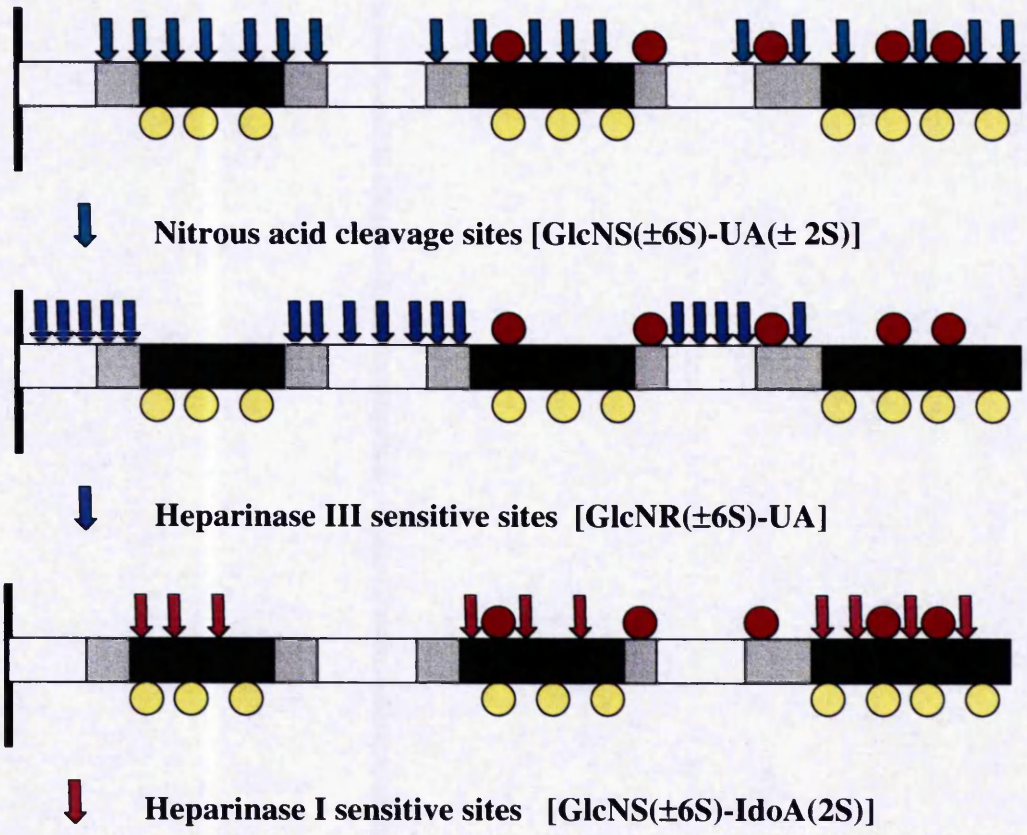

Figure 1.3 : Methods for investigating the structure of heparan sulphate. Nitrous acid cleaves extensively within the S-domains (black boxes) and at sites of N-sulphated glucosamine in the transition zones (grey boxes). Heparinase III cleaves in the relatively unmodified N-acetylated regions (white boxes) and transition zones liberating intact S-domains. Heparinase I disrupts the S-domains releasing highly sulphated disaccharides whereas predominantly N-acetylated oligosaccharides with intact transition zones are resistant. The products of chain scission range from disaccharides (dp2) to longer fragments (≥dp14) that can be separated by gel filtration. From the profiles obtained, the content and positioning of susceptible linkages in the intact chain can be inferred. Yellow circles = 2-O-sulphate, red circles = 6-O-sulphate.

Each of the heparinases depolymerise HS/heparin by an eliminative mechanism that results in the introduction of an unsaturation between C4 and C5 of the non-reducing terminal uronate residue upon cleavage of the glycosidic bond (Linker & Hovingh, 1972). This results in loss of the asymmetry that separates GlcA and IdoA and generates a UV chromaphore (max absorption at 232nm) that allows the digestion of heparin/HS to be monitored. Heparinase II has broad specificity and so is usually used in combination with heparinases I and III to completely degrade GAGs to component disaccharides for calculation of the proportions of mono-, di-, and tri-sulphated disaccharides present. When compared to known standards 2-O-, 6-O-, and N-sulphate substitutions can also be determined but IdoA and GlcA cannot be differentiated due to loss of asymmetry as outlined above. In contrast, the more restricted specificities of heparinases I and III enable each to be used alone to determine the proportions and distributions of susceptible linkages within a chain.

Detection of HS/heparin and degradation products

Various chromatographic (eg anion exchange, gel filtration, SAX-HPLC) and electrophoretic (eg PAGE) methods are used to separate, purify and analyse GAGs. The large quantities of heparin available from animal tissue extracts enable detection by standard assay techniques such as spectophotometric detection of unsaturated uronate residues by absorption at 232nm (Linhardt *et al.*, 1988). However, quantities of HS derived from cell culture are typically too small to detect by these means. This problem has been overcome by incorporating a radiolabel either by chemical means to end-label oligosaccharides (Bienkowski & Conrad, 1985; Delaney & Conrad, 1983) or by providing radiolabelled precursors in cell-culture media (^{3}H-glucosamine, Sodium ^{35}S-sulphate) to enable metabolic labelling throughout newly synthesised chains (Gallagher & Walker, 1985).

Novel sequencing methods for glycosaminoglycans

Methods to order disaccharides analogous to DNA or peptide sequencing have only recently been developed (Keiser *et al.*, 2001; Merry *et al.*, 1999; Rhomberg *et al.*, 1998; Turnbull *et al.*, 1999; Vives *et al.*, 2001; Vives *et al.*, 1999). Three of these techniques extend the fundamental techniques outlined above by incorporating specific recombinant exoenzymes to remove 6-O- or 2-O-sulphate groups, or monosaccharide groups (glucuronate or iduronate) selectively from the non-reducing ends of saccharides

(Merry *et al.*, 1999; Turnbull *et al.*, 1999; Vivès *et al.*, 1999). Saccharides either end labelled with a fluorescent (Turnbull *et al.*, 1999) or ^{3}H tag (Vivès *et al.*, 1999), or metabolically radio-labelled (Merry *et al.*, 1999) are purified to homogeneity using various combinations of gel filtration, SAX-HPLC separation and PAGE. In general the end-tagged methods are suitable for use with highly heterogeneous heparin/HS from sources that cannot be metabolically radio-labelled. In contrast, the method of Merry *et al.*,1999, termed step sequencing, was developed specifically to sequence metabolically radio-labelled material and avoids additional handling procedures required for end-labelling. In brief, homogeneous saccharides are chemically depolymerised to a range of intermediates by controlling and stopping the activity of nitrous acid at various time points. The composition and order of disaccharides in the original sequences are then inferred from PAGE (Turnbull *et al.*, 1999) or SAX-HPLC (Merry *et al.*, 1999; Vivès *et al.*, 1999) profiles of intermediates before and after treatment with specific exoenzymes. The step sequencing technique of Merry *et al.*,1999, is shown in Figure 1.5.

A further strategy is based on the use of Mass spectrometry and incorporates heparin binding proteins to select for short oligosaccharides (dp4-6) with affinity (Keiser *et al.*, 2001; Rhomberg *et al.*, 1998). It is applicable for use with small quantities (picomolar) of cell culture derived HS and a 'one step' method to select biologically relevant saccharide sequences is an attractive possibility. One drawback is that minimal protein binding binding sequences within HS/heparin do not imply bioactivity. For example, bFGF binds tightly to a hexasaccharide but requires longer saccharides of dp10-14 for signalling (see next section). In comparison the former methods, although developed on oligosaccharides of dp4-10 have potential to sequence longer oligosaccharides and utilise standard laboratory equipment (Merry *et al.*, 1999; Vives *et al.*, 2001). However, the complex range of structures in HS from whole tissue extracts such as bovine lung, require multistep purification methods to generate pure species for sequencing and methods by which homogeneous sequences of longer eg. $\geq$ 10/12 oligosaccharides may be obtained are still being perfected (Vives *et al.*, 2001). Although there are few reports of the application of these novel GAG sequencing techniques to the structural analysis of HS recognition sites for proteins it is anticipated that they will have a significant impact in this field.

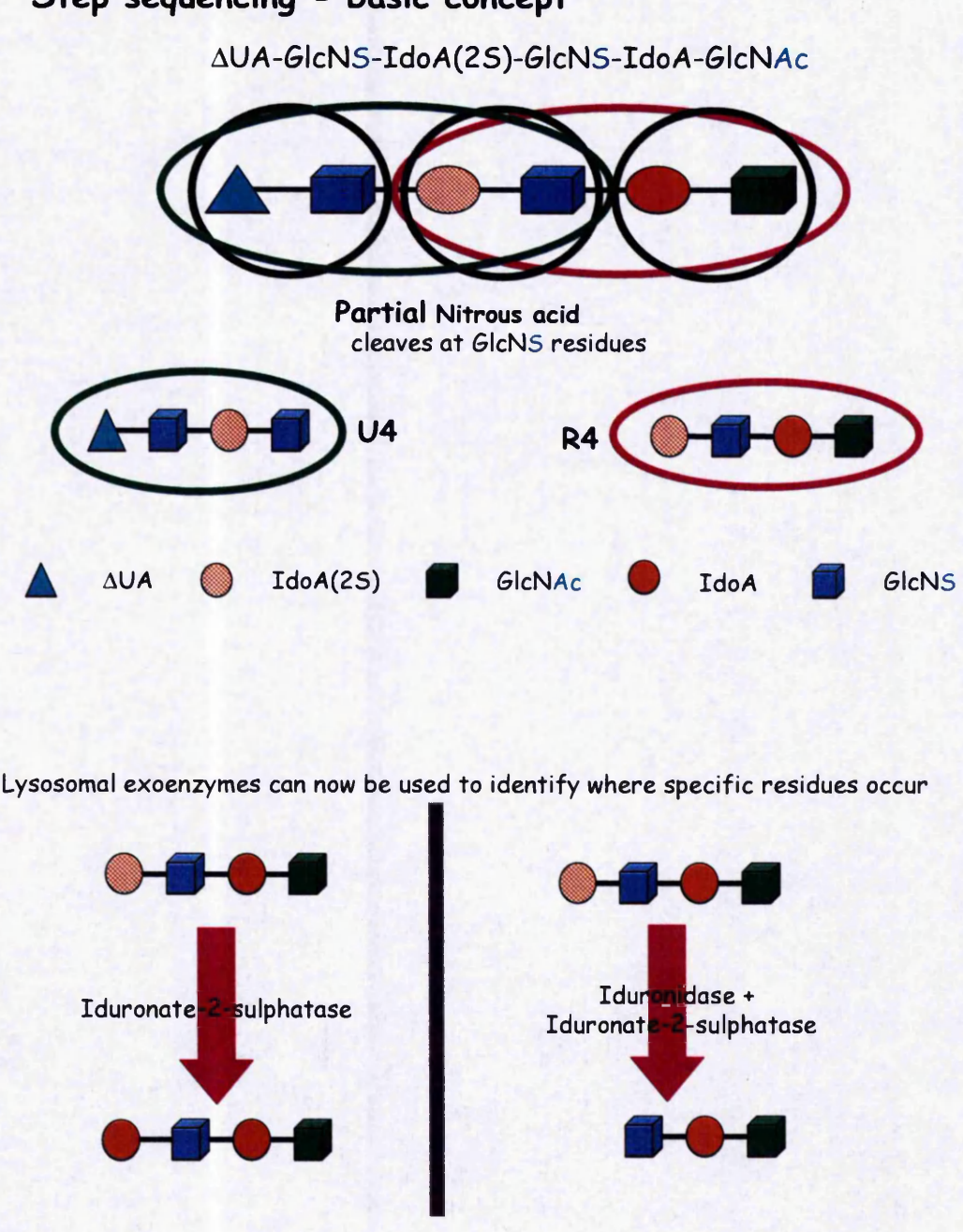

Figure 1.4 : Step Sequencing. The basic principle of the technique is to open up the oligosaccharide, exposing all of the 'hidden' internal information to investigation using specific enzymatic digests. This is done by using a partial nitrous acid depolymerisation to cleave the chain at GlcNS residues. By stopping the reaction on small aliquots at various timepoints a range of oligosaccharides can be generated from which the susceptible GlcNS residues can be pinpointed. For example, from a hexasaccharide containing two internal GlcNS residues, partial nitrous acid scission will result in three disaccharides, two distinct tetrasaccharides and a small amount of residual intact hexasaccharide. In contrast, if a hexasaccharide has one internal GlcNAc residue, then only one tetrasaccharide can be formed. The degradation products of partial nitrous acid scission are resolved by SAX-HPLC. The positions of O-sulphate modifications can then be determined by using specific exoenzymes and observing for shifts in elution position of peaks in the initial profile of partial nitrous acid scission. Similarly, the GlcA/IdoA content can be derived from the effects of digestion with glucuronidase or iduronidase. Information from a total disaccharide analysis is also used to complement the data derived from partial nitrous scission although this cannot indicate the content of GlcA versus IdoA. *Merry et al.,1999*

HS recognition sites for proteins

Antithrombin III – the prototypic heparin binding protein

To date, the best characterised recognition site within HS for a heparin-binding protein is that for ATIII. Heparin/endothelial cell HS plays a central role in the co-ordination of multiple proteins involved in haemostasis (see Conrad, 1998 for extensive review). Before the discovery of heparin, thrombin was known to lose its activity in plasma or serum, and this was attributed to a specific 'anti-thrombin' activity. When the anticoagulant activity of heparin was identified, it was noted that this also required an accessory protein in the blood, named heparin co-factor. It turned out that the 'anti-thrombin' and heparin co-factor were both ATIII. This is a serine protease inhibitor of the serpin superfamily that targets proteases by forming inactive complexes that are subsequently cleared from the circulation. Although most serpins combine rapidly with their target proteases, several of them, including ATIII, heparin cofactor II, protease nexin I, and protein C inhibitor, are poor inhibitors unless complexed with heparin. The heparin-ATIII interaction is mediated by a specific binding site that comprises a pentasaccharide sequence with a rare, and critical, 3-O-sulphated GlcNS (Conrad, 1998; Lindahl *et al.*, 1998).

Binding to this sequence induces a conformational change in ATIII that accelerates the rate at which the procoagulant proteases thrombin and factor Xa are inactivated (Evans *et al.*, 1992; Lindahl *et al.*, 1984). This has been exploited in the clinical use of heparin for many years. However, heparin is not the natural activator of ATIII. Patients with genetic defects that reduce ATIII activity have a propensity for thrombosis and studies of endothelial cell derived HSPGs and mast cell deficient mice have confirmed HS, rather than heparin, to be the naturally occuring activator *in vivo* (Conrad, 1998).

To date, no other heparin-binding protein has been identified with the sequence-specificity of ATIII. Studies of variant pentasaccharides have demonstrated that the activity of ATIII is impaired by either substitutions of additional sulphate groups or removal of essential groups (Conrad, 1998; Marcum & Rosenberg, 1989). Other proteins involved in coagulation such as thrombin appear to have less stringent requirements. The pentasaccharide enables ATIII to neutralise factor Xa activity but much longer heparin sequences of at least 18 monosaccharide units are required for ATIII to inactivate thrombin. In the case of thrombin, heparin is required as a template

to bring ATIII and thrombin together, side by side, to react. This approximation effect is also observed for factors IXa and XIa. The longer oligosaccharide sequence required to bind ATIII and thrombin simultaneously is composed of the specific pentasaccharide but there appears to be tolerance of sequence variation within the additional saccharides that bind to thrombin. This information has evolved over at least 3 decades and resulted from a combination of strategies that remain valid for investigating GAG-protein interactions as summarised by Conrad, 1998 below:

Physical methods

- NMR characterisation of protein and oligosaccharide structures
- X-ray crystallography for determining the three-dimensional structure of the heparin-binding proteins
- Calorimetry and circular dichroism for observing the interactions between proteins or peptides and heparin oligosaccharides
- Molecular modelling to deduce the three-dimensional structure of antithrombin and the docking of heparin pentasaccharide to antithrombin

Chemical approaches

- Synthesis of peptides and oligosaccharides

Biochemical approaches

- cDNA cloning of proteins to deduce amino acid sequences and site directed mutagenesis to identify critical amino acids for binding
- Biological assays to measure heparin and heparin oligosaccharide activities *in vitro*
- Affinity chromatography for isolation of specific antithrombin-binding heparin oligosaccharides and specific heparin-binding fragments
- Measurement of binding and kinetic constants to observe the interactions between heparin and antithrombin or peptides

Animal models

- To determine the biological activity of endothelial cell heparan sulphate *in vivo* and the effects of genetic defects in antithrombin on normal haemostatic mechanisms.

HS recognition epitopes for angiogenic regulators

- Basic FGF -

Basic FGF (bFGF) is the best studied heparin-binding angiogenic regulator. It is implicated in neural differentiation, mesoderm induction and blood vessel growth in embryonic and adult tissues (Folkman & Klagsbrun, 1987) and signals through

fibroblast growth factor receptors (FGFRs) that are classical signal transduction receptors with multiple Ig-loops in the ectodomain, a single membrane spanning sequence and an intrinsic (split) tyrosine kinase in the intracellular region (Ornitz, 2000). FGFRs belong to four closely related gene families from which multiple receptor isoforms are generated by alternative splicing of mRNA. The FGFR isoforms have different ligand binding properties and bFGF acts on the two and three loop variants of FGFR-1 and FGFR-2 (Ornitz, 2000). In cells lacking HS but expressing FGFR, the affinity of bFGF for its FGFR is reduced and signal transduction is impaired (Rapraeger *et al.*, 1991; Yayon *et al.*, 1991). As previously mentioned, studies in *Drosophila* have demonstrated that HS is required for FGF signalling (Lin *et al.*, 1999). The HS binding site for bFGF and the mechanism by which it functions as a co-receptor for FGFR have been widely debated.

Initially, using bFGF affinity chromatography, a sequence in HS was identified comprising S-domains of 6-7 N-sulphated disaccharide units rich in IdoA residues and 2-O-sulphate groups (Turnbull *et al.*, 1992). The notable feature of this sequence was uniform sulphation of the internal repeating unit [IdoA(2S)-GlcNS]. However, it was not possible to prepare adequate quantities of this for testing in biological assays. In addition to this high affinity binding site, a pentasaccharide site was also reported (Maccarana *et al.*, 1993). From X-ray crystallographic studies of heparin saccharides and bFGF it was concluded that the minimal binding sequence for bFGF comprised five saccharides including a key IdoA(2S) residue (Fahem *et al.*, 1996). Iduronate residues exhibit conformational plasticity, oscillating between chair and skew boat forms with minimal change in linkage geometries. Notably, in the bFGF binding pentasaccharide [GlcNS–IdoA(2S)-GlcNS-IdoA-GlcNS] the two internal IdoA residues are locked in different conformations that increase the area of contact with the protein surface (Fahem *et al.*, 1996). The ability to test soluble heparin/HS in bioassays using cells lacking surface HS but expressing FGFR, has enabled functional evaluation of bFGF binding saccharides and provided some unanticipated results. Pentasaccharides bind but do not activate bFGF. Instead, optimal activation of bFGF requires longer sequences of 6-7 disaccharide units based on the aforementioned sequence described by Turnbull *et al.*,1992. However, the additional presence of a 6-O-sulphated, N-sulphated glucosamine is required for activation (Guimond *et al.*, 1993; Ishihara *et al.*, 1993; Pye *et al.*, 1998). As outlined above crystal studies do not implicate 6-O-sulphate in the

binding site and the role of 6-O-sulphate in the mechanism of activation of bFGF by heparin/HS remains unsolved. When it was first discovered that bFGF was dependent on HS it was believed that the polysaccharide converted bFGF from a latent to an active form by inducing a conformational change in the protein (Yayon *et al.*, 1991). However, FGFR-1 also binds to HS, and synthetic peptides based on the sequence of the putative HS binding region in the receptor block the mitogenic action of bFGF (Kan *et al.*, 1993). Recent crystallographic data support a model in which HS contains binding domains for both the growth factor and the receptor (Figure 1.5) (Pellegrini *et al.*,2000; Schlessinger *et al.*,2000). In these models the polysaccharide is conceived as a template bringing the ligand and the receptor in close proximity and 6-0–sulphate groups may be required to bind the FGFRs (Guimond *et al.*, 1993; Ornitz *et al.*, 1992). A further theory, is that HS presents dimers of the growth factor either in a cis or trans (by virtue of the bilateral arrangement of sulphate clusters) orientation, to facilitate the FGFR dimerization that is a prerequisite for signal transduction (Herr *et al.*, 1997; Moy *et al.*, 1997). Since the minimal pentasaccharide sequence is unable to promote bFGF mitogenic activity it is feasible that longer oligosaccharides are active because they can accommodate two bFGF monomers. However, covalent complexes of HS and bFGF in a 1:1 ratio are active, therefore oligosaccharide induced dimerisation is not crucial for activation of bFGF (Pye & Gallagher, 1999).

Further examination of heparin/HS saccharides of known size and composition have identified that heparins, and naturally occuring HS saccharides deficient in 6-O-sulphate such as the high affinity structure initially identified by Turnbull *et al.*,1992, can inhibit bFGF mitogenic activity (Guimond *et al.*, 1993; Pye *et al.*, 1998). Therefore, the balance of sequences at the cell surface may direct the cellular response to bFGF. This notion is consistent with results of HS analyis from five different mammary cell lines (Rahmoune *et al.*, 1998). Two distinct sites have been identified to which the affinity for bFGF and binding kinetics differ. HS containing only one site (denoted slow/low), could promote bFGF mitogenic activity whereas HS from two of the cell lines contained a second site denoted fast/high and was inactive (Rahmoune *et al.*, 1998). Thus, the bFGF story illustrates that the affinity of a saccharide for a protein does not necessarily define the activity. Furthermore, the detection of saccharide sequences with differential activity ie. inhibition or activation, provides a previously unsuspected mechanism of modulatory control by HS.

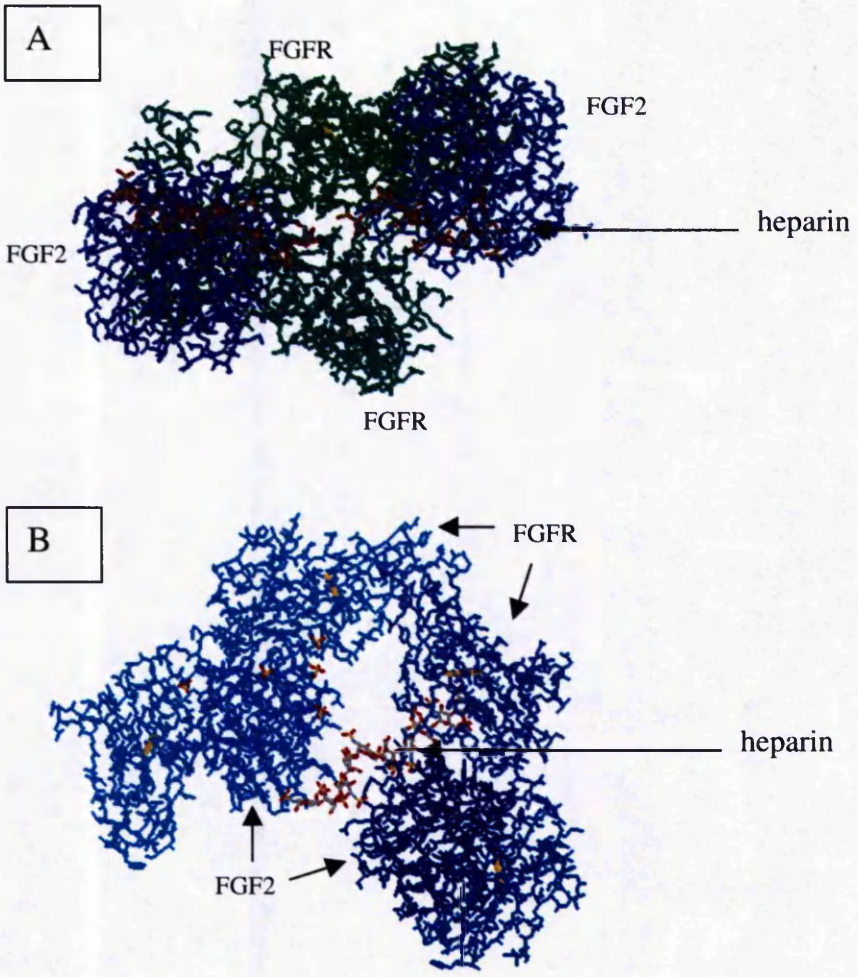

Figure 1.5 : Molecular architecture of FGF-FGFR-Heparin complexes. A : The crystal structure studies of Schlessinger *et al.*, 2000 reveal that the ligand (FGF-1 and FGF-2) and receptor form a 2:2 tetrameric assembly with each of the FGF/FGFR dimers in association with separate heparin decasaccharides. The saccharides are arranged in an antiparallel fashion and make extensive contacts with a canyon of positive charge that extends across the ligand receptor pairs. **B :** A contrasting view of the role of heparin was deduced from crystal structures of FGF2 and FGFR1 (Pellegrini *et al.*,2000). A 2:2 tetrameric assembly of FGF2 and FGFR1 forms but only a single asymmetric heparin decasaccharide is present that binds the two non-contacted FGF2 molecules in an offset trans arrangement and tethers two FGFRs into the assembly. The saccharide interacts with only one FGFR and induces a modification in receptor structure that may be essential for active signalling complex formation. Further studies are required to examine the molecular architecture of FGF-FGFR-HS complexes and to determine interactions between HS oligosaccharides that differ in sulphate pattern. These studies also imply the possibility that there may be more than one solution to the problem of how to form signalling complexes.

A pivotal role for HS in the regulation of angiogenesis ?

In contrast to the intense effort that has been directed towards the HS-bFGF interaction over the last decade, there is less information about the HS binding sites for other angiogenic regulators. A summary of current information is presented in Table 1.5. The HS epitopes have not been characterised for all the heparin-binding angiogenic regulators, although for a proportion, the heparin binding properties are known. Comparing the HS epitopes, several conclusions can be drawn. The first is that all the recognition sequences contain sulphated disaccharides and, in contrast to the ATIII site, unique and rare modifications such as 3-O-sulphate have not been identified. Instead, the proteins bind to arrangements of the commonly occurring disaccharides. Secondly, there does not appear to be a universal recognition epitope for either an inhibitor, or stimulator, of angiogenesis. Indeed, with our current understanding, the recognition epitopes do not provide any insight into the role of HS in the bioactivity of the protein. Thirdly, the differences between some of the binding sites appear subtle, with potential to overlap, for example compare that for TSP-1 and aFGF. This raises the possibility that there may be direct competition between angiogenic regulators for HS binding sites. This has been proposed for the mechanism of inhibition of bFGF induced angiogenesis by endostatin (O'Reilly *et al.*, 1997; Sasaki *et al.*, 1999). Also, there may be competition for certain saccharide modifications that are not actively participating in binding but required for activation. For example, TSP-1 may bind to/compete for 6-O-sulphate that is necessary for bFGF activation.

However, the binding affinities for these proteins vary widely, the structure – activity relationships of the sequences are not well characterised and the techniques used to elucidate them have not employed the novel sequencing strategies now available. In addition, it is difficult to ascertain the absolute specificities of these binding sites. For example, it is often not possible to obtain sufficiently distinct saccharide structures to determine whether redundant modifications are present in binding sequences. A further consideration is that the role of HS differs depending on the protein (Table 1.4 and see below). Thus, it is probably naive to regard direct competition between inhibitors and stimulators as a unifying mechanism of regulation of angiogenesis by HS, although this may be relevant for a subset of proteins.

ANGIOGENIC REGULATOR (reference(s) reporting GAG binding site)	HEPARAN SULPHATE RECOGNITION SEQUENCE FOR BINDING			HEPARIN BINDING DETERMINANTS (if HS recognition sequence is unknown)
	Disaccharide units	Domain organisation ■ = GlcN-sulphated □ = GlcN-acetylated	*Modifications required for maximal affinity	
Acidic FGF *(Kreuger'99)*	3-7		6S, IdoA2SGlcNS6S	
Basic FGF *(Turnbull,1992)*	3-7		Ido2S, GlcNS	
‡$VEGF_{165}$	> 7		2S>6S,NS	6S and NS*(Ono,1999)*
HGF *(Lyon,1994)*	3 -7		6S>2S,NS	
TNFα	?	?	?	?
TGFβ 1, 2 *(Lyon,1997)*	> 7 (heparin)		?	NS>2S>6S
PDGF *(Feyzi,1997)*	3-4	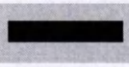	NS,2S,6S, IdoA2SGlcNS6S	
IL 8 *(Spillmann,1998)*	11-12		IdoA2SGlcNS6S	
Angiogenin *(Soncin,1997)*	3-6 (heparin)	?	?	?
HIV-tat	?	?	?	?
Midkine *(Kaneda,1996)*	15 (heparin)	?	?	NS>2S,6S
Endostatin *(Sasaki,1999)*	6 (heparin)	?	?	2S,6S
IFN γ *(Lortat-Jacob ,1995)*	22	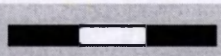	? highly sulphated S-domains	
IL 12 *(Hasan et al.,1999)*	4 (heparin)	?	?	NS,2S>6S
PF 4 *(Stringer, 1997)*	15-20		2S,NS>6S	
16K prolactin	?	?	?	?
Arresten	?	?	?	?
Fibronectin *(Lyon,2000)*	4-7		6S, at least two Ido2S residues	
TIMP	?	?	?	?
**TSP 1 *(Feitsma,2000)*	6-7		NS,6S>2S IdoA2SGlcNS6S	

Table 1.5

Heparan sulphate recognition sequences for heparin-binding regulators of angiogenesis.*For example, NS>6S indicates that both modifications are found in binding sites but the contribution of NS to the interaction is greater.**Binding site characterised using endothelial cell HS. ‡personal communication C Robinson, S Stringer , ? = not known

Finally, a pattern of binding site is emerging for oligomeric proteins, particularly the chemokines. IFN γ, PF4, IL8, and TGFβ recognise composite sites comprising unmodified N-acetylated regions of the HS chain in addition to highly modified 'S'-domains (Gallagher & Lyon, 2000). Heparin lacks the domain structure of HS and these composite sites underline the importance of examining HS in these studies rather than solely relying on heparin as a surrogate. The N-acetylated regions are thought to confer a conformational flexibility to the saccharides as illustrated by PF4 (see below).

Platelet factor 4 binds a composite HS epitope

PF4 is a tetrameric chemokine released from the α-granules of activated platelets that has a number of properties associated with inflammation, wound healing, and inhibition of angiogenesis. It exerts procoagulant activity by preventing formation of the heparin-ATIII-thrombin ternary complex and inhibits binding of bFGF, VEGF, and transforming growth factor β1 to their receptors (Zucker & Katz, 1991). Antiangiogenic and anticancer activity of PF4 has also been demonstrated *in vitro* and *in vivo* (Sharpe *et al.*, 1990). Two pairs of C-terminal lysines on an amphipathic α-helix in each PF4 monomer are thought to be important in binding heparin, since guanidation of these or digestion with carboxypeptidase decreases binding. However NMR studies of PF4 suggested that arginines in other regions of the protein are also critical to the interaction with heparin, and site directed mutation of these arginines reduces heparin binding 7 fold. Models proposed from x-ray crystallographic and NMR studies suggested that heparin may wrap around the tetramer, binding to a ring of positive charges running perpendicular to the lysine containing α-helices (Gallagher & Lyon, 2000).

The PF4-HS interaction was investigated by Stringer & Gallagher, 1997b. Competition studies with partially desulphated heparins provided initial clues that 2-O-sulphation of IdoA residues was more important than N or 6-sulphation of glucosamines in the interaction and provided evidence that the interaction was not solely dependent upon charge. Heparinase III derived S-domains of porcine mucosal HS were found to be poorer competitors than the parent HS suggesting that the binding site for PF4 was not confined to a sulphated domain. Using a protection approach in which PF4 and 3T3 HS

were incubated in the presence of heparinase III, a large 9.3kDa (21 disaccharide) fragment was isolated. Subsequent analysis suggested that this fragment was composed of a central poorly sulphated region flanked by 1 long, or 2 shorter eg octasaccharide and hexasaccharide S-domains at either end (Figure 1.6, Table 1.5). It has not been possible to sequence this fragment exactly and it is likely that a 'mix' of similar fragments was obtained. In addition, these fragments have not been tested in biological assays for modulation of PF4 activity.

The mechanism of regulation of PF4 by heparin/HS is unknown. A biophysical study using NMR to investigate the interaction between PF4 and a heparin dodecasaccharide has provided some evidence that heparin may induce a conformational change in PF4. At certain ratios of protein:heparin oligosaccharide, the protein undergoes a transition to a less folded state (Mikhailov *et al.*, 1999). Interestingly, a number of the basic residues in the ring of charges on PF4 are conserved within the family of intercrine chemokines that also includes interleukin-8 which is dimerised by HS. Therefore, the model of an extended region of HS tethered by peripheral S-domains encircling subunits of PF4 could be a common mechanism of interaction with multimeric cytokines and provides evidence that the spacing of the S-domains within HS may be as critical for binding as the sulphation patterns. (Stringer & Gallagher, 1997b)

Mechanisms of protein regulation by HS

HS can immobilize ligand, increase its local concentration, protect ligand from proteolytic degradation, change its conformation and present it to a signalling receptor (Bernfield *et al.*, 1999). This repertoire of activities is evident in the interactions between HS and the angiogenic regulators (Table 1.3). HS is employed as a co-receptor for tyrosine kinase receptors of the FGF family, VEGF and HGF, and for the integrins interacting with ECM components such as fibronectin (Gallagher & Lyon, 2000). It accelerates dimerisation of midkine (Iwasaki *et al.*, 1997) and IL8 (Spillmann *et al.*, 1998) thereby facilitating receptor activation. In addition, it restricts the diffusion of chemokines creating high local concentrations that exceed the threshold for receptor activation (Gallagher & Lyon, 2000). Heparin/HS has long been known to protect proteins from proteolysis and thermal denaturation thereby prolonging their biological lifetime (Bernfield *et al.*, 1999). Notably, it can restore damaged protein

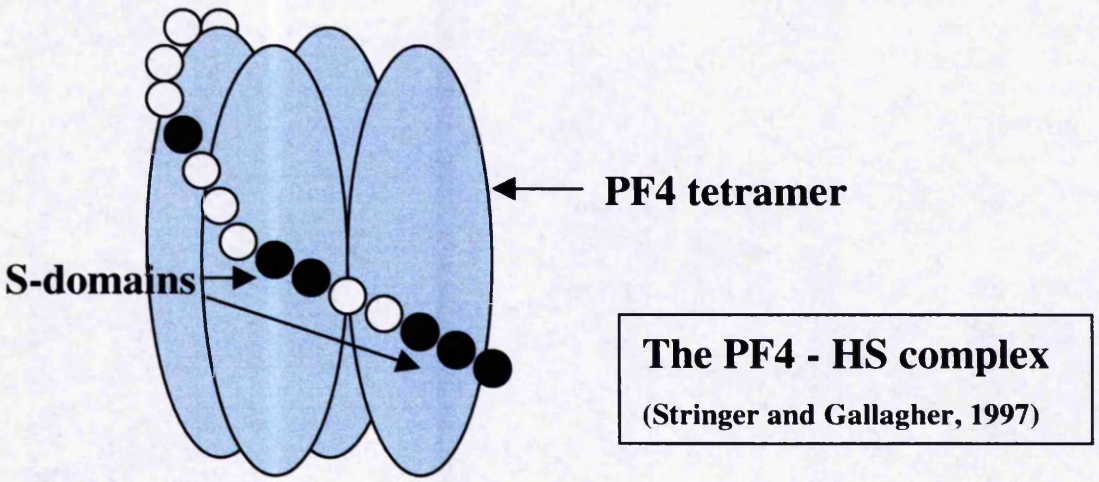

Figure 1.6 : Simplified model of PF4 binding to a composite HS domain. A 21 saccharide long section of HS wraps around the PF4 tetramer and the two small S-domains (forming a 'split' S-domain) denoted by black circles at either end, interact with the positively charged α-helices located on the external face of the PF4 dimer pairs.

oxidised by exposure to free radicals which may be particularly pertinent to the tumour milieu, especially in areas of tissue necrosis and hypoxia (Gengrinovitch *et al.*, 1999). HS does not always potentiate the activity of its ligands. In the case of IFN γ, binding to HS stabilises the protein but the complex is inert. IFN γ must dissociate from HS to engage its signalling receptor because of the partial overlap of the GAG and receptor binding domains in the protein (Sadir *et al.*, 1998). Additional factors in the protein environment may induce a conformational change in IFN γ to liberate it from sequestration by the GAG. For a proportion of angiogenic regulators including endostatin, the role of heparin/HS is not known and it is possible that as yet unidentified mechanisms exist.

The function of HS has been a longstanding enigma and a unifying hypothesis, based on the heparin mediated acceleration of thrombin inactivation by ATIII, is that HS catalyses molecular interactions at the cell surface (Lander, 1998). It has been calculated that the length of a typical HS chain (MW 30,000) when fully extended would be ~50nm. Given that a cell of ~15 μm radius bears $10^5/10^6$ uniformly placed HSPGs, HS would encompass the entire cell surface (Yanagishita & Hascall, 1992). This 'halo' of polyanionic HS chains is believed to provide a plane for capture and concentration of ligands to restrict their diffusion and reduce 'dimensionality'. In this way, HS can accelerate ligand-receptor encounters, enhance peptide diffusion and establish concentration gradients even for soluble factors that do not have high affinity for heparin/HS (Lander, 1998).

This may explain the potentiation of growth factor activity that is often seen with increasing heparin/HS concentrations. Stimulation of activity at low concentrations would occur due to reduced dimensionality, whereas the reduction in activity at high concentrations would be due to the large number of surfaces to which the growth factor can bind (Schlessinger *et al.*, 1995). The effect of HS would be expected to vary as a function of relative abundance of the HS chains and the reactants, their relative affinities, and the size and nature of the HS chain (Bernfield *et al.*, 1999). This unifying theory for the function of HS is attractive but it does not adequately explain two key observations. Firstly, the requirements for specific growth factor recognition sequences (such as the ATIII site) in this context are unclear as 'universal' binding sites may enable accommodation of a wider range of ligands and increase the chance of

'collision'. Secondly, in the absence of cell surface HS, the activity of HS-dependent growth factors cannot always be fully restored by just increasing the growth factor concentration (Delehedde *et al.*, 2000; Fannon *et al.*, 2000).

The regulation of proteins involved in angiogenesis by HS may be modulated by several other factors in addition to those already described. The core protein to which the HS chains are attached may impose specific functions and these will be discussed in the next section. As illustrated by bFGF, the balance of HS structures presented at the cell surface may be of significance in directing the cellular response. Also, HS expression is altered with consequent changes in growth factor binding activity in various pathophysiological states including malignant transformation (Jayson *et al.*, 1998; Winterbourne & Mora, 1981), as outlined previously, and it is not known whether endothelial cells alter their HS when recruited for angiogenesis by tumours. Degradation of HS by heparanase enzymes will also influence bioavailability of ligands sequestered by HS (usually in the ECM), and cellular responses to ligands (Kato *et al.*, 1998). In general, there has been some progress in identifying HS recognition epitopes and the functions of these for individual proteins. However, the role of HS in angiogenesis, particularly in the coordination of both positive and negative regulators, remains poorly understood.

1.3 Functions of membrane HSPGs

The HS chains are responsible for much of the biological role of the HSPGs and it is well known that heparin or HS can often substitute for HSPG functions in bioassays (Salmivirta *et al.*, 1996). The core proteins may have evolved to maximise the efficiency of HS *in vivo* (Bernfield *et al.*, 1999). In general, the core proteins determine when, where, and to what extent the HS chains are expressed; and the rate and mechanism of HS turnover. For example, 2-3 HS chains are usually positioned in close proximity on the core protein which may be necessary for a co-operative mode of action *in vivo* (Stringer & Gallagher, 1997a). However, syndecans and glypicans are expressed in cell-, tissue- and development specific patterns (Table 1.6) and some domains of these proteins are remarkably stable throughout evolution. These characteristics imply specific interactions that expand the functional diversity of the HSPGs.

The transmembrane syndecans

There are four distinct but homologous syndecan core proteins (19-35KD) named types 1-4 based on the order of cloning of their cDNAs (Bernfield *et al.*, 1992). All are type 1 transmembrane proteins, with an N-terminal signal peptide, an ectodomain containing GAG attachment Ser-Gly sequences, a single hydrophobic transmembrane domain and a short C-terminal cytoplasmic domain (Kim *et al.*, 1994) (Figure 1.7). In syndecan 1 and 3 the GAG attachment sites occur in two distinct clusters, one near the N-terminus, and the other near the membrane attachment site, separated by a proline-and-threonine rich 'spacer'. The transmembrane and cytoplasmic domains are highly conserved whereas the ectodomains show little homology except in the regions of glycanation by HS. (Bernfield *et al.*, 1992; Carey, 1997) .

Based on similarities within these regions syndecans 1 and 3, and syndecans 2 and 4, can be considered as subfamilies (Carey, 1997). The cytoplasmic domains contain a 13 amino acid segment (designated C-1) immediately following the transmembrane domain that is identical in all vertebrate and invertebrate syndecans. All syndecan core proteins also contain an identical tetrapeptide (EFYA) sequence at their C-terminal ends designated C-2. C-1 and C-2 are thought to confer key syndecan functions such as signalling and/or core protein oligomerisation (Woods *et al.*, 1998). The C-1 region of

	EXPRESSION PATTERNS OF VERTEBRATE SYNDECANS
Syndecan-1	Fibroblastic and epithelial cells (esp keratinocytes), embryonic mesenchyme, skin, liver, kidney, lung
Syndecan-2 (Fibroglycan)	Non-epithelial cells - endothelial, neural and fibroblastic cells, liver
Syndecan-3 (N-syndecan)	Neural cells, endothelial cells, primitive mesenchymal cells, brain, heart
Syndecan-4 (ryudocan /amphiglycan)	Most cell types - epithelial, endothelial, fibroblastic, neural cells Liver, kidney, brain, lung

	EXPRESSION PATTERNS OF VERTEBRATE GLYPICANS
Glypican –1	Developing and adult brain, kidneys, perichodrium
Glypican –2	Developing nervous system
Glypican –3	Developing intestine and mesoderm-derived tissues
Glypican –4	Blood vessels, kidney, brain, adrenal cortex
Glypican –5	Developmentally regulated expression in kidney, limb, brain, adult brain
Glypican –6	Smooth muscle cells of major blood vessels, mesenchymal cells of intestine, kidney, lung, tooth and gonad in development

Table 1.6 : Expression patterns of membrane heparan sulphate proteoglycans.

(David *et al.*, 1993; Kim *et al.*, 1994; Veugelers *et al.*, 1999)

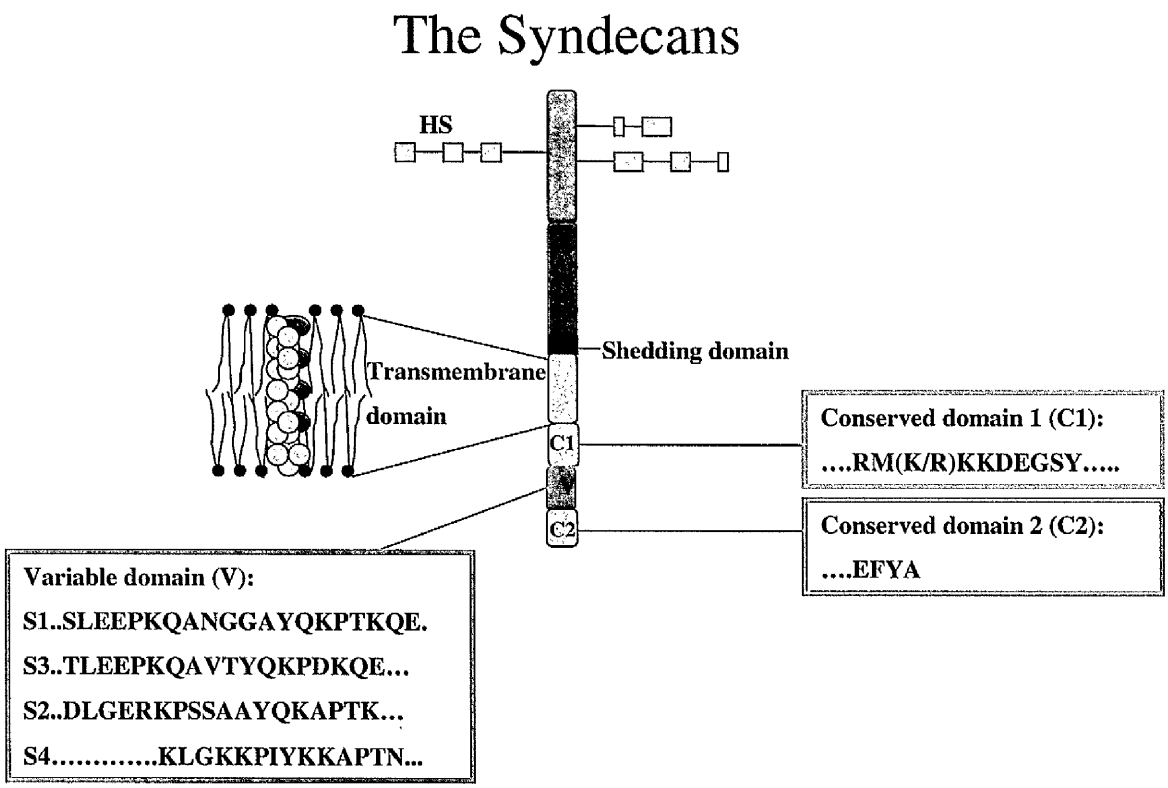

Figure 1.7 : Syndecan core protein structure. The extracellular domains of the four vertebrate syndecans conatin several sites for heparan sulphate attachment. Shedding occurs at a site proximal to the plasma membrane. The transmembrane domain is highly conserved among the family members and contains an unusual motif of glycine/alanine that aligns on one face of the domain in the outer membrane leaflet. The cytoplasmic domains contain regions (C1 and C2) that are exactly conserved in each of the four syndecans (the exception being a conservative substitution of arginine for lysine in syndecan-2). These flank a central variable (V) region that is distinct for each family member. *Adapted from Rapraeger, 2001*

syndecan-3 interacts with members of the src/cortactin signaling pathway (Kinnunen *et al.*, 1998) and the sole serine present in this region of syndecan 4 is dephosphorylated in response to bFGF (Horowitz & Simons, 1998). The FYA sequence of C-2 interacts with PDZ proteins including CASK/Lin-2, and the syntenin adaptor protein that couples syndecans to cytoskeletal proteins or cytoplasmic downstream signalling effectors (Grootjans *et al.*, 1997; Rapraeger, 2001).

Between C-1 and C-2 there is a highly variable (V) region that is conserved across species for each syndecan type (Carey, 1997). This region may confer unique properties. For example, syndecan-4 co-operates with integrins and ECM proteins such as fibronectin in formation of specialised cell-matrix contact points called focal adhesions (Woods *et al.*, 1998) and the peptide sequences within the V region of syndecan 4 regulate the distribution and activity of PKC in focal adhesions (Oh *et al.*, 1997; Oh *et al.*, 1998). In addition, V-region phosphorylation has been implicated in the assembly of matrix components fibronectin and laminin by syndecan-2, that is independent of integrins, and not demonstrated by other syndecan members (Itano *et al.*, 1996; Klass *et al.*, 2000).

Syndecan-1 is induced in endothelial cells that form the neovasculature of granulation tissue during wound healing (Elenius *et al.*, 1991; Gallo *et al.*, 1996) and enhanced syndecan 3 expression is associated with stromal blood vessels in hepatocellular carcinoma (Roskams *et al.*, 1998). These altered expression patterns are thought to mirror changes in ligands that require syndecans for their activities (Bonneh-Barkay *et al.*, 1997) and the recent demonstration that syndecan-1 is essential for wnt-1 induced mammary tumourigenesis in mice (Alexander *et al.*, 2000) provides direct evidence for a role of this HSPG in growth factor signalling. Interestingly, syndecan-4 deficient mice are viable, fertile, and develop normally but they exhibit defective wound healing with impaired angiogenesis (Echtermeyer *et al.*, 2001). This has been attributed to a defect in cell migration due to altered cell-matrix interaction but a ligand is not yet assigned.

In experimental studies of cancer, syndecan-1 expression is associated with maintenance of epithelial morphology, anchorage-dependent growth and inhibition of invasiveness (Inki & Jalkanen, 1996). Immunohistochemical studies reveal

downregulation of syndecan-1 in many of the commonest epithelial tumours and correlation of this with reduced survival (Blackhall *et al.*, 2001) Since loss of syndecan-1 is thought to be an early genetic event (Soukka *et al.*, 1997) it has been proposed as a tumour suppressor with a usual role in maintaining adhesion and preventing cellular migration (Sanderson, 2001) .

The breakdown products of syndecans also exhibit distinct physiological roles. Syndecans are shed from the cell surface as soluble molecules (ectodomains) that regulate protease and GF activity (Bernfield *et al.*, 1999). In contrast to their cell surface precursors, S1 ectodomains inhibit bFGF signalling. In turn, heparanase reverses the inhibitory activity of shed ectodomains by liberating fragments of HS that activate bFGF (Kato *et al.*, 1998). These mechanisms are believed to 'fine tune' GFs recruited for tissue repair and remodelling. Enhanced shedding of S1 is observed in cancer but its role is poorly understood (Stanley *et al.*, 1999). An intriguing property of S1 ectodomains is that they inhibit growth of various cancer cell lines *in vitro* (Mali *et al.*, 1994) and S1 ectodomains shed from myeloma cells induce apoptosis of myeloma allografts in SCID mice (Dhodapkar *et al.*, 1998). In clinical studies of multiple myeloma serum S1 is an independent prognostic indicator with 'high' levels conferring an adverse prognosis (Seidel *et al.*, 2000). A further property of shed S1 ectodomains is their ability to modulate protease and antiprotease activity. For example, elastase is protected from inactivation by its plasma-derived inhibitor, the serpin α1-antiprotease in acute dermal wound fluid (Kainulainen *et al.*, 1998). Thus, there are various roles that syndecans may play in angiogenesis and further definition is required.

The glypican family of GPI-anchored proteoglycans

Six glypican family members (glypican-1 - 6) have been identified in vertebrates. They are thought to have arisen from a series of gene and genome duplications since the GPC3/GPC4 genes cluster on chromosome Xq26 and the GPC5/GPC6 genes cluster on 13q32. Based on similarities in sequence and gene organisation, glypican-1, -2, -4 and –6 appear to define a subfamily of glypicans that differs from the subfamily comprising so far glypican-3 and glypican-5 (Veugelers *et al.*, 1999). The structures of individual glypicans are highly conserved across species (for example, human and mouse glypican-6 share 96% identity) suggesting specific roles.

The core proteins of all glypicans are roughly similar sizes (60kDa) and contain Ser-Gly repeats in their C-termini that compose sites for substitution with HS. An important distinction between the syndecans and glypicans is that the glycanation sites (usually 2-3) for HS attachment are located close to the cell membrane (Yanagishita & Hascall, 1992). In addition, all glypicans, including the glypican encoded by the *dally* gene in *Drosophila,* attach to the cell membrane via a glycophosphatidyl-inositol (GPI) anchor and share conservation of a unique pattern of 14 cysteine residues (David *et al.*, 1990; DeCat & David, 2001; Filmus *et al.*, 1995; Nakato *et al.*, 1995) (Figure 1.8).

The HS chains attached to the glypicans often share the ligand binding properties of the syndecans and ECM PGs (Bonneh-Barkay *et al.*, 1997) but the core protein characteristics are assumed to confer different signalling properties. The GPI-anchor may confer greater mobility in the cell membrane and in polarised cells it may serve to direct glypican to the apical surface. Many GPI-anchored proteins are concentrated to caveolae, specific plasmalemmal structures believed to be involved in endo-transcytosis and signaling (for review, see Anderson, 1998). All glypicans are highly expressed during embryonic development in tissue specific patterns (Table 1.6) and, like the syndecans, the expression patterns of glypicans often coincide with those of growth factors, such as FGFs and BMPs, and their receptors (Bonneh-Barkay *et al.*, 1997).

Genetic evidence for HSPGs in growth factor regulation

Studies in *Drosophila* provide the first direct evidence that a single glypican (*dally*) is capable of affecting patterning mediated by a growth factor during development and that other PGs cannot substitute for its absence. Mutations in *dally* affect cell division in the *Drosophila* visual system and lead to morphological defects in the eyes, antenna, genitalia, and wings (Nakato *et al.*, 1995). *Drosophila dally* influences patterning by affecting the activity of two known HS-binding growth factors, *Decapentaplegic* (Dpp), the transforming growth factor-β-related morphogen (Jackson *et al.*, 1997) and *Wingless* (Wg), a *Drosophila* wnt (Reichsman *et al.*, 1996). The findings support a model in which PGs enhance the activity of growth factors at the cell surface by promoting the assembly of signalling complexes (Selleck, 2000).

The ability of *dally* to enhance Dpp as well as Wg signalling raises a question about the specificity of HSPGs in modulating growth-factor signalling. Interestingly, during

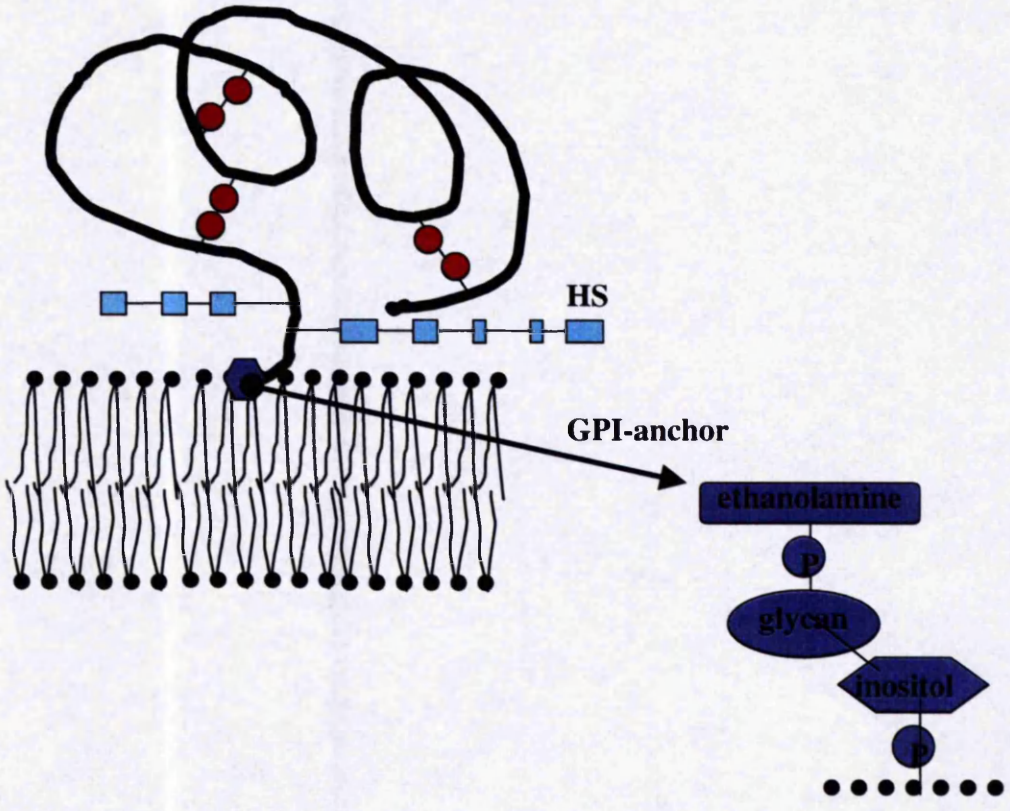

Figure 1.8 : Schematic representation of the glypicans. The glypican core protein locates completely in extracellular or luminal compartments. Numerous disulphide bridges organise the core protein as a highly compact globular domain. HS chains are covalently bound to serine residues that form part of Ser-Gly-X-Gly motifs in the polypeptide chain. The protein is covalently linked to the plasma membrane at its carboxyterminus, via a GPI anchor. The glycan component of the GPI anchor consists of a trimannose-glucosamine core. *Adapted from DeCat and David, 2001*

genitalia development in *Drosophila, dally* affects Dpp and not Wg signalling, whereas in the embryonic epidermis, *Dally* influences Wg but not Dpp-directed patterning. While the molecular mechanism of these differential activities of *Dally* is not known, it is apparent that a PG can serve as a tissue-specific modulator of a growth-factor signalling pathway. This property may be determined by the HS chain so that the structure of the chain regulates participation in one signalling pathway or another (Perrimon & Bernfield, 2000; Selleck, 2000).

Glypican 3 – a negative regulator of cell growth

The glypican-3 knockout mouse exhibits developmental overgrowth, perinatal death, cystic and dysplastic kidneys and abnormal lung development (Cano-Gauci *et al.*, 1999). The phenotype resembles that of human Simpson-Golabi-Behmel syndrome (SGBS) , an X-linked syndrome characterised by pre- and post-natal overgrowth and an increased frequency of embryonal tumours such as Wilm's tumour of the kidney and neuroblastoma. SGBS is due to mutations in the glypican-3 gene (GPC3) (Pilia *et al.*, 1996) and is the first inherited syndrome to involve a HSPG, confirming the critical role of this PG in vertebrate morphogenesis. Consequent defects in GF signalling pathways, are believed to account for the abnormalities in SGBS (Veugelers *et al.*, 1999) and possible candidate pathways include insulin-like growth factor 2 (Pilia *et al.*, 1996) and bone morphogenetic protein 4 (BMP4) (Paine-Saunders *et al.*, 2000).

A tumour suppressor role for GPC3 has been proposed due to the incidence of embryonal tumours in SGBS, and ability of GPC3 to induce cell line specific apoptosis (Gonzalez *et al.*, 1998). The mechanism of apoptosis is independent of glycosylation which, uncharacteristically, suggests a direct interaction between a ligand and the core protein rather than the HS chain (Filmus, 2001). Loss of GPC3 has also been implicated in sporadic cancers (see Filmus, 2001 for review) although it is not yet clear whether GPC3 suppression is a primary oncogenic or downstream event, possibly conferring a more invasive phenotype.

Glypicans and angiogenesis

Few studies have directly examined the role of glypicans in angiogenesis although glypican-1 is known to regulate FGF family members. In keratinocytes glypican-1 inhibits the mitogenic response to FGF-7 (KGF) while enhancing the response to FGF-1

(aFGF) (Bonneh-Barkay *et al.*, 1997). Glypican-1 may have a specific role in the regulation of $VEGF_{165}$, a widely expressed angiogenic promoter that signals through the tyrosine kinase receptors KDR and flt-1. Glypican-1 can restore binding of $VEGF_{165}$ to KDR and flt-1 expressed by human umbilical vein endothelial cells (HUVEC) denuded of cell surface HS and restores the receptor binding ability of oxidised $VEGF_{165}$ suggesting a role for this HSPG as an extracellular chaperone (Gengrinovitch *et al.*, 1999). In addition to this putative role in potentiating VEGF mediated angiogenesis, a recent study has proposed glypican-1 as a low affinity co-receptor for endostatin (Karumanchi *et al.*, 2001). This would suggest that glypican-1 may either stimulate or inhibit angiogenesis depending on the ligand. However, neither study convincingly excluded the ability of other HSPGs to bind these proteins and structure-function relationships require further exploration before glypican-1 can be assigned as the key PG coordinating the activities of $VEGF_{165}$ and endostatin.

HSPGs of the extracellular matrix – distinct roles in angiogenesis

The ECM is a dynamic continuum of protein and PG complexes that imparts shape and form to organs and tissues and profoundly influences the activity of cells associated with it. The ECM provides structural or adhesive support, growth factor sequestration, and regulation of cell growth, differentiation, and morphogenesis. Proteinaceous ECM components include fibronectin, laminins, vitronectin, and collagens, many of which bind to various $\alpha\beta$ integrins and elicit intracellular signals (Giancotti & Ruoshlati, 1999). Basement membranes (BM) are specialised zones of ECM that perform essential mechanical and signalling roles in development (Erickson & Couchman, 2000).

The HSPGs found in the ECM/BM such as perlecan and agrin are large modular proteins, that contribute to the structure, hydration, and permeability of the matrix (Figure 2) (Noonan *et al.*, 1991; Tsen *et al.*, 1995). Collagen XVIII is a recent addition to the ECM PG family with the discovery that it is invariably substituted with HS chains (Halfter *et al.*, 1998) (see later section). Experimental data support a role for perlecan in the promotion of angiogenesis and collagen XVIII encodes the potent angiogenic inhibitor, endostatin (O'Reilly *et al.*, 1997). Other matrix proteins also encode cryptic fragments that modulate angiogenesis. For example, arresten (Table 1.2) is a heparin binding angiogenic inhibitor derived from collagen type IV implicating the BM as a key modulator of angiogenesis (Colorado *et al.*, 2000).

Perlecan

The best characterised ECM HSPG is perlecan (Iozzo *et al.*, 1994; Noonan *et al.*, 1991; Olsen, 1999), so-named because of its 'beads on a string' appearance when imaged by electron microscopy. It is produced by Engelbreth Holm Swarm tumour and has been used experimentally as a prototype for the BM HSPGs but is also found in close association with chondrocytes in cartilage matrix. Perlecan is one of the largest gene products known (400 KDa) and is organised into five domains (Figure 1.9). The amino terminus (domain 1) bears 2-3 HS chains and the other domains include regions that are homologous to the LDL receptor, the laminin A chain, immunoglobulin-like repeats, and epidermal growth factor (Olsen, 1999).

Perlecan spans the BM and, in addition to binding proteins via its HS chains, the protein domains interact with multiple ligands including collagen type IV, nidogen 1, FGF-7, fibronectin, heparin, laminin-1, PDGF-BB, integrins and FGF-binding protein, a modulator of FGF-2 activity (Iozzo *et al.*, 1994). Embryos homozygous for a null mutation in the perlecan gene are normal at embryonic day 10 (E10), suggesting that perlecan is not critical for BM assembly (Timpl & Brown, 1996). However, between E10 and E12, most embryos die of cardiac arrest, at the stage when intraventricular blood pressure is thought to increase. There is evidence of bleeding into the pericardial sac and loss of normal BM structure around myocardial cells. Embryos that survive this critical period develop lethal brain defects, including exencephaly, and die perinatally. These abnormalities have been attributed to stress sensitivity of BMs (Costell *et al.*, 1999).

An unexpected finding in embryos surviving the cardiac crisis period is that of skeletal defects including striking abnormalities in the growth plates of long bones. An abnormal fibrillar collagen network is observed and altered expression of other cartilage ECM genes. This implicates perlecan in cartilage growth and endochondral ossification but its role is uncertain. It may protect the ECM of cartilage from proteolytic degradation (Costell *et al.*, 1999) and/or may modulate signalling pathways for growth and differentiation. Candidates include the FGF family since FGFR3 is a negative regulator of chondrocyte proliferation and hypertrophy (Deng *et al.*, 1996) and Indian hedgehog (Ihh), which regulates chondrocyte maturation by controlling the expression of parathyroid hormone-related peptide (PTHrP) (Olsen, 1999).

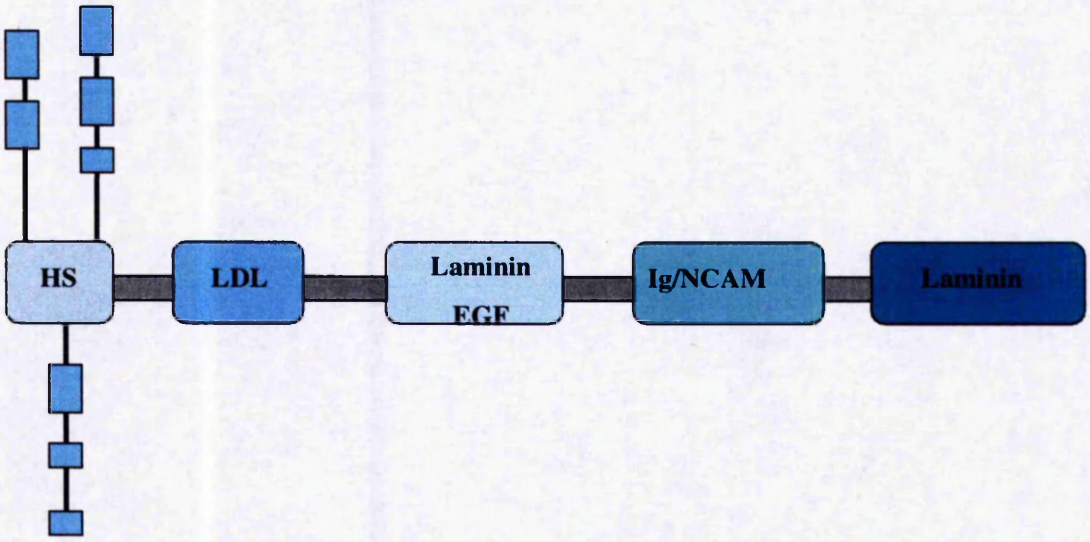

Figure 1.9 : The domain structure of perlecan. The 400-450 kDa core protein of perlecan has several distinct protein modules that are organised in five domains. The attachment sites for heparan sulphate (HS) are in domain I at the amino terminus. *Adapted from Olsen, 1999.*

Interestingly, perlecan mutations have recently been attributed to the human Schwartz-Jampel syndrome (chondrodystrophic myotonia) (Nicole, 2000). These patients have a myotonic phenotype (failure of muscle relaxation) and skeletal dysplasia (reduced stature, kyphoscoliosis, bowing of the diaphyses and irregular epiphyses) but do not show craniofacial abnormalities nor lethal heart defects. The perlecan mutations include missense and splicing mutations that generally give rise to a truncated protein in which the N terminus bearing HS chains is retained. It is not yet known whether these HS chains can still bind and effect the functions of ligands normally in the absence of full length perlecan, nor whether mutations in the N-terminus, that lack HS, produce a different phenotype.

Perlecan modulates angiogenesis

In development perlecan is expressed early in tissues of vasculogenesis. It is deposited along all endothelial-lined vascular beds, both fenestrated and non-fenestrated, and this correlates with the onset of tissue differentiation (Handler *et al.*, 1997). In adults, perlecan expression is upregulated at sites of tissue remodelling and active angiogenesis. Increased perlecan levels are detected surrounding blood vessels in invasive breast carcinomas (Iozzo *et al.*, 1994), hepatocellular carcinomas (Roskams *et al.*, 1998), and human prostate cancer xenografts deposit human perlecan along the BM of newly formed murine vessels (Iozzo *et al.*, 1994).

Perlecan is believed to sequester and protect GFs such as bFGF from proteolytic degradation (Bernfield *et al.*, 1999; Chang *et al.*, 2000). The action of tumour heparanases on the HS chains in concert with proteases such as the matrix metalloproteases is one mechanism by which tumour cells bring about the generation of bioactive molecules, released from perlecan, at sites of invasion (Vlodavsky *et al.*, 1999; Whitelock *et al.*, 1996). A signalling role for perlecan has also been proposed since perlecan, but not syndecan or glypican, promotes binding of bFGF to HS-deficient CHO cell mutants engineered to express FGFR-1 (Aviezer *et al.*, 1994b) and can stimulate angiogenesis *in vivo* (Aviezer *et al.*, 1994a). However, in the latter experiment the cooperation of other HSPGs could not be excluded and the former findings may be peculiar to the CHO cell mutants. Nevertheless, inhibition of endogenous perlecan levels suppresses autocrine and paracrine functions of bFGF in human melanoma cells (Aviezer *et al.*, 1997), blocks melanoma cell proliferation and

invasion (Adiata *et al.*, 1998) and inhibits tumour growth and neovascularisation in human colon carcinoma cell and mouse melanoma cell xenografts (Sharma *et al.*, 1998). In contrast, suppression of perlecan in fibrosarcoma cells leads to stimulation of their growth that is independent of FGF-2 (Mathiak *et al.*, 1997), reinforcing the concept that HSPG mediated effects are cell and GF-specific.

Collagen XVIII

The collagens comprise a family of structurally related proteins and in vertebrate tissues, there are at least 20 genetically distinct types (I-XX) based on the order of their discovery, comprising more than 30 different α chains. They are composed of one or more triple helical sequences with a repeated Gly-Xaa-Yaa motif and there are two major groups. The fibril-forming collagens (types I,II, III, V, and XI) are characterised by long and uninterrupted repetition of the Gly-Xaa-Yaa sequence. In contrast, the non-fibril-forming (IV, VI-X, and XII-XIX) exhibit one or more interruptions in the collagenous sequence and are heterogeneous in structure, macromolecular organization, tissue location, and function (see Prockop & Kivirikko, 1995 for review).

Collagen XVIII was initially identified by screening cDNA libraries with probes for collagen-like proteins (Abe *et al.*, 1993; Oh *et al.*, 1994b; Oh *et al.*, 1994) and found to be highly homologous with type XV collagen (Rehn & Pihlajaniemi, 1994). Collagen XV and XVIII are homotrimers that share 200 residues of sequence homology in the N-terminus corresponding to the N-terminus of thrombospondin-1, and 7 homologous triple-helical collagenous domains that are separated and flanked by non-triple-helical / non-collagenous (NC) domains. Due to a domain structure that differs from other collagens, they have been assigned to a novel subgroup termed MULTIPLEXINS (multiple triple helix domains with interruptions) (Oh *et al.*, 1994). In contrast to many other collagens that are rigid and inextensible with one large triple-helix domain, the interruptions of collagen XVIII probably allow for flexibility between triple helical regions (Figure 1.10). The human genes are encoded by chromosome 9q21-q22 for α1(XV)collagen (Huebner *et al.*, 1992) and chromosome 21q22.3 for α1(XVIII) collagen (Oh *et al.*, 1994b) and their genomic organisation suggests a common ancestor (Hagg *et al.*, 1998). Collagen XV and XVIII are both secreted by endothelial cells (Kivirikko *et al.*, 1995; Muragaki *et al.*, 1995) and are widely distributed in BMs, including those of the endothelium, epidermis, kidney, lung, liver, peripheral nerves,

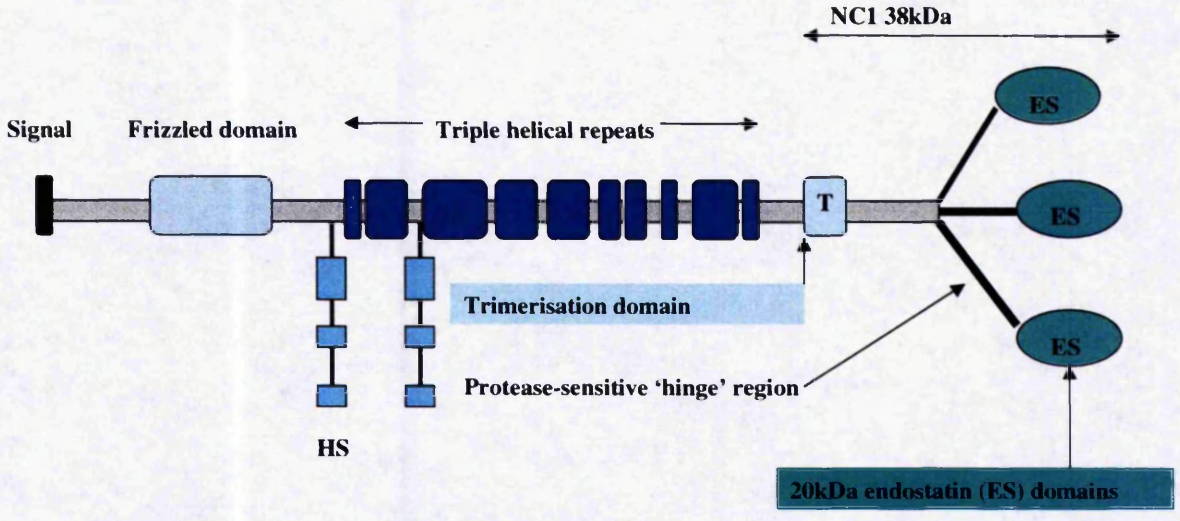

Figure 1.10 : Schematic representation of type XVIII collagen. Endostatin is a proteolytic fragment of the NC1 domain of collagen XVIII. The domain structures include a signal peptide, triple helical collagenous repeats and a region with frizzled homology that is removed by alternative splicing in non-hepatic tissues. HS attaches to consensus sequences in the non-collagenous domains. The NC1 domain comprises a protease-sensitive 'hinge' region interposed within the trimerisation and the globular endostatin (ES) domains. *Adapted from Kuo et al, 2001.*

and brain (Hagg *et al.*, 1997; Muragaki *et al.*, 1995; Musso *et al.*, 2001; Oh *et al.*, 1994b; Rehn & Pihlajaniemi, 1994; Rehn & Pihlajaniemi, 1995; Saarela *et al.*, 1998b; Saarela *et al.*, 1998a; Sasaki *et al.*, 1998). Notably, collagen XV expression is enhanced in muscle tissue compared to collagen XVIII and the converse is true in liver (Hagg *et al.*, 1997; Muragaki *et al.*, 1995; Rehn & Pihlajaniemi, 1994) suggesting that different mechanisms regulate their expression (Hagg *et al.*, 1998). The functions of multiplexins have attracted increased interest since the discovery of endostatin, a 20kD fragment (184 amino acids) of the C-terminal NC1 domain of collagen XVIII. Indeed, this is the most homologous region of collagen XV and collagen XVIII; and restin, the endostatin homologue of collagen XV, is also an inhibitor of angiogenesis (Ramchandran *et al.*, 1999).

Due to the potent antiangiogenic activity of endostatin, and their expression patterns, putative functions of collagen XV and XVIII include a role in vascular assembly. However, the collagen XVIII knockout mouse appears to develop normally with no vascular abnormalities (O'Reilly *et al.*, 1997). Mice with a null mutation in collagen XV also develop and reproduce normally with no apparent abnormalities during the first months following birth. In particular, the number of vessels and vascular architecture does not differ from the wild type. However, with increasing age beyond 3 months collagen XV deficient mice develop functional changes in the myocardium exacerbated by increased workload, and focal changes in skeletal muscle characteristic of myopathy. Ultrastructural analysis of these tissues reveals collapsed capillaries and endothelial cell degeneration whereas these vascular abnormalities are absent in tissues such as the lung and brain where capillary associated collagen XV is sparse. This may indicate a tissue-specific structural role for coll XV in stabilising muscle cells and microvessels (Eklund *et al.*, 2001). In addition, the data reinforce that collagen XV and XVIII are distinct, despite extensive homology.

Collagen XVIII is a HSPG

The overall homology between the mouse and human α1(XVIII) collagen chains is high (79% identity) and most marked in their C-terminal NC domains that encode endostatin (85% identity, 99% homology) (O'Reilly *et al.*, 1997). Characterisation of mouse collagen XVIII has demonstrated 3 variants arising from two alternate promoters that result in the synthesis of either short or long N-terminal NC domains, and the latter is

subject to alternate splicing (Muragaki *et al.*, 1995; Rehn & Pihlajaniemi, 1995). Interestingly, the longest murine α1(XVIII) chain has a motif of ten cysteine residues homologous to the extracellular part of the frizzled receptors involved in the *Wingless* signaling pathway in *Drosophila* (Bhanot *et al.*, 1996). Other putatively biologically significant motifs are an RGD sequence important in cell attachment, and within the non-triple helical regions are several ser-gly-containing sequences that conform to consensus sequences for GAG attachment sites (Pihlajaniemi & Rehn, 1995; Saarela *et al.*, 1998a).

Two human α1(XVIII) variants designated short (1336 amino acids, 136kD) and long (1516 amino acids, 154kD) have been reported with different signal peptides and N-terminal NC domains (Saarela *et al.*, 1998a). Both retain GAG attachment sequences and examination of collagen XVIII from human kidney and placenta by Western blotting and treatment with heparitinase (degrades HS) confirm substitution with HS chains in these tissues (Saarela *et al.*, 1998b). Under non-denaturing conditions collagen XVIII exists as an oligomer/trimer due to non-covalent association of core protein monomers that does not require the presence of HS (Halfter *et al.*, 1998). Members of the collagen family, such as collagen IX and XII, can carry CS side chains and exist as part-time PGs, but this is the first identified HS-substituted collagen/proteoglycan. Interestingly, collagen XV is also substituted with GAG chains of the CS class (Oh *et al.*, 1994).

Immunohistochemical and *in situ* hybridisation studies using human fetal and adult tissues demonstrate that collagen XVIII colocalises in epithelial and endothelial BM zones with the α1 and α2 chains of type IV collagen (Saarela *et al.*, 1998b). Notably, the tissue distribution of the human α1(XVIII) isoforms differs in that the long variant is detected almost exclusively in the liver sinusoids (Saarela *et al.*, 1998a). It is expressed by hepatocytes (Saarela *et al.*, 1998b) and the promoter of the long variant has subsequently been shown to contain liver-specific regulatory elements (Lietard *et al.*, 2000). In a recent study of hepatocellular carcinomas, tumours expressing high levels of the α1(XVIII) long variant were smaller, with lower microvessel density, and recurred earlier following resection of the primary tumour (Musso *et al.*, 2001). However, further studies are required to demonstrate the extent to which this association may be causal.

1.4 Endostatin – a natural cleavage product of collagen XVIII

Endostatin was initially detected in the conditioned media from a non-metastatic murine haemangioendothelioma cell line (EOMA) (Obeso *et al.*, 1990) during a screen for novel antiangiogenic factors. When this media was applied to bovine capillary endothelial cells that had been stimulated with bFGF a potent inhibitory activity was observed (O'Reilly *et al.*, 1997). Subsequent purification (by heparin affinity) and characterisation, distinguished it from previously identified inhibitors such as angiostatin (O'Reilly *et al.*, 1994) and partial amino acid sequencing of endostatin from EOMA culture media revealed sequence homology with the C-terminal fragment of collagen XVIII as outlined above (O'Reilly *et al.*, 1997).

The proteolytic mechanisms by which endostatin is cleaved from collagen XVIII are currently being elucidated. Structural analyses of the recombinant 38kDa C-terminal NCI domain of murine α1(XVIII) suggest that it consists of three main regions: a 5 kDa N-terminal association domain that induces trimerization, a central protease-sensitive hinge region and the C-terminal 22 kDa endostatin domain (Sasaki *et al.*, 1998). Examination of the EOMA cell cultures confirmed production of collagen XVIII and proteolytic activities responsible for generation of endostatin (Felbor *et al.*, 2000). Procathepsin L is activated to cathepsin L in a slightly acidic medium that generates endostatin from collagen XVIII. Cysteine protease inhibitors block generation of collagen XVIII and EOMA cells also secrete matrix metalloproteases (MMPs) that produce a larger, 30kDa endostatin containing fragment in a parallel processing pathway (Felbor *et al.*, 2000).

The hinge region is also sensitive to elastase but this has not been confirmed *in vivo* (Wen *et al.*, 1999). Nevertheless, both NC1 and endostatin circulate in human plasma and exist in human tissues, notably lung and liver, suggesting that both exist as physiological cleavage products that may also be glycosylated (Sasaki *et al.*, 1998). Crucially, NC1 domains oligomerise noncovalently into trimers through their association domain, whereas endostatin remains monomeric (Kuo *et al.*, 2001; Sasaki *et al.*, 1998).

Endostatin – a heparin binding inhibitor of angiogenesis ?

Endostatin inhibits endothelial cell proliferation, migration and angiogenesis both *in vitro*, and *in vivo* (O'Reilly *et al.*, 1997; Yamaguchi *et al.*, 1999). It induces apoptosis of appropriately stimulated endothelial cells *in vitro* (Dhanabal *et al.*, 1999) and treatment of experimental tumours in mice with endostatin can result in tumour regression and dormancy (Boehm *et al.*, 1997; O'Reilly *et al.*, 1997). Endostatin is currently in early (Phase I) clinical trials, however its mechanism of action is unknown.

Endostatin was originally found to elute between 0.4 and 0.6M NaCl from heparin-sepharose during purification indicating a moderate heparin affinity and suggesting a physiological interaction with HS (Hohenester *et al.*, 1998; O'Reilly *et al.*, 1997). The primary sequence revealed conservation of basic arginine residues (11 in the human sequence and 14 in the mouse) and three-dimensional analysis of the 22 kDa endostatin fragment by x-ray crystallography at 1.5Å resolution revealed a compact molecule (Hohenester *et al.*, 1998) with a large basic binding patch of arginine residues constituting a putative heparin binding site (Figure 1.11).

Mutagenesis of key arginine residues (R158/R270) reduced the affinity of endostatin for heparin and this correlated with inability to inhibit bFGF in the chick embryo chorioallantoic membrane (CAM) assay of angiogenesis (Sasaki *et al.*, 1999). Crystal structure analysis of human recombinant endostatin also revealed a zinc ion near the N-terminus (Ding *et al.*, 1998). It was initially reported that zinc-binding was essential for the anti-angiogenic mechanism of endostatin (Boehm *et al.*, 1998) but later studies, including mutagenesis of the zinc-binding site failed to confirm this (Sasaki *et al.*, 1999; Yamaguchi *et al.*, 1999).

Following the first reports of the bioactivity of endostatin by O'Reilly *et al.*,1997, the antiproliferative effect of endostatin proved difficult to replicate by other groups (Yamaguchi *et al.*, 1999). Varying solubility and unfolding of protein depending on the system used for expression of recombinant proteins, and deterioration of endostatin in transit were attributed (Zatterstrom *et al.*, 2000). However, the proliferation assay was superseded by a migration assay that observed antagonism of VEGF induced endothelial cell migration, rather than bFGF induced endothelial cell proliferation. In

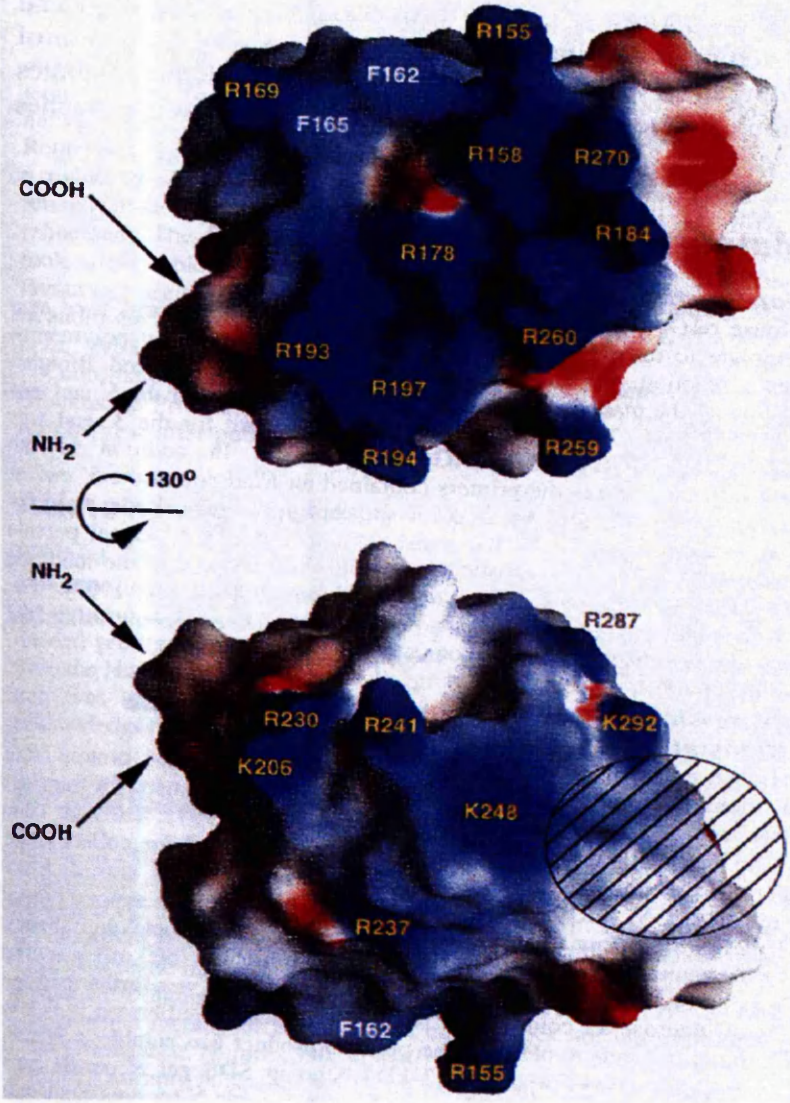

Figure 1.11 : Electrostatic surface representation of endostatin. Endostatin is a 20kD protein with conserved arginine residues in murine (14) and human (11) sequences and the crystal structure predicts an external position of these residues in a putative heparin-binding domain. Blue indicates regions of positive potential and red regions of negative potential. The hatched box defines a region that corresponds to the oligosaccharide – binding site of the C-type lectin carbohydrate recognition domain (Hohenester *et al.*,1998)

this assay the endostatin mutants with decreased heparin affinity did not differ from the native protein (Yamaguchi *et al.*, 1999) and this non-heparin dependent effect of VEGF inhibition was also observed in the CAM assay (Sasaki *et al.*, 1999). Although these reports have questioned the role of heparin in the mechanism of action of endostatin, it is possible that both heparin-dependent and heparin-independent mechanisms exist (see below, and discussed in Chapter 7).

In addition to binding HS, endostatin binds to matrix proteins such as sulphatides, fibulins, perlecan and laminin-1 (Sasaki *et al.*, 1998; Sasaki *et al.*, 2000). This may explain why endostatin can still bind to tissue sections from which GAGs have been eliminated using degradative enymes (heparinases)(Chang *et al.*, 1999) and does not exclude a function for HSPGs. Interestingly, a signalling receptor for endostatin has not yet been identified. However, tyrosine kinase (TK) activity has been shown to mediate endostatin induced apoptosis via the shb adaptor protein, but only if the heparin binding site is intact (Dixelius *et al.*, 2000).

Endostatin also binds to integrins of endothelial cells *in vitro* and modulates adhesive and migratory cellular responses (Rehn *et al.*, 2001). Although the ability of HSPGs to act as co-receptors or factors in TK or integrin signalling is well documented (Gallagher & Lyon, 2000), this has not been explored in these studies. Notably, the heparin binding angiogenic inhibitors fibronectin, and arresten, require the co-operative action of integrins and HSPGs to effect cell adhesion (Colorado *et al.*, 2000; Woods *et al.*, 1998). The role of heparin/HS in the regulation of endostatin is therefore open to debate.

Collagen XVIII, NC1 and endostatin – a novel autoregulatory mechanism ?

Since collagen XVIII is the core protein of an HSPG in vascular and epithelial basement membranes, a physiological role as a positive co-factor for angiogenesis, possibly together with perlecan, has been proposed (Olsen, 1999). During sprouting angiogenesis, endothelial cells release proteolytic enzymes, including cathepsin L and MMPs, that cleave peptide bonds within the protease-sensitive hinge region of the NC1 domain of collagen XVIII, and liberate endostatin. This may provide an autoregulatory loop whereby endostatin acts locally to inhibit angiogenesis and 'switches off'

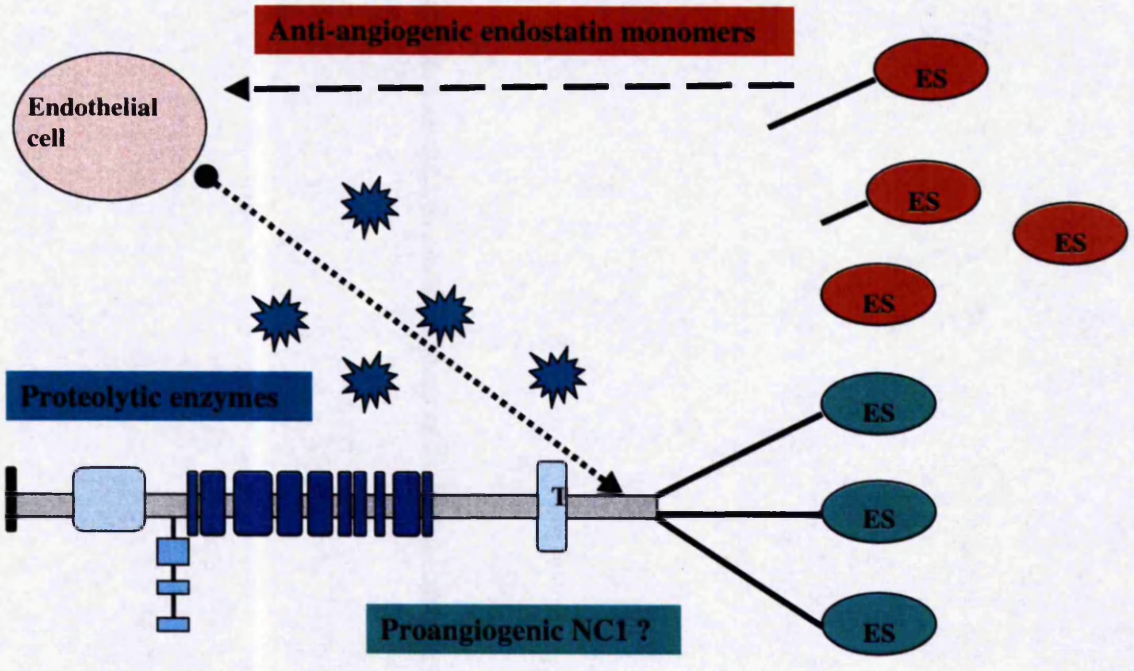

Figure 1.12 : Collagen XVIII/endostatin as a local regulator of angiogenesis. Local secretion of cathepsins and matrix metalloproteases (MMPs) by stimulated endothelial cells leads to cleavage within the protease-sensitive C-terminal hinge region of collagen XVIII. This results in release of endostatin and inhibition of angiogenesis which in turn causes a reduction in the release of cathepsins and MMPs. *Adapted from Felbor, 2000; Zatterstrom, 2000.*

stimulation of angiogenesis by collagen XVIII and or/proteases (Zatterstrom *et al.*, 2000) (Figure 1.12). Further support for a potentially antagonistic relationship between endostatin and its precursor has been derived from genetic studies. A collagen XV/XVIII homologue has been identified in the avascular nematode, *Caenorhabditis elegans*, designated *cle-1* (Ackley *et al.*, 2001). Together with collagen IV, these are the only conserved collagens between *C.elegans*, *Drosophila* and vertebrates (Hutter *et al.*, 2000; Kramer, 1997) indicating a likely fundamental role.

At the sequence level, CLE-1 is equally similar to α1(XV) and α1(XVIII) collagen. However, both *cle-1* and vertebrate collagen XVIII are expressed as three isoforms, whereas collagen XV has no identified isoforms (Muragaki *et al.*, 1995; Rehn & Pihlajaniemi, 1995). Notably, both the CLE-1 and vertebrate α1(XVIII) endostatin domains have a four-amino acid loop that is not present in α1(XV) collagen (Sasaki *et al.*, 2000). This loop contains Arg 158 that contributes strongly to the heparin-binding property of endostatin (Sasaki *et al.*, 1999). Based on these comparisons CLE-1 is most similar to collagen XVIII, except in the N-terminal domain. There is a region related to the Wingless receptor *frizzled* in α1(XVIII) collagen whereas the equivalent CLE-1 domain is related to the netrin receptor *unc-40* (Chan *et al.*, 1996). CLE-1 is broadly distributed in BMs but accumulates to highest levels in association with the nervous system. A deletion of *cle-1, cg 120* deletes the C-terminal NC1 domain resulting in expression of a stable truncated protein lacking the endostatin homologue (Ackley *et al.*, 2001). The pattern of expression is similar to the wild type except at the junctions between body wall muscles, suggesting that the NC1 domain is necessary for this localisation. Type IV collagen assembly is not affected by the *cg120* deletion, showing that general BM structure is not disrupted. However, loss of the NC1 domain causes migration defects of multiple cells and axons and a similar, but more severe, phenotype, is observed using RNA interference of *cle-1* (Ackley *et al.*, 2001).

Particular migration defects can be rescued by ectopic NC1 domain expression but not by its endostatin subdomain, or the association-hinge region. Indeed, ectopic endostatin expression in the wild-type phenocopies the *cg120* mutant by inducing similar migration defects. No effect of ectopic endostatin was observed in the *cg120* mutant suggesting that presence of NC1 is essential for endostatin activity. Together, these findings argue for a direct antagonism between NC1 and its endostatin subdomain, with

endostatin acting as a dominant negative regulator of NC1 induced cell motility (Ackley *et al.*, 2001).

Nematodes lack endothelial cells and the effects of NC1 and endostatin appear to regulate neuronal cell motility. Both neurogenesis and angiogenesis involve extensive cell migration and related mechanisms may control these processes. Neuropilin (Soker *et al.*, 1998) and HGF (Gallagher & Lyon, 2000) also affect migration of neural and endothelial cells. In addition, collagen XVIII has recently been identified as the genetic lesion in Knobloch syndrome, an autosomal recessive condition characterised by scalp and/or neural tube closure deficits and retinal degeneration (Sertie *et al.*, 2000).

Endostatin oligomers – a novel class of scatter factor ?

Antagonistic roles of collagen XVIII NC1 and endostatin have been described for endothelial cells, *in vitro* (Kuo *et al.*, 2001). On complex matrix substrates, such as matrigel, endothelial cells assemble into densely multicellular capillary-like tubular structures (Folkman & Haudenschild, 1980; Grant *et al.*, 1991). Since fibroblasts exhibit similar changes this assay best reflects ECM-induced changes in cell adhesion and morphogenesis. Recombinant human collagen XVIII NC1(a trimer) disrupts these tubular structures by inducing cell migration and activation of the MAPK signalling pathway but the effect is blocked by preincubation with endostatin (a monomer) (Kuo *et al.*, 2001). Artificially constructed recombinant dimers of the endostatin domain exactly reproduce the activity of collagen XVIII NC1, suggesting that the motogenic effect of collagen XVIII NC1 is dependent on oligomerisation of the endostatin domain (Kuo *et al.*, 2001).

Interestingly, the motogenic activity of collagen XVIII NC1 is neither replicated nor antagonised by collagen XV NC1. As outlined previously, the foremost distinction between these proteins is that the collagen XV endostatin domain (restin) does not bind heparin due to the absence of arginine 158 (Sasaki *et al.*, 2000). Also, the effects of collagen XVIII NC1 resemble the activities of HGF/scatter factor and macrophage stimulatory protein (MSP) in migration assays (Kuo *et al.*, 2001). HGF has a high affinity signalling receptor c-met, but also requires the co-operation of HSPGs to effect its cellular responses (Gallagher & Lyon, 2000). Notably, the motogenic effects of collagen XVIII NC1 require the complex matrigel matrix that is manufactured by the

Engelbreth Holm Swarm tumour and abundant in HSPG (perlecan). Neither collagen I, nor fibrin matrices support the motogenic activity of α1(XVIII) NC1 and the identity of the co-factor remains under active investigation. Together, these findings reinforce a potential role for HS in the regulation of endostatin. An intriguing concept is whether the substitution of collagen XVIII with HS chains is coincidental, or necessary for regulation of its NC1 and endostatin cleavage products. If so, this would define a novel mechanism for regulation of heparin-binding proteins by HSPGs.

1.5 Summary and Objectives

Many regulators of angiogenesis are united by their ability to bind heparin, and key stimulatory factors such as bFGF, HGF, and VEGF depend on this interaction for their biological activity (Gallagher & Lyon, 2000). Following the discovery of a specific recognition epitope for ATIII, progress in characterising other GAG-protein partnerships has been slow. This is partly because of the inherent heterogeneity of these polysaccharides and difficulty in obtaining sufficiently homogeneous quantities of binding saccharides for analysis but also due to the cumbersome sequencing technology for GAGs (Bernfield *et al.*, 1999). Indeed, the GAG-ATIII relationship remains, by far, the best defined (Conrad, 1998). Nevertheless, the last decade has witnessed significant advances in analytical tools that have accelerated understanding of GAG-mediated processes (Turnbull *et al.*, 2001). Oligosaccharide recognition sequences have been identified for a proportion of angiogenic regulators (Table 1.5). Of these, bFGF has been investigated most intensively and in all cases, the structure-activity relationships require further exploration to better define the role of HS in angiogenesis.

Among the inhibitors of angiogenesis, potent activity was demonstrated for endostatin in preclinical experiments (O'Reilly *et al.*, 1997). This also provided the first proof that anti-endothelial cell treatment is not associated with development of drug resistance (Boehm *et al.*, 1997) and endostatin is currently in clinical trial. Its mechanism of action is unknown but a role for HS has been proposed (O'Reilly *et al.*, 1997; Sasaki *et al.*, 1999; Zatterstrom *et al.*, 2000). Importantly, endostatin binds to heparin with moderate affinity via a surface patch of arginine residues that are highly conserved (Hohenester *et al.*, 1998) and required for antiangiogenic activity as demonstrated by site directed mutagenesis (Sasaki *et al.*, 1999). Although heparin released from mast

cells may play a role *in vivo* (Azizkhan *et al.*, 1980), it is HS, present on the cell surface and in the ECM, that is the principal GAG modulating the heparin-binding proteins involved in angiogenesis (Conrad, 1998). For practical reasons, most studies of GAG-protein interactions relevant to angiogenesis have utilised heparin/HS prepared from whole organs/tissues such as porcine intestine and bovine lung (Conrad, 1998). HS derived from the endothelial cells of large vessels (eg bovine aorta, human umbilical vein) has rarely been used for detailed studies. However, structural analyses of HS have demonstrated cell-type specific heterogeneity (Gallagher *et al.*, 1992) and more recently, evidence from genetic models with defects in HS biosynthesis and structure, supports the concept of tissue-specific HS function (Perrimon & Bernfield, 2000; Selleck, 2000). It is the microvessel endothelial cells that are recruited in angiogenesis but the structure of this HS has not been reported.

The initial objective of this thesis was to perform a detailed structural analysis of microvessel and macrovessel endothelial cell HS. We were interested to determine the expression of HS recognition and activation sites for angiogenic regulators and establish whether there were unique features of microvessel endothelial cell HS that could potentially be exploited in the therapeutic control of angiogenic regulators. We planned to extend standard approaches (Figure 1.3) by applying a recently developed profiling and sequencing method (Merry *et al.*,1999) to examine the S-domains in unprecedented detail. It was anticipated that this information would provide a basis from which to examine the molecular interaction between endothelial cell HS and an angiogenic regulator. Endostatin was chosen due to its potent antiangiogenic activity and its unknown mechanism of action. We aimed firstly to determine whether a specific HS recognition site for endostatin was present within endothelial cell HS. A sensitive filter binding assay was used to define the size, composition and specificity of HS derived oligosaccharides with affinity for endostatin in solution. Secondly, we wished to address the mechanism by which monomeric endostatin antagonises artificially engineered dimeric endostatin in functional assays by applying a zero-length covalent crosslinking technique to analyse the binding stoichiometries and conformations of GAG-endostatin complexes. Ultimately, it was hoped to provide novel structural information to provide a basis from which functional relationships between endostatin and HS could be examined in biological assays and extend our knowledge of the role HS plays in the coordination of angiogenesis.

2. MATERIALS

Cell culture and immunohistochemistry

Primary human neonatal dermal microvascular endothelial cells (HMVEC), endothelial cell basal medium (EBM-MV) plus bovine brain extract, epidermal growth factor, 10% fetal bovine serum, hydrocortisone , gentamicin and amphotericin-B were obtained from Clonetics at TCS Biologicals (Botolph Claydon, Buckingham, UK). Bovine corneal endothelial cells (BCE) were a gift from T Hickling (Glaxo-Wellcome, Stevenage, UK) and bovine aortic endothelial cells (BAEC) were from the Department of Medical Oncology (PICR, Christie Hospital, Manchester, UK). Dulbecco's modified eagle medium (DMEM) with sodium pyruvate, 4500g/L-glucose and pyridoxine; donor calf serum (DCS), penicillin – streptomycin and L-glutamine were from Gibco BRL (Paisley, UK). L-ascorbic acid and trypsin/EDTA were from Sigma (Poole, Dorset, UK). Gelatin (EIA grade) was from Bio-Rad (Hemel Hempstead, Hertfordshire, UK). Plasticware and dual chamber slides were from Falcon (Becton Dickinson and Co., Lincoln Park, NJ, USA). Mouse IgG, human polyclonal von Willebrand's factor, human monoclonal CD31, human monoclonal α smooth muscle actin antibodies, haematoxylin counterstain and Dako Envision+ system were from Dako (Denmark). BB4 antibody (Syndecan-1) was from Serotec (Kidlington, UK), and mouse antihuman syndecan-2 (10H4),-3 (1C7),-4 (8G3), glypican-1 (S1) and perlecan were a generous gift from G David (Leuven, Belgium). Tween 20 was from Sigma, (Poole, Dorset, UK); formaldehyde and methanol were from BDH Ltd, (Poole, Dorset, UK). Cells in culture were photographed using phase contrast microscopy (Leitz, Germany) onto black and white film (Kodak, Boots, UK) and scanned into Microsoft Photo editor, Microsoft (USA).

Metabolic radiolabelling and characterisation of heparan sulphate

D-[6-^{3}H] Glucosamine hydrochloride (20-45Ci/nmol) and $Na_2{}^{35}SO_4$ (carrier-free ;1200-1400Ci/nmol) were purchased from DuPont NEN (Boston, MA). DEAE-Sephacel was from Sigma (Poole, Dorset, UK), Sepharose CL-6B and PD-10 prepacked, disposable columns containing Sephadex G-25 were from Pharmacia Biotech (Uppsala, Sweden). Bio-Gel P10 (fine grade) and Bio-Gel P2 were from Bio-Rad (Hemel Hempstead, Herts, UK) and ProPac PA-1 analytical columns were obtained from Dionex (Camberley, Surrey, UK). Chondroitinase ABC (*Proteus vulgaris*;EC4.2.2.4) and pronase were

from Sigma (Poole, Dorset, UK). Heparinase I (*Flavobacterium heparinum*; heparin lyase, EC 4.2.2.7), heparinase II (*F. heparinum*; no EC number assigned) and heparinase III (*F. heparinum*; heparitin-sulphate lyase EC 4.2.2.8) were purchased from Grampian enzymes (Orkney, UK). β-D-glucuronidase from bovine liver (EC 3.2.1.31.) was from Sigma (Poole, Dorset, UK). Human α-L-iduronate-2-sulphatase (Bielicki *et al.*, 1993) and human α-L-iduronidase (Unger *et al.*, 1994) were purified recombinant enzymes and a generous gift from Professor John Hopwood, Adelaide, Australia. Anhydromannose containing disaccharide standards derived from heparin and radiolabelled by reduction with Na^+ boro[3]hydride were purchased from Chirazyme (Urbana, IL). Optiphase 'Hisafe' liquid scintillation cocktail (added at 3:1 v/v) was obtained from Fisher chemicals (Loughborough, UK). Human recombinant bFGF and aFGF for the filter binding assay (see below) were from R&D systems, (Abingdon, UK). All solutions were prepared using MilliQ (Millipore;Watford, UK) ultra pure water and chemicals were analar grade, BDH Ltd (Poole, Dorset, UK).

The filter binding assay and investigation of the interaction between endostatin and HS.

For the filter binding assay a vacuum assisted, manifold membrane filtration apparatus was used from Millipore (Watford, Herts, UK) with cellulose nitrate filters (pore size, 0.2μM) from Sartorius (Goettingen, Germany). Human recombinant endostatin monomer (HEM), dimer (HED), R-A mutated monomer and dimer, polyclonal rabbit anti-human endostatin antibody, monoclonal antibody (mAb)12C1 and mAb PDM were generous gifts from Dr K Javaherian and Professor J Folkman, Children's Hospital, Harvard (Boston, USA). HS and S-domains from 3T3 cell fibroblasts and HS from 2-O-sulphotransferase knockout and wild type mouse fibroblasts were obtained from Dr C Merry, Paterson Institute with kind permission. For competition assays, bovine lung heparin was kindly provided by Dr B Mulloy (National Institute for Biological Standards and Control, Hertfordshire, UK); porcine mucosal HS was obtained from Sigma (Poole, UK); De-N-sulphated/re-N-acetylated HS (loss of 92% N-sulphates), selectively de-2-O-sulphated HS (loss of 83.4% 2-O-sulphates) and selectively 6-O-sulphated HS (loss of 54.8% 6-O-sulphates, 9.6% loss of 2-O-sulphates) were prepared in house by G Rushton (Paterson Institute of Cancer Research, Christie Hospital, Manchester, UK) (Lyon *et al.*, 2000); Chondroitin sulphate C (from shark cartilage) and dermatan sulphate (chondroitin sulphate B from bovine mucosa) were

from Sigma, (Poole, Dorset, UK). Sized oligosaccharides were prepared in-house by gel filtration from low molecular weight heparin (innohep, Leo Laboratories, UK). All solutions were prepared using MilliQ (Millipore;Watford, UK) ultra pure water and chemicals were analar grade, BDH Ltd (Poole, Dorset, UK).

Two step, zero-length covalent crosslinking

Porcine intestinal mucosal heparin, heparin-agarose beads and bovine serum albumin (BSA) were from Sigma (Poole, Dorset, UK) and heparin dodecasaccharides, prepared as described above. Sephadex G50 resin was from Pharmacia Biotech (Uppsala, Sweden). The crosslinkers, EDC (1-Ethyl-3-[3-dimethylaminopropyl]carbodiimide Hydrochloride) and S-NHS (N-Hydroxysulfosuccinimide) were from Pierce (Perbio Science UK Ltd, Cheshire, UK). All other reagents and chemicals were from BDH Ltd (Poole, Dorset, UK).

SDS-PAGE and Western blotting

Acrylamide, TEMED, bromophenol blue, Tween, SDS, methanol and the semi-dry blot apparatus were from Sigma (Poole, Dorset UK). Glycine, TRIS-base, glycerol, 2-mercaptoethanol and ammonium persulphate (APS) were from BDH Ltd (Poole, Dorset, UK). The minigel electrophoresis kit and low molecular weight prestained colour markers were from Bio-Rad (Hemel Hempstead, Hertfordshire, UK). Chromatography paper was from Whatman, UK. Non-fat dried milk was from Asda stores, UK. Protran nitrocellulose transfer membrane, Schleicher and Schuell GmbH, Dassel, West Germany was obtained from Scientific Laboratory Supplies Ltd (Nottingham, UK). High performance chemiluminescence film (Hyperfilm) and enhanced chemiluminescence (ECL) detection kit was from Amersham Pharmacia Biotech (St Albans, UK).

Matrigel tube formation / morphogenesis assay

BAEC, culture media, HEM and HED were obtained as previously decribed. Tissue culture plates (24 well) were from Falcon (Becton Dickinson and Co., Lincoln Park, NJ, USA) and matrigel was from Pharmingen (Becton Dickinson UK Ltd, Oxford, UK). Plates were photographed using phase contrast microscopy (Leitz, Germany) onto black and white film (Kodak, Boots, UK) and scanned into Microsoft photo editor, Microsoft (USA).

3. METHODS

Cell culture

Bovine aortic endothelial cells (BAEC) and bovine corneal endothelial cells (BCE) were grown on 0.1% gelatin coated tissue culture flasks and maintained in 3g/l glucose (50:50 mix 1g/L and 4.5g/L) DMEM supplemented with 100 IU/ml penicillin-streptomycin, 50 μg/ml ascorbic acid and 10% DCS at 37^0C in humidified air containing 5% CO_2. Cells were used within 12 passages, the medium changed every two days and routinely subcultured in a 1:3 split ratio every 5 days. Primary cultures of human microvessel neonatal dermal endothelial cells (HMVEC) were maintained in endothelial cell basal medium (EBM-MV) supplemented with bovine brain extract, human epidermal growth factor (10ng/ml), hydrocortisone (1μg/ml), 10% fetal bovine serum , gentamicin (50μg/ml) and amphotericin-B (50ng/ml) at 37^0C in humidified air containing 5% CO_2. HMVEC were used within 9 passages, the medium changed every 2 days, and subcultured in a 1:3 split ratio every 7-10 days. For routine subculture, the medium was removed, cells were overlaid with 2-10 mls trypsin/EDTA at 37°C depending on the size of the tissue culture flask, for 3 minutes at room temperature, or until cells were observed, using light microscopy, to round up and detach with gentle agitation. The action of trypsin was inhibited by adding an equal volume of complete medium. Centrifugation was avoided due to the increased sensitivity of endothelial cells to this procedure.

Immunohistochemistry

Cells at about 80% confluence were seeded at a density of 10^5/chamber in 2 mls of complete medium for 24 hours then fixed in dual chamber slides. The medium was removed, then cells were washed twice with warm PBS before overlaying with 4% formaldehyde in phosphate buffered saline (PBS) at room temperature for 1 hour. Cells were washed extensively with warm PBS, then permeabilised where applicable, with 100% methanol at minus 20°C for 10 minutes. After further washing with PBS, cells were overlaid with PBS/Tween 20 (0.05% v/v) for 5 minutes. Endogenous peroxidase activity was blocked with 0.03% hydrogen peroxide (Dako EnVision + system) for 5 minutes then slides were washed with MilliQ water and overlaid with PBS/Tween 20. Primary antibodies were applied in total volumes of 100μl PBS for 30 minutes in the following dilutions; syndecan 1 (BB4 10μg/ml) 1:10, syndecan 2(10H4, 10μg/ml)

1:100, syndecan 3 (1C7, 10μg/ml)1:100, syndecan 4 (8G3, 10μg/ml) 1:100, perlecan (5 μg/ml) 1:50, glypican (S1, 10μg/ml) 1:100,CD31 1:50, vWF 1:50, α smooth muscle actin 1:50, mouse IgG1 1:100. Following primary antibody incubations cells were washed 3 x 10 minutes with PBS/Tween 20 then incubated with peroxidase labelled polymer conjugated to goat anti-mouse immunoglobulins in Tris-HCl buffer (Dako EnVision + system) for 30 minutes. After a further 3 x 10 minute washes cells were overlaid with a buffered substrate solution, pH 7.5, containing hydrogen peroxide and 3,3'-diaminobenzidine chromogen solution (DAB, Dako EnVision + system) for 10 minutes, then washed extensively with water before and after staining with haematoxylin counterstain and mounting.

Metabolic radiolabelling

Subconfluent cell cultures (~ 70 %) were metabolically radiolabelled by incubation with the above medium containing 10μCi [^{3}H] glucosamine hydrochloride/ml and 20 μCi $Na_2{}^{35}SO_4$/ ml for 48 hours. BAEC cultures were expanded to 20-30 x 175cm^2 flasks for radiolabelling. BCE and HMVEC cultures were expanded to 10 x 175cm^2 flasks for radiolabelling.

Extraction of glycosaminoglycans

The medium was removed from radiolabelled near confluent cultures and the remaining cell monolayers were washed twice with 0.15M NaCl, 20mM sodium phosphate buffer, pH 7.4 (PBS). The first wash was added to the pooled medium and the second discarded. To extract proteoglycans from the cell layer and matrix, the monolayers were overlaid with PBS containing 1% (v/v) Triton-X-100 detergent for 1 hour at room temperature with gentle shaking. A rubber policeman was used to scrape the matrix into the PBS / Triton-X-detergent. The cell extracts and the cell culture media were pooled and the protein cores of extracted PGs degraded with pronase at a final concentration of 100μg/ml by incubation for 4 hours at 37^{0}C. Pronase treated extracts were stored at –20^{o}C until required for further processing.

Ion – exchange chromatography

After pronase digestion, GAGs attached to small, residual peptide fragments of the protein core, were applied to a DEAE-Sephacel column (1x 5cm) pre-equilibrated with PBS and washed with 10 column volumes of PBS. Bound GAG chains were resolved

by elution from the column with a linear gradient of 0.15 to 0.825M NaCl in 20mM sodium phosphate buffer, pH7.4, at a flow rate of 15 mls/hour. 100 x 2ml fractions were collected and small aliquots taken for scintillation counting. Fractions corresponding to HS (material eluting at ~ 0.5-0.6 M NaCl) was pooled for further analysis and remaining material (non-HS GAGs) was pooled according to elution position and stored at -20^0C.

To reduce the volume of eluted samples for further analysis, material was first diluted 3:1 (v/v) with milliQ water then applied at a flow rate of 15mls / hour to a small DEAE-Sephacel column (1cm x 1cm). Aliquots of the sample before and after loading were checked for radioactivity to ensure greater than 90% binding of GAGs to DEAE-Sephacel. Bound material was step-eluted with 1.5 M NaCl, 20mM phosphate buffer, pH7.4 in 15 x 1 ml fractions. Small aliquots were taken for scintillation counting. Fractions containing radioactivity were pooled and the volume further reduced to 1ml by centrifugal evaporation.

De-salting

Salt was removed by size exclusion chromatography on a 5.1ml PD-10 column containing Sephadex G-25. Samples were applied in 0.5 ml aliquots and eluted with milliQ water in 12 x 1 ml fractions. Small aliquots were taken for scintillation counting, fractions containing radioactivity pooled, and samples lyophilised by centrifugal evaporation.

Purification of heparan sulphate

Digestion with chondroitinase ABC

Lyophilised samples were reconstituted in 50mM Tris / HCL, 50mM NaCl, pH 7.9 and incubated with 40mIU chondroitinase ABC for 24 hours at 37^0C to remove any contaminating chondroitin sulphate (CS) and dermatan sulphate (DS) present. Fragments (disaccharides) resulting from CS degradation were resolved from HS by gel filtration chromatography on a Sepharose CL-6B column (1.5 x 66 cm). Samples were eluted in 0.2 M NH_4HCO_3 at 12 mls / hour. Dextran blue and sodium dichromate were used to mark total (Vo) and void (Vt) volumes respectively. Fractions of 1ml were

collected, aliquots taken for scintillation counting and fractions corresponding to HS pooled, lyophilised and reconstituted with MilliQ water.

Peptide elimination

Residual peptide attached to HS chains was eliminated by alkaline borohydride treatment. HS chains were treated with 50mM NaOH, 1 M $NaBH_4$ at 45^0C for 48 hours. The reaction was neutralised with acetic acid using phenol red as the indicator. HS was recovered by gel filtration chromatography on a Sepharose CL-6B column using the running conditions described previously and lyophilised.

Characterisation of heparan sulphate

Estimation of chain size

The molecular size distribution of purified HS was analysed by gel filtration chromatography on a Sepharose CL-6B column using the running conditions described previously. Alternatively, when the column was not being used preparatively, material was eluted with 0.2 M NaCl, pH 8.8 at a flow rate of 12 mls / hour; fractions of 1ml were collected and monitored for radioactivity by scintillation counting.

Specific scission reagents

Nitrous acid depolymerisation was performed by the low pH method of Shively and Conrad (Shively & Conrad, 1976). Samples were dried down by centrifugal evaporation, reconstituted in 100µl freshly generated nitrous acid (1M HNO_2) and maintained at room temperature for 30 minutes. The reaction was then stopped by addition of ~ 10µl of 2M Na_2CO_3 with phenol red as the indicator.

Exhaustive enzymatic digestion with heparinase I or III was performed with two additions of enzyme (20mIU/ml) in 0.1M sodium acetate, 0.1mM calcium acetate, 1 mg/ml bovine serum albumin, pH 7.0 to samples of lyophilised HS over a minimum of 18 hours at 37^0C. To ensure that maximum depolymerisation of HS chains was achieved, non-radiolabelled heparan sulphate (from bovine kidney) was added to the digest at a final concentration of 100µg/ml and digestion was followed spectrophotometrically by monitoring the increase in absorbance at 232nm.

Products of chemical or enzymatic depolymerisation were separated according to size by gel permeation chromatography on a Bio-Gel P10 column (1cm x 140cm) eluted with 0.1M NH_4HCO_3 or 0.1M NaCl, pH 8.8 at a flow rate of 4mls/hour. Bovine haemoglobin and sodium dichromate were used as Vo and Vt markers respectively. Fractions of 1ml were collected and the radioactivity present in each was assessed by scintillation counting. Alternatively, for preparative experiments, aliquots of fractions were checked for scintillation counting and peaks of interest pooled, volume-reduced and de-salted as outlined previously. Products of heparinase I digestion were also analysed by Sepharose CL-6B chromatography using the running conditions outlined previously.

Calculation of susceptible linkages

The proportion of glycosidic linkages susceptible to each of the three scission reagents used were calculated from the formula :

% susceptible glycosidic linkages = $\Sigma(An/n)$ / total [^3H] x 100

where An is the number of ^3H counts in the area under a peak for an oligosaccharide of length, n disaccharides (Turnbull *et al.*, 1992). Information regarding the arrangement of susceptible linkages within the intact polymer can also be derived with this formula. It can be deduced that disaccharide products will result from scission of susceptible glycosidic linkages occurring in contiguous sequence, tetrasaccharides will result from cleavage of susceptible glycosidic linkages alternating with resistant linkages and larger oligosaccharides with six or more monosaccharide units will result from scission of widely spaced susceptible glycosidic linkages.

Disaccharide composition

Samples were completely depolymerised by combined treatment with 10µl each of heparinases I, II and III (all at 20mIU/ml) in 0.1M sodium acetate, 0.1mM calcium acetate, 1 mg/ml bovine serum albumin, pH 7.0. Heparinases I, II and III were added sequentially at time 0, 24 and 48 hours respectively to lyophilised sample containing 10µl of non-radiolabelled bovine kidney HS (100mg/ml) as a carrier at 37^{0}C for a total incubation time of 72 hours. Disaccharides were separated from resistant oligosaccharides by gel permeation chromatography on a Bio-Gel P2 column (1cm x 140cm) eluted with 0.1M NH_4HCO_3, pH 8.8 at a flow rate of 4mls/hour. 1 ml fractions were collected, small aliquots checked for scintillation counting, disaccharides pooled

and freeze dried repeatedly to remove salt. Near complete depolymerisation to disaccharides was typical so in experiments with very small quantities of HS (~3-10K cpm ^{3}H) P2 chromatography was omitted to prevent further losses. The disaccharides were then separated by SAX-HPLC using a ProPac PA-1 analytical anion-exchange column (4.8 x 250 mm). The column was first equilibrated with filtered, MilliQ water (adjusted to pH3.5 with HCl) at 1ml/min. Samples were then injected and disaccharides resolved with a linear gradient of 0-1M NaCl over 45 minutes in filtered, MilliQ water, pH 3.5. Fractions of 0.5 ml were collected, monitored for radioactivity by scintillation counting and elution positions compared to HS disaccharide standards used to calibrate the column and detected by absorbance at 232nm by the in-line UV detector in the HPLC apparatus. Peaks that did not co-elute with the disaccharide standards were assumed to represent longer resistant oligosaccharides resulting from incomplete degradation in experiments that omitted purification of disaccharides by gel permeation on Bio-Gel P2.

Purification and characterisation of S-domains

Purification of S-domains

Radiolabelled HS chains were extracted, digested with heparinase III and the enzyme resistant fragments were further purified as described previously (Pye *et al.*, 1998). Briefly, following heparinase III digestion, enzyme resistant fragments were separated by size using a Bio-Gel P10 gel filtration column (170 cm x 1 cm). Samples were eluted at 4 ml/ hour in 0.1 M NaCl, pH 8.8 and 1.0 ml fractions were collected. Aliquots were monitored for radioactivity by scintillation counting. Peaks of radioactivity were pooled separately, volume reduced by centrifugal evaporation, de-salted and lyophilised. Individual size fractionated samples could then be further purified or analysed.

S-domain profiling by SAX-HPLC

Individual size fractionated samples corresponding to dp4-dp12 were further resolved by strong anion-exchange (SAX) HPLC chromatography. Samples were applied to a ProPac PA-1 (4.6 x 250mm) column pre-equilibrated in distilled water adjusted to pH3.5 with HCl and eluted with increasing NaCl (maximum of 1.5M). Oligosaccharides were fractionated using a range of linear gradients optimised for the separation of each size group (Merry *et al.*,1999). Fractions of 0.5ml were collected and

aliquots taken for scintillation counting. Peaks of interest were pooled, de-salted and lyophilised for further analysis.

Disaccharide analysis of S-domains

Lyophilised samples, typically containing ~ 3-5K cpm of ^{3}H, were re-suspended in 0.1M sodium acetate, 0.1mM calcium acetate, pH 7.0 to which was added a combination of heparinase I and heparinase II (in that order) and 1µl cold disaccharide standards (100µg/ml) to mop up any contaminating sulphatase activity. Each digestion step lasted ~8 hours before addition of the next enzyme. All digests were at 37°C for a total of 24 hours and the digest volume did not exceed 50 µl. Following digestion, samples were separated by SAX-HPLC using a single ProPac PA-1 (4.6 x 250 mm) column as described previously.

S-domain sequencing

Partial nitrous acid scission

The step sequencing technique of Merry *et al.*,1999 was used. Each oligosaccharide is subjected to partial depolymerisation using dilute nitrous acid as described (Radoff & Danishefsky, 1985), with aliquots of the reaction being stopped at a number of time points to generate a range of intermediates of the depolymerisation process. Briefly, each oligosaccharide was lyophilised, then re-suspended in 80µl of MilliQ water to which was added 10 µl each of 10 mM $NaNO_2$ and 190 mM HCl. At each stop point (usually 30 minutes, 1 hour, 2 hours, 3 hours and 4 hours), 20 µl of 0.2 M sodium acetate, pH 5.0. All procedures and reagents were at 4°C. Aliquots were then taken for treatment with exo-enzymes (see below), or adjusted to 1 ml by addition of MilliQ water, pH 3.5 (HCl) for separation by HPLC. Products were identified using ^{3} H radiolabelled HS/heparin-derived disaccharide standards which contained reducing-terminal anhydromannose residues and the known elution positions of 3T3 fibroblast tetrasaccharides.

Lysosomal exo-enzyme digestion

Following nitrous acid depolymerisation, samples to be digested with enzymes were desalted by passage over PD-10 size exclusion columns eluted with MilliQ water, then lyophilised. Digests of α-L-iduronidase (0.29 mU per digest), α-L-iduronate-2-sulphatase (0.54 mU per digest), and β-D-glucuronidase (1,000 U per digest) were in a

total volume of 25 µl of 40 mM sodium acetate, pH 4.5 for 12 hours at 37°C. After treatment with the enzymes, samples were adjusted to 1 ml by addition of H_2O / HCl pH 3.5 for loading onto HPLC.

HPLC separation conditions for sequence analysis

A single ProPac PA-1 SAX column (4.6 x 250 mm), was used with a linear gradient running from 0 – 0.75 M NaCl over 110 min. Samples were loaded using a 1 ml sample injection loop. Following sample loading, the loop was washed onto the column with 1 ml of MilliQ water before application of the gradient. The column was eluted at a flow rate of 1 ml/ minute collecting 0.5 ml fractions and radioactivity in each fraction was measured by scintillation counting.

The filter binding assay

A modified version of the filter binding assay (FBA) (Maccarana & Lindahl, 1993) was used. Metabolically radiolabelled HS was incubated with protein plus any non-radioactive GAG inhibitors or antibodies for 2 hours at room temperature in 25-200 µl 0.15M or 0.05M NaCl containing 10 mM Tris-HCl at pH 7.0. The proteins used were human recombinant endostatin monomer (HEM, 40µM), human recombinant endostatin dimer (HED, 5µM), bFGF (1µg/100µl) and aFGF(2µg/100µl). Samples were applied to buffer-equilibrated cellulose nitrate filters (0.2µM) under a vacuum manifold and unbound radiolabelled material eluted with aliquots (3x1ml, unless specified otherwise) of either 0.05M NaCl, 10mM Tris-HCl, pH 7.0 or 0.15M NaCl, 10mM Tris-HCl, pH 7.0, as indicated. Bound HS was eluted from protein with increasing concentrations of NaCl in 10mM Tris-HCl, pH 7.0 for affinity studies. Increments of 0.05 to 0.1 M NaCl were typical with 3 x 1 ml aliquots at each NaCl concentration (detailed in results). For competition studies, bound radiolabelled material was eluted with 3 x 1ml aliquots of 1.0 M NaCl, 10mM Tris-HCl, pH 7.0. In all assays, 1 ml fractions were collected. Filters, 1 ml fractions (analytical assays) or small aliquots of fractions (preparative assays) were monitored for radioactivity by scintillation counting.

Recovery of HS with affinity for endostatin and further analysis

In preparative assays, material was pooled according to the NaCl concentration required to elute and the volumes decreased to ~ 0.5ml by centrifugal evaporation. Samples were desalted as described previously using PD-10 columns containing Sephadex G-25,

then lyophilised by centrifugal evaporation and resuspended in various volumes of milliQ water, usually not exceeding 100µl. S-domain profiling, disaccharide compositional analysis, and heparinase III digestion of heparinase I resistant oligosaccharides were performed as outlined above. Samples were also tested for rebinding to endostatin using identical conditions of incubation and elution using the FBA as described previously.

Two step zero length covalent cross-linking

Cross-linking was carried out essentially as described previously by Grabarek & Gergely, 1990. Non-radiolabelled porcine intestinal mucosal heparin or low molecular weight heparin derived dodecasaccharides in coupling buffer (0.1 M NaCl, 0.1 M MES, pH 6.0) were incubated for 15 minutes at room temperature with 27mM EDAC and 23mM S-NHS in a final volume of 100µl to activate carboxyl groups. The reaction was terminated by size separation of activated GAG from EDC and S-NHS by chromatography on a 1 ml Sephadex-G50 column, pre-equilibrated in coupling buffer. Sample (applied in a volume of 100 µl) was eluted with 250 µl aliquots of coupling buffer and activated GAG recovered in the void (usually fraction 4). Dextran blue and sodium dichromate were used as Vo and Vt markers, respectively. Activated GAGs (in a volume of 250µl) were then added to a solution of endostatin (minimum 10µM) in PBS or coupling buffer to a give a final endostatin : GAG molar ratio of 1:10 and incubated at room temperature for 2 hours. Products of zero-length crosslinking were subsequently stored at 4°C and analysed by standard SDS-PAGE (15%gel) and Western blotting, followed by enhanced chemiluminescence (ECL) immunodetection prior to purification (see below).

Characterisation of cross-linked conjugates

Heparinase I digestion

Crosslinked conjugates in 0.1M MES, 0.1M NaCl, pH 6.0 were diluted 10 fold to a final concentration of 1x heparinase buffer (0.1M sodium acetate, 0.1mM calcium acetate, 1 mg/ml bovine serum albumin, pH 7.0) and treated for 18 hours at 37° C with heparinase I. The enzyme digested crosslinked conjugates were then recovered into a smaller volume for further analysis by precipitation with BSA and 10% trichloroacetic acid (TCA). BSA (50 µg) was added to the digest with $1/10^{th}$ of the sample volume of 100%

TCA, left for 10 minutes at 4°C, then centrifuged for 10 minutes at 10000rpm. The supernatant was removed and the pellet washed in acetone then centrifuged for a further 10 minutes at 10000 rpm. The acetone was removed, the pellet airdried and dissolved in 30µl sample buffer for analysis by SDS-PAGE and Western blotting.

Heparin affinity of crosslinked conjugates

To check heparin affinity, aliquots of protein from the crosslinking reaction (maximum 5µg) were mixed with 30µl heparin-agarose beads. The beads were centrifuged for 10 minutes at 10000 rpm, the supernatant removed then buffer equilibrated into 0.1M MES, 0.1M NaCl, pH 6.0 before they were mixed with sample for 10 minutes on a rotator and centrifuged for 10 minutes at 10000 rpm. The supernatant containing unbound product of the crosslinking reaction was reserved and the beads containing bound product suspended in sample buffer for further analysis.

To separate crosslinked monomer from native, uncrosslinked protein, a 0.5ml heparin-agarose column was prepared and equilibrated with 10 column volumes of 0.1M MES, 0.1M NaCl, pH 6.6. To decrease non-specific binding the column was blocked with 0.5mg BSA and 0.5mg porcine intestinal heparin in the above buffer. Samples (not greater than 100 µg) in a volume of 100µl 0.1M MES, 0.1M NaCl, pH 6.0 were applied and recirculated 5 times. The eluant was retained for analysis by SDS-PAGE and Western blotting as described below.

Sodium dodecyl sulphate-polyacrylamide gel electrophoresis (SDS-PAGE)

Crosslinked conjugates were separated by minigel electrophoresis on 15% (w/v) SDS polyacrylamide gels (Laemmli, 1970). The glass plate apparatus was assembled and the 15% (w/v) SDS polyacrylamide resolving gel made using 5mls milliQ water, 5mls 1.5M Tris, pH8.8, 10mls 30% degassed acrylamide, 200µl SDS, 200µl of fresh 10% ammonium persulphate and 75µl TEMED. The gel was poured gently between the glass plates, ensuring that there were no bubbles. The gel was overlaid with water-saturated butanol and allowed to set. A 4% (w/v) SDS polyacrylamide stacking gel was made using 12.2 mls milliQ water, 5mls 0.5M Tris, pH 6.6, 2.6ml degassed 30% acrylamide, 200µl SDS, 200µl 10% ammonium persulphate and 75µl TEMED. The water-saturated butanol was removed and the interface washed with water, before pouring the stacking gel on top. A comb was placed in the stacking gel to create wells

for the protein samples and the gel was allowed to set for ~ 30 minutes. The gel plates were placed in the protein tank apparatus. The protein and standard colour marker samples were diluted at least 1:4 with SDS sample buffer containing 4.4ml milliQ water, 1ml 0.5M Tris-HCl, pH 6.8, 0.8ml glycerol, 1.6 ml 10% (w/v) SDS and 0.2ml 0.05% (w/v) bromophenol blue x SDS sample buffer (non-reducing) or as above with 0.4ml 2-β-mercaptoethanol for SDS reducing buffer, then boiled for 10 minutes. The samples (30μl) were loaded in the wells and electrophoresed in 1 x SDS running buffer (25mM TRIS base, 192mM glycine, pH 8.3, 0.1%SDS) at 200V for 40 minutes. Low molecular weight prestained colour standard markers were used to estimate the size of the resolved proteins.

Western blotting

SDS-PAGE gels were transferred to nitrocellulose membranes using semi-dry blot apparatus at 200mA for 1 hour in which the gel and membrane were sandwiched between 6 layers of chromatography paper soaked in transfer buffer (25mM TRIS-base, 192mM glycine, pH 8.3, 0.1% SDS and 20% methanol). After transfer the nitrocellulose mambranes were washed with milliQ water and blocked for 1 hour with 10% marvel in PBS and then washed 3 x 5 minutes with PBS/(0.05%v/v)Tween 20. The membrane was then incubated overnight on a rotator at 4^0C with a 1:1000 dilution of rabbit anti-human endostatin polyclonal antibody. The antibody solution was then removed, the membrane washed 3 x 10 minutes in PBS/Tween 20 and then incubated with a 1:5000 dilution of horseradish peroxidase-conjugated swine anti-rabbit IgG for 60 minutes. Next, the membrane was washed extensively in PBS/Tween 20 for 30 minutes, and the presence of endostatin visualised by enhanced chemiluminescence (ECL) following the manufacturer's protocol. Briefly, after 1 minute incubation of the nitrocellulose membrane with the ECL reagents in the dark room , the membrane was wrapped in cling film and exposed to hyperfilm (high performance chemiluminescence film) in a Kodak autoradiography plate for exposure times ranging from 1 minute to 1 hour. The hyperfilm was developed by immersion in a 1:3 dilute solution of GBX developer fluid for 3 minutes or until bands were visible, fixed by immersion in a 1:3 dilute solution of GBX fixer fluid for 3 minutes then washed extensively in water before drying in air. Blots were scanned into Microsoft Photo editor.

The matrigel tube formation / morphogenesis assay

The assay was performed according to the method described by Kuo *et al.,* 2001. Multiwell dishes (24 well) were coated with 250µl Matrigel at 4°C and incubated at 37°C for 20 minutes. Wells were then seeded with $5x10^5$ cells per well (BAEC) in 1 ml complete medium. Recombinant endostatin monomer (HEM) and/or dimer (HED) were added at concentrations of 3000nM and 50nM respectively, either at the time of plating or after 16 hours of tube formation. Where relevant, the cells were preincubated with HEM for 30 minutes prior to the addition of dimer. The plates were observed for tubule formation and cell morphology at 16 and 24 hours after the cells were seeded by phase contrast microscopy. Photographs taken at low power (x 100 magnification) on black and white film were scanned into Microsoft photo editor.

4. RESULTS

PART 1 : COMPARATIVE ANALYSIS OF HEPARAN SULPHATE FROM MACROVESSEL AND MICROVESSEL ENDOTHELIAL CELLS

The initial aim of this project was to examine the structure of HS from human microvessel endothelial cells (HMVEC) that had not previously been characterised. We were interested to know whether this HS differed significantly from that of other endothelial cell (EC) populations for studies of HS-protein interactions relevant to angiogenesis. To address this, comparative analyses were also performed on bovine macrovessel (BAEC) and microvessel (BCE) EC HS.

4.1 Preparation of HS from endothelial cells

Characterisation of endothelial cells

All endothelial cells exhibited typical morphology in routine culture with a cobblestone appearance on reaching confluence (Schor & Schor, 1983) (Figure 4.1A,B) and expressed the endothelial cell marker, von Willebrand's factor (vWF) detected by immunohistochemistry with human polyclonal vWF antibody (Figures 4.2, 4.3). HMVEC also immunostained positive for the endothelial cell marker CD31 and negative for smooth muscle actin (Figure 4.3). In addition, HSPG expression was examined in HMVEC by immunohistochemistry. The cells stained strongly for perlecan, syndecan-3 and syndecan-4 and weakly for glypican-1, syndecan-1 and syndecan-2 (Figure 4.4). The findings were consistent with previous reports that cells usually express more than one class of HSPG (Bernfield *et al.*, 1999; Carey, 1997; Costell *et al.*, 1999).

Extraction and purification of heparan sulphate

Subconfluent monolayers of BAEC, BCE and HMVEC were metabolically labelled with ^{3}H -glucosamine ± sodium ^{35}S-sulphate and extracts digested with pronase to convert PGs to one or more GAG chains attached to peptide fragments. Charged species were first separated by salt elution of the digests from a DEAE anion-exchange column. Figure 4.5 shows the elution profiles of secreted and/or shed GAGs resolved

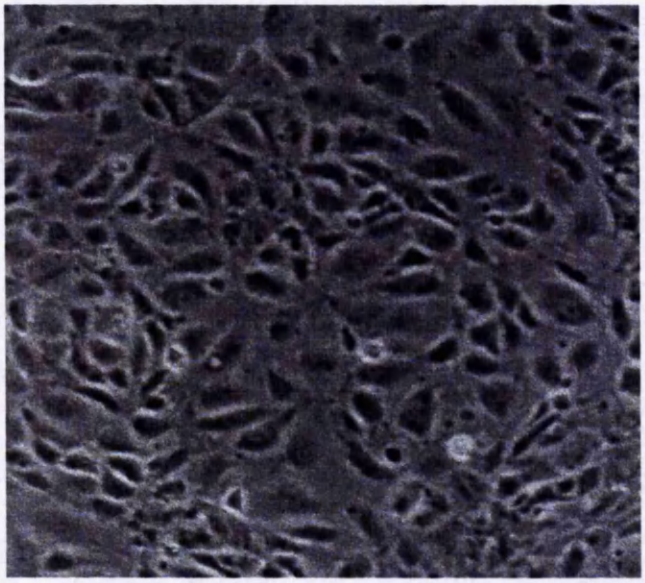

Confluent HMVEC
(x 120 magnification)

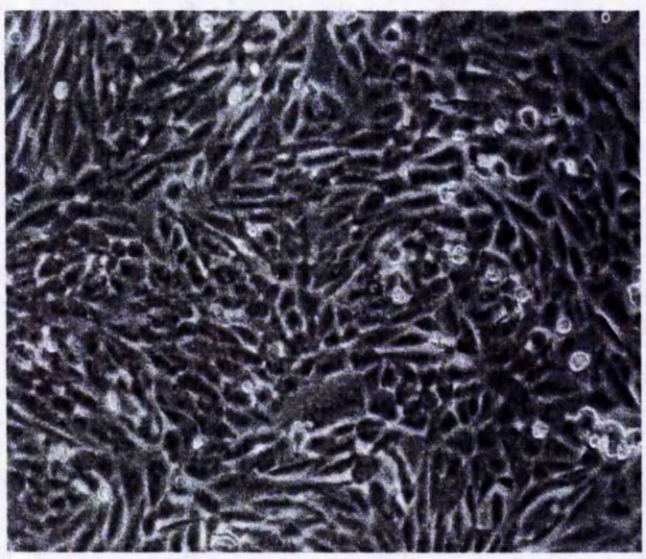

Confluent BCE
(x 150 magnification)

Figure 4.1A : Phase contrast microscopy of endothelial cells in culture. Confluent HMVEC and BCE cells exhibit a cobblestone morphology characteristic of endothelial cells.

Subconfluent BAEC

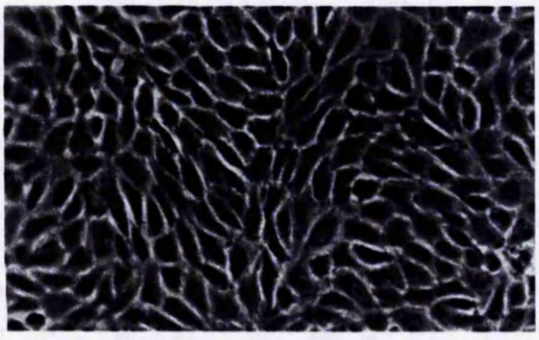

Confluent BAEC

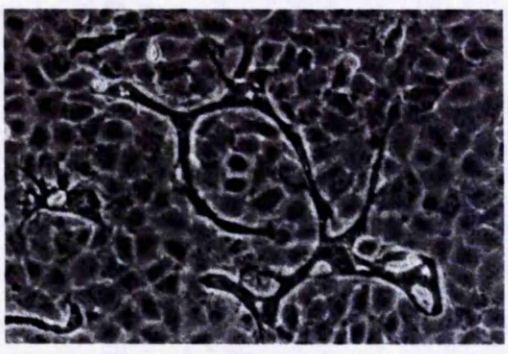

Postconfluent BAEC

Figure 4.1B : Phase contrast microscopy of endothelial cells in culture. BAEC exhibit typical endothelial cell morphology. Subconfluent 'tear drop' cells are shown. Confluent cells have a cobblestone appearance and postconfluent cells undergo a morphological change to a sprouting phenotype. All photographed at x 150 magnification.

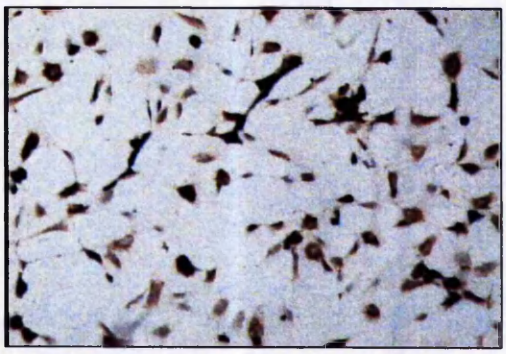

BAEC immunostained for vWF

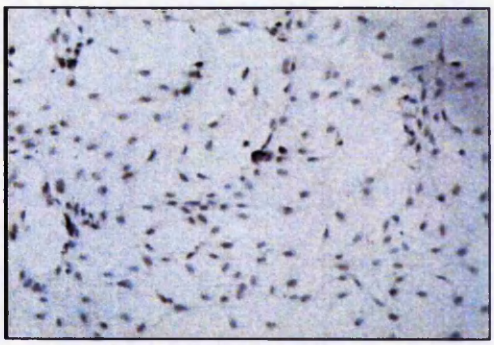

BAEC negative control

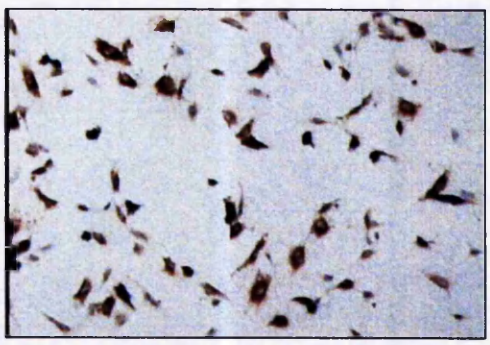

BCE immunostained for vWF

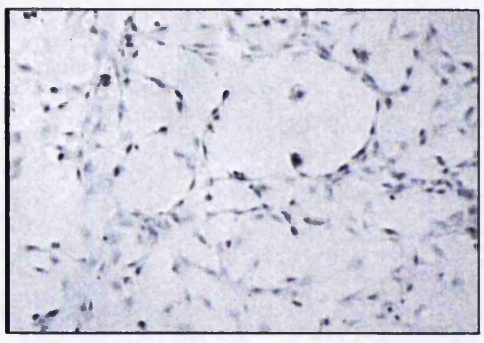

BCE negative control

Figure 4.2 : Immunohistochemistry of bovine endothelial cells for von Willebrands Factor (vWF). Cells were cultured for 24 hours in glass chamber slides then permeabilised, fixed and stained as described in methods. The perinuclear staining of vWF is shown alongside negative controls using mouse IgG as the primary antibody. Immunoperoxidase was counterstained with haematoxylin, slides visualised by light microscopy and photographed at x100 magnification.

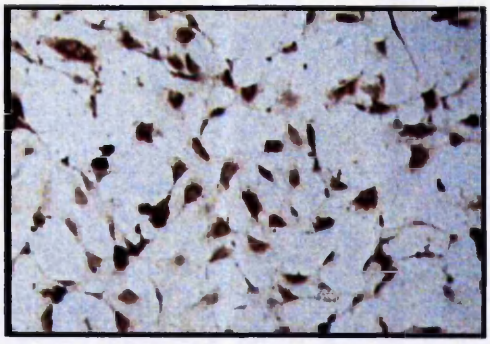

HMVEC immunostained for vWF

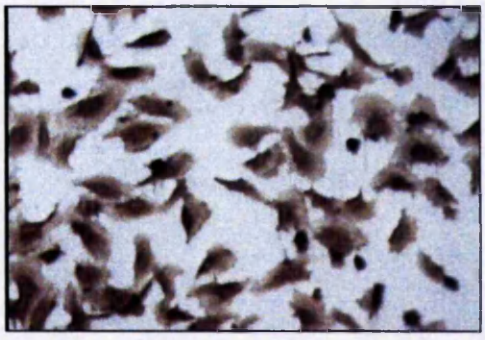

HMVEC immunostained for CD31

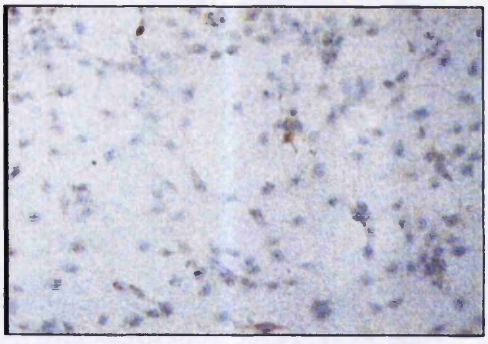

HMVEC immunostained for αsmooth muscle actin

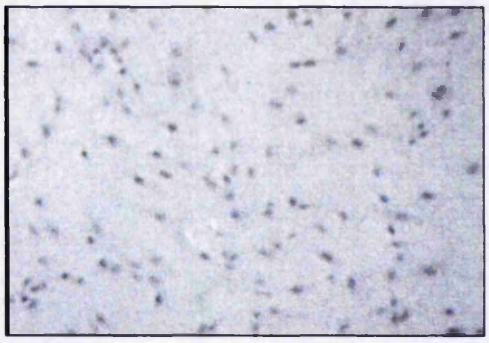

HMVEC negative control

Figure 4.3 : Immunohistochemistry of HMVEC for endothelial cell markers. Cells were cultured for 24 hours in glass chamber slides then permeabilised (if required), fixed and stained as described in methods. The perinuclear staining of vWF and surface staining of CD31 is shown alongside negative controls using mouse IgG as the primary antibody and α smooth muscle actin. Immunoperoxidase was counterstained with haematoxylin, slides visualised by light microscopy and photographed at x100 magnification.

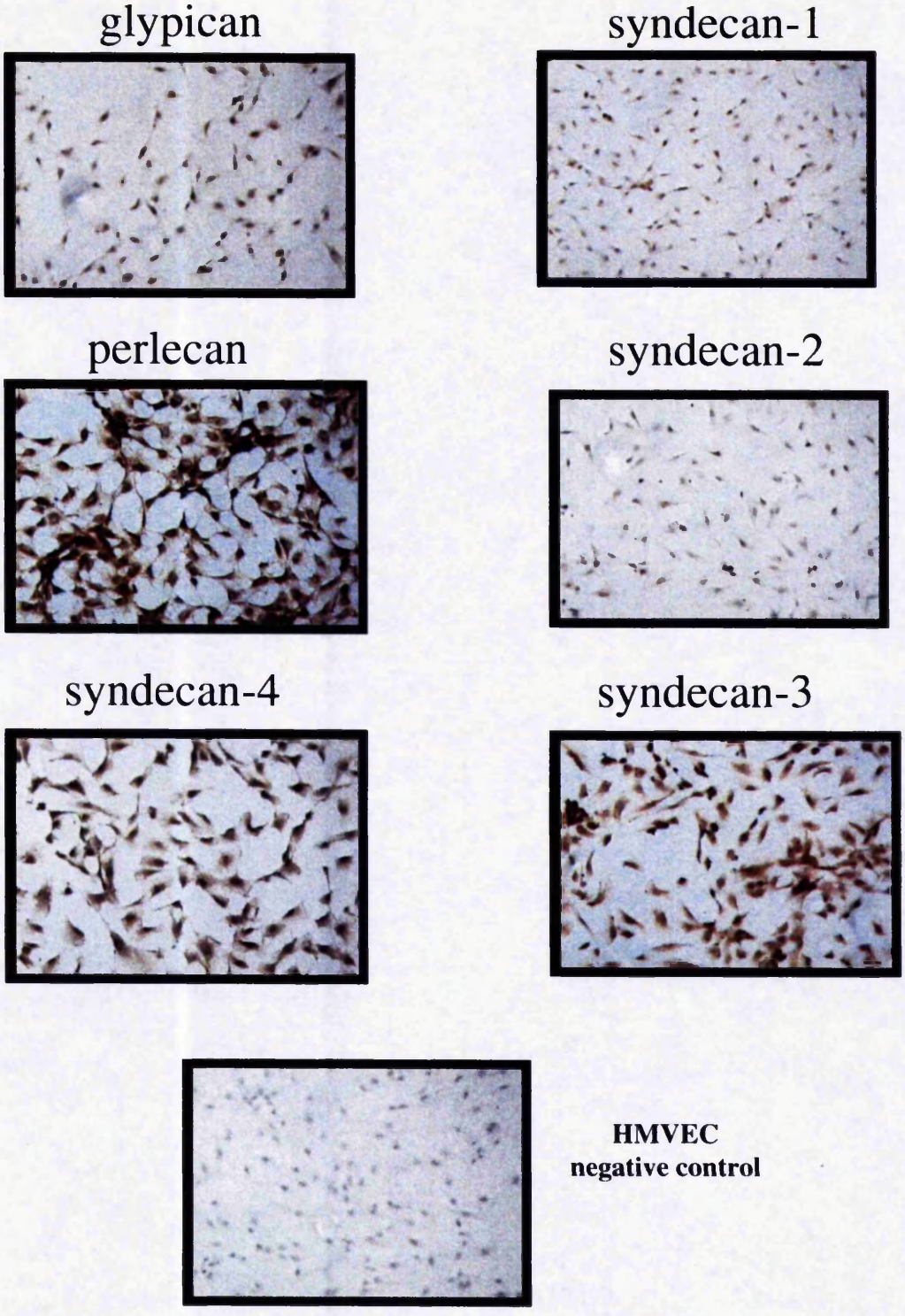

Figure 4.4 : Immunohistochemistry of HMVEC for proteoglycan expression. Cells were cultured for 24 hours in glass chamber slides then permeabilised (if required), fixed and stained as described in methods. HMVEC stain strongly positive for perlecan, syndecan-3 and syndecan-4. Weak staining for glypican-1, syndecan-1 and syndecan-2 is also demonstrated compared to the negative controls using mouse IgG as the primary antibody. Immunoperoxidase was counterstained with haematoxylin, slides visualised by light microscopy and photographed at x100 magnification.

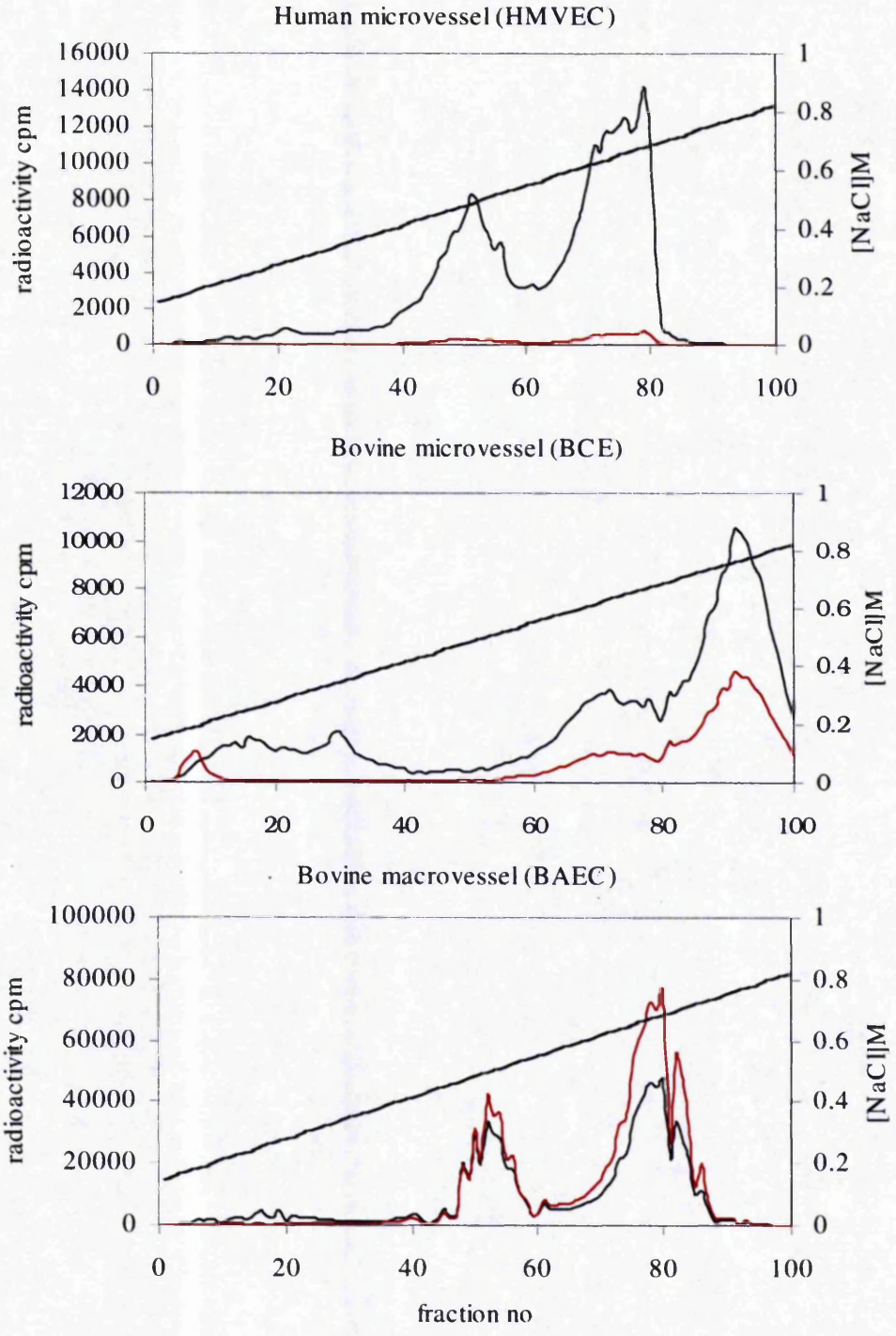

Figure 4.5 : DEAE-anion exchange separation of GAG chains released by pronase digestion of endothelial cell PGs. The pronase digests were loaded onto 5cm pre-equilibrated columns and washed with 10 column volumes of low salt buffer (0.15M NaCl, 20mM sodium phosphate, pH7.4). Bound material was eluted with a linear gradient of 0.15-0.825M NaCl, 20mM sodium phosphate, pH 7.4 at a flow rate of 15ml per hour. One hundred 2ml fractions were collected and the elution profile monitored by taking small aliquots for scintillation counting. Material eluting ~ 0.5-0.6M NaCl is HS. ^{3}H black line, ^{35}S red line.

by anion – exchange chromatography on DEAE-Sephacel. In accordance with previous reports, material eluting at ~ 0.5-0.6 M NaCl was predominantly HS (Gallagher & Walker, 1985). Unsulphated hyaluronan has been shown to elute at lower salt concentrations, and more highly sulphated CS has been shown to elute at higher salt concentrations. Material from the remaining peaks was treated with nitrous acid and/or chondroitinase ABC to confirm the absence of HS (data not shown). There is poor incorporation of ^{35}S in preparations from HMVEC relative to [^{3}H] uptake. Incorporation of ^{35}S into GAGs can be inhibited by the presence of sulphated antibiotics and sulphated compounds such as magnesium sulphate in the culture medium (C Merry and P Hyde, personal communication). The medium (EBM-MV) for HMVEC contains a relatively high content of sulphated compounds and a low sulphur preparation is not available. Due to the fastidious culture requirements of these cells measures were not taken to adapt the cells to a different medium such as DMEM since it is the ^{3}H rather than the ^{35}S label that is critical for these analyses.

4.2 Estimation of molecular weight and length of HS chains

The first characteristic of the HS chains to be detailed following elution from DEAE was their relative size. This was approximated from their elution position on a Sepharose CL-6B column. Following removal of contaminating CS by digestion with chondroitinase ABC and residual peptide by alkaline borohydride treatment, the HS chains from each endothelial cell population eluted from Sepharose CL-6B as single peaks (Figure 4.6). The peak maximum Kav values are calculated using the formula (Vt-Ve/Vt-Vo) and used to derive the corresponding molecular weights from the calibration of Wasteson, 1971. For each HS species, the first major peak is the putative HS containing peak and the second, minor peak represents the disaccharide breakdown products of CS. Figure 4.7 shows the material following alkaline borohydride elimination of residual peptide. A shift nearer to Vt has occurred representing a lower molecular weight. Given the structure of PGs, the shift may also indicate the dissociation of single HS chains from small, residual peptide cores to which two or more HS chains were attached in close proximity. The number of disaccharides per chain is calculated by assuming that each disaccharide has an average molecular weight of 450. The profiles indicate polydispersity of chain length within each population that is most marked in HMVEC HS.

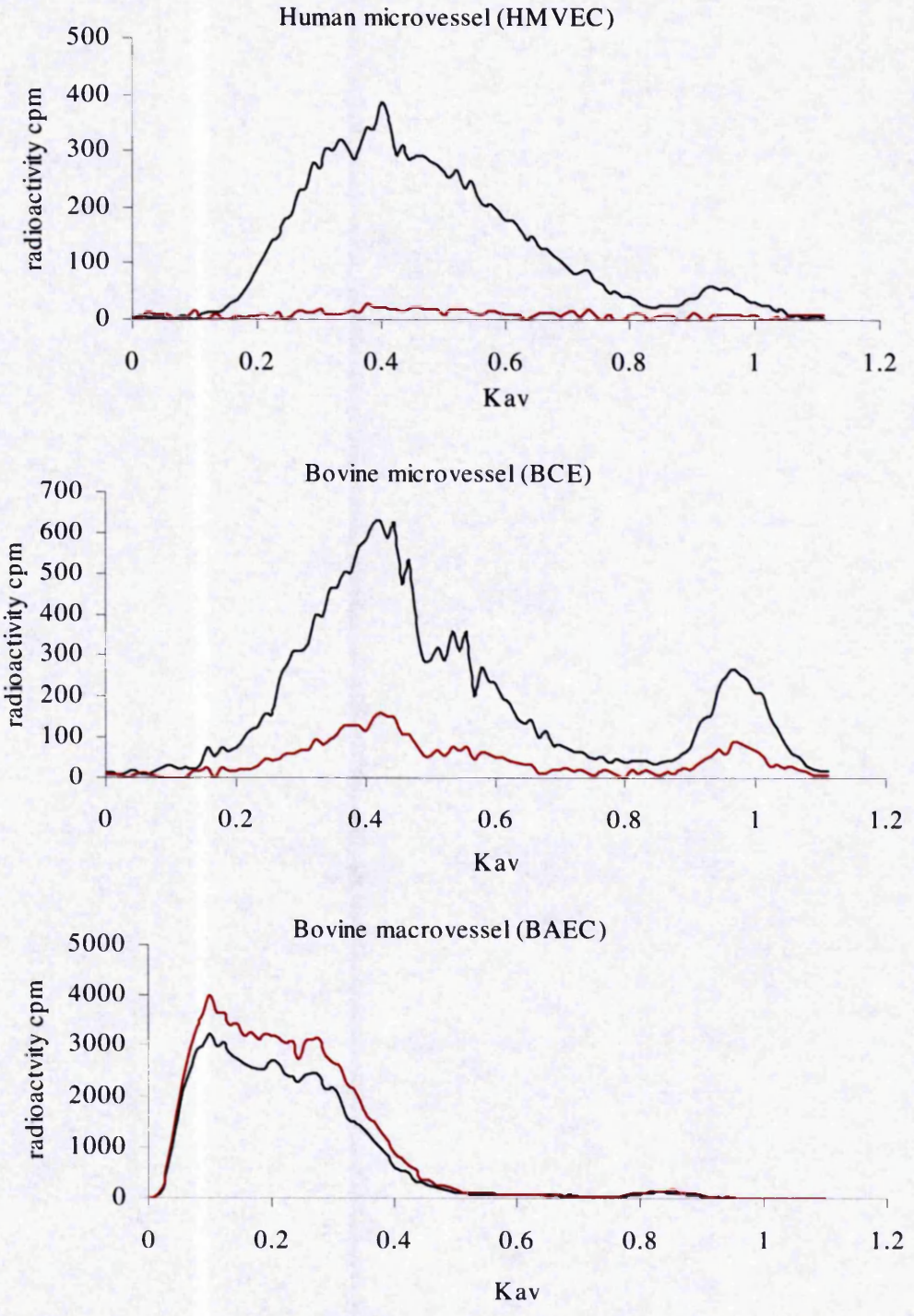

Figure 4.6 : Sepharose CL-6B separation of HS chains from endothelial cells following digestion with chondroitinase ABC. HS chains from DEAE, treated with chondroitinase ABC were loaded onto a CL-6B column (1.5 x 66 cm) in 1 ml 0.2M ammonium hydrogen carbonate. The column was eluted with 0.2M ammonium hydrogen carbonate at a flow rate of 12ml per hour. 1 ml fractions were collected. K_{av} was calculated from elution positions of sodium dichromate (V_t, K_{av} = 1.0) and dextran blue (V_o,K_{av} = 0). The elution profile was monitored by taking small aliquots for scintillation counting. ^{3}H black line, ^{35}S red line.

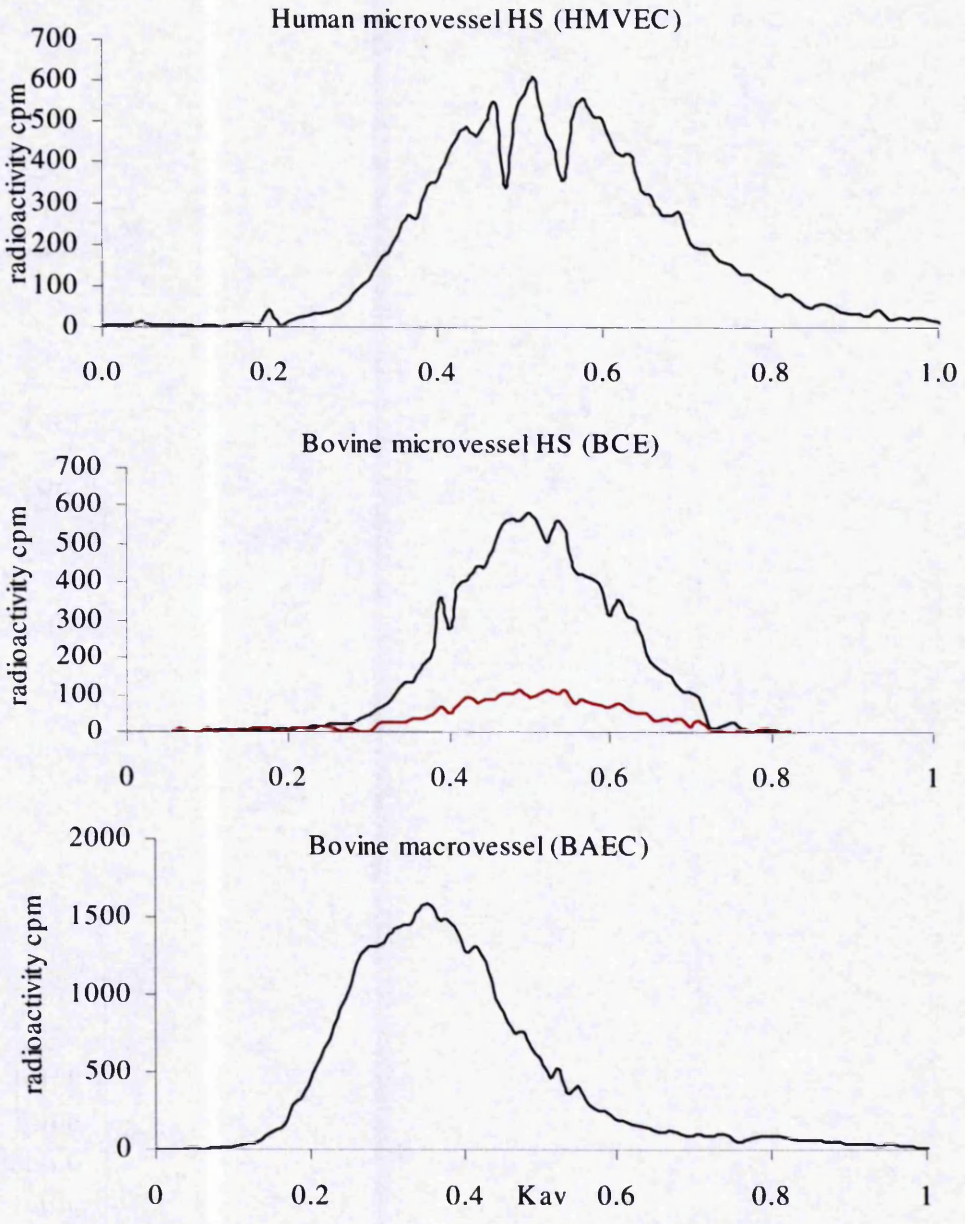

Figure 4.7 : Sepharose CL-6B separation of HS chains from endothelial cells following alkaline borohydride peptide elimination. HS chains from DEAE, treated with alkaline borohydride were loaded onto a CL-6B column (1.5 x 66 cm) in 1 ml 0.2M ammonium hydrogen carbonate. The column was eluted with 0.2M ammonium hydrogen carbonate at a flow rate of 12ml per hour. 1 ml fractions were collected. K_{av} was calculated from elution positions of sodium dichromate (V_t, K_{av} = 1.0) and dextran blue (V_o,K_{av} = 0). The elution profile was monitored by taking small aliquots for scintillation counting. ^{3}H black line ^{35}S red line.

Endothelial Cell species	Kav	Mr	No. disaccharides per chain
HMVEC (human microvessel)	0.5	20000	~ 45
BCE (bovine microvessel)	0.5	20000	~ 45
BAEC (bovine macrovessel)	0.35	50000	~ 110

Table 4.1 : Molecular weights and lengths of endothelial cell HS chains. Kav values obtained from Sepharose CL-6B gel filtration were used to calculate the average molecular weights and numbers of disaccharides comprising the EC HS chains.

Chain size analyses did not differ with subsequent preparations of HS (HMVEC n=3, BCE n=1, BAEC n=3). The average molecular weights and numbers of disaccharides per chain are summarised in Table 4.1. The HS chains from HMVEC and BCE are significantly shorter (both ~ 45 disaccharides) than those of BAEC (~ 110 disaccharides). These sizes are consistent with previous reports defining the size range of HS chains to be 50-200 disaccharides in length (Gallagher & Walker, 1985) and the BAEC HS chain size compares well with previous analyses (Hiscock *et al.*, 1995; Pye & Kumar, 1995). HUVEC cells are also reported to have HS chains of over 100 disaccharides in length (Lindblom & Fransson, 1990), suggesting that this marked distinction between chain lengths of macrovessel and microvessel HS may be conserved between species.

4.3 Characterisation of endothelial cell HS using specific scission techniques

To characterise the HS purified from each EC species, the chains were exposed to specific scission reagents known to cleave at well-defined linkages (see Table 1.4, Figure 1.3). The products of depolymerisation following exposure to these reagents can be resolved according to size by Bio-Gel P10 chromatography and the resulting profiles used to generate an overall picture of the organisation of the intact chains (the macrostructure). An important function of these analyses is that the structural assignment is strengthened by combining data derived from using different scission reagents either alone or in combination, rather than replicate analyses of a single scission method. Therefore, analyses were usually performed in triplicate using material from different cell preparations. However, due to limited quantities of HS and time constraints, this was not always possible and resources were prioritised to obtain complementary data from different scission reagents.

Low pH nitrous acid causes specific and near quantitative release of N-sulphate groups with concomitant cleavage of the adjacent hexosaminidic bond. The gel filtration profiles suggest a typical domain structure of these EC HS species with N-sulphated disaccharides occuring in clusters (S-domains) throughout the chain (Figure 4.8). Consistent with the properties of BioGel P-10, there is good separation of generated oligosaccharides in the size range dp2-12 with less resolution of longer oligosaccharides eluting near Vo. The numbers of the glycosidic linkages susceptible to

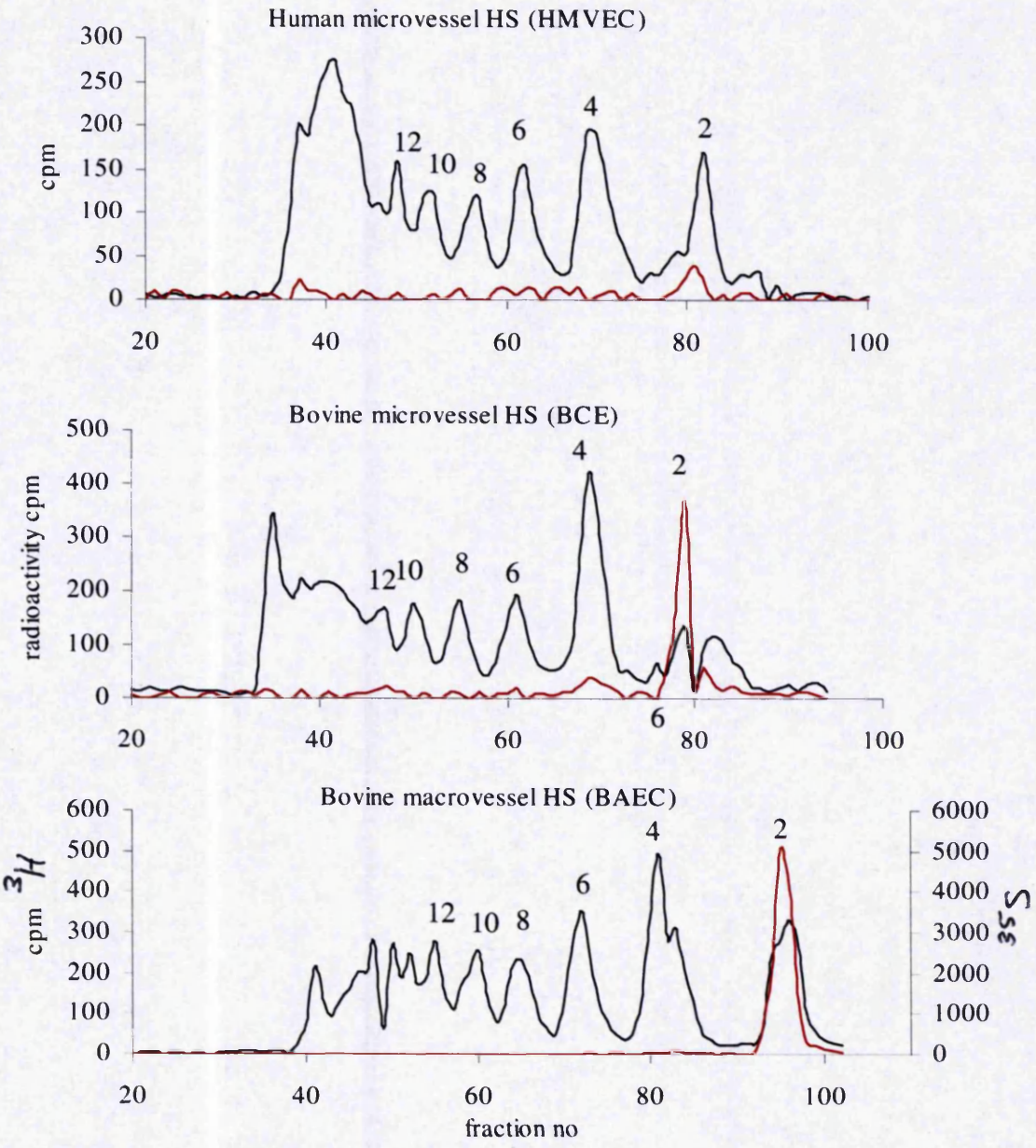

Figure 4.8 : BioGel P-10 separation of fragments generated by nitrous acid scission of endothelial cell HS. Low pH nitrous acid depolymerisation was performed on ≥10 K cpm of ^{3}H from each endothelial cell HS species. Following neutralisation, samples were loaded onto a P-10 column (1cm x 140 cm) in a maximum of 1ml. The column was eluted with 0.1M NaCl, buffered with NaOH to pH8.8, at a flow rate of 4ml/hour and 1 ml fractions collected. The elution profiles were monitored by scintillation counting (^{3}H black line ^{35}S red line). The numbers above the peaks correspond to the degree of polymerisation (dp) or number of saccharide units, therefore dp2 = disaccharide etc.

nitrous acid for each ECHS species were calculated by using the formula $\sum An/n$ where An was defined as the relative amount of ^{3}H-glucosamine radioactivity within a chromatographic peak of a certain oligosaccharide size (dp) and n is dp (Turnbull & Gallagher, 1990). In contrast to the distinctions observed for chain length the proportion of N-sulphated disaccharides is similar for all the EC HS species that we examined (36 – 40%). This is consistent with previous analyses for BAEC (Hiscock *et al.*, 1995; Pye & Kumar, 1995) and HUVEC HS (Lindblom & Fransson, 1990). This reflects a low level of sulphation given that the average range of N-sulphation in HS is ~ 40-50% (Gallagher & Walker, 1985). The spacing of susceptible linkages was derived by comparing the amounts of di-, tetra- and larger oligosaccharides on the chromatograms to estimate contiguous, alternate and spaced linkages, respectively. A summary of this data in Figure 4.11 suggests that there is no significant variation in the distribution of the N-sulphated disaccharides between the EC HS species. Approximately 34 - 46 % of the N-sulphated disaccharides occur contiguously in clusters (forming S-domains), 26-31% occur in alternate disaccharides and the remainder (32-35%) occur more than two disaccharides apart suggesting that the positioning and organisation of the S-domains is very similar. The data obtained for BAEC HS was in line with previous analyses (Pye & Kumar, 1995) and not repeated to conserve material.

Heparinase I (cleavage of GlcNS±6S-IdoA2S) is believed to act within the most sulphated regions of HS (Linhardt *et al.*, 1990) (Figure 1.3, Table 1.4). In contrast to the extensive degradation to oligosaccharides of ≥dp2-12 seen with nitrous acid, digestion with heparinase I results in few low molecular weight products and a large peak at the void in each case (Figure 4.9). From 3 independent experiments, the proportion of material eluted as disaccharides (calculated from the proportion ^{3}H-HS present in the disaccharide peak at Vt compared to the total) did not differ significantly, with 8.2 ± 2.6% for HMVEC, 7.5 ± 0.7% for BCE and 7.3 ± 2.8% for BAEC HS. These profiles suggest that the proportions of iduronate 2-O-sulphate containing disaccharides are similar between the EC HS species, consistent with their relatively low level of N-sulphation and localisation in clusters, within the S-domains.

Heparinase III (cleavage of GlcNAc/S±6S-GlcA) can be broadly considered to have the opposite activity to heparinase I (Linhardt *et al.*, 1990) (Table 1.4, Figure 1.3). Highly

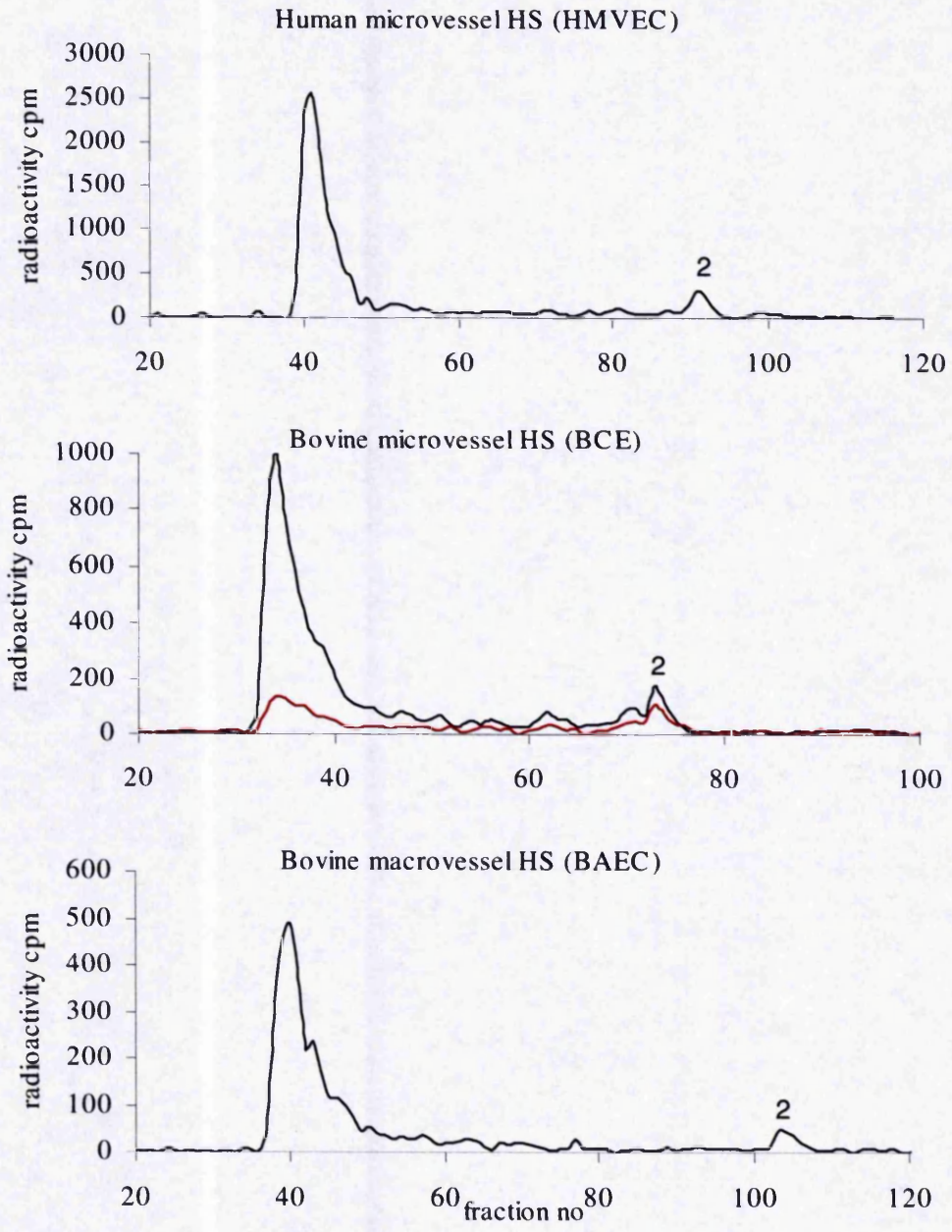

Figure 4.9 : BioGel P-10 separation of fragments generated by heparinase I digestion of endothelial cell HS. Heparinase I digestion was performed on ≥10 K cpm of ^{3}H from each EC HS species. Following digestion, samples were loaded onto a P-10 column (1cm x 140 cm) in a maximum of 1ml. The column was eluted with 0.1M NaCl, pH8.8, at a flow rate of 4ml/hour and 1 ml fractions collected. The elution profiles were monitored by scintillation counting (^{3}H black line ^{35}S red line). The numbers above the peaks correspond to the degree of polymerisation (dp) or number of saccharide units, therefore dp2 = disaccharide etc.

sulphated disaccharides, enriched in IdoA(2S), are resistant to degradation by this enzyme so oligosaccharides bearing contiguously N-sulphated disaccharides with a high proportion of IdoA(2S) residues are excised and defined as S-domains. Importantly, GlcA containing linkages can evade scission by heparinase III if located in close proximity to highly sulphated disaccharides (Merry *et al.*,1999, Appendix 1). Exposure of the EC HS chains to heparinase III results in very similar profiles (Figure 4.10) that are highly reproducible allowing for slight variations in column behaviour (Figure 4.11). Combining data from all EC HS species the total number of susceptible linkages ranges from 72 – 76% with 84-86% of these occurring in contiguous sequence. This is reflected in the dominant disaccharide peak that results from the release of enzyme-susceptible disaccharides that are mainly N-acetylated (see later, Table 4.3) and confirms a typical domain structure with IdoA(2S) residues largely confined to the S-domains. There are very few non-contiguous IdoA(2S) residues as indicated by the minor tetrasaccharide peaks in all the profiles that correspond to 3-5% of susceptible linkages arranged alternately. In addition, the profiles show that the S-domains (dp6 to dp14) decrease in abundance with increasing S-domain length. The relative abundance of S-domains according to size is shown for each EC species in Figure 4.12.

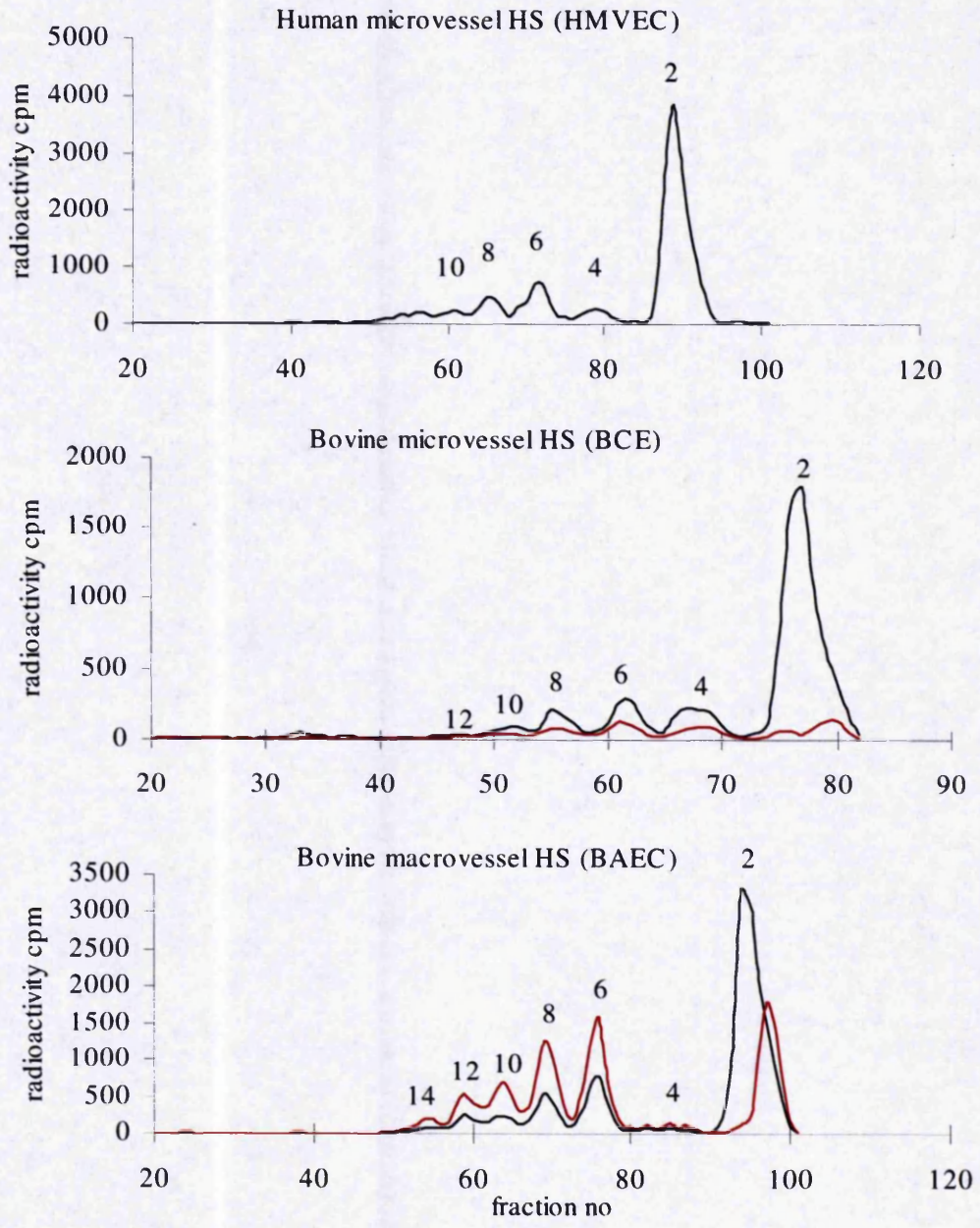

Figure 4.10 : BioGel P-10 separation of fragments generated by heparinase III digestion of HS chains from endothelial cells. Heparinase III digestion was performed on ≥10 K cpm of ^{3}H from each EC HS species. Following digestion, samples were loaded onto a P-10 column (1cm x 140 cm) in a maximum of 1ml. The column was eluted with 0.1M NaCl, pH8.8, at a flow rate of 4ml/hour and 1 ml fractions collected. The elution profiles were monitored by scintillation counting (^{3}H black line ^{35}S red line). The numbers above the peaks correspond to the degree of polymerisation (dp) or number of saccharide units, therefore dp2 = disaccharide etc.

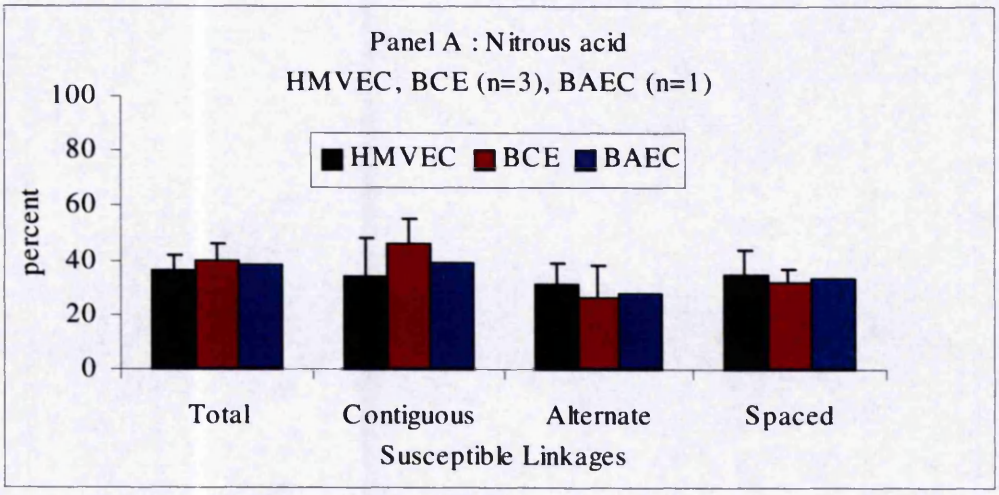

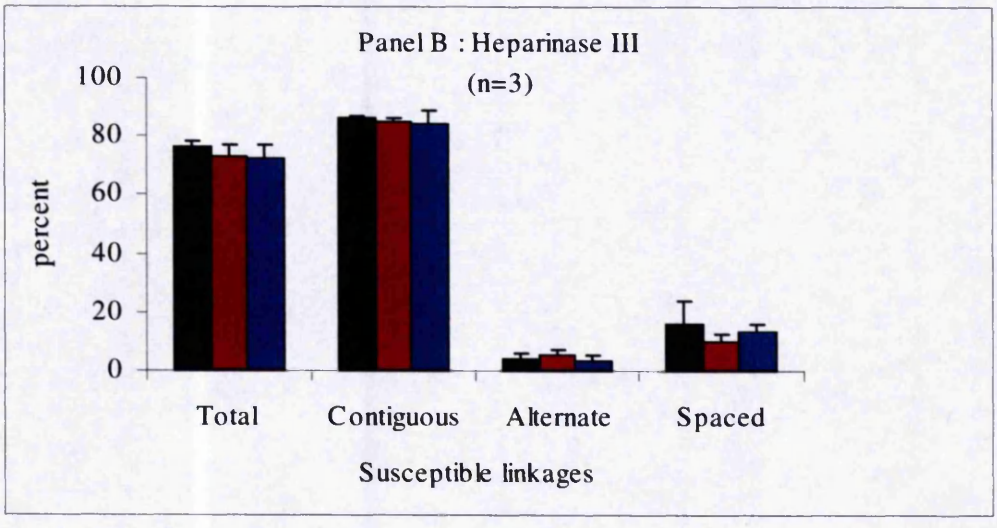

Figure 4.11 : Comparison of linkages susceptible to nitrous acid scission (Panel A) and heparinase III digestion (Panel B) in endothelial cell HS species. BioGel P-10 filtration profiles of nitrous acid depolymerisation or heparinase III digestion, performed on ≥10 K cpm of ^{3}H from each endothelial cell HS species, were used to derive the linkages susceptible to each scission reagent using the formula $\sum An/n$ where An = relative amount of ^{3}H-glucosamine radioactivity within a chromatographic peak of a certain oligosaccharide size (dp) and n is dp. Mean values plus sd are shown.

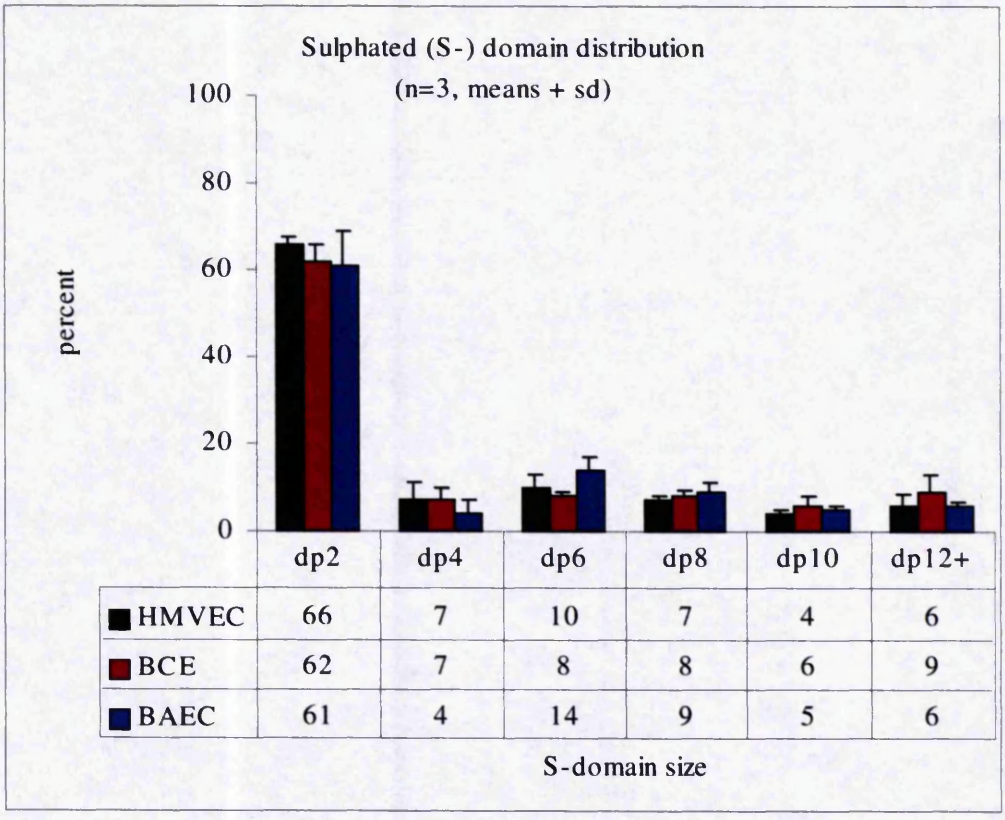

Figure 4.12 : Relative abundance of heparinase III derived S-domains from endothelial cell HS species. BioGel P-10 filtration profiles of heparinase III digestion, performed on ≥10 K cpm of ^{3}H from each endothelial cell HS species, were used to derive the percentages of each S-domain size per digest. Mean values of 3 independent analyses are tabulated and error bars show standard deviations.

4.4 Total disaccharide composition of endothelial cell HS

Disaccharides were prepared from each EC HS species by combined digestion with heparinases I,II and III. Resistant oligosaccharides (usually tetrasaccharides) were excluded by gel filtration of digests using Bio-Gel P2, and recovered disaccharides separated by strong anion-exchange (SAX) HPLC analysis. In practice, > 97% disaccharide yields were usually obtained. Also, the SAX-HPLC elution position of contaminating tetrasaccharides was found to be distinct from those of the disaccharides (Figure 4.13). Therefore, to minimise losses from recovery following Bio-Gel P2 filtration and enable smaller quantities of material (~5Kcpm ^{3}H-HS) to be used, this step was often omitted.

The SAX-HPLC profiles obtained for each EC HS species reinforce the findings obtained previously using specific scission reagents (Figure 4.13, 4.14, Table 4.2). The majority of disaccharides are unmodified (ie. UA-GlcNAc) with the proportion of N-sulphated disaccharides varying from 37 to 40% (compared to 36 to 40% by nitrous acid scission). Disaccharides modified by 0-sulphation are least abundant and the analyses reveal that 2-O-sulphation is a more common modification than 6-O-sulphation. There is a clear difference in the level of 6-O-sulphation between the microvessel and macrovessel EC HS. In HMVEC, the most modified tri-sulphated disaccharide [ΔUA(2S)-GlcNS(6S)] constitutes 6±0% of the total HMVEC pool compared to 1.9±0.2% of the total BAEC disaccharides. The increase in 6-O-sulphation is even more marked comparing BAEC HS to BCE HS. In BCE EC HS, there is increased frequency of all the 6-O-sulphated disaccharides although there was insufficient material to confirm this observation. However, Figure 4.5 shows that BCE HS elutes ~ 0.1M NaCl later than HMVEC and BAEC HS from DEAE-Sephacel consistent with a relatively higher sulphate content.

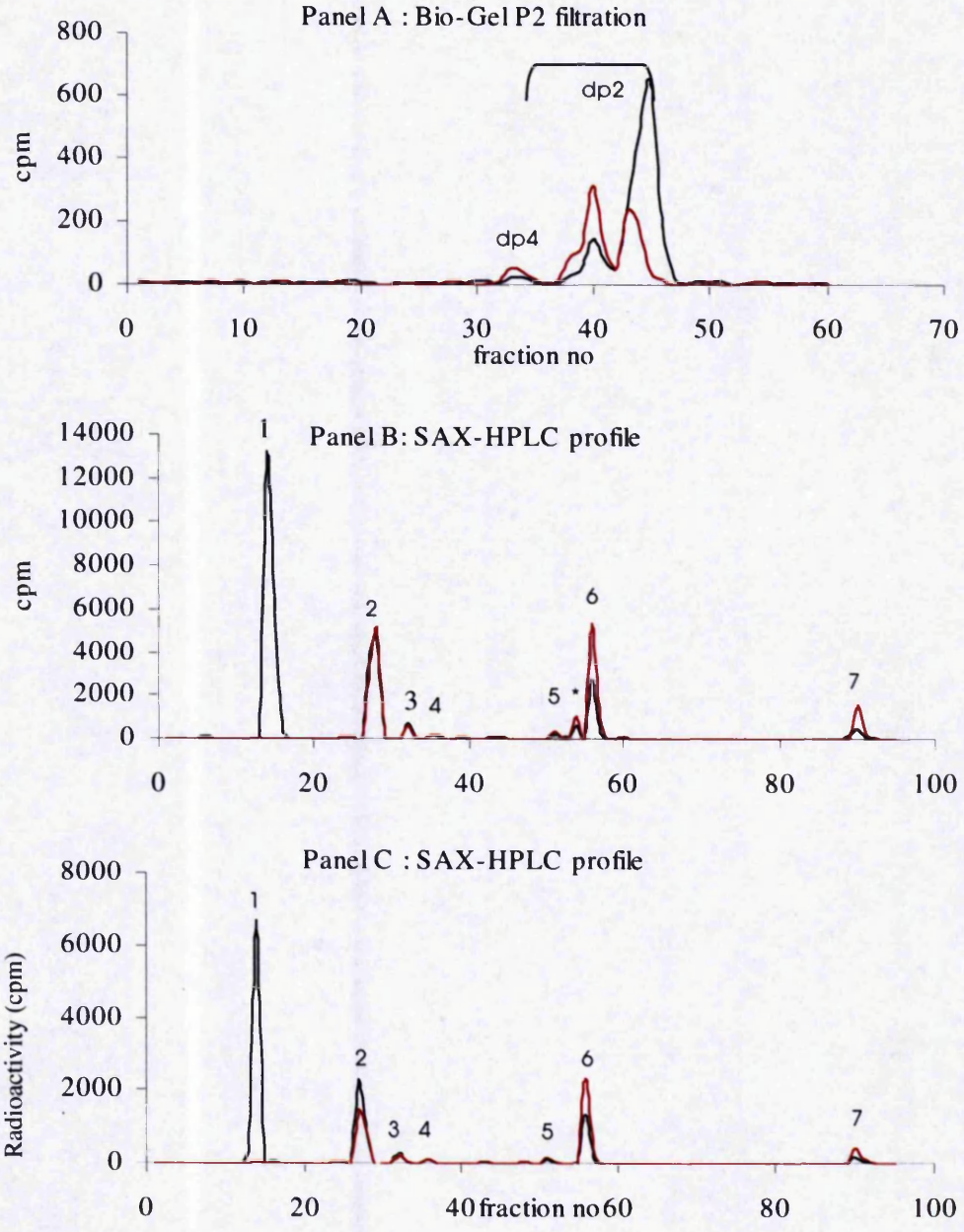

Figure 4.13 : Total disaccharide composition of BAEC HS by strong anion exchange HPLC analysis. Disaccharides were prepared by exhaustive digestion with a combination of heparinases I, II and III, purified by Bio-Gel P2 filtration (Panel A), then resolved on a Pro-Pac PA1 SAX-HPLC column eluted with a 0-1M NaCl, pH3.5 gradient. Fractions collected (1ml for Bio-Gel P2, 0.5ml for SAX-HPLC) were monitored by scintillation counting. The numbered peaks correspond to the elution positions of known disaccharide standards as follows:- 1= UA-GlcNAc; 2=UA-GlcNS; 3=UA-GlcNAc(6S); 4=UA(2S)-GlcNAc; 5=UA-GlcNS(6S); 6=UA(2S)GlcNS; 7=UA(2S)GlcNS(6S). The disaccharide yield obtained from Bio-Gel P2 filtration was 97%. The SAX-HPLC profiles are shown before (Panel B, *denotes resistant tetrasaccharide peak) and after (Panel C) separation of disaccharides using Bio-Gel P2 (^{3}H black line, ^{35}S red line, UA=unsaturated uronic acid).

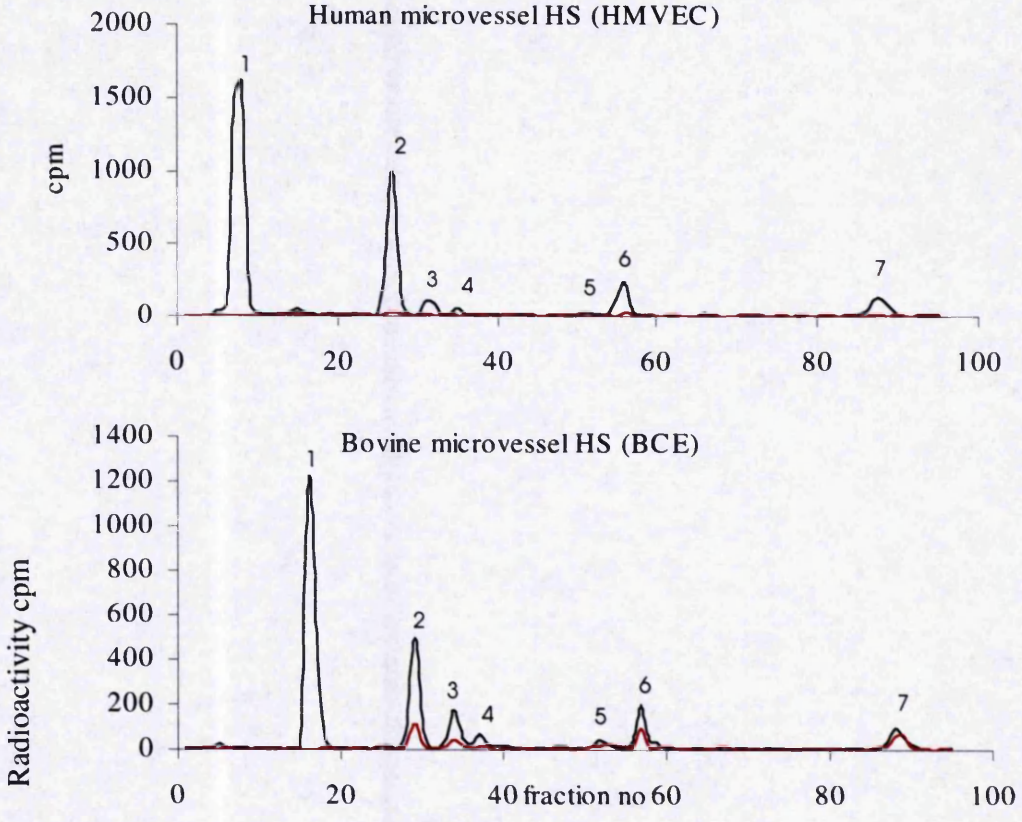

Figure 4.14 : Strong anion-exchange HPLC analysis of human and bovine microvessel HS disaccharides. Disaccharides were prepared by exhaustive digestion with a combination of heparinases I, II and III, then resolved on a Pro-Pac PA1 SAX-HPLC column eluted with a 0-1M NaCl, pH3.5 gradient. Fractions collected (0.5ml) were monitored by scintillation counting. The numbered peaks correspond to the elution positions of known disaccharide standards as follows:- 1= UA-GlcNAc; 2=UA-GlcNS; 3=UA-GlcNAc(6S); 4=UA(2S)-GlcNAc; 5=UA-GlcNS(6S); 6=UA(2S)GlcNS; 7=UA(2S)GlcNS(6S). The disaccharide yield obtained from Bio-Gel P2 filtration was >97% (^{3}H black line ^{35}S red line, UA=unsaturated uronic acid).

Table 4.2a

Standard peak no. (in order of elution)	Disaccharide structure	Total Disaccharides (%) (Means ±SD)		
		HMVEC (n=3)	BCE (n=1)	BAEC (n=3)
1	UA-GlcNAc	58 ± 2	50	58 ± 1.5
2	UA-GlcNS	24 ± 1.6	19	25 ± 1.2
3	UA-GlcNAc(6S)	3 ± 0.6	8	2.6 ± 0.3
4	UA(2S)-GlcNAc	1 ± 0	4	1 ± 0
5	UA-GlcNS(6S)	0.3 ± 0.6	3	1 ± 0
6	UA(2S)-GlcNS	7 ± 3	9	10 ± 0.8
7	UA(2S)-GlcNS(6S)	6 ± 0	6	1.9 ± 0.2

Table 4.2b

Sulphate modification	Content per 100 disaccharides (Means ±SD)		
	HMVEC (n=3)	BCE (n=1)	BAEC (n=3)
N-sulphate	38 ± 3	37	38 ± 2
2-O-sulphate	14 ± 3	19	13 ± 0.8
6-O-sulphate	10 ± 0.6	17	5.4 ± 0.5
Total sulphate	62 ± 5	73	56 ± 2

Table 4.2 : Disaccharide compositions of endothelial cell HS species. The total ^{3}H cpm contributing to each peak in Figures 4.13 and 4.14 was calculated as a percentage of the total ^{3}H of all peaks to obtain the disaccharide compositions (4.2a) and sulphate contents and distributions (4.2b) of HMVEC, BCE and BAEC HS. The data are presented as means ± sd of three independent experiments except for BCE HS due to insufficient material.

4.5 Profiling of endothelial cell S-domains

The preceding investigations suggested that these EC HS species were closely related with the exception of a significantly longer chain length in BAEC HS and variation in the level of 6-O-sulphation. To examine the fine structure of the chains heparinase III digests of between 100K and 4 x 10^6Kcpm ^{3}H-HS were separated using Bio-Gel P10 chromatography to obtain disaccharides and S-domains in the range dp 4 - ≥dp12. The gel filtration profiles from which the S-domains were pooled did not differ significantly from the analytical profiles shown in Figure 4.10. Preparative heparinase III digests were performed identically to analytical digests but were more likely to be incomplete, therefore small aliquots were tested (by Bio-Gel P-10 filtration) and further aliquots of enzyme added as necessary. Once complete digestion was confirmed the total digest was resolved by Bio-Gel P10 chromatography and the eluant monitored by taking small aliquots for scintillation counting. The resulting profile was used to determine the central regions of the peaks corresponding to dp2,4,etc. for recovery (Figure 4.15). The ^{3}H cpm present in pooled samples was checked at all purification steps to ensure that significant losses during purification (mainly de-salting) were minimal. Disaccharides elute close to the void on PD-10 desalting columns. However this problem did not need to be addressed as the abundant radioactivity in the sample enabled small ≤20µl volumes in 0.1M NaCl from Bio-Gel P10 to be diluted in 1ml water for direct application to a Pro-Pac PA1 SAX-HPLC column.

The heparinase III released disaccharides from the EC HS species were consistent with the specificity of this enzyme and are presented in Table 4.3. The majority of the disaccharides (68-77%) were non-sulphated [UA-GlcNAc] in each case and of the remainder, [UA-GlcNS] type disaccharides were predominant reflecting the preference of heparinase III for linkages between poorly sulphated disaccharides. Comparing these results to the total disaccharide compositions given in Table 4.3, the 2-O-sulphated disaccharides resist heparinase III consistent with the tendency for 2-O-sulphation to occur on iduronate residues. This also locates these disaccharides in the heparinase III resistant S-domains. Similarly, heparinase III does not release any trisulphated disaccharides, positioning them exclusively within the S-domains. In contrast the majority of unmodified and mono- N-sulphated disaccharides are not located within the S-domains.

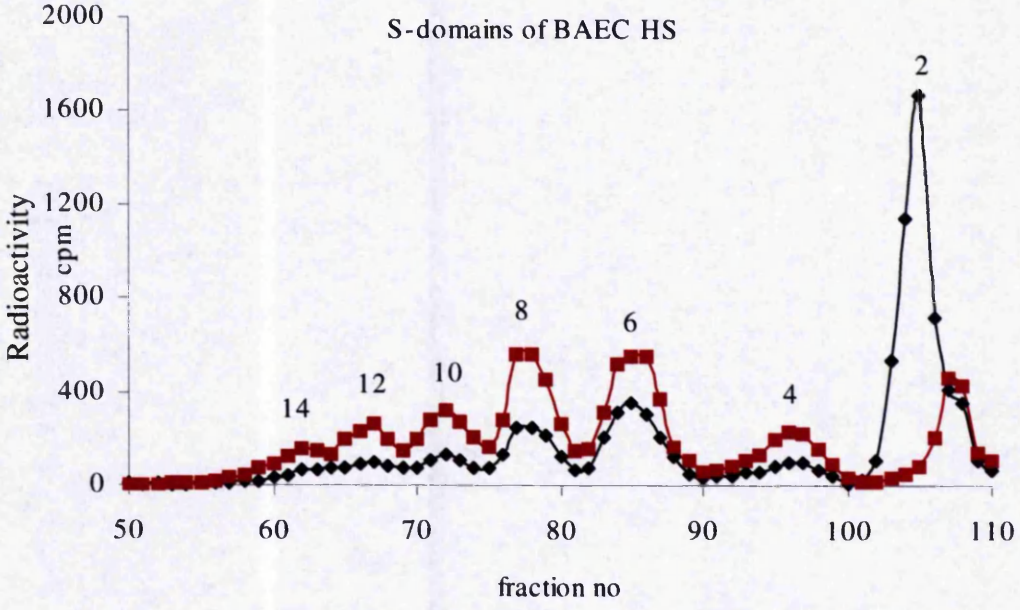

Figure 4.15 : BioGel P-10 separation of S-domains generated by heparinase III digestion of HS chains from bovine macrovessel endothelial cells (BAEC). Heparinase III digestion was performed on 100K- $4x10^6$K cpm of ^{3}H-HS. Following digestion, the sample was loaded onto a P-10 column (1cm x 140 cm) in a maximum of 1ml. The column was eluted with 0.1M NaCl, pH8.8, at a flow rate of 4ml/hour and 1 ml fractions collected. The elution profiles were monitored by taking 20-100µl aliquots for scintillation counting (^{3}H black line ^{35}S red line). The numbers above the peaks correspond to the degree of polymerisation (dp) or number of saccharide units, therefore dp2 = disaccharide etc. The central regions of each peak (usually 3-5 fractions) were pooled and de-salted.

STANDARD PEAK NO. (in order of elution)	DISACCHARIDE STRUCTURE	HEPARINASE III RELEASED DISACCHARIDES %		
		HMVEC	BCE	BAEC
1	UA-GlcNAc	68	77	71
2	UA-GlcNS	26	17	26
3	UA-GlcNAc(6S)	6	6	2
4	UA(2S)-GlcNAc			
5	UA-GlcNS(6S)	0	0	1
6	UA(2S)-GlcNS			
7	UA(2S)-GlcNS(6S)			

Table 4.3 : Disaccharide composition of heparinase III sensitive regions of EC HS. Disaccharides recovered from Bio-Gel P10 chromatography of heparinase III digested ^{3}H-HS were resolved on a Pro-Pac PA1 SAX-HPLC column eluted with a 0-1M NaCl, pH 3.5 gradient. Fractions collected (0.5 ml) were monitored by scintillation counting and identified according to elution positions of known standards. Proportions of disaccharides were calculated from the total cpm ^{3}H in each peak.

Interestingly, a significant proportion of the [UA-GlcNAc(6S)] disaccharides, are also excised by heparinase III. This is consistent with the location of these disaccharides in the transition zones (Figure 1.2).

Following recovery, de-salting and rehydration in water, size-defined S-domains were resolved, according to charge, by SAX-HPLC, using the conditions for purification of homogeneous saccharides and S-domain profiling as described in Methods. Sufficient quantities of S-domains were generated to examine dp4,6 and 8 for all EC HS species. For BAEC HS, four analyses on three independent preparations of cells were performed, two independent analyses were carried out on HMVEC HS and only one on BCE HS. Two independent analyses of BAEC S-domains of dp10 and dp12 were also possible but there was insufficient HS from the microvascular ECs to profile their S-domains in this size range.

The profiles were found to be highly reproducible as previously demonstrated for 3T3 fibroblast cell HS (Merry *et al.*, 1999). The S-domains of dp4 were compared by resolution on SAX-HPLC and found to contain one dominant tetrasaccharide species (denoted 4a, Figure 4.16) with 2-3 minor species. The, S-domain dp4a eluted at an identical position to the dominant heparinase III resistant tetrasaccharide isolated from 3T3 fibroblast HS (Merry *et al.*, 1999). In addition, resolution of dp6 S-domains by SAX-HPLC, revealed four main species denoted 6a-d, that shared almost identical elution positions to each other and to 3T3 HS dp6 (Figure 4.17). Closer inspection of the profiles revealed proportional differences in expression of these species. Notably, dp6d, the most highly charged S-domain of this size, was relatively increased in both of the microvessel EC species compared to the macrovessel HS.

In contrast, the SAX-HPLC profiles of resolved dp8 S-domains from the BAEC macrovessel ECs are distinct from the two microvessel species, but exhibit close identity to the 3T3 cells (Figure 4.18). Inspection of the BAEC dp8 profiles reveals 6 main (a-e) and 2 minor (c* and f*) species reflecting increasing scope for structural heterogeneity within longer oligosaccharides compared to the dp6. Greater heterogeneity of structures compared to dp6 is also apparent on examination of the microvessel dp8 profiles but in contrast to BAEC and 3T3 there are fewer dominant

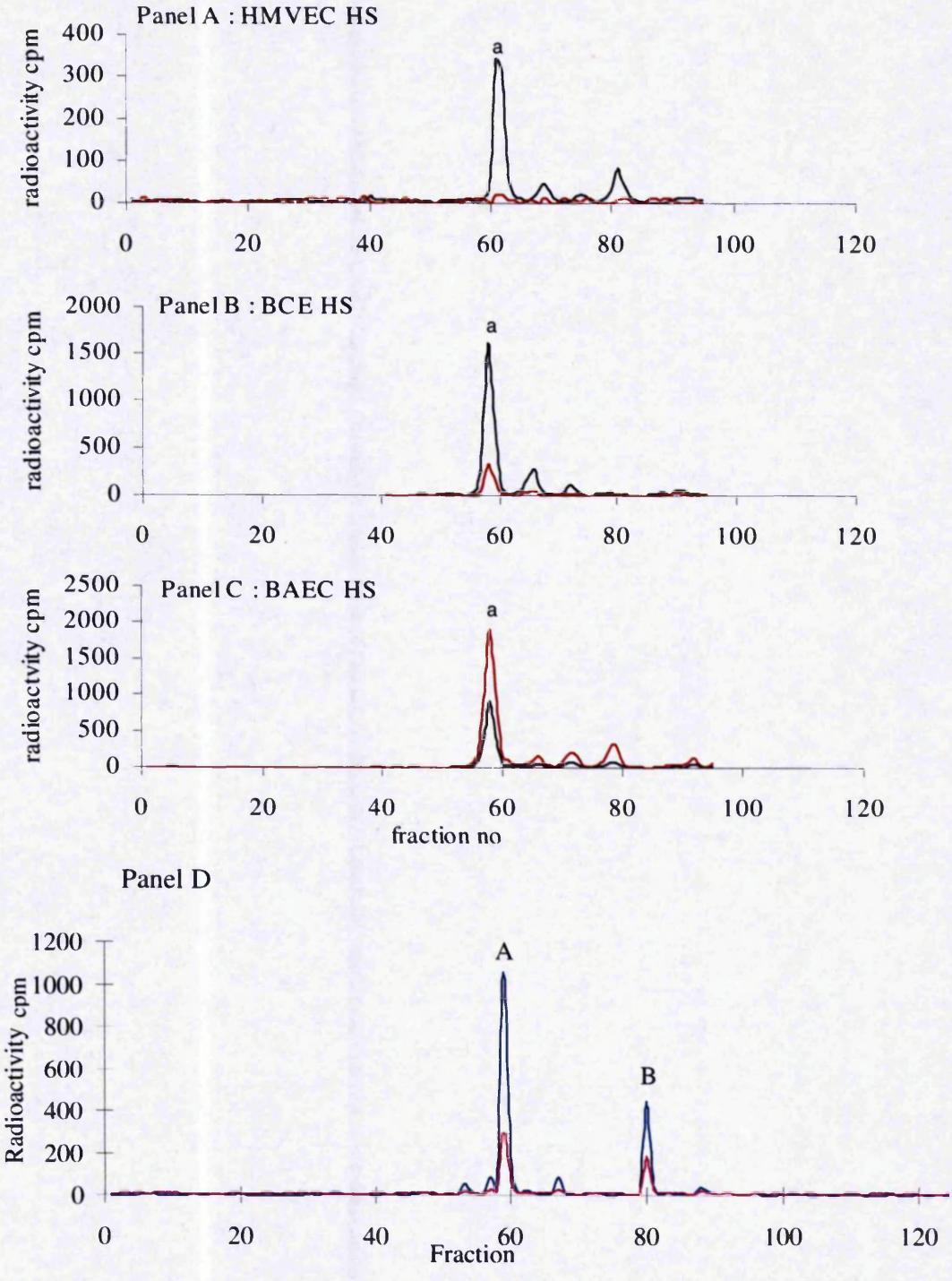

Figure 4.16 : S-domain profiling by SAX chromatography of S-domains (dp4)
Heparinase III generated dp4 from ^{3}H-HS were recovered from Bio-Gel P10 filtration, desalted and eluted from a single Pro-Pac PA1 column with a linear gradient of 0-1M NaCl in milliQ water, pH 3.5 over 80 minutes, at a flow rate of 1 ml/min and 0.5ml fractions were collected. Elution profiles were monitored by scintillation counting (^{3}H black line ^{35}S red line). Typical profiles are shown for HMVEC (Panel A), BCE (Panel B), BAEC (Panel C), and 3T3 fibroblast HS (Panel D). Profile in Panel D obtained from C Merry, with kind permission, ^{3}H blue line ^{35}S pink line.

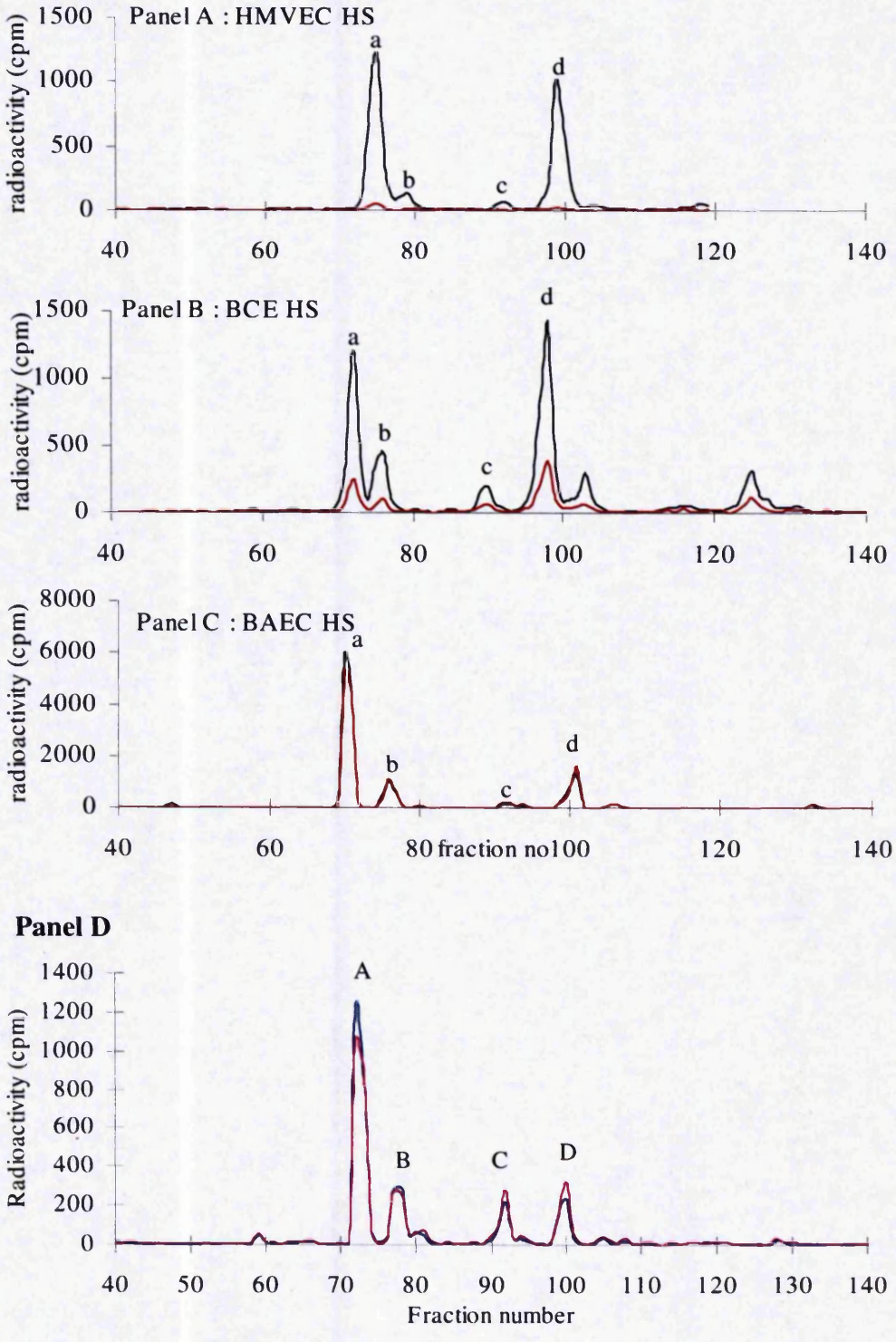

Figure 4.17 : S-domain profiling by SAX chromatography of S-domains (dp6) Heparinase III generated dp6 from ^{3}H-HS were recovered from Bio-Gel P10 filtration, desalted and eluted from a single Pro-Pac PA1 column with a linear gradient of 0-1M NaCl in milliQ water, pH 3.5 over 80 minutes, at a flow rate of 1 ml/min and 0.5ml fractions were collected. Elution profiles were monitored by scintillation counting (^{3}H black line ^{35}S red line). Profiles are shown for HMVEC (Panel A), BCE (Panel B), BAEC (Panel C), and Panel D of 3T3 dp6 is reproduced from Merry et al.,1999 with kind permission, ^{3}H blue line ^{35}S pink line.

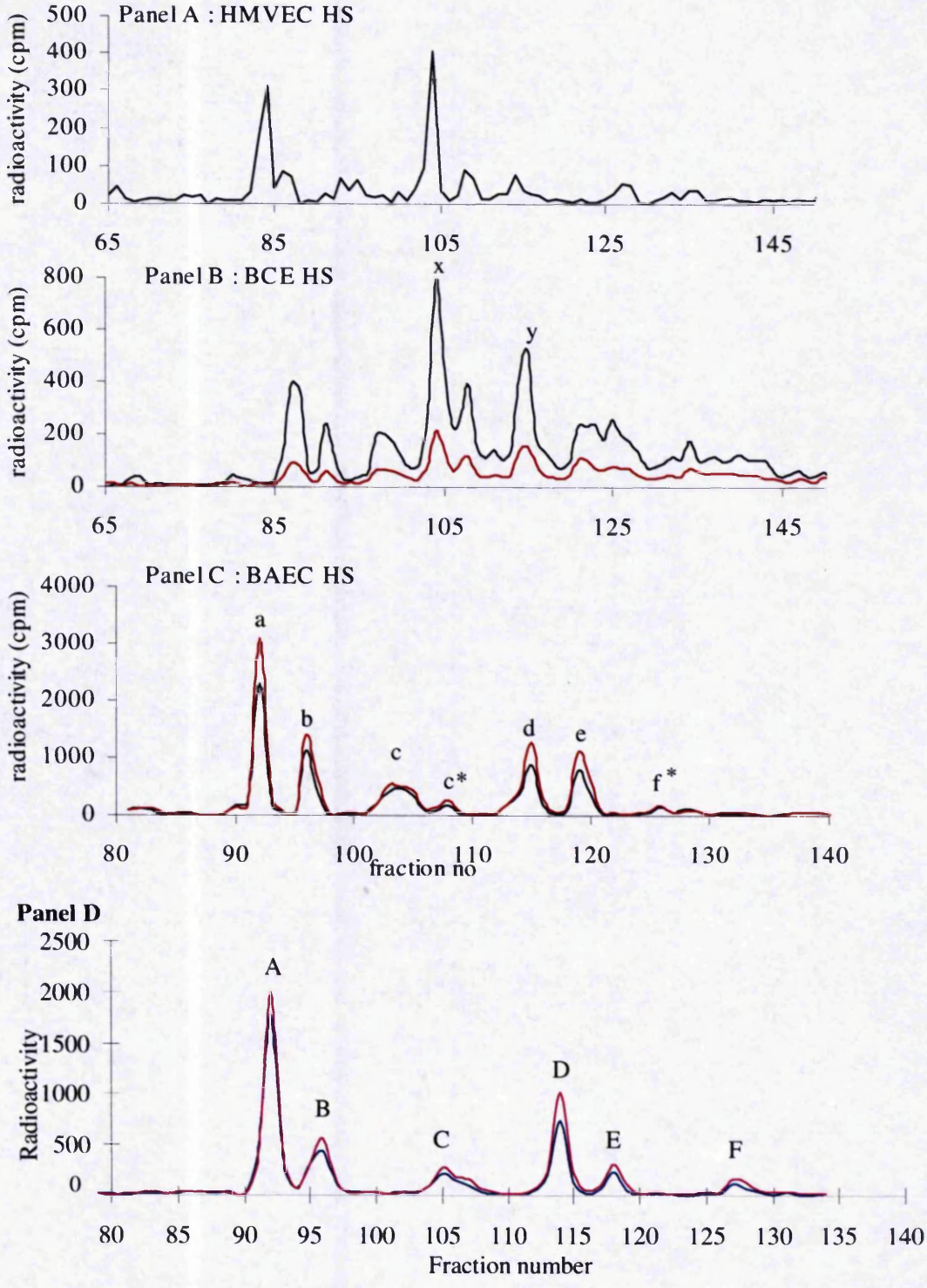

Figure 4.18 : S-domain profiling by SAX chromatography of S-domains (dp8)
Heparinase III generated dp8 from ^{3}H-HS were recovered from Bio-Gel P10 filtration, desalted and eluted from a single Pro-Pac PA1 column with a linear gradient of 0-1.2M NaCl in milliQ water, pH 3.5 over 90 minutes, at a flow rate of 1 ml/min and 0.5ml fractions were collected. Elution profiles were monitored by scintillation counting (^{3}H black line ^{35}S red line). Profiles are shown for HMVEC (Panel A), BCE (Panel B), BAEC (Panel C), and Panel D of 3T3 dp8 is reproduced from Merry et al.,1999 with kind permission, ^{3}H blue line ^{35}S pink line.

species and multiple minor species occurring in a less well resolved cluster around the middle of the NaCl gradient. Interestingly, although distinct from the BAEC and 3T3 cell HS profiles, the microvessel profiles are similar to each other, suggesting that there may be a predetermined design of these S-domains.

In view of the unexpected identity between the S-domains of BAEC and 3T3 fibroblast HS the cells were checked for EC morphology and markers. The 3T3 fibroblasts exhibited a typical fibroblastic morphology and were negative for the EC markers, vWF and CD31 (data not shown). As previously demonstrated (Figures 4.1-3), the ECs had a cobblestone morphology and strong immunostaining for EC markers. Culture of BCE cells in identical media to 3T3 and BAEC cells also indicated that the conserved S-domain structures could not be explained as an artefact of growth conditions *in vitro*.

Profiling of the dp10 and dp12 S-domains of BAEC HS by SAX-HPLC is shown in Figure 4.19. The S-domain structures are more heterogeneous than the shorter S-domains described above. The complex profiles show several major peaks and a number of minor peaks in each that indicate structures of similar charge with positional differences in sulphate pattern. These profiles reflect the increasing sequence variation as a function of domain length consistent with previous analyses (Vives *et al.*,1999). Also, in contrast to the shorter S-domains the dp10 and dp12 profile in BAEC HS is quite distinct from that of 3T3 fibroblast HS (3T3 dp12 profile not shown) confirming their separate identities.

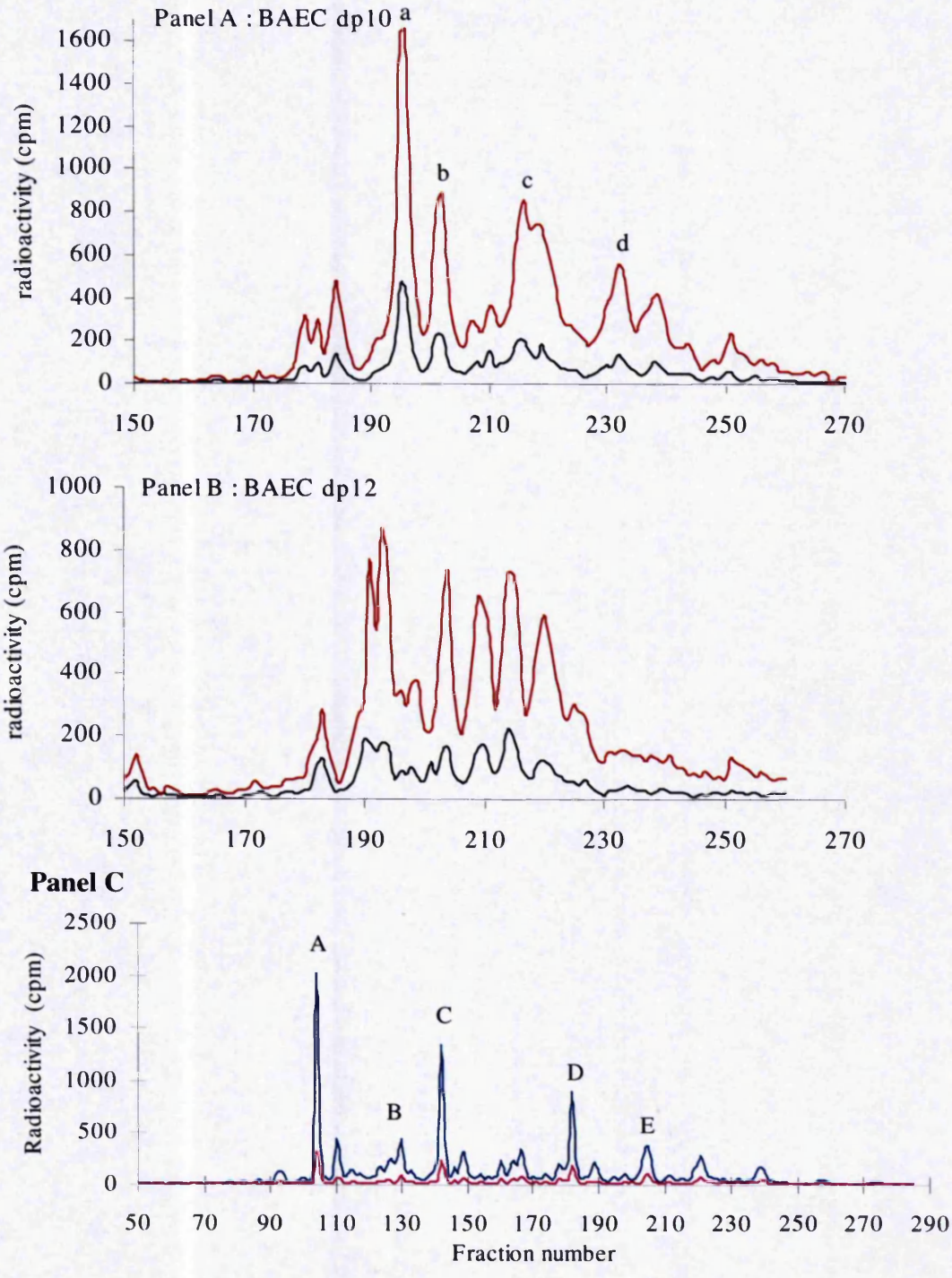

Figure 4.19 : S-domain profiling by SAX chromatography of S-domains (dp10 and dp12) Heparinase III generated dp10 & 12 from ^{3}H-HS were recovered from Bio-Gel P10 filtration, desalted and eluted from a single Pro-Pac PA1 column with a linear gradient of 0-1.2M NaCl in milliQ water, pH 3.5 over 180 minutes, at a flow rate of 1 ml/min and 0.5ml fractions were collected. Elution profiles were monitored by scintillation counting (^{3}H black line ^{35}S red line). Panel C of 3T3 dp10 is reproduced from Merry et al.,1999 with kind permission (^{3}H blue line ^{35}S pink line). Note that fraction 50 in Panel C corresponds to fraction 150 in Panels A and B etc.

4.6 Sequencing of selected S - domains from BAEC HS

For sequencing of metabolically radiolabelled HS using the technique of Merry *et al.*,1999, 30-40Kcpm ^{3}H-HS is optimal. It was possible to generate this quantity of BAEC S-domain 6a, and ~20K of BAEC S-domain 8a, for sequencing. This allowed us to determine whether their identical elution positions to 6A and 8A from 3T3 fibroblast HS on SAX-HPLC purification corresponded to the same structures.

The technique essentially involves :

1. Partial nitrous acid digestion to open up the oligosaccharide at internal GlcNS residues (Figure 1.4). By stopping the reaction at various time points intermediates are generated for further profiling by SAX-HPLC. The effects of specific exoenzymes on the elution positions of the partial nitrous acid generated fragments enable O-sulphate groups, glucuronate and iduronate residues to be pinpointed and component disaccharides to be ordered within the chain.
2. Analysis of disaccharide composition by SAX-HPLC and their stoichiometry (calculated from the ^{3}H content present in each peak) in the oligosaccharide to confirm the sequence.

Sequencing of 6a

BAEC S-domain species 6a (~5K cpm ^{3}H) was depolymerised to disaccharides using heparinases I and II and the products resolved by SAX-HPLC. The resulting profile shown in Figure 4.20 shows three disaccharide peaks UA-GlcNAc: UA-GlcNS: UA(2S)-GlcNS corresponding to a molar ratio of 1:1:1 (derived from the ^{3}H content) relative to that of the common disaccharide that occurs once at the nonreducing end of each oligosaccharide due to the specificity of heparinase III. The ^{35}S:^{3}H ratio provides further confirmation of 1 nonsulphated : 1 monosulphated : 1 disulphated disaccharide. This disaccharide composition exactly matched that of 3T3 dp6A eluting in the same position (See Appendix 1 for 3T3 fibroblast HS S-domain structures).

Next, to establish the order of the disaccharides and assign the uronate residues as either GlcA or IdoA, the remaining material ~35K cpm ^{3}H, was partially depolymerised using dilute nitrous acid and the scission products separated by SAX-HPLC. Nitrous acid

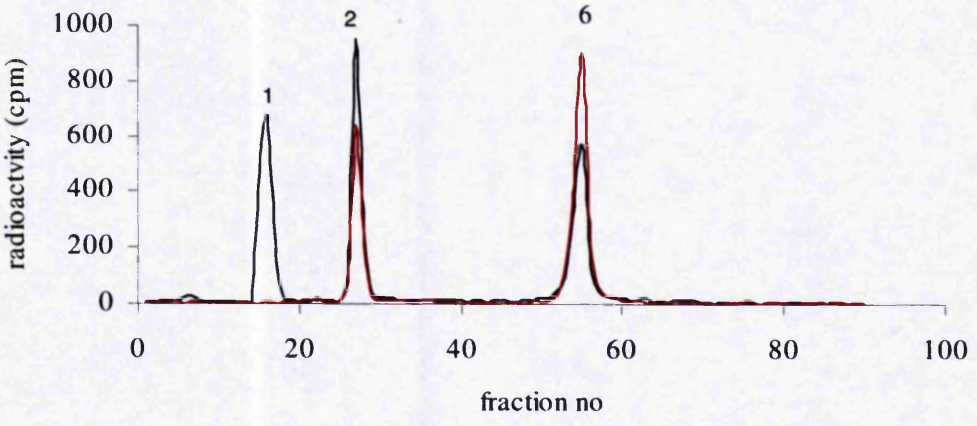

Figure 4.20 : Disaccharide composition of BAEC S-domain dp6a by strong anion exchange HPLC analysis. Disaccharides were prepared by digestion with a combination of heparinases I and II then resolved on a Pro-Pac PA1 SAX-HPLC column eluted with a 0-1M NaCl, pH3.5 gradient over 45 minutes. Fractions collected (0.5ml) were monitored by scintillation counting. The numbered peaks correspond to the elution positions of known disaccharide standards as follows:- 1=UA-GlcNAc; 2=UA-GlcNS; 6=UA(2S)GlcNS. (^{3}H black line, ^{35}S red line, UA=unsaturated uronic acid).

effects deaminative scission of glycosidic linkages of GlcNS-HexA, releasing inorganic $^{35}SO_4$, and converting GlcNS to anhydromannose (aMan). By using dilute nitrous acid as described (Radoff & Danishefsky, 1985) with aliquots of the reaction stopped at a number of time points, a range of intermediates is generated. Figure 4.21, Panel A, shows peaks corresponding to nonsulphated disaccharides (labelled non-S; IdoA-aMan, GlcA-aMan, Δ UA-aMan, Δ UA-GlcNAc), the sulphated disaccharide IdoA(2S)-aMan (fraction 45, ISM), free $^{35}SO_4$ (fraction 38), two tetrasaccharides (fractions 78 and 95, designated R4 - reducing end and U4 - unsaturated uronate from heparinase III/nonreducing end) and the original hexasaccharide at fraction 118. The disaccharides were identified by comparison with known standards and the tetrasaccharides by comparison with 3T3 fibroblast HS species that were sized by Bio-Gel P10 and of known elution position. The presence of two tetrasaccharides indicates two internal GlcNS residues (Figure 1.4) and species U4, due to its unsaturated uronate is resistant to exoenzymes whereas R4 is susceptible.

After desalting the nitrous acid treated material, aliquots of ≥5K cpm ^{3}H, were treated with exoenzymes as described in methods and Figure 4.21 shows the resulting products of glucuronidase (Panel B), iduronidase (Panel C) and 2-sulphatase (Panel D) digestion. The profiles are compared to the partial nitrous acid profile (Panel A) and Panel B shows no shifts in peaks to indicate the presence of GlcA. Neither U4 or R4 change in elution position after treatment with iduronidase (Panel C). However, an early GlcNAc peak appears with a decrease in the non-S peak identifying one disaccharide as IdoA-GlcNAc. Since there are two tetrasaccharides, there must be two internal GlcNS residues so this places IdoA-GlcNAc at the reducing end of the hexasaccharide. From the specificity of heparinase III, Δ UA-GlcNS is positioned at the non-reducing end and the internal disaccharide must be UA2S-GlcNS. This is confirmed by the action of 2-O-sulphatase with a shift in R4 to fraction 45. The uronate in R4 from which 2-O-sulphate was removed is then identified by the ability of iduronidase or glucuronidase, to cause a further shift in the peak to the left however there was insufficient material to perform this analysis. Alternatively, it can be inferred from the presence of the ISM peak, since the other 2 disaccharides are not O-sulphated. This peak also shifts to the left (and co-elutes with the non-S peak) upon treatment with 2-O-sulphatase.

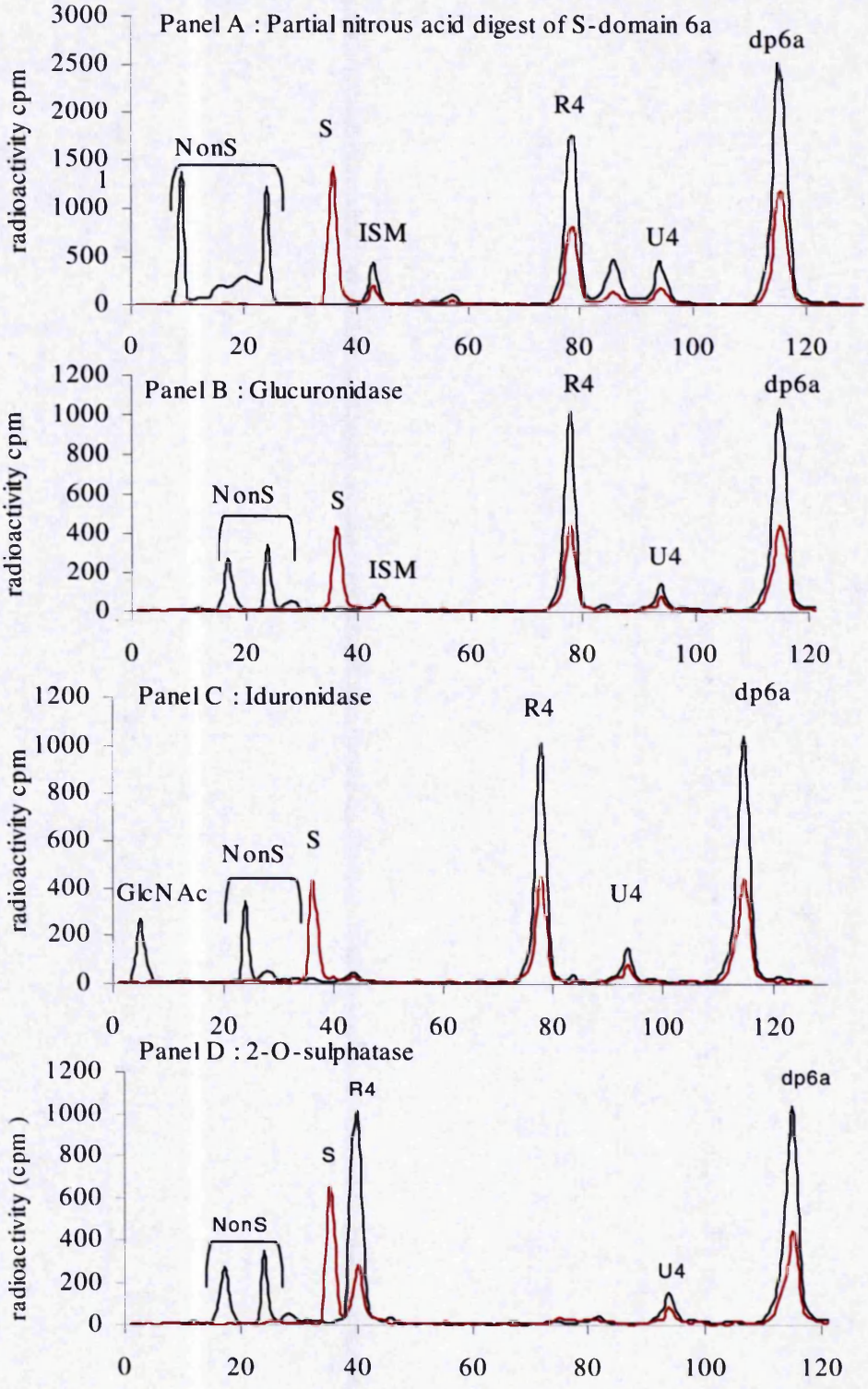

Figure 4.21: Sequence analysis of BAEC S-domain 6a. Dilute nitrous acid scission was used to generate a range of fragments from dp6a that were resolved on a Pro-Pac PA1 column eluted with a linear 0-0.75M NaCl gradient over 110 minutes (Panel A). Aliquots of these fragments (≥5K cpm ^{3}H), were treated with glucuronidase (Panel B), iduronidase (Panel C) or 2-O-sulphatase (Panel D). Fractions (0.5ml) were collected and monitored for radioactivity by scintillation counting (^{3}H black line, ^{35}S red line). Identified peaks are nonsulphated disaccharides (non-S), the IdoA(2S)-aMan (fraction 45, ISM), free $^{35}SO_4$(S, fraction 38), two tetrasaccharides (fractions 78 and 95, designated R4 - reducing end and U4 - unsaturated uronate from nonreducing end) and the original hexasaccharide at fraction 118.

The structure of BAEC dp6a was therefore found to be identical to 3T3 dp6a (Merry *et al.*,1999, Appendix 1) :

ΔUA-GlcNS – IdoA(2S)-GlcNS – IdoA - GlcNAc

ΔUA-GlcNS – IdoA(2S)-GlcNS **U4**

R4 IdoA(2S)-GlcNS – IdoA - GlcNAc

Sequencing of BAEC S-domain 8a

BAEC S-domain species 8a (~5K cpm ^{3}H) was depolymerised to disaccharides using heparinase I and II and the products resolved by SAX-HPLC. The resulting profile shown in Figure 4.22 shows three peaks UA-GlcNAc, UAGlcNS and UA(2S)GlcNS corresponding to a molar ratio of 1:1:2 (derived from the ^{3}H content) relative to that of the common disaccharide that occurs once at the nonreducing end of each oligosaccharide due to the specificity of heparinase III (UAGlcNS). The ^{35}S:^{3}H content provides further confirmation of 1 nonsulphated : 1 monosulphated : 2 disulphated disaccharides. This disaccharide composition exactly matched that of 3T3 dp8A that co-eluted on SAX-HPLC (Merry *et al.*,1999, Appendix 1).

A sufficient quantity of BAEC 8a was available for depolymerisation with partial nitrous acid and subsequent treatment with iduronidase. As observed for BAEC 6a, the partial nitrous acid generated intermediates of BAEC 8a co-eluted on SAX-HPLC with those obtained previously for 3T3 dp8A (Figure 4.23). Iduronidase treatment identified the presence of an IdoA-GlcNAc, again positioned at the reducing end due to the action of heparinase III and the presence of 3 internal GlcNS residues inferred from the generation of three different tetrasaccharides and two hexasaccharides by nitrous acid. Thus, although there was insufficient material for all the sequencing steps it was possible to use data from

sequencing of 3T3 fibroblast HS S-domains as a standard to assign the following structure to 8a :

ΔUA-GlcNS – Ido(2S)-GlcNS- Ido (2S) – GlcNS – IdoA – GlcNAc

ΔUA-GlcNS – Ido(2S)-GlcNS **U4**

R4 Ido (2S) – GlcNS – IdoA – GlcNAc

M4 Ido(2S)-GlcNS- Ido (2S) – GlcNS

R6 Ido(2S)-GlcNS- Ido (2S) – GlcNS – IdoA – GlcNAc

ΔUA-GlcNS – Ido(2S)-GlcNS- Ido (2S) – GlcNS **U6**

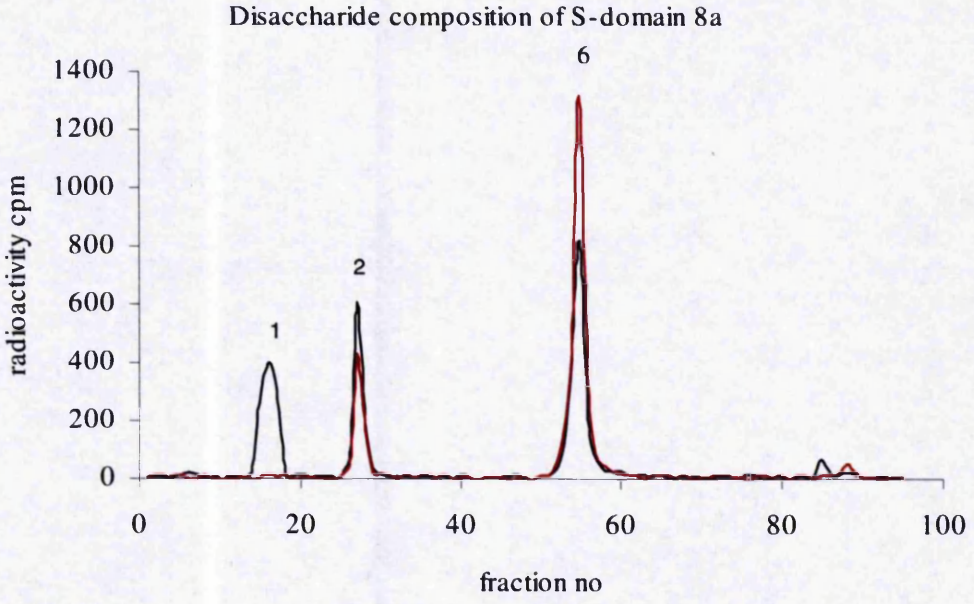

Figure 4.22 : Disaccharide composition of BAEC S-domain 8a by strong anion exchange HPLC analysis. Disaccharides were prepared by digestion with a combination of heparinases I and II then resolved on a Pro-Pac PA1 SAX-HPLC column eluted with a 0-1M NaCl, pH3.5 gradient over 45 minutes. Fractions collected (0.5ml) were monitored by scintillation counting. The numbered peaks correspond to the elution positions of known disaccharide standards as follows:- 1= UA-GlcNAc; 2=UA-GlcNS; 6=UA(2S)GlcNS. (^{3}H black line, ^{35}S red line, UA=unsaturated uronic acid).

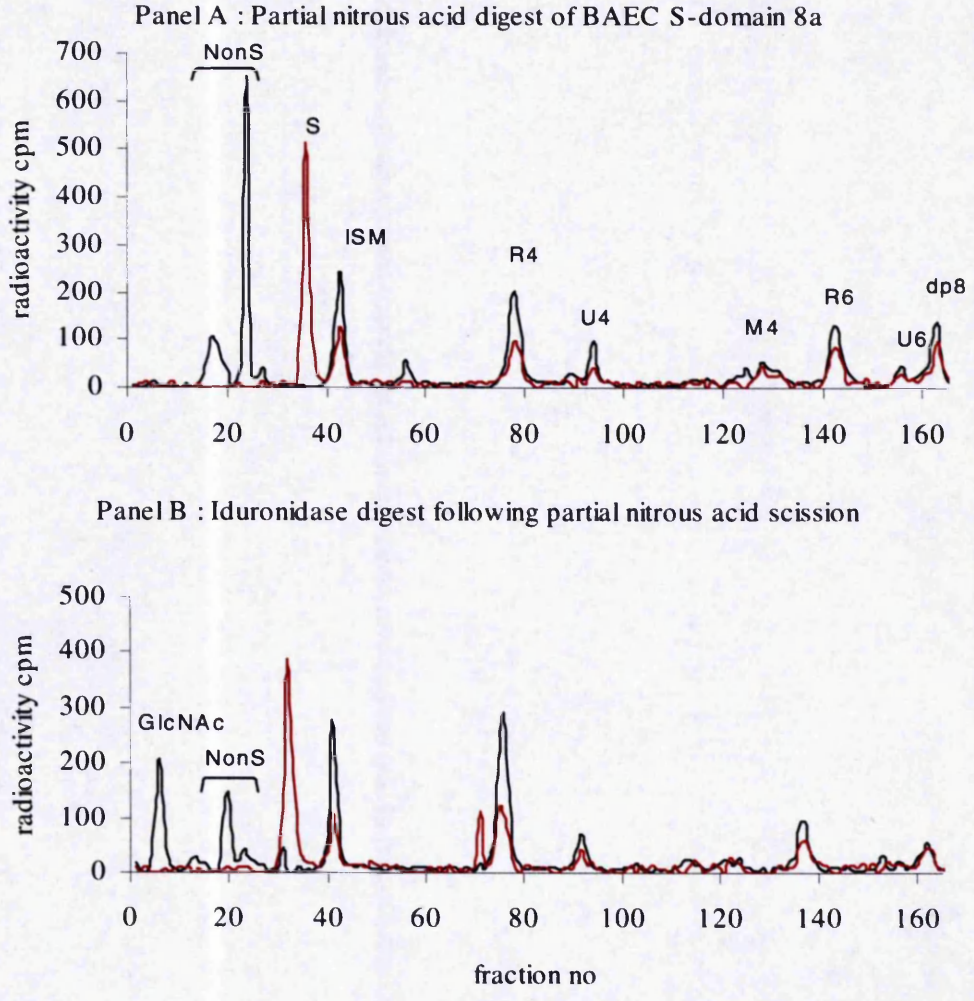

Figure 4.23: Sequence analysis of BAEC S-domain 8a. Dilute nitrous acid scission was used to generate a range of fragments from dp8a that were resolved on a Pro-Pac PA1 column eluted with a linear 0-0.75M NaCl gradient over 110 minutes (Panel A). The sample was treated with iduronidase (Panel B) Fractions (0.5ml) were collected and monitored for radioactivity by scintillation counting (^{3}H black line, ^{35}S red line). Identified peaks are nonsulphated disaccharides (non-S; IdoA-aMan, GlcA-aMan, Δ UA-aMan), the sulphated disaccharide IdoA(2S)-aMan (fraction 45, ISM), free $^{35}SO_4$(fraction 38), three tetrasaccharides (fractions 78,95,125 designated R4 - reducing end, U4 - unsaturated uronate from heparinase III/nonreducing end, M4 – middle tetrasaccharide) hexasaccharides R6 and U6 and the intact octasaccharide at fraction 165.

These analyses confirmed the broad applicability of this novel sequencing technique to other metabolically radiolabelled HS species and demonstrated unanticipated conservation of S-domain structure between HS from different cell types.

4.7 Disaccharide composition of BAEC octasaccharide S-domains

The disaccharide compositions of aliquots of the remaining BAEC S-domain octasaccharides (~3-5K cpm) were obtained by digestion of oligosaccharides with heparinases I and II, followed by separation on SAX-HPLC as previously described. The profiles are shown in Figure 4.24 and the disaccharide compositions in Table 4.4. The compositions of four of the octasaccharides 8a,b,d and e exactly matched those obtained previously for 3T3 fibroblast HS dp8 that co-eluted on SAX-HPLC (Figure 4.18, Appendix 1). The disaccharide compositional analysis does not indicate the epimer of uronate residues. However, sequencing of 3T3 8A,B,D and E (Merry *et al.*, 1999) gave the following structures ;

8A ΔUA-GlcNS-Ido(2S)-GlcNS-Ido(2S)-GlcNS-IdoA-GlcNAc
8B ΔUA-GlcNS-Ido(2S)-GlcNS-Ido(2S)-GlcNS-GlcA-GlcNAc
8D ΔUA-GlcNS-Ido(2S)-GlcNS(6S)-Ido(2S)-GlcNS-IdoA-GlcNAc
8E ΔUA-GlcNS-Ido(2S)-GlcNS(6S)-Ido(2S)-GlcNS-GlcA-GlcNAc

It can be seen that the only difference between 3T3 8A and B, is the C5 epimer of the reducing end uronate residue. This is also the case for 3T3 8D and E. The structure of BAEC dp8a was found to contain a reducing end iduronate residue by sequencing, therefore, from the disaccharide analyses and SAX-HPLC elution positions for BAEC b,d and e, it is reasonable to infer identity to their 3T3 fibroblast HS counterparts 8,B,D and E.

In contrast the stoichiometry of disaccharides present in 8c and 8c* reveal that neither species is pure, as may have been anticipated from the less well resolved peak of the initial separation profile (Figure 4.18). Nevertheless, both of these species contain 6-O-sulphate but species substituted with 6-O-sulphate were not detected at these elution

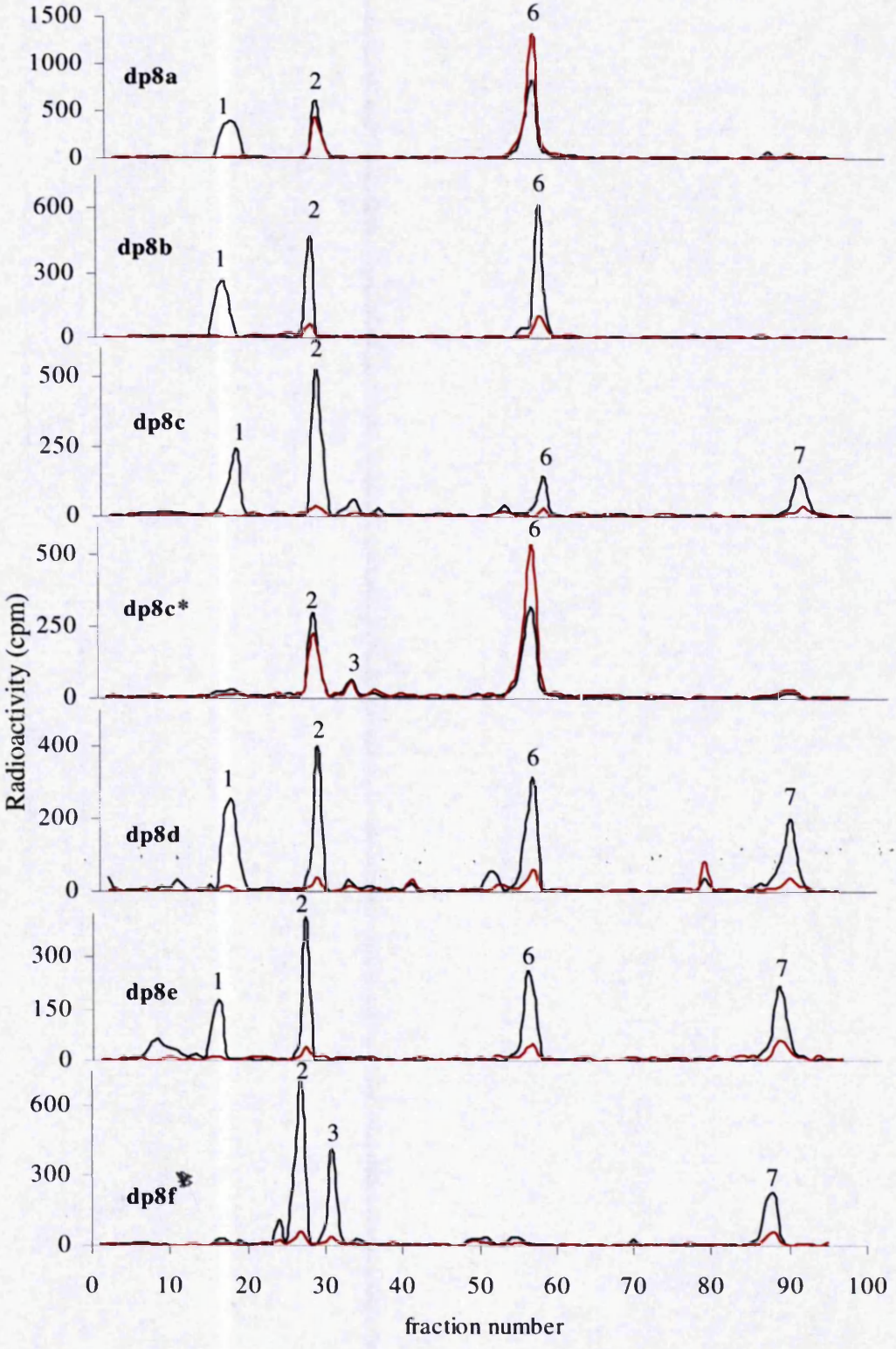

Figure 4.24 : Disaccharide composition of BAEC octasaccharide S-domains by SAX-HPLC analysis. Disaccharides were prepared by digestion with a combination of heparinases I and II, then resolved on a Pro-Pac PA1 SAX-HPLC column eluted with a 0-1M NaCl, pH3.5 gradient over 45 minutes. Fractions collected (0.5ml) were monitored by scintillation counting. The numbered peaks correspond to the elution positions of known disaccharide standards as follows:- 1= UA-GlcNAc; 2=UA-GlcNS; 3=UA-GlcNAc(6S); 4=UA(2S)-GlcNAc; 5=UA-GlcNS(6S); 6=UA(2S)GlcNS; 7=UA(2S)GlcNS(6S). (^{3}H black line ^{35}S red line, UA=unsaturated uronic acid).

Table 4.4A

DISACCHARIDE STRUCTURE	(%) DISACCHARIDE PER OCTASACCHARIDE						
	Dp8a	Dp8b	Dp8c	Dp8c*	Dp8d	Dp8e	Dp8f*
UA-GlcNAc	28	27	24		28	26	
UA-GlcNS	26	27	45	39	24	24	51
UA-GlcNAc(6S)				9			26
UA(2S)-GlcNAc							
UA-GlcNS(6S)							
UA(2S)-GlcNS	46	46	12	52	29	26	
UA(2S)-GlcNS(6S)			18		18	26	23

Table 4.4B

SULPHATE MODIFICATION	NUMBER OF SULPHATE GROUPS PER OCTASACCHARIDE						
	Dp8a	Dp8b	Dp8c	Dp8c*	Dp8d	Dp8e	Dp8f*
N-sulphate	2.88	2.92	3.00	3.64	2.84	3.03	2.96
2-O-sulphate	1.84	1.84	1.20	2.08	1.88	2.06	0.94
6-O-sulphate	0	0	0.72	0.36	0.72	1.03	1.98
Total sulphate	4.72	4.76	4.92	6.08	5.44	6.12	5.88

Table 4.4 : Disaccharide composition and sulphate distribution of BAEC octasaccharide S-domains. The total ^{3}H cpm contributing to each peak in Figure 4.24 was calculated as a percentage of the total ^{3}H of all peaks to obtain the disaccharide compositions (4.4A). The proportions were used to estimate the number of sulphate modifications per octasaccharide (4.4B).

positions for 3T3 fibroblast HS octasaccharide S-domains. The remaining BAEC S-domain 8f* is a minor and complex peak. The stoichiometry of this species suggested that it was near homogeneous with a 2:1:1 ratio of ΔUA-GlcNS, UA-GlcNAc(6S) and UA(2S)GlcNS(6S). This would suggest a structure like :

ΔUA-GlcNS - UA(2S)GlcNS(6S) - UA-GlcNS - UA-GlcNAc(6S)

This type of S-domain was not observed in 3T3 HS. Therefore within the octasaccharide S-domains some variations in structure are evident between 3T3 and BAEC HS despite conservation of the dominant forms (8a,b,d,e).

4.8 Disaccharide composition of BCE octasaccharide S-domains

The disaccharide compositions of aliquots of the dominant BCE S-domain octasaccharides (~3-5K cpm) denoted 8x and 8y (Figure 4.18, Panel B) were obtained by digestion of oligosaccharides with heparinases I and II, followed by separation on SAX-HPLC, as previously described. Ideally, particularly if sequencing is planned, after pooling an S-domain peak of interest, an aliquot should be reapplied to the SAX-HPLC column and eluted with the same conditions as the initial purification to ensure the presence of a single species. The small quantities of material available for these experiments prevented this. Nevertheless, resulting profiles of the disaccharide compositions are shown in Figure 4.25.

Component disaccharides of BCE S-domains 8x and 8y

8x = UA-GlcNS : UA(2S)-GlcNS(6S) : UA(2S)-GlcNS : UA-GlcNAc

8y = UA-GlcNS : UA-GlcNS : UA(2S)-GlcNS(6S) : UA-GlcNAc(6S)

The profiles are consistent with the presence of a major species in each and they are distinct from each other. BCE dp8x elutes in a similar position on SAX-HPLC to BAEC 8c and its component disaccharides are the same. Interestingly, considering the relative increase in 6-O-sulphation in BCE compared to BAEC, both of these species, that dominate this S-domain size class in BCE HS, contain a trisulphated [UA(2S)-GlcNS(6S)] disaccharide. Notably, exclusively 2-O-sulphated octasaccharide S-domains do not appear to dominate in BCE HS as seen for 3T3 fibroblast and BAEC HS. BCE dp8y also contains a disaccharide of the structure UA-GlcNAc(6S) and resembles the composition of BAEC dp8f* (Figure 4.24).

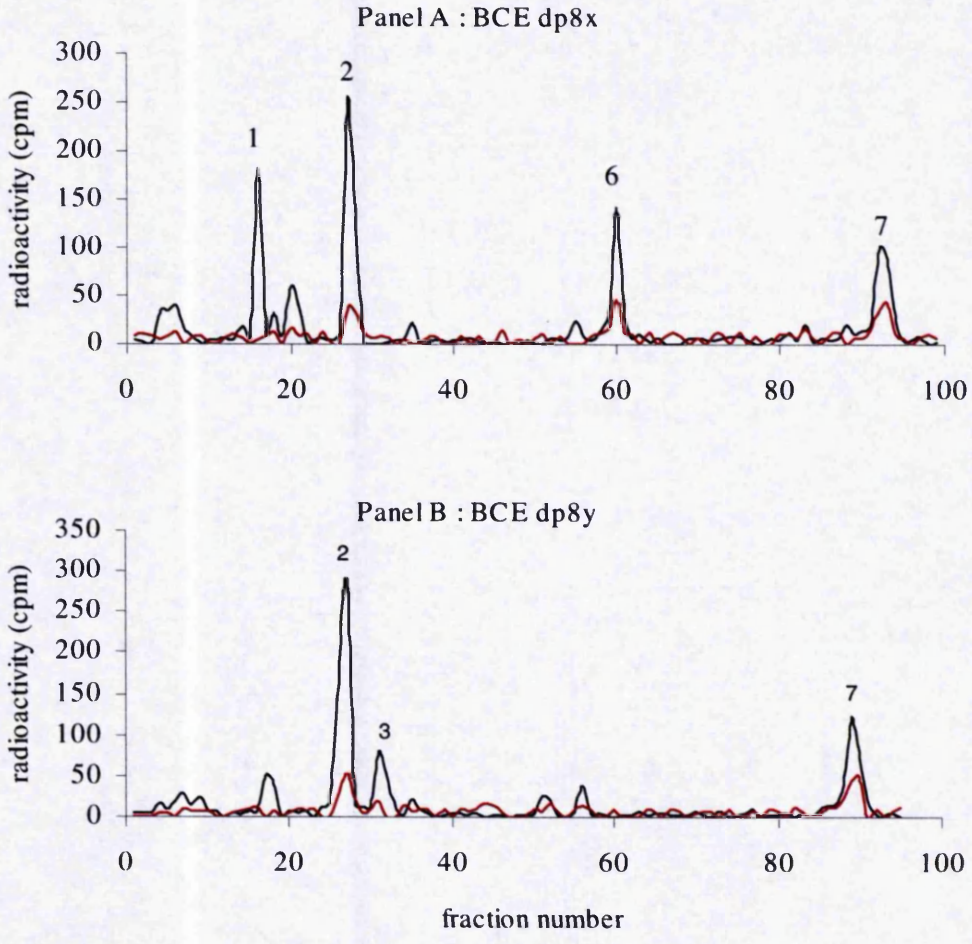

Figure 4.25: Disaccharide composition of BCE octasaccharide S-domains by strong anion exchange HPLC analysis. Disaccharides were prepared by digestion with a combination of heparinases I and II, then resolved on a Pro-Pac PA1 SAX-HPLC column eluted with a 0-1M NaCl, pH3.5 gradient over 45 minutes. Fractions collected (0.5ml) were monitored by scintillation counting. Panel A : BCE dp8x, Panel B : BCE dp8y. The numbered peaks correspond to the elution positions of known disaccharide standards as follows:- 1= UA-GlcNAc; 2=UA-GlcNS; 3=UA-GlcNAc(6S); 4=UA(2S)-GlcNAc; 5=UA-GlcNS(6S); 6=UA(2S)GlcNS; 7=UA(2S)GlcNS(6S). (^{3}H black line ^{35}S red line, UA=unsaturated uronic acid).

However, it elutes ~10 fractions earlier than BAEC dp8f* suggesting that the uronate epimers or the order of the disaccharides within the respective sequences must differ. Again, there was insufficient material to sequence these oligosaccharides but it is interesting that S-domains containing [UA-GlcNAc(6S)] were not identified in 3T3 fibroblast HS (Merry *et al.*,1999). These findings confirm that there is structural heterogeneity within the S-domains between HS species and suggest that structures of co-eluting oligosaccharides on SAX-HPLC should be inferred with caution, especially if derived from complex and/or minor peaks. In addition, oligosaccharides with similar disaccharide compositions that do not co-elute on SAX-HPLC profiling should be assumed to have subtly different structures.

4.9 Structural characterisation of dominant BAEC decasaccharide S-domains

The disaccharide compositions of BAEC S-domains dp10a-d (from the profile shown in Figure 4.19) were obtained by digestion of ~3-5K cpm ^{3}H-HS with heparinases I and II, followed by separation on SAX-HPLC as previously described. The results are shown in Figure 4.26. The earlier eluting dp10a and b are comprised of the same disaccharides and the stoichiometry suggests homogeneous species that are deficient in 6-O-sulphate. The shift in elution position of ~ 5 fractions between dp10a and dp10b is most likely due to a difference in epimerisation of the reducing end uronate residue. Later eluting species dp10c and d, represent 2 fractions pooled from the centre of complex peaks and so are less likely to be homogeneous. They both comprise disaccharides substituted with 6-O-sulphate in addition to 2-O-sulphate.

This finding confirmed a pattern of S-domain organisation within BAEC HS that was also detected in 3T3 fibroblast HS (Merry *et al.*,1999; Appendix I). Within each size class from dp6-10, all S-domains are 2-O-sulphated. In contrast, a subpopulation are substituted with 6-O-sulphation that indicates selective expression of this modification by the 6-O-sulphotransferases.

4.10 Affinity of endothelial cell HS for aFGF and bFGF

The filter binding assay was used to compare the affinity of HMVEC, BCE and BAEC HS for bFGF and aFGF. BFGF (1μg) or aFGF (2μg) were incubated with ~10K ^{3}H-HS

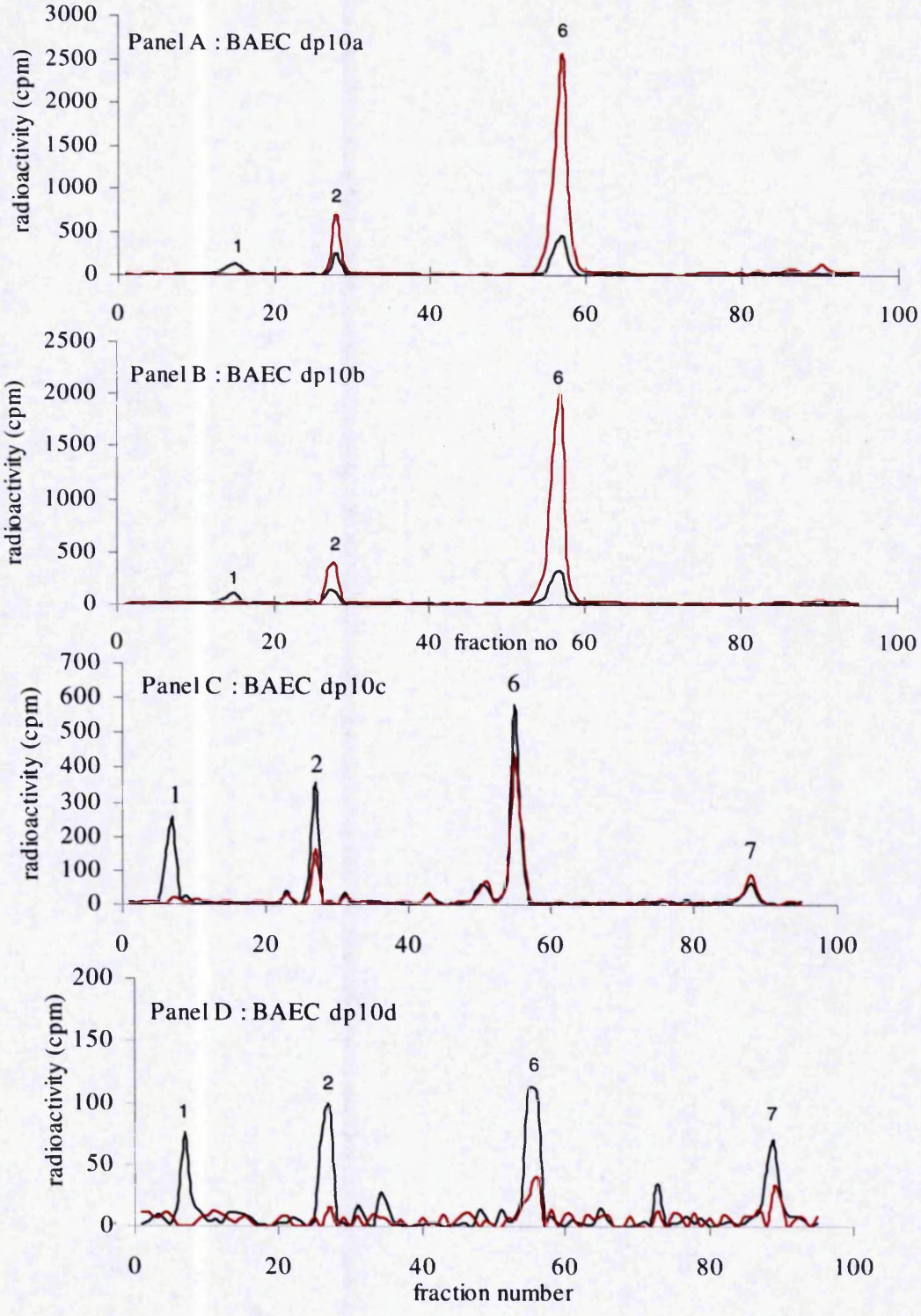

Figure 4.26: Disaccharide composition of BAEC decasaccharide S-domains by strong anion exchange HPLC analysis. Disaccharides were prepared by digestion with a combination of heparinases I and II, then resolved on a Pro-Pac PA1 SAX-HPLC column eluted with a 0-1M NaCl, pH3.5 gradient over 45 minutes. Fractions collected (0.5ml) were monitored by scintillation counting. The numbered peaks correspond to the elution positions of known disaccharide standards as follows:- 1= UA-GlcNAc; 2=UA-GlcNS; 3=UA-GlcNAc(6S); 4=UA(2S)-GlcNAc; 5=UA-GlcNS(6S); 6=UA(2S)GlcNS; 7=UA(2S)GlcNS(6S). (^{3}H black line ^{35}S red line, UA=unsaturated uronic acid).

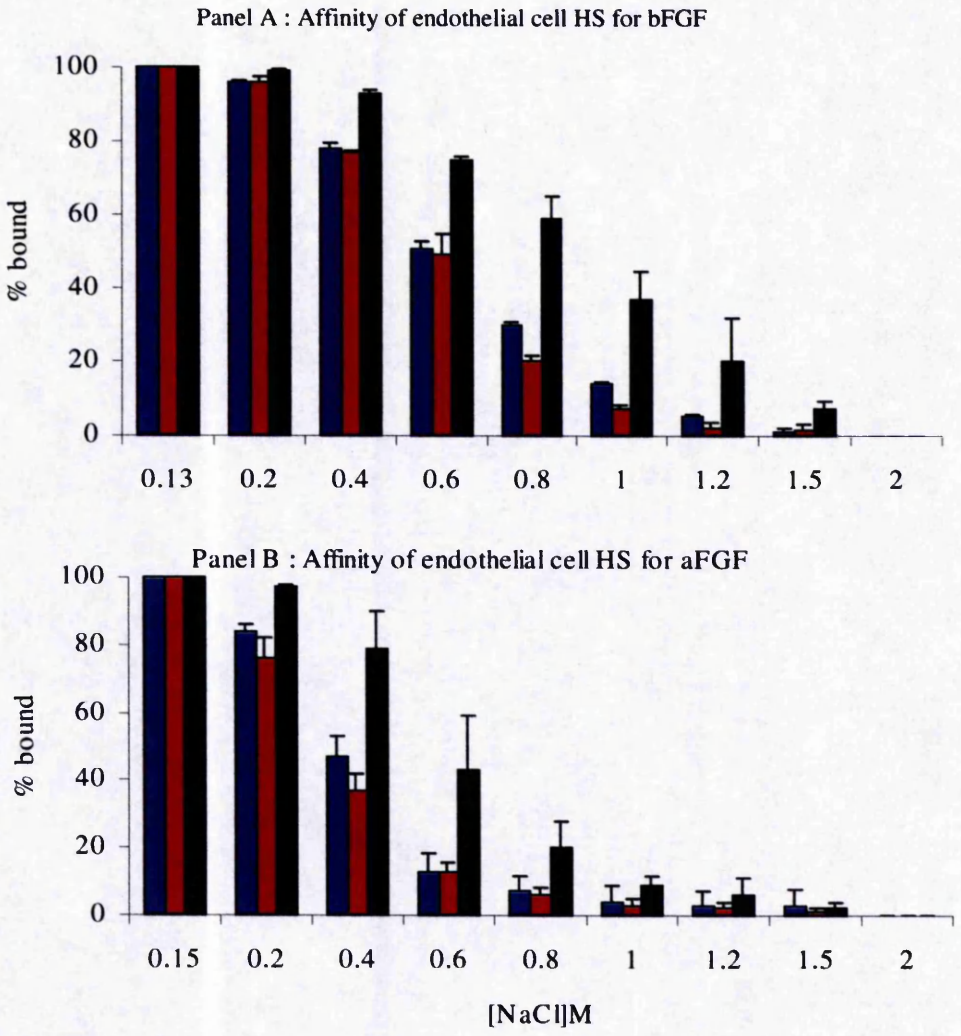

Figure 4.27 : Comparison between HMVEC, BCE and BAEC HS of affinity to bFGF and aFGF using the filter binding assay. ~10K ^{3}H-HS from HMVEC (black bars), BCE (red bars) and BAEC (blue bars) was incubated with either 1µg bFGF or 2µg aFGF in 100µl of 0.13M NaCl, 50mM Tris, pH 7.0 for one hour at room temperature then applied to cellulose nitrate filters using a vacuum assisted apparatus. Unbound HS was eluted with 2 X 5 ml washes of 0.13M NaCl, 50mM Tris, pH 7.0 and bound HS eluted with 2 X 5 ml washes of increasing 0.2M NaCl increments. The proportion of bound HS was greater than 50% in all cases (data not shown). The bars represent the means + sd of the proportion of bound HS remaining after each NaCl wash from 3 experiments.

5 : DISCUSSION

PART 1 : COMPARATIVE ANALYSIS OF MACROVESSEL AND MICROVESSEL ENDOTHELIAL CELL HS

The structural characteristics of microvessel and macrovessel EC HS have been obtained using standard and novel analytical approaches. All the EC HS species share a relatively low level of sulphation and the sequences of the short S-domains (dp4-6) are highly conserved. In contrast, the microvessel HS chains are shorter (~ 45 disaccharides), the 6-O-sulphate and trisulphated disaccharide [UA(2S)-GlcNS(6S)] contents are increased, and the structure of the longer S-domains (dp≥8) differs significantly from the macrovessel HS chains. These findings support the concept that the design of HS can differ depending on its tissue of origin. The occurrence of preserved S-domains has not been reported previously and may reflect a common function of EC HS. However the trisulphated disaccharide is frequently implicated in the binding sites for angiogenic regulators (Table 1.5, and see Chapter 6) and the enhanced expression of this motif in microvessel HS compared to macrovessel HS may signify an important functional distinction.

Large vessel ECs cultured from human or bovine aorta and human umbilical vein are frequently used to study vascular pathology and physiology due to relative ease of isolation. However, differences exist between macro- and microvessel ECs, with respect to morphology, cell surface molecules, antigenic determinants, permeability, and metabolic properties (Craig *et al.*, 1998; Hewett *et al.*, 1993; Kuzu *et al.*, 1993). In consequence, human microvessel ECs are the preferred model for the study of many aspects of vascular biology.

There are no previous characterisations of HMVEC HS although HS has been characterised from human, bovine, and porcine macrovessel EC sources (Feitsma *et al.*, 2000; Hiscock *et al.*, 1995; Lindblom & Fransson, 1990; Pye & Kumar, 1995). HMVEC have a limited lifespan and fastidious culture requirements in comparison to other EC types. To study HS synthesised by cells in culture, bulk preparations of cells are required to yield sufficient quantities for detailed analysis. We were therefore interested to determine whether bovine ECs were a good model for HMVEC since these cells are

easier to culture on a large scale. This also provided an opportunity to compare microvessel EC HS from different species and micro- versus macrovessel HS from the same species.

All EC species synthesised similar ratios of HS compared to CS/DS that eluted from DEAE-anion exchange with ~0.5-0.6M NaCl, consistent with other HS forms (Gallagher & Walker, 1985). HMVEC did not readily incorporate ^{35}S into their HS chains probably due to competition from sulphur in the culture medium and antibiotics, but all EC species incorporated ^{3}H into glucosamine residues thereby labelling disaccharides throughout the chain. The most striking difference in the macrostructure of the ECHS species was their size. Analysis of chain length revealed that both microvessel EC species had much shorter chains (~ 45 disaccharides) than BAEC HS (~ 110 disaccharides). Chain length is known to alter depending on the cellular origin of HS, for example ~ 50 disaccharides for rat liver HS (Lyon *et al.*, 1994) compared to ~ 100 disaccharides for skin fibroblast HS (Turnbull & Gallagher, 1990) and HUVEC HS (Lindblom & Fransson, 1990). Although determinants of chain length, and functional implications, are poorly understood, the data suggest that conserved mechanisms may exist that dictate this distinction for macro and microvessel ECs.

Conservation and variation in molecular design of EC HS

Scission reagents with known specificities were used to assign the proportions of particular disaccharides and their organisation within the chains. The findings were remarkably similar with levels of N-sulphated glucosamine between 36-40% for all EC types. This represents a relatively low level of sulphation compared to other HS species and is consistent with previous reports (Feitsma *et al.*, 2000; Hiscock *et al.*, 1995; Lindblom & Fransson, 1990; Pye & Kumar, 1995). For example HS extracted from rat liver has a high proportion of N-sulphated glucosamine (~ 60%) (Lyon *et al.*, 1994) and skin fibroblast HS has ~ 47% N-sulphated glucosamine (Turnbull & Gallagher, 1990).

The gel filtration profiles of products following treatment of HS with specific scission reagents indicated the typical domain organisation, characteristic of HS, for each EC type. The nitrous acid profiles confirm the predominant distribution of sulphated disaccharides in clusters either contiguously (S-domains) or alternately (flanking domains). Correspondingly, the heparinase III profiles indicate the relatively abundant,

unmodified, GlcA containing disaccharides (ie GlcA-GlcNAc) are located in contiguous sequences between the heparinase III resistant S-domains. The S-domains vary from 2 to 6-7 disaccharides and those of 3-4 disaccharide repeats (dp6 and dp8) are most common. The heparinase I generated profiles revealed a low frequency of iduronate 2-O-sulphate containing disaccharides that were widely spaced, consistent with the location of these disaccharides within the S-domains (Gallagher *et al.*, 1992). (Figure 1.2, 1.3)

Combined digestion with heparinases I, II and III, also revealed similar disaccharide compositions but there were notable variations. The proportion of N-sulphated disaccharides (37-40%) obtained in this way compared well with the nitrous acid derived figures (36-40%) demonstrating the complementary nature of these analyses. The most striking variation was the increased content of the trisulphated disaccharide [UA(2S)-GlcNS(6S)] in the microvessel EC HS, compared to the macrovessel EC HS. This disaccharide has been implicated in the binding sites of several angiogenic regulators such as aFGF, PDGF, IL-8 and TSP-1 (see Table 1.5). In addition, 6-O-sulphation is a prerequisite for bFGF activation (Pye *et al.*, 1998) suggesting that this structural distinction may have functional importance.

S-domain profiling is part of the method by which pure, homogeneous S-domains of defined size can be extracted from HS for sequence analysis (Merry *et al.*,1999; Vives *et al.*,1999). For the majority of S-domains in this study, it was not possible to obtain sufficient quantities of material to sequence due to the difficulty in preparing bulk quantities of HS from ECs. However, S-domain profiling did provide insight into the structural heterogeneity within the heparinase III resistant S-domains of the EC HS types. This revealed variation in S-domains from different cellular origins, but also conservation of the most abundant S-domains to a degree that was not anticipated.

When previously obtained information from 3T3 fibroblast cell HS was used for comparison the S-domains of dp4-8 from BAEC HS, and of dp4-6 from HMVEC and BCE HS, were noted to co-elute on SAX-HPLC. Sequence analysis of the most abundant BAEC S-domains 6a and 8a confirmed identity to their 3T3 fibroblast HS counterparts. In contrast, variation in S-domain structure was observed for the HMVEC

and BCE HS S-domains of dp8, minor species of BAEC HS dp8 and within the longer BAEC HS S-domains of dp10 and dp12.

Disaccharide compositional analysis of BAEC HS dp8 and selected dp10, indicated that most S-domains lacked a 6-O-sulphate group as detected previously during analysis of 3T3 fibroblast HS (Merry *et al.*,1999). Structural analysis of microvessel dp8 was limited, but the dominant species were both substituted with 6-O-sulphation, possibly reflecting the increased prevalence of this modification in the total disaccharide composition. The sparing distribution of 6-O-sulphation suggests that this modification may be tightly regulated to determine ligand interactions (see also Conclusions, Chapter 8). This finding also supports the concept that sequences capable of both inhibiting, and activating bFGF, are present at the cell surface (Pye *et al.*, 1998).

Interestingly, the BAEC and BCE HS, despite structural distinctions, both bound the the angiogenic stimulators, bFGF and aFGF with equivalent affinity but there was a small increase (~0.2M NaCl) in the affinity of HMVEC HS for these proteins. This suggests an as yet unidentified distinction in the design of HMVEC HS, either within the heterogeneity of the longer S-domains, and/or in S-domain position within the chain. The latter has been proposed to explain different affinities of 3T3 fibroblast and BAEC HS to bFGF (Pye & Kumar, 1998). However, it is not known to what extent these differences in affinity have functional implications for the regulation of these ligands.

In summary, novel data on the structural characteristics of HMVEC HS have been obtained and compared to BCE and BAEC HS. Overall, the EC HS species examined are closely related and generally conform to the typical structural characteristics of HS (Gallagher & Walker, 1985; Turnbull & Gallagher, 1990) indicating the potential for bovine EC HS species to substitute for HMVEC HS. However, fine structural distinctions are also inherent in the design of each EC HS species suggesting caution when extrapolating findings from different HS sources to the physiologically relevant target HS.

6. RESULTS

PART 2 : THE INTERACTION OF ENDOTHELIAL CELL HEPARAN SULPHATE WITH ENDOSTATIN

6.1 The filter binding assay.

The filter binding assay (FBA) of (Maccarana & Lindahl, 1993) was chosen to investigate the interaction between endostatin and HS. As described in methods and Chapter 4.10, HS and protein are bound in solution which avoids coupling protein to a solid phase support that may alter its reactivity due to changes in conformation or masking of GAG binding domains. This assay is particularly suited for use with trace quantities of metabolically radiolabelled HS. Bound ^{3}H-HS and protein are incubated for two hours in a saline buffer then applied to cellulose nitrate filters. Unbound ^{3}H-HS is eluted with incubation buffer and bound ^{3}H-HS eluted with increasing increments of NaCl at physiological pH (or as specified). Thus, eluted ^{3}H-HS is readily recovered for detection by scintillation counting and further analysis.

The assay was optimised for use with ^{3}H-HS in the range 3 – 300K cpm ^{3}H. Binding of BAEC ^{3}H-HS to human recombinant endostatin monomer (HEM) in 0.13M NaCl, 10mM Tris, pH 7.0, approached saturation (~80% HS bound) with 30-40 μM protein (Figure 6.1, Panel A). Neither the length of incubation (range 30 mins to 24 hours) (Figure 6.1, Panel B), or the presence of BSA (Figure 6.1, Panel C) significantly altered the proportion of HS bound.

All assays were subsequently performed with 40μM HEM to shift the binding equilibrium in favour of association. Further modifications were added to the technique of Maccarana *et al.*, 1993 as follows: initial incubation volumes were reduced from 100-200μl to 25μl to conserve protein used per assay and the volume of salt used to elute HS was reduced from 3x1ml from 1-3x5ml without altering the elution profiles (not shown). This enabled recovery of eluted HS in smaller volumes and reduced error in scintillation counting due to aliquoting.

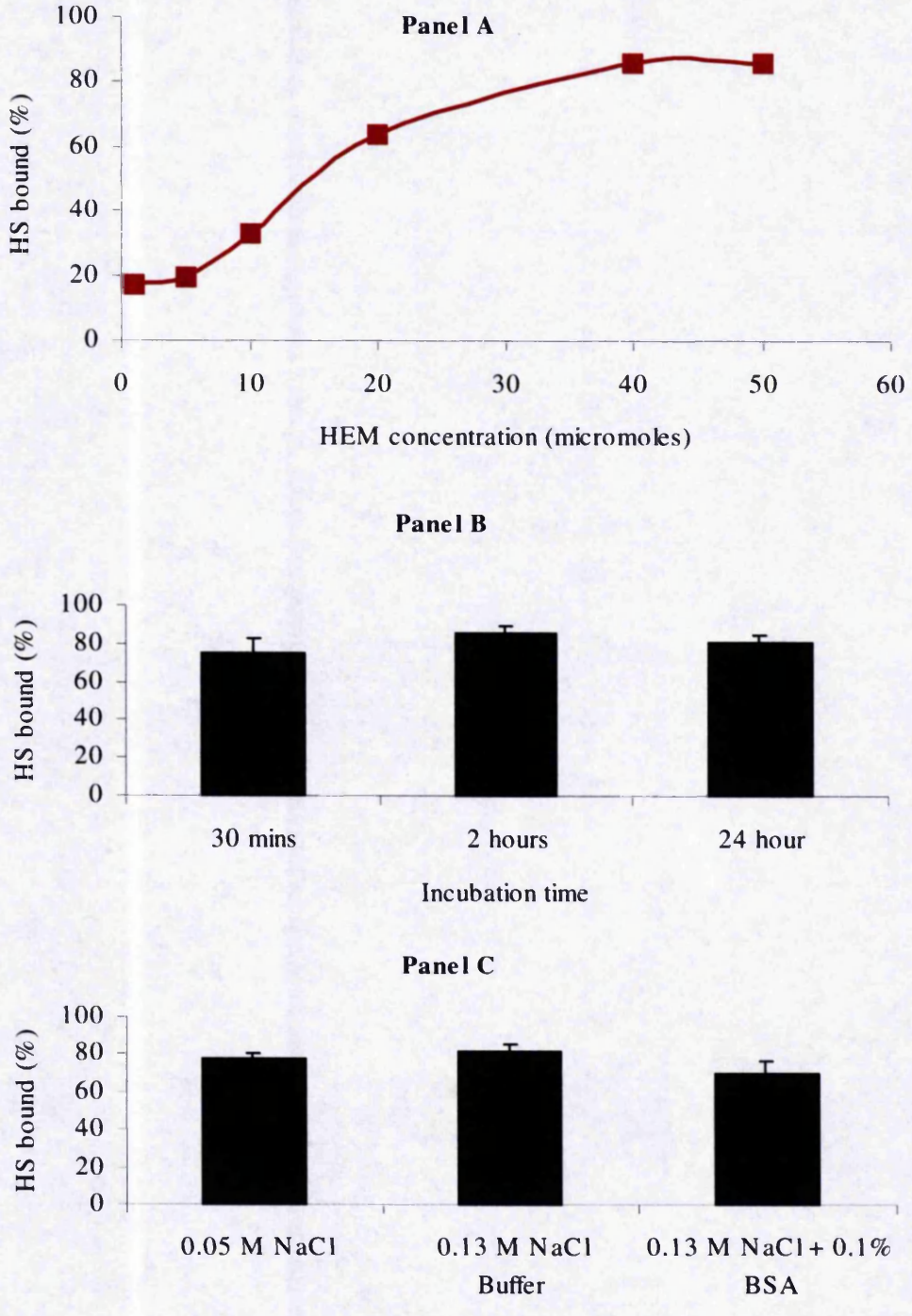

Figure 6.1 : Optimisation of Filter binding assay ~ 10K ^{3}H- HS from BAEC was incubated with HEM and bound ^{3}H-HS determined by the FBA with 3 x 1 ml washes of 1.0M NaCl. Panel A: Effect of varying concentrations of HEM (0.5 to 40 µM) in 100µl 0.13M NaCl, 10mM Tris, pH7.0 for 2 hours. Panel B : Effect of varying incubation times; 40 µM HEM in 100µl 0.13M NaCl, 10mM Tris, pH7.0 for 0.5,2 or 24 hours. Panel C: Effect of varying incubation buffer; 40 µM HEM in 100µl 0.05 or 0.13M NaCl ± 0.1% BSA, 10mM Tris, pH7.0 for 2 hours. Bars show means + SD from 3 independent experiments of cpm ^{3}H bound as a percent of total cpm. No binding was observed in negative controls substituting BSA for HEM and ^{3}H-HS retained on the filter was <0.1% (data not shown).

Affinity of endostatin (HEM) for HS

Figure 6.2 compares the affinities of BAEC, BCE, HMVEC and 3T3 HS for HEM. HS (~ 10K ^{3}H cpm) from HMVEC, BCE, BAEC or 3T3 fibroblasts was incubated with 40μM HEM in 25μl 0.05M NaCl, 10mM Tris, pH7.0 for 2 hours, and bound ^{3}H-HS determined by the FBA with 3 x 1 ml washes of increasing, 0.05M increments of NaCl. Similar binding profiles were obtained. The majority of bound HS is eluted with 0.2 - 0.25M NaCl and there is no detectable binding beyond 0.35 – 0.4 M NaCl. These findings are consistent with the moderate affinity (Kd = 0.3μM) obtained for heparin to recombinant murine endostatin monomer by Scatchard analysis and elution of bovine kidney HS from a murine recombinant endostatin affinity column with 0.22M NaCl (Sasaki *et al.*,1998).

Similar to the results obtained for HMVEC HS binding to bFGF and aFGF (Figure 4.27), there is a slight (~0.05M NaCl) shift to the right for HMVEC HS binding to HEM. BAEC HS most closely matches the affinity of HMVEC; 3T3 HS and BCE HS appear to have a comparatively lower affinity. Therefore, where possible, HMVEC HS was used for further studies and other HS species or S-domains, used to provide supplementary information.

A preparative assay was performed to examine whether HS eluted by different concentrations of NaCl behaved similarly upon rebinding or redistributed across the whole NaCl concentration range. For this, ~200K cpm ^{3}H-HS was incubated with 40μM HEM in 100μl 0.05M NaCl, 10mM Tris, pH7.0, for 2 hours, and bound ^{3}H-HS determined by the FBA with 3 x 1 ml washes of increasing, 0.05M increments of NaCl. Aliquots (100μl) were taken for scintillation counting and the profile shown in Figure 6.3, Panel A, used to pool the remaining HS into low (eluting ≤ 0.1M NaCl) medium (eluting at 0.15 and 0.2M NaCl) and high (eluting at ≥0.25M NaCl) affinity samples. After de-salting ~ 5K cpm ^{3}H aliquots of the samples were re-incubated with 40μM HEM and bound ^{3}H-HS determined by the FBA as described above. The profile obtained on rebinding is shown in Figure 6.3, Panel B. Allowing for some spread, particularly in the low affinity sample due to the dynamic binding equilibrium, the samples retained their different apparent affinities upon rebinding. Therefore, exhaustive rebinding of low affinity species was not performed routinely in subsequent experiments except where indicated.

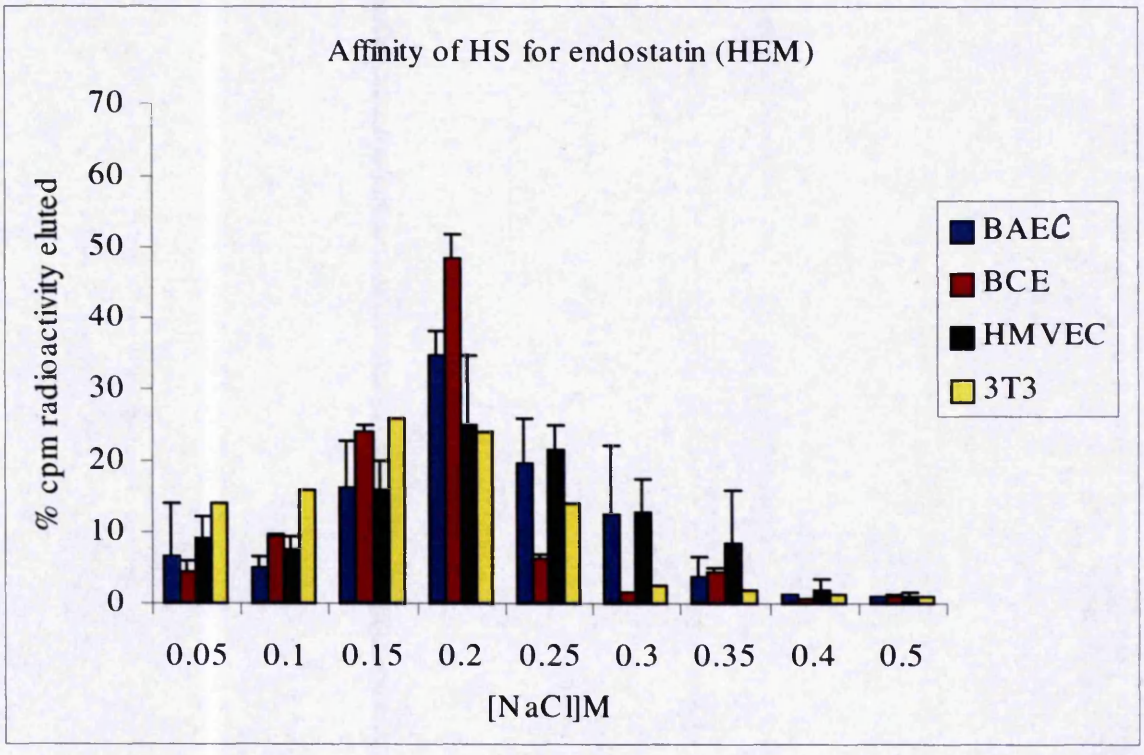

Figure 6.2 : Affinity of HS for endostatin. ~ 10K ^{3}H-HS from HMVEC, BCE, BAEC or 3T3 fibroblasts was incubated with 40µM HEM in 25µl 0.05M NaCl, 10mM Tris, pH7.0 for 2 hours, and bound ^{3}H-HS determined by the FBA with 3 x 1 ml washes of increasing, 0.05M increments of NaCl. The bars show means + SD obtained from 5 independent experiments of cpm ^{3}H eluted as a percent of total cpm (except 3T3 HS, n=1). No binding was observed in negative controls substituting BSA for HEM and ^{3}H-HS retained on the filter was <0.1% (data not shown).

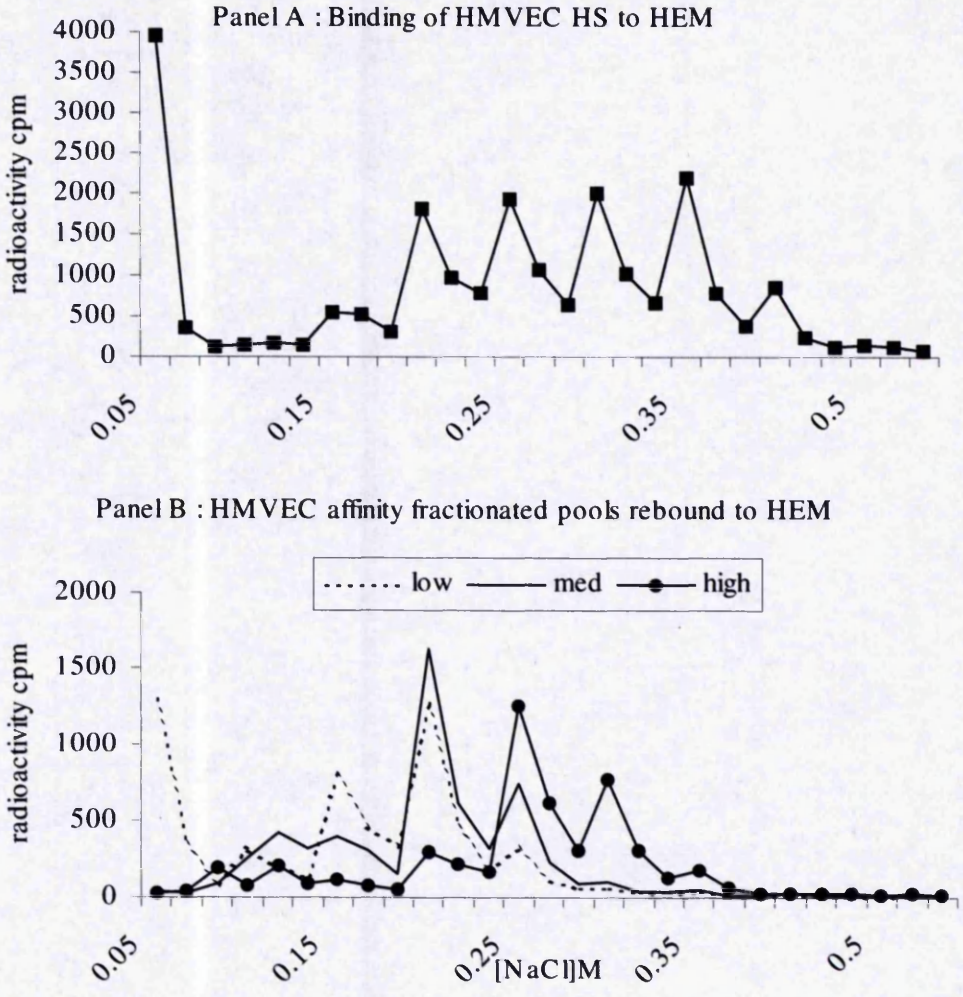

Figure 6.3 : Subfractionation of HMVEC HS by affinity for endostatin. ~ 200K cpm ^{3}H- HS from HMVEC was incubated with 40µM HEM in 100µl 0.05M NaCl, 10mM Tris, pH7.0, for 2 hours, bound ^{3}H-HS determined by the filter binding assay with 3 x 1 ml washes of increasing, 0.05M increments of NaCl and 100µl aliquots taken for scintillation counting (Panel A). Eluted ^{3}H-HS was pooled into low (eluting ≤ 0.1M NaCl) medium (eluting at 0.15 and 0.2M NaCl) and high (eluting at ≥0.25M NaCl) affinity samples. After de-salting ~ 5K cpm ^{3}H aliquots of the samples were re-incubated with 40µM HEM in 25µl 0.05M NaCl, 10mM Tris, pH7.0, for 2 hours and bound ^{3}H-HS determined by the FBA as above. Whole fractions were monitored by scintillation counting (Panel B). No binding was observed in negative controls substituting BSA for HEM and ^{3}H-HS retained on the filter was <0.1% (data not shown).

In addition, this experiment suggested the presence of a high affinity subspecies of HMVEC inferring a structurally heterogeneous population of this HS.

6.2 The role of the primary heparin binding site in the affinity of HEM for HS.

Affinity of mutant (R-A) HEM for endostatin

Based on the crystal structure of recombinant murine endostatin and site directed mutagenesis data, primary and secondary heparin binding sites have been proposed (Sasaki *et al.*,1998). Mutagenesis studies have previously implicated two critical arginine residues (R158, 270) (Figure 1.11) in the primary heparin binding site as the principal determinants of affinity to heparin and HS. HEM mutated to display alanine residues in place of these arginine residues was compared to native HEM for affinity to HMVEC HS in 0.13M NaCl, 10mM Tris, pH 7.0 using the FBA as described. Figure 6.4 shows that there is no measurable affinity of the R-A mutant HEM to HMVEC HS at physiological ionic strength. This is consistent with the proposal that R158 and 270 in the primary heparin binding site are also the principal determinants of affinity to HS (Sasaki *et al.*,1998).

Competition with neutralising mAb 12C1

To further test the specificity of the heparin/HS binding epitope a monoclonal antibody (mAb12C1) was tested for ability to inhibit binding between HEM to HMVEC HS. This Ab recognises arginines within the primary heparin binding site and neutralises the activity of endostatin in bioassays (K Javaherian, personal communication). Using the FBA as previously decribed, ~ 10-20 K ^{3}H- HMVEC HS and HEM were incubated in the presence of 10μM mAb. The elution profiles in Figure 6.5, Panel A show that 12C1 can completely inhibit binding of HEM to HMVEC. A control mAb PDM, that recognises a peptide sequence distinct from the heparin binding epitope in the primary endostatin sequence, and is non-neutralising in bioassays, did not inhibit binding (Figure 6.5, Panel A). This suggested that 12C1 was not blocking binding of HS by steric hindrance. In addition, 12C1 had no effect on the binding of HMVEC HS to bFGF, excluding a nonspecific interaction between 12C1 and a basic heparin binding epitope (Figure 6.5, Panel B).

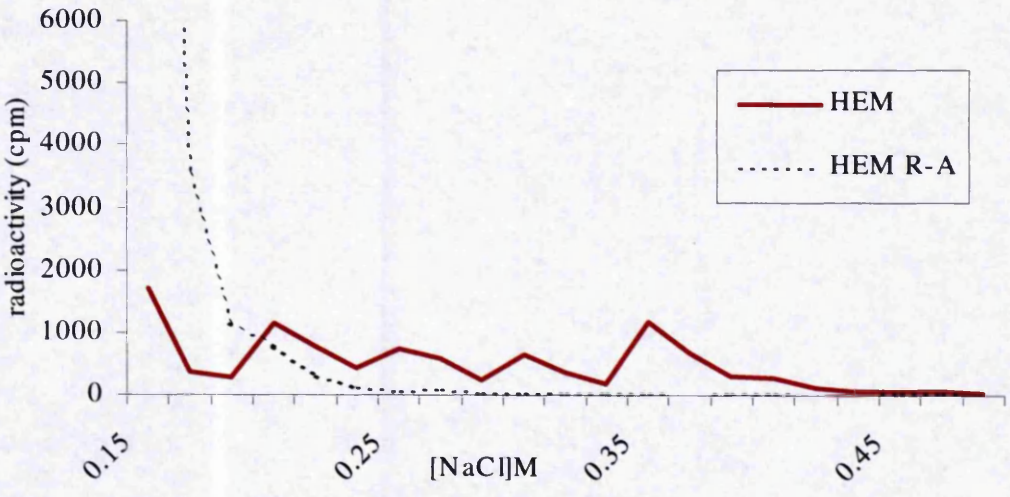

Figure 6.4 : Affinity of mutated R-A HEM for HMVEC HS. ~ 10-20 K ^{3}H-HMVEC HS was incubated in 25 µl 0.15M NaCl, 10mM Tris, pH7.0 with 40µM HEM or 40µM R-A mutant HEM. Bound ^{3}H-HS was determined by the FBA with 3 x 1 ml washes of increasing, 0.05M increments of NaCl. 1 ml washes were monitored for radioactivity by scintillation counting. ^{3}H-HS retained on the filter was <0.1%, experiments were performed in duplicate with identical results and no binding was observed in negative controls substituting BSA for HEM (data not shown).

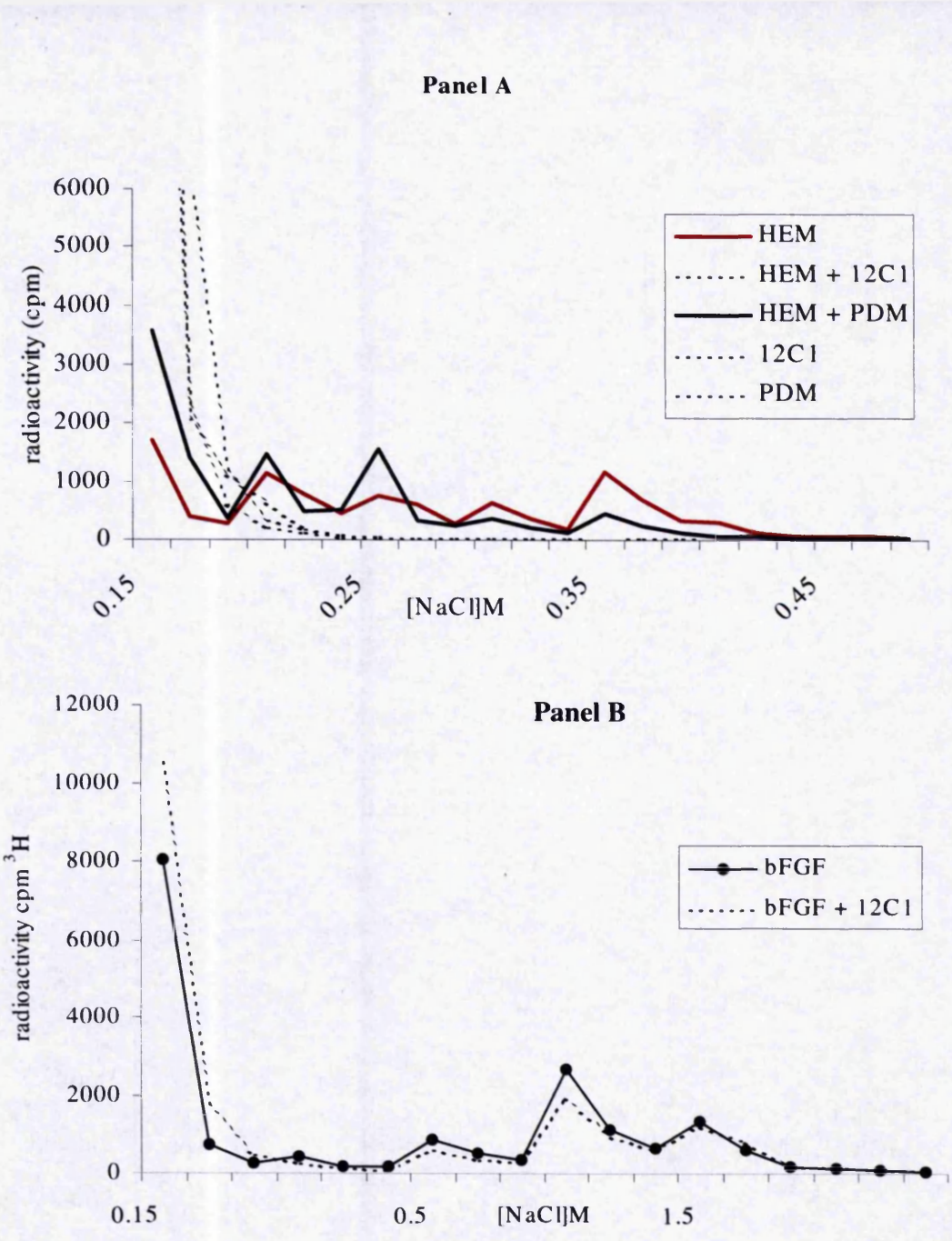

Figure 6.5: Competition with neutralising mAb 12C1. ~ 10-20 K ^{3}H- HMVEC HS were incubated in 25 µl 0.15M NaCl, 10mM Tris, pH7.0 with 40µM HEM (Panel A) or 1µg bFGF (Panel B) in the presence of 10µM neutralising mAb 12C1 or non-neutralising PDM (HEM only). 12C1 and PDM were also incubated with HMVEC HS in the absence of HEM (Panel A). Bound ^{3}H-HS was determined by the FBA with 3 x 1 ml washes of increasing, 0.05M increments of NaCl. 1 ml washes were monitored for radioactivity by scintillation counting. ^{3}H-HS retained on the filter was <0.1%, experiments were performed in duplicate with identical results and no binding was observed in negative controls substituting BSA for HEM (data not shown).

6.3 Oligosaccharide size for optimal binding to endostatin

Competitive binding

The first characteristic of the HS binding domain for HEM to be examined was its size. To do this, non-radiolabelled heparin–derived oligosaccharides of dp4-20, were screened for ability to compete with ^{3}H-HMVEC HS and ^{3}H-BAEC HS. As shown in Figure 6.6, the shortest oligosaccharides able to compete were the octasaccharides but longer, ≥dp10/12 were optimal. From the crystal structure of endostatin, Sasaki *et al.*, 1998 predicted that a highly sulphated tetrasaccharide could be accommodated in the primary HB site with a longer oligosaccharide (dp10/12) required to extend into the putative secondary binding site (see Figure 7.2). Our data showed no competition by tetrasaccharides in physiological conditions, however, the possibility that short oligosaccharides (with weak affinity) might associate with HEM in reduced ionic strength buffer was tested by direct binding (see below).

Direct binding –heparinase III generated S-domains

Before testing size-defined S-domains for affinity to HEM, HMVEC HS was treated with nitrous acid, an aliquot checked for complete degradation by Bio-Gel P10 chromatography, and the remainder desalted on a PD10 column and incubated with HEM in 0.05M NaCl, 10mM Tris, pH7.0. This resulted in total inhibition of binding between HMVEC HS and HEM indicating that contiguous N-sulphated disaccharides are essential for binding (data not shown).

Therefore, a range of S-domains was generated by heparinase III treatment of HMVEC HS as previously described, and an aliquot checked for complete digestion (Figure 6.7, Panel A). Heparinase III was denatured by boiling for 10 minutes. To avoid losses from desalting, the digest buffer was adjusted to 0.05M NaCl, 10mM Tris, pH7.0 and the presence of 10μM calcium acetate and 10mM sodium acetate from dilution of the heparinase buffer was not found to affect binding of a control sample (data not shown). The total digest was incubated with HEM and bound ^{3}H-HS eluted using the FBA as previously described. Figure 6.7, Panel B, shows that ~17% of the digest compared to ~80% of control samples bound, and ~6% of the heparinase III digested HMVEC HS bound HEM

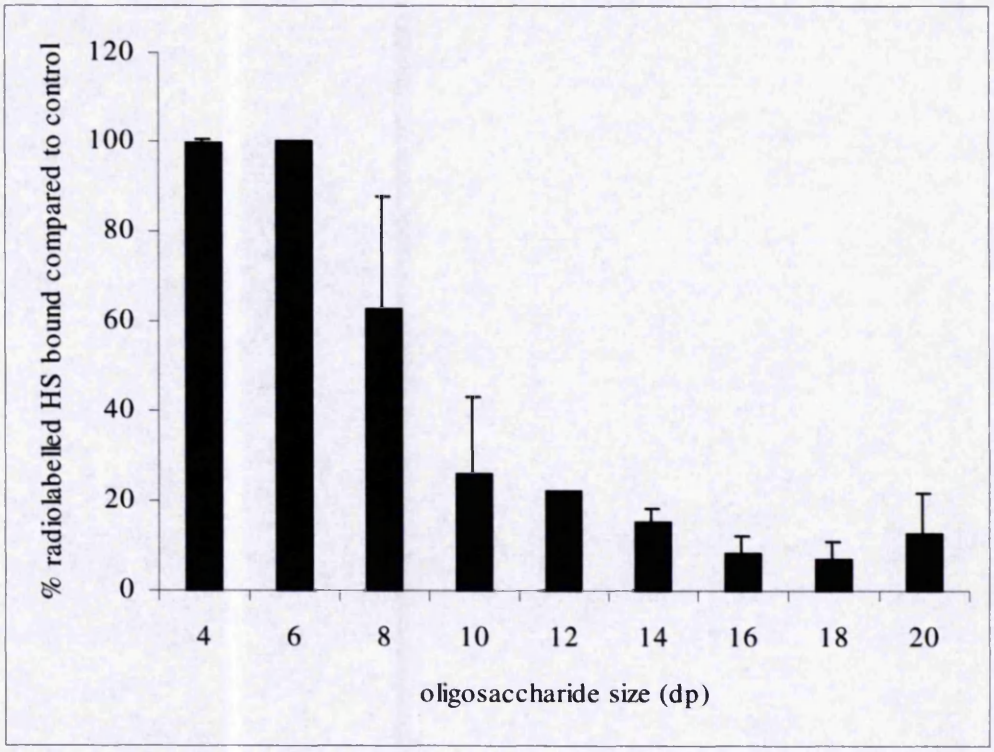

Figure 6.6 : The ability of non-labelled heparin-derived oligosaccharides of defined size to compete with ^{3}H-HS for HEM in the filter binding assay. ~ 2K cpm ^{3}H-HMVEC or ^{3}H-BAEC HS was incubated in the presence of 10μM non-radiolabelled oligosaccharide ranging from 2 - 10 disaccharides in length (dp4 - 20) and 40μM endostatin monomer (HEM) in 0.13M NaCl, 10mM Tris, pH7.0 for two hours. The proportions of unbound and bound ^{3}H-HS were determined by the filter binding assay with 3 x 1 ml washes of 0.13M NaCl, 10mM Tris, pH7.0 then 3 x 1 ml washes of 1.0M NaCl, 10mM Tris, pH7.0 respectively. 1 ml washes were monitored for radioactivity by scintillation counting. Bars show means + standard deviations as a percentage of radiolabelled HS bound compared to control from combined results of HMVEC (n=1) and BAEC (n=1). ^{3}H-HS retained on the filter was <0.1%.

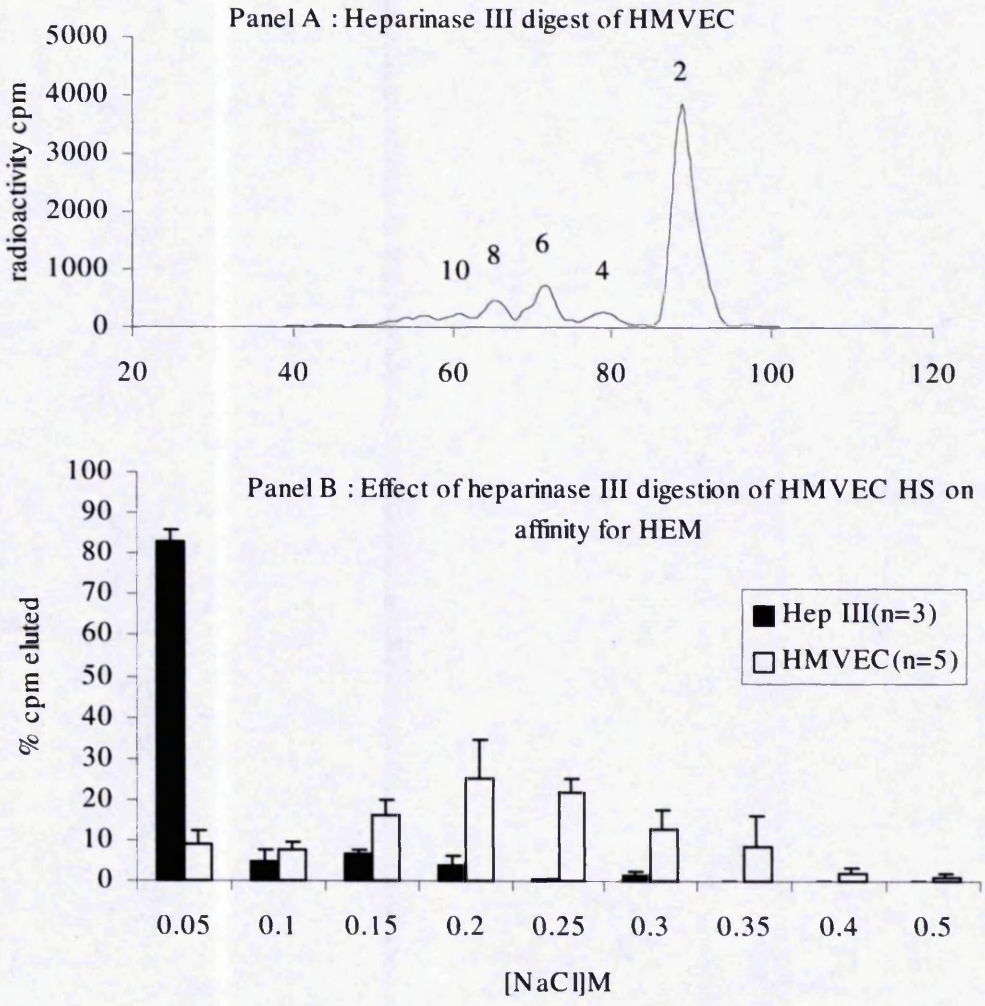

Figure 6.7 : Affinity of heparinase III derived S-domains for endostatin. Panel A ~ 200K ^{3}H- HMVEC HS was digested with heparinase III and a 10K ^{3}H –HS aliquot checked for complete digestion by Bio-Gel P10 chromatography as previously described. Panel B : The remaining heparinase III digest of HMVEC HS was adjusted to 0.05M NaCl, 10mM Tris, 10mM sodium acetate, 10μM calcium acetate, pH7.0, incubated with 40μM HEM and bound ^{3}H-HS determined by the FBA with 3 x 1 ml washes of increasing 0.05M NaCl increments. Either 1 ml washes or 100 μl (preparative) aliqouts were monitored by scintillation counting. ^{3}H-HS retained on the filter was <0.1% of the total radioactivity. Bars show means + sd for heparinase III digested HMVEC HS (Hep III) compared to undigested HMVEC HS (HMVEC) of cpm ^{3}H –HS eluted as a percent of total radioactivity of the sample.

beyond 0.13M NaCl. A reduction in affinity was evident with no binding of any components of the heparinase III digest beyond 0.2M NaCl. Combined results from 3 digests are shown. For preparative digests ~ 200K cpm heparinase III treated ^{3}H-HS was incubated with HEM, bound material eluted using the FBA as described, aliquots of 100µl checked for scintillation counting and the remaining heparinase III digested ^{3}H-HS pooled according to elution position.

After desalting, these pools (~ 3-10K cpm ^{3}H) were chromatographed on Bio-Gel P10 to establish the size range of S-domains present in each (Figure 6.8, Panels A-C). Samples were chromatographed in random order on the same column, with a Vt marker (sodium dichromate), to ensure that shifts in elution of peaks were not due to changes in column behviour. Identical results were obtained from two independent experiments. The size distribution of the S-domains changes with increasing NaCl concentration required for elution from HEM. In the unbound fraction eluted with 0.05M NaCl (Figure 6.8, Panel A), S-domains of dp2-8 are present. The relative decrease in the proportion of dp2 is due to selective loss of disaccharides during desalting on PD10 columns. The weakest binding fraction eluted with 0.1M NaCl (Figure 6.8, Panel B), comprises dp6-8, with no dp2-4. A further increase in chain length is observed in Figure 6.8, Panel C, with dp8-10 and possibly dp12 eluted by 0.15M NaCl. In both experiments, the highest affinity fraction, eluted by 0.2 M NaCl, contained a poorly resolved peak between the void and dp10 elution position, just discernible from the background radioactivity, and absence of shorter S-domains. The proportion of bound heparinase III treated ^{3}H –HS in this fraction was consistent with the ~ 6% of S-domains known to be ≥dp12 (Figure 4.12) but it was not possible to confirm this from the quality of the profiles (data not shown). Therefore direct binding followed by size fractionation of heparinase III treated HMVEC HS indicated that hexasaccharides could bind HEM weakly, but that longer oligosaccharides of ≥ dp10/12 were required to bind HEM in physiological ionic conditions.

To investigate this further and ensure that binding of shorter oligosaccharides was not inhibited by competition from longer oligosaccharides in the incubation, S-domains of defined size (dp4-12) were purified from HMVEC HS as previously described (see Figure 4.15). Disaccharides generated by heparinase III are predominantly unsulphated so to

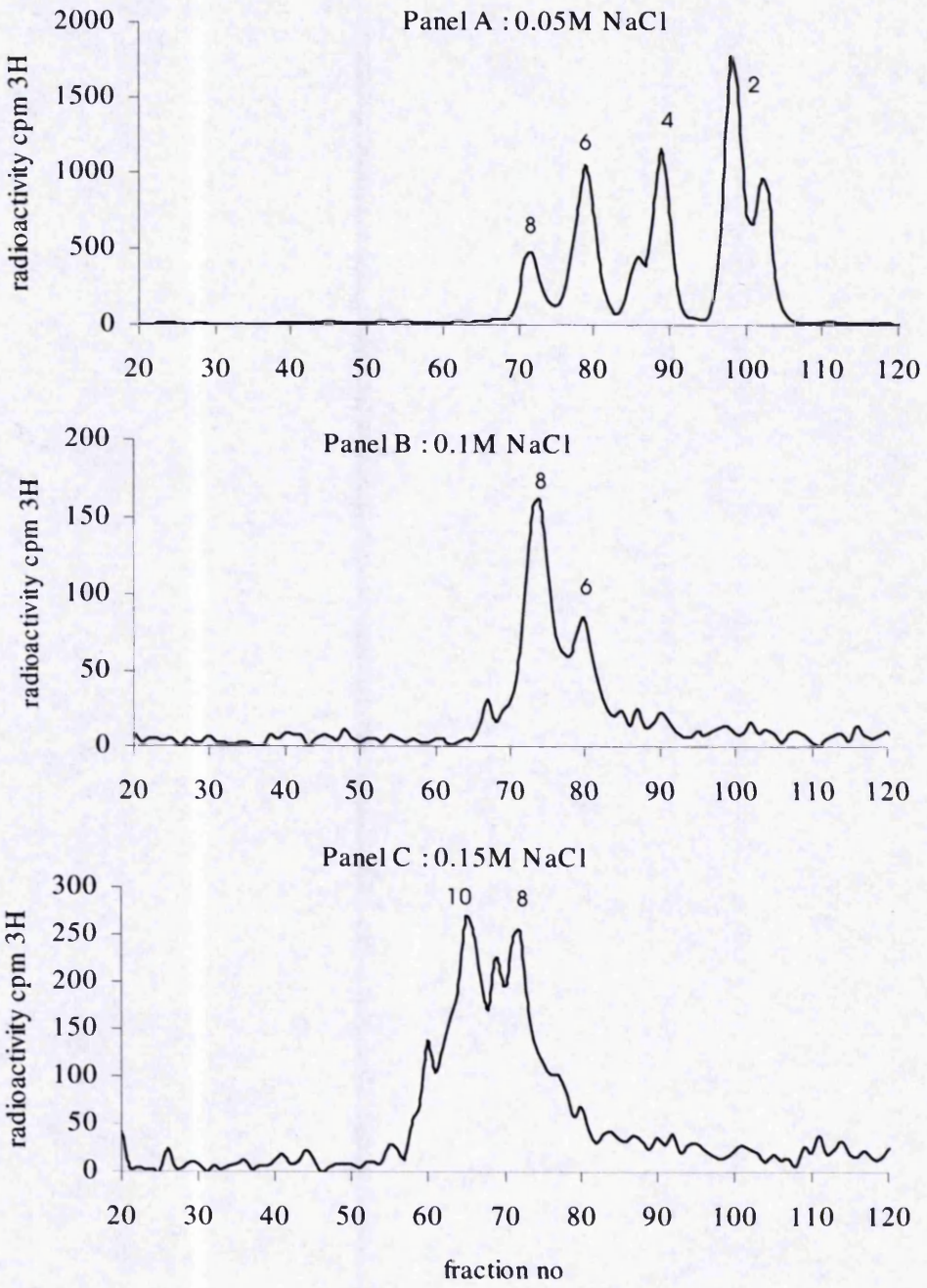

Figure 6.8 : Bio-Gel P10 separation of S-domains fractionated by affinity for HEM. S-domains were generated by heparinase III digestion of ~200K cpm ^{3}H-HMVEC HS, and subfractionated by affinity to HEM, indicated by elution [NaCl] using the FBA. Panel A =0.05M NaCl pool, Panel B=0.1M NaCl, Panel C=0.15M NaCl. Desalted samples were loaded onto a Bio-Gel P10 column (1cm x 140cm) in a maximum of 1ml, and eluted in 1 ml fractions with 0.1M NaCl, pH8.8, at a flow rate of 4ml/hour. Elution profiles were monitored by scintillation counting and numbers above the peaks correspond to the degree of polymerisation where dp2=disaccharides etc.

check the affinity of highly sulphated disaccharides a multiheparinase digest of HMVEC HS was performed to obtain all component disaccharides.

The disaccharides and size defined S domains (dp4-12) were incubated in duplicate (~5-10 Kcpm ^{3}H per sample) with 40μM HEM in 0.05M NaCl, 10mM Tris, pH7.0 alongside control samples substituting BSA for HEM as a negative control. Bound material was eluted with 3x1 ml increasing 0.05M NaCl increments and 1 ml washes monitored by scintillation counting. The results in Figure 6.9 confirm that hexasaccharides are the smallest S-domains with weak but measurable affinity for HEM, whereas decasaccharides are the smallest S-domains with affinity for HEM in physiological conditions.

6.4 Structural characterisation of hexasaccharides with affinity for HEM

S-domain profiling of hexasaccharides (dp6) previously demonstrated four conserved species (Figure 4.17). To determine whether all bound to HEM, a preparative FBA was used in which ~50K cpm ^{3}H-dp6 from HMVEC obtained by heparinase III digestion then gel filtration on Bio-Gel P10, was bound to 40μM HEM in 0.05M NaCl, 10mM Tris, pH7.0. Bound ^{3}H-dp6 were eluted with 3 x 1ml 0.1M NaCl, 10mM Tris, pH7.0. Bound and unbound pools were monitored by taking small aliquots for scintillation counting, and desalted for further analysis. Sufficient ^{3}H-HS was present in each fraction to obtain a SAX-HPLC profile and a disaccharide analysis. The SAX-HPLC profiles of bound and unbound HMVEC dp6 S-domains compared to the total pool are shown in Figure 6.10.

Figure 6.10, Panel A shows four dp6 species, as obtained previously and panels B and C indicate that HEM binds preferentially to dp6d and possibly, dp6c. In the non-binding pool, the proportion of 6d is significantly reduced compared to 6a and 6b whereas 6d is enhanced in the binding pool. The contribution of 6c to the binding pool cannot be determined due to the low abundance of this species.

The remaining ^{3}H-dp6 in each pool were digested with heparinase I and II to yield disaccharides and the resulting SAX-HPLC profiles are shown in Figure 6.11. The

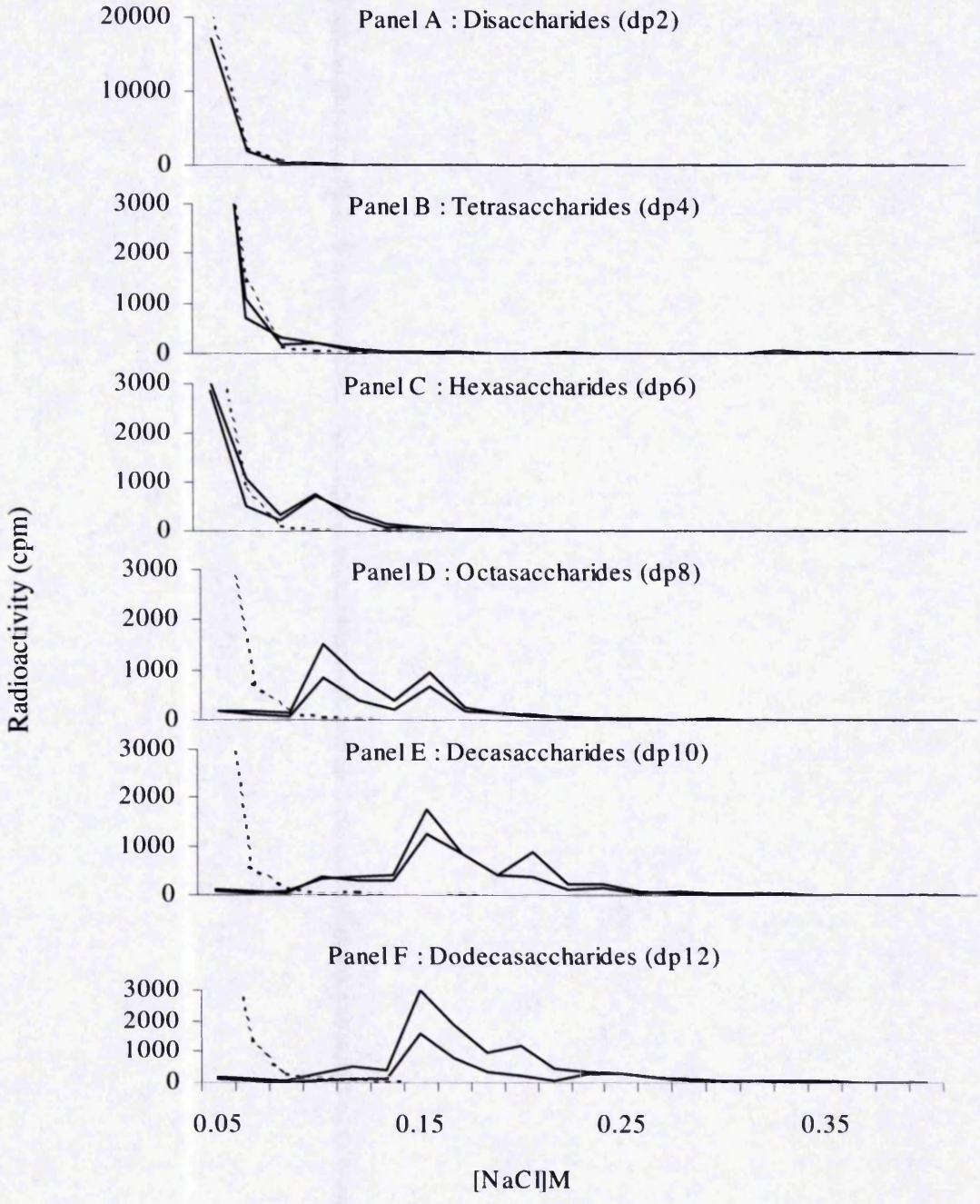

Figure 6.9: Binding of disaccharides and S-domains (dp4-12) to HEM
Panels A – F ~ 5-10K cpm ^{3}H-dp2 from a heparinase I, II and III digest of HMVEC HS and ^{3}H-S-domains (dp4-12), isolated from heparinase III digestion of ~$1x10^{6}$ cpm ^{3}H-HMVEC HS as previously described, were incubated with 40μM HEM in 0.05 M NaCl, 10mM Tris, pH7.0. Bound ^{3}H-S-domains were determined by the FBA with 3 x 1 ml washes of increasing 0.05M NaCl increments and 1 ml washes monitored by scintillation counting. Assays were performed in duplicate, ^{3}H-HS retained on the filter was <0.1%, hashed lines = negative control with BSA substituting for HEM.

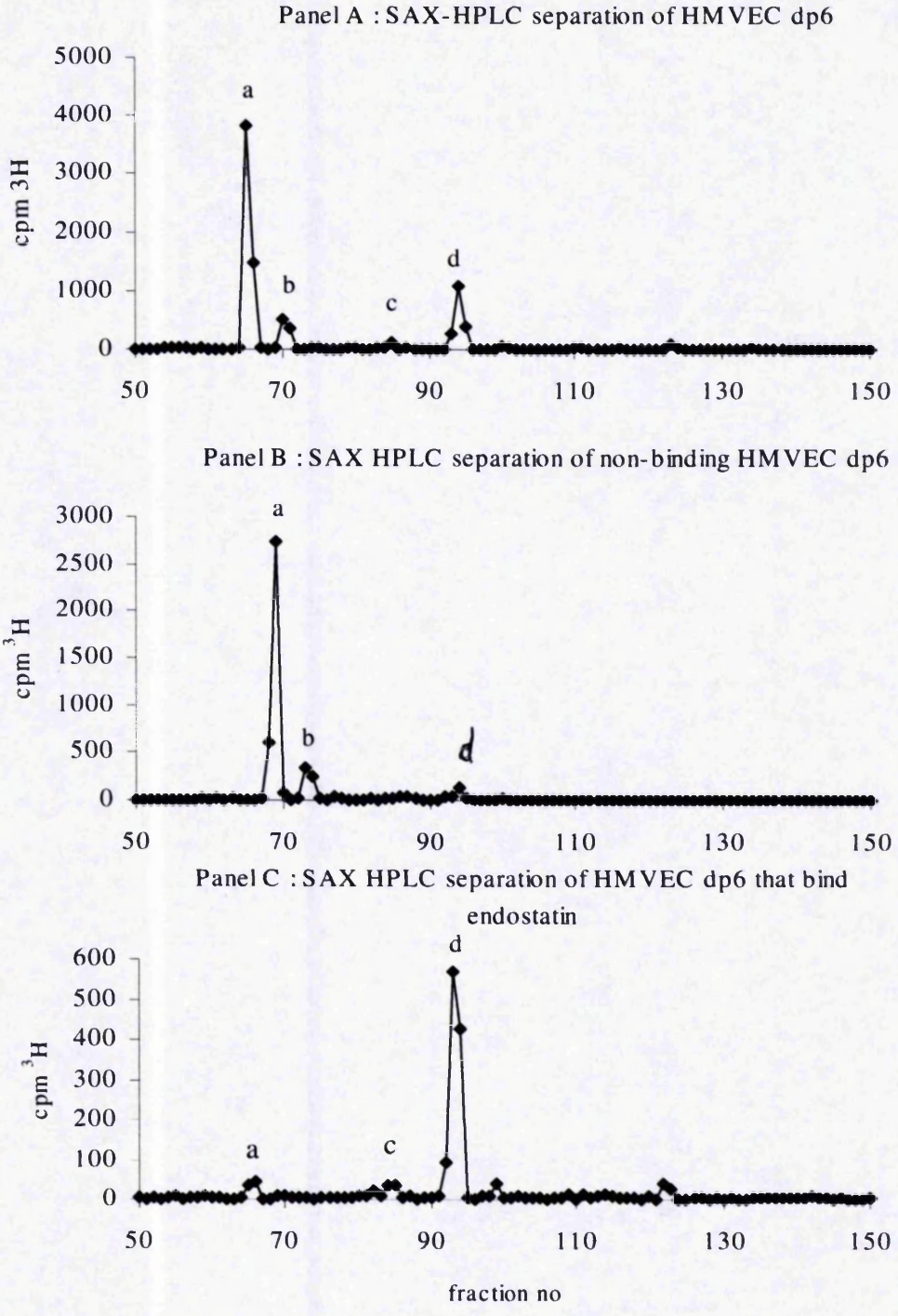

Figure 6.10 : SAX-HPLC S-domain profiling of HMVEC hexasaccharides (dp6) fractionated by affinity for HEM. ~50K cpm ^{3}H-dp6 from HMVEC HS were generated by heparinase III digestion, purified by Bio-Gel P10 chromatography, and incubated with 40µM HEM in 0.05M NaCl, 10mM Tris, pH7.0. Bound ^{3}H-dp6 were eluted with 3 x 1ml 0.1M NaCl, 10mM Tris, pH7.0 using the FBA as previously described. Bound and unbound fractions were desalted and resolved on a single Pro-Pac PA1 column with a linear gradient of 0-1M NaCl in milliQ water, pH 3.5 over 80 minutes, at a flow rate of 1 ml/min and 0.5ml fractions were collected. Elution profiles were monitored by sccintillation counting. Panel A- HMVEC dp6 before subfractionation; Panel B- Unbound dp6; Panel C – Bound dp6.

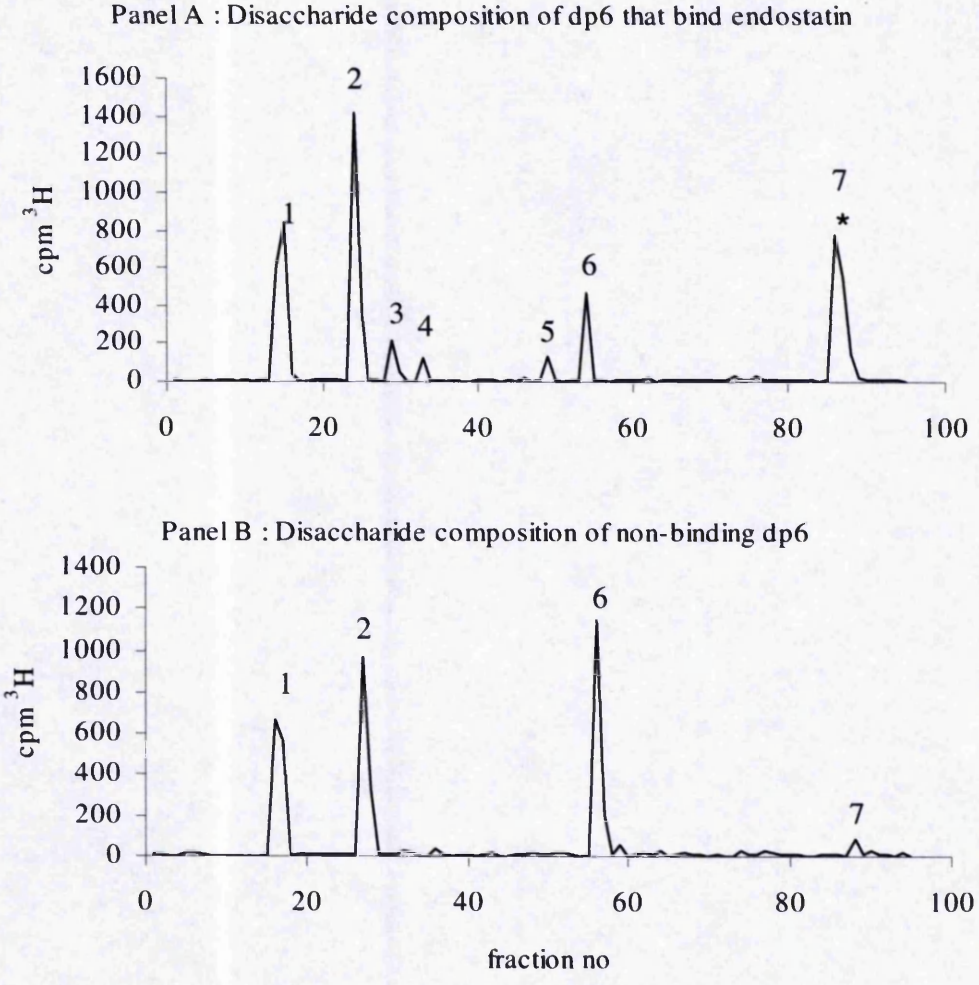

Figure 6.11 : SAX-HPLC analysis of disaccharides comprising HMVEC hexasaccharides fractionated by affinity for HEM. ~50K cpm ^{3}H-dp6 from HMVEC generated by heparinase III digestion and purified by Bio-Gel P10 chromatography, were incubated with 40µM HEM in 0.05M NaCl, 10mM Tris, pH7.0, and bound ^{3}H-dp6 eluted with 3 x 1ml 0.1M NaCl, 10mM Tris, pH7.0 using the FBA as previously described. Bound and unbound fractions were desalted, digested with heparinase I and II to disaccharides, then resolved on a Pro-Pac PA1 SAX-HPLC column eluted with a 0-1M NaCl, pH3.5 gradient over 45 minutes. Fractions collected (0.5ml) were monitored by scintillation counting. The numbered peaks correspond to the elution positions of known disaccharide standards as follows:- 1= UA-GlcNAc; 2=UA-GlcNS; 3=UA-GlcNAc(6S); 4=UA(2S)-GlcNAc; 5=UA-GlcNS(6S); 6=UA(2S)GlcNS; 7=UA(2S)GlcNS(6S). (^{3}H black line ^{35}S red line, UA=unsaturated uronic acid). Panel A- Unbound dp6; Panel B – Bound dp6.

Table 6.1A

STANDARD PEAK NO. (in order of elution)	DISACCHARIDE STRUCTURE	TOTAL DISACCHARIDES (%)	
		Non-binding	Binding (0.1M NaCl)
1	UA-GlcNAc	31	26
2	UA-GlcNS	33	32
3	UA-GlcNAc(6S)		5
4	UA(2S)-GlcNAc		2
5	UA-GlcNS(6S)		
6	UA(2S)-GlcNS	34	8
7	UA(2S)-GlcNS(6S)	2	27

Table 6.1B

SULPHATE MODIFICATION	NUMBER OF SULPHATE GOUPS PER HEXASACCHARIDE	
	Non-binding	Binding (0.1M NaCl)
N-sulphate	2.07	2.01
2-O-sulphate	1.08	1.11
6-O-sulphate	0.06	0.96
Total sulphate	3.21	4.08

Table 6.1 : Disaccharide composition and sulphate distribution of affinity fractionated HMVEC dp6 S-domains. The total ^{3}H cpm contributing to each peak in Figure 6.11 was calculated as a percentage of the total ^{3}H of all peaks to obtain the disaccharide compositions (6.1A). The proportions were used to estimate the number of sulphate modifications per hexasaccharide (6.1B).

SAX-HPLC profiles confirm that the compositions of the hexasaccharides with affinity for HEM are different. Notably, peak 7 (Figure 6.11, Panel B), the trisulphated disaccharide [UA(2S)GlcNS(6S)] is enriched in the binding pool. Analysis of the stoichiometry of disaccharides from the total cpm ^{3}H in each peak suggested the presence of more than one dp6 species in the binding pool (Table 6.1). By combining data from these analyses with the SAX-HPLC elution profiles (Figure 6.10), and sequencing data from BAEC and 3T3 HS dp6 that co-elute (Figure 4.17, Merry *et al.*,1999, Appendix 1), structures of hexasaccharides that bind HEM can be inferred :

Hexasaccharide structures that do not bind HEM

6a = ΔUA-GlcNS-IdoA(2S)-GlcNS-IdoA-GlcNAc

6b = ΔUA-GlcNS-IdoA(2S)-GlcNS-GlcA-GlcNAc

Hexasaccharide structures that bind HEM

6c = ΔUA-GlcNS-IdoA(2S)-GlcNS-IdoA(2S)-GlcNAc

6d = ΔUA-GlcNS-IdoA(2S)-GlcNS(6S)-IdoA-GlcNAc

However, the presence of minor quantities of [UA-GlcNS(6S)] and [UA-GlcNAc(6S)] in the binding pool (Table 6.1) suggest additional minor contaminants. In addition, due to the low abundance of dp6c, it was unclear whether it also bound HEM. To clarify this, purified dp6 from BAEC HS were tested individually for ability to bind HEM. This confirmed affinity to both dp6c and dp6d (Figure 6.12). In order to establish whether a small but measurable difference in affinity existed between dp6c and dp6d the FBA was repeated using smaller 0.025M NaCl increments to elute the dp6. This did not enable further subfractionation (data not shown). However, combining data from this experiment, and those shown in Figure 6.12 and Figure 6.13, a statistically significant (TTEST $p<0.01$) higher proportion of dp6d (56.5%±3.87%, n=4) bound to HEM, compared to dp6c (40±6%, n=3). This indicates that an additional 6-O-sulphate in place of a 2-O-sulphate, or the trisulphated disaccharide [UA(2S)-GlcNS(6S)] may confer stronger binding. Significantly, mAb 12C1 inhibited binding of dp6d to HEM, suggesting that dp6d binds to the primary heparin binding epitope of HEM (Figure 6.13).

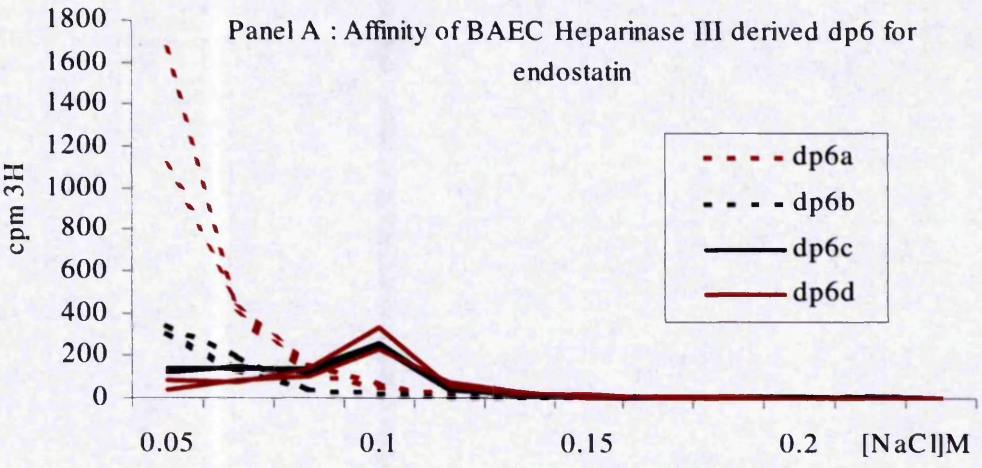

Figure 6.12 : Affinity of BAEC S-domains dp6a-d for HEM. BAEC S-domains (dp6) were extracted following heparinase III digestion of $4x10^6$ cpm ^{3}H-HS by Bio-Gel P10 filtration, resolved by SAX-HPLC to obtain single species, and desalted. ~3Kcpm ^{3}H dp6 a-d were incubated with 40μM HEM in 0.05 M NaCl, 10mM Tris, pH7.0. Bound ^{3}H-dp6 were determined by the FBA with 3 x 1 ml washes of increasing 0.05M NaCl increments and 1 ml washes were monitored for radioactivity by scintillation counting. Results of assays performed in duplicate are shown.

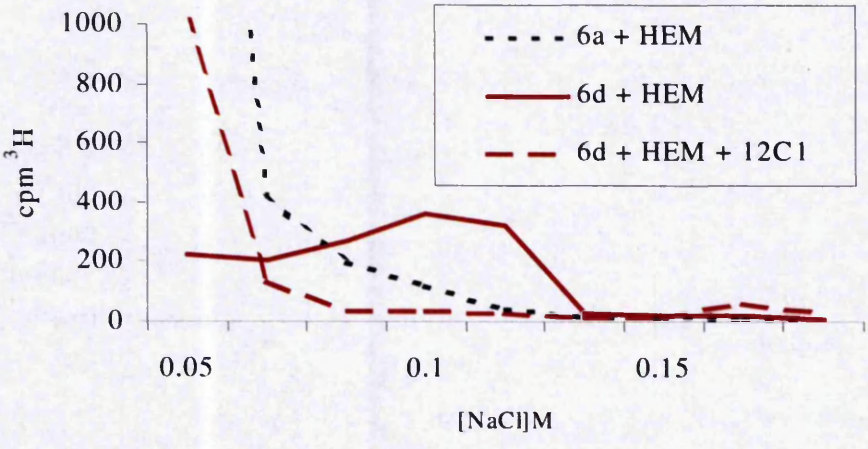

Figure 6.13 : Binding of BAEC 6d in the presence of neutralising mAb 12C1.
~ 3 K cpm ^{3}H- dp6d were incubated in 25 μl 0.05M NaCl, 10mM Tris, pH7.0 with 40μM HEM in the presence or absence of 10μM neutralising mAb 12C1. Bound ^{3}H-HS was determined by the filter binding assay with 3 x 1 ml washes of increasing, 0.05M increments of NaCl. 1 ml washes were monitored for radioactivity by scintillation counting. ^{3}H-HS retained on the filter was <0.1% and 6a, incubated with HEM as above was included as a negative control.

6.5 Structural characterisation of octasaccharides with affinity for HEM

Octasaccharides from HMVEC HS

Heparinase III derived octasaccharides (dp8) were investigated to gain further insight into the structural determinants of the HEM-HS interaction using a similar approach to that for the dp6 above. Thus, a preparative FBA was performed to affinity fractionate ~ 70K cpm ^{3}H-dp8 S-domains from HMVEC HS as described in section 6.3 with the exception that higher NaCl concentrations were required to elute the bound ^{3}H-dp8. The elution profile was as shown in Figure 6.9, Panel D. Three pools were obtained; an unbound, eluting with 0.05M NaCl, a low affinity, eluting with 0.1M NaCl and a pool eluting with 0.15M NaCl, denoted high affinity.

The material in each pool was recovered, desalted, and divided for S-domain profiling or disaccharide compositional analysis by SAX-HPLC. The minor yield from the non-binding fraction (0.05M NaCl) was insufficient for S-domain profiling. The S-domain profiles of the low and high affinity fractions were compared to the S-domain profile of dp8 before fractionation by HEM affinity (Figure 6.14). As obtained previously (Fig 4.18, Panel A,) the total pool shows two dominant octasaccharide species, denoted 8* and 8**. The profiles after fractionation show that the dominant octasaccharides differ in affinity for HEM with enrichment of the more highly charged 8**, in the high affinity binding fraction.

The ^{3}H-dp8 in each pool were then digested with heparinase I and II to yield disaccharides and the resulting SAX-HPLC profiles are shown in Figure 6.15. As expected, the SAX-HPLC profiles show that the profiles of the dp8 with affinity for HEM are different. Again, an increase in peak 7 (Figure 6.15), the trisulphated disaccharide [UA(2S)-GlcNS(6S)] is associated with stronger binding. Analysis of the stoichiometry of disaccharides from the total cpm ^{3}H in each peak is consistent with the presence of more than one dp8 species in each pool (Table 6.2A). As suggested by the SAX-HPLC profiles (Figure 6.15) the most highly sulphated octasaccharides bind strongest (Table 6.2B) and the higher sulphation is principally determined by an increase in the trisulphated disaccharide (Table 6.2A).

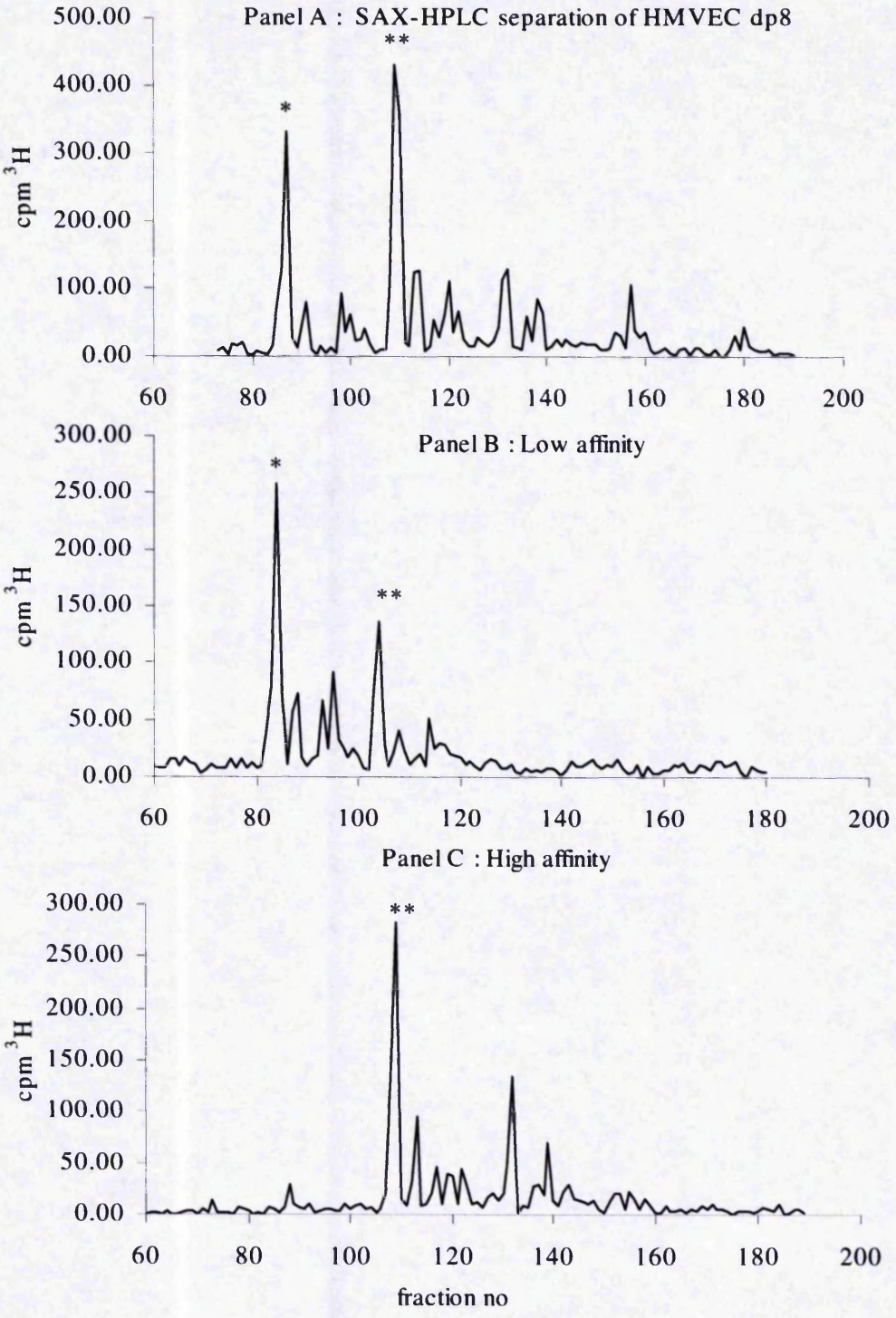

Figure 6.14 : SAX-HPLC S-domain profiling of HMVEC octasaccharides fractionated by affinity for HEM. ~70K cpm ^{3}H-dp8 from HMVEC generated by heparinase III digestion and purified by Bio-Gel P10 chromatography, were incubated with 40μM HEM in 0.05M NaCl, 10mM Tris, pH7.0, and bound ^{3}H-dp8 eluted with 3 x 1ml increasing 0.05M NaCl increments using the FBA as previously described. Low affinity (eluted with 0.1M NaCl, Panel B) and high affinity (eluted with 0.15M NaCl, Panel C) were desalted and resolved on a single Pro-Pac PA1 column with a linear gradient of 0-1.2M NaCl in milliQ water, pH 3.5 over 90 minutes, at a flow rate of 1 ml/min and 0.5ml fractions were collected. Elution profiles were monitored by scintillation counting. Panel A shows dp8 before subfractionation by HEM affinity resolved on SAX-HPLC as above.

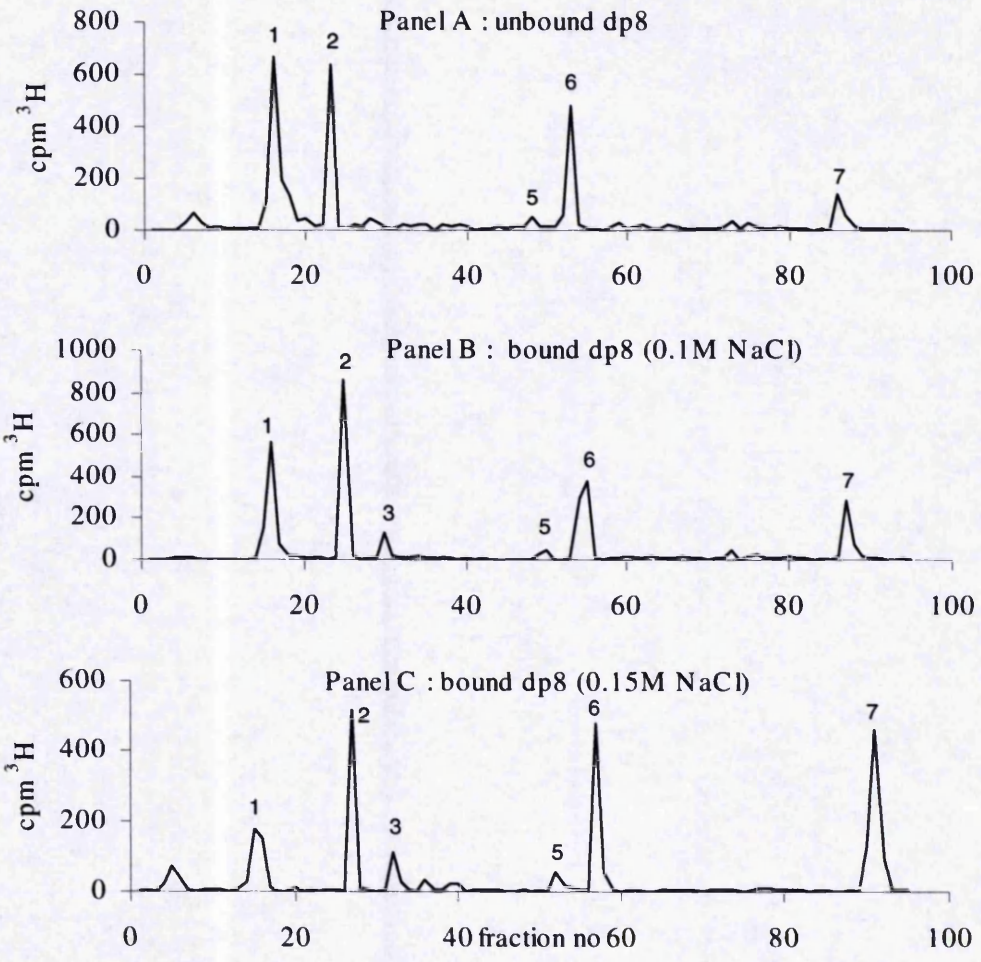

Figure 6.15 : SAX-HPLC analysis of disaccharides comprising HMVEC octasaccharides fractionated by affinity for HEM. ~70K cpm ^{3}H-dp8 generated by heparinase III digestion of HMVEC HS and purified by Bio-Gel P10 chromatography, were incubated with 40μM HEM in 0.05M NaCl, 10mM Tris, pH7.0, and bound ^{3}H-dp8 eluted with increasing 0.05M NaCl increments using the filter binding assay as previously described. Pooled fractions were desalted, digested with heparinase I and II to disaccharides, then resolved on a Pro-Pac PA1 SAX-HPLC column eluted with a 0-1M NaCl, pH3.5 gradient over 45 minutes. Fractions collected (0.5ml) were monitored by scintillation counting. The numbered peaks correspond to the elution positions of known disaccharide standards as follows:- 1= UA-GlcNAc; 2=UA-GlcNS; 3=UA-GlcNAc(6S); 4=UA(2S)-GlcNAc; 5=UA-GlcNS(6S); 6=UA(2S)GlcNS; 7=UA(2S)GlcNS(6S). Panel A- Unbound dp8; Panel B – Low affinity dp8; Panel C – High affinity dp8.

Table 6.2A

STANDARD PEAK NO. (in order of elution)	DISACCHARIDE STRUCTURE	TOTAL DISACCHARIDES (%)		
		Non-binding	Low affinity (0.1M NaCl)	High affinity (0.15M NaCl)
1	UA-GlcNAc	45	27	20
2	UA-GlcNS	26	30	21
3	UA-GlcNAc(6S)		5	6
4	UA(2S)-GlcNAc			
5	UA-GlcNS(6S)		2	3
6	UA(2S)-GlcNS	20	23	22
7	UA(2S)-GlcNS(6S)	8	12	28

Table 6.2B

SULPHATE MODIFICATION	NUMBER OF SULPHATE GOUPS PER OCTASACCHARIDE		
	Non-binding	Low affinity (0.1M NaCl)	High affinity (0.15M NaCl)
N-sulphate	2.16	2.68	2.96
2-O-sulphate	1.12	1.40	2.00
6-O-sulphate	0.32	0.76	1.48
Total sulphate	3.6	4.84	6.44

Table 6.2 : Disaccharide composition and sulphate distribution of affinity fractionated HMVEC dp8 S-domains. The total ^{3}H cpm contributing to each peak in Figure 6.15 was calculated as a percentage of the total ^{3}H of all peaks to obtain the disaccharide compositions (6.1A). The proportions were used to estimate the number of sulphate modifications per octasaccharide (6.1B).

Direct binding of S-domain dp8 species from BAEC HS

BAEC dp8 S-domains were previously shown to comprise 7 structural variants denoted 8a,b,c,c*,d,e,f* according to previous nomenclature used for sequencing of 3T3 dp8 with * denoting BAEC variants (Figure 4.18). Species c*, d,e and f* were noted to have similar overall charge density but distinctions in structure (Figure 4.24, Table 4.4). Small (~2K cpm ^{3}H) quantities were available to test these species individually for affinity to HEM using the FBA as previously described. The result in Figure 6.16 shows a correlation between increased affinity for HEM and charge density.

As predicted by the weak affinity of dp6c for HEM, dp8a and 8b, that contain the structure of dp6c, bind between 0.05 and 0.1M NaCl and the presence of an additional mono N-sulphated disaccharide in dp8a and dp8b does not confer stronger binding.

6c = ΔUA-GlcNS-IdoA(2S)-GlcNS-IdoA(2S)-GlcNAc

8a = ΔUA-GlcNS-IdoA(2S)-GlcNS-IdoA(2S)-GlcNS-IdoA-GlcNAc

8b = ΔUA-GlcNS-IdoA(2S)-GlcNS-IdoA(2S)-GlcNS-GlcA-GlcNAc

BAEC dp8c to dp8f* exhibit progressively stronger binding. Again, the trisulphated disaccharide is associated with the highest affinity binding species. However, comparing 8c* to 8e and 8f* (Figure 4.24, Table 4.4) there are also possible indications of specificity for 6-O-sulphate groups, rather than a purely charge based interaction. These octasaccharides are of similar overall sulphation. Although 8c* is a mixed species, it has a similar level of 2-O-sulphate, higher N-sulphate, lower 6-O-sulphate and a slightly reduced affinity compared to 8e.

An interesting distinction is observed between 8e and 8f*. The disaccharide compositions of these octasaccharides suggest the following structures :

8e = ΔUAGlcNS – IdoA(2S)GlcNS(6S) – IdoA(2S)GlcNS – GlcAGlcNAc

8f* = ΔUAGlcNS - IdoA(2S)GlcNS(6S) - UAGlcNS – UAGlcNAc(6S)

These dp8 exhibit strongest binding, have a similar overall charge, and both comprise a trisulphated disaccharide with a positional difference in a further O-sulphate substitution. The binding profiles show that the apparent affinity of dp8f* is slightly

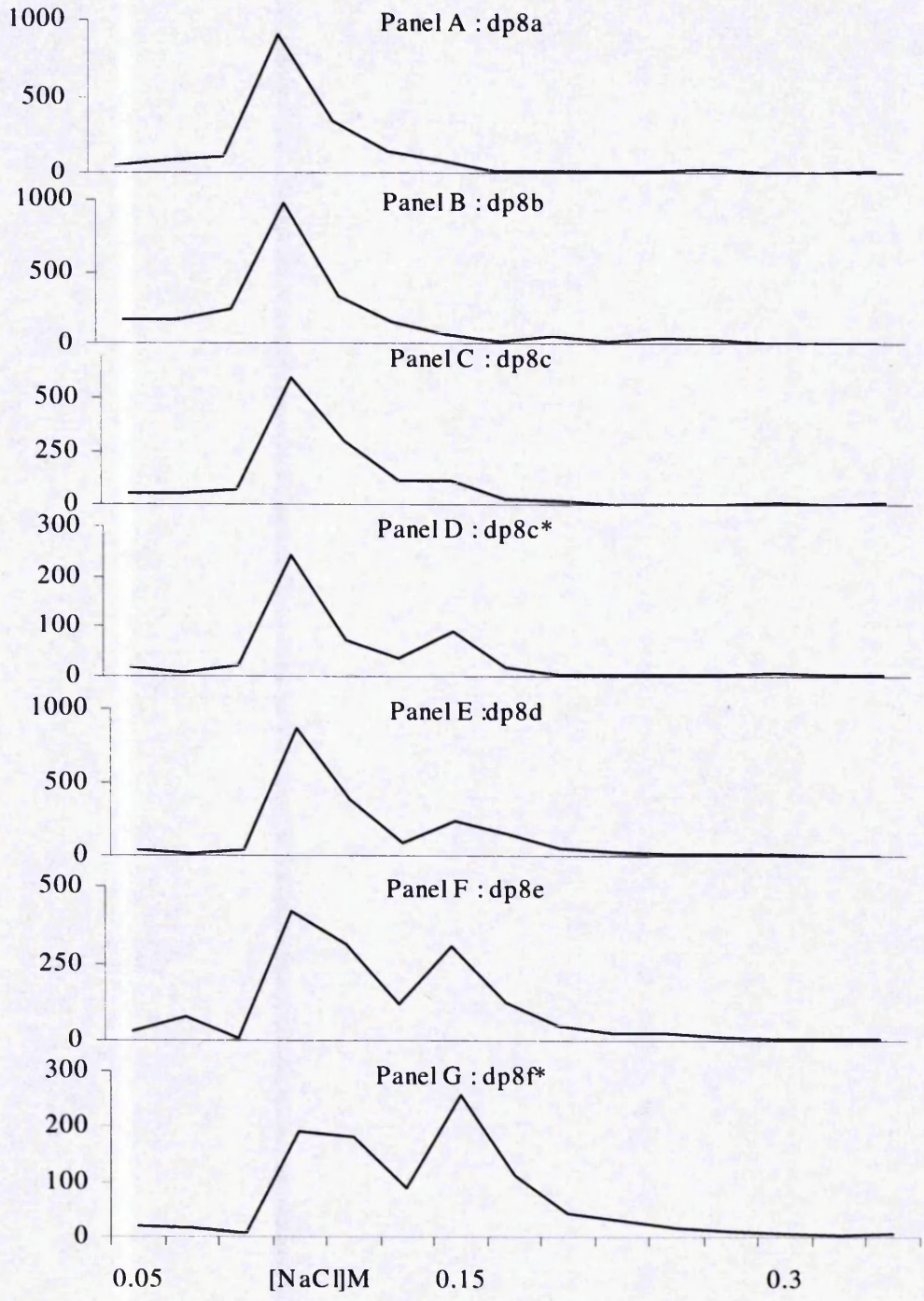

Figure 6.16 : Affinity of single species BAEC S-domains (dp8) for HEM using the filter binding assay. Panels A – G : BAEC S-domains, dp8: a,b,c,c*,d,e,f*, were extracted after heparinase III digestion of $4x10^6$ cpm ^{3}H-HS by Bio-Gel P10 filtration, resolved by SAX-HPLC to obtain single species, and desalted. ~2Kcpm ^{3}H of each dp8 was incubated with 40μM HEM in 0.05 M NaCl, 10mM Tris, pH7.0, bound ^{3}H-dp8 determined by the FBA with 3 x 1 ml washes of increasing 0.05M NaCl increments and 1 ml washes monitored for radioactivity by scintillation counting.

increased compared to dp8e, suggesting a small advantage in favour of an additional 6-O-sulphate rather than 2-O-sulphate. However, the difference is small. In addition, the N-sulphate and 2-O-sulphate content of dp8f* is significantly reduced compared to 8c* favouring the increase in 6-O-sulphation and the presence of the trisulphated disaccharide as consistent features of higher affinity binding species. However, it has not been possible to obtain sufficient quantities of material to confirm these observations since 8f* is a minor species that is frequently part of a complex peak (Figure 4.18).

6.6 Characterisation of S-domains (dp12 and dp18)

Affinity of 3T3 derived dp12 and dp18 for HEM

Previous experiments suggested that S-domains of dp10/12 were optimal for binding to HEM in physiological conditions. These S-domains are relatively rare in HMVEC HS and it was not possible to obtain sufficient quantities for affinity fractionation and structural analysis. Instead, S-domains of dp12 and dp18 (the longest available) from 3T3 HS (provided by C Merry) were examined. First, to confirm the suitability of 3T3 dp12 as a surrogate for HMVEC dp12, binding profiles were compared and are shown in Figure 6.17, panel A. The HMVEC and 3T3 dp12 behave similarly although, interestingly, the affinity of those from 3T3 HS appears slightly reduced (by ~ 0.05M NaCl), matching the reduced affinity of intact (parent) 3T3 chains compared to intact HMVEC HS. This was also observed for the dp18 (Figure 6.17, Panel B), suggesting that the determinants for the affinity of the intact chains are associated with the longer S-domains.

Characteristics of affinity fractionated dp12 and dp18

A preparative FBA was performed to subfractionate ~ 100K cpm ^{3}H each of dp12 and dp18 S-domains from 3T3 fibroblast HS as described previously. Four pools were obtained; an unbound (non), eluted with 0.05M NaCl, a low affinity, eluted with 0.1M NaCl, a medium affinity eluted with 0.15M NaCl, and a pool eluted with 0.3M NaCl denoted high affinity. The material in each pool was recovered and desalted then half the radioactivity present in each (~ minimum of 3K cpm ^{3}H) was taken for disaccharide compositional analysis by SAX-HPLC as previously described.

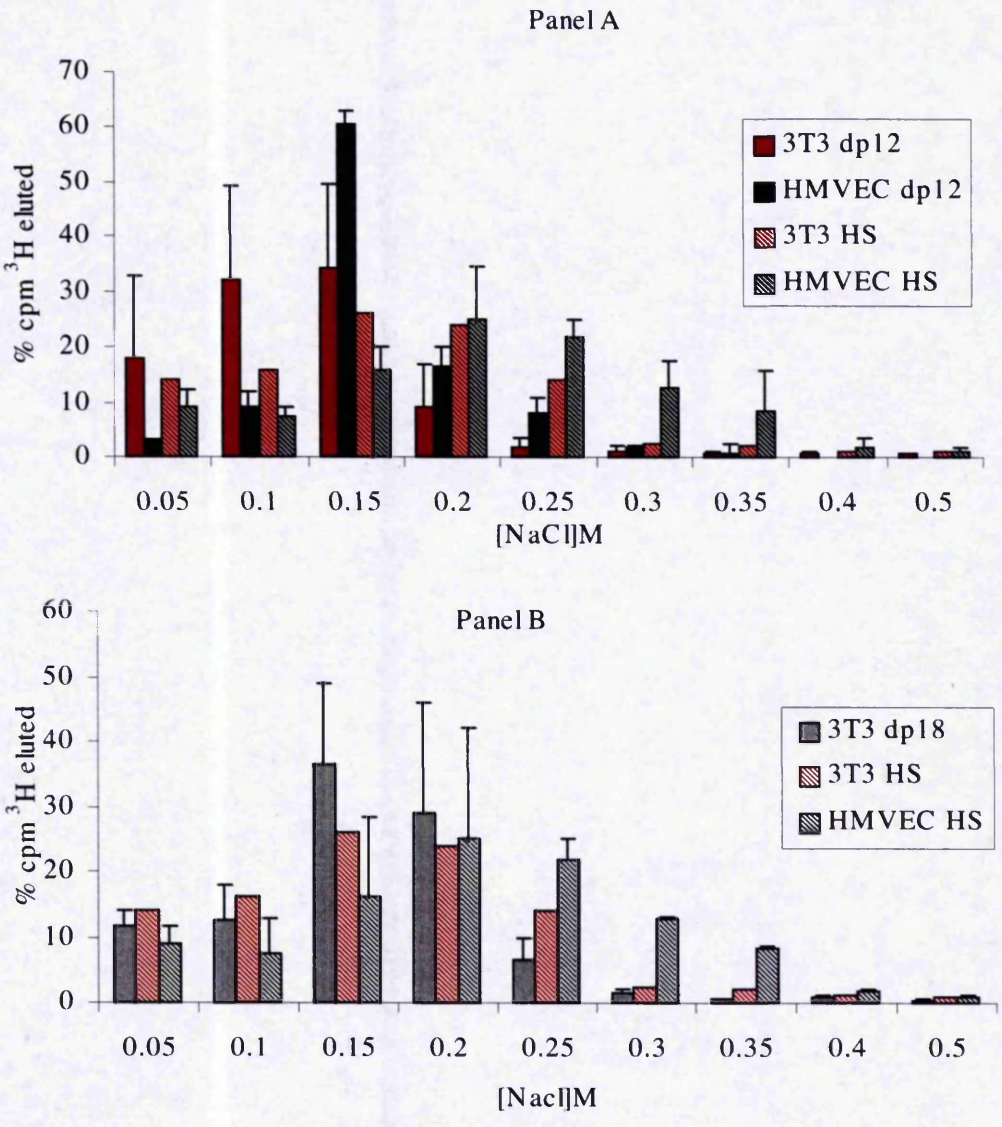

Figure 6.17 : Affinity of 3T3 S-domains (dp12 and dp18) for HEM. ~ 10K cpm ^{3}H-HMVEC or 3T3 fibroblast HS and ~ 10K cpm heparinase III generated ^{3}H -dp12 from HMVEC or 3T3 fibroblast HS (Panel A) or dp18 from 3T3 fibroblast HS (Panel B) were incubated with 40µM HEM in 25µl 0.05M NaCl, 10mM Tris, pH7.0, and bound ^{3}H-HS determined by the FBA with 3 x 1 ml washes of increasing, 0.05M increments of NaCl. The bars show means + SD obtained from 2-5 independent experiments of cpm ^{3}H eluted as a percent of total cpm ^{3}H (except 3T3 HS, n=1). No binding was observed in negative controls substituting BSA for HEM and ^{3}H-HS retained on the filter was <0.1% (data not shown).

The profiles are shown in Figure 6.18 and 6.19 and the results are summarised in Table 6.3. The main observation is that increased sulphate content confers stronger binding for both dp12 and dp18. Note that in the dp18 medium affinity fraction there is an unidentified peak arising from incomplete digestion of the oligosaccharides so the proportions of disaccharides and sulphate contents given for this fraction will be an overestimate. Nevertheless, the presence of 6-O-sulphation in the medium and high affinity binding species distinguishes these from the non and low affinity binding species for the dp12 and dp18 S-domains. However, the low affinity binding fractions are more sulphated than the corresponding dp6 and dp8 that bind with this affinity. Therefore, the remainder of each pool was rebound to HEM, and eluted using the FBA as previously described, to determine the extent of subfractionation. Figure 6.20 shows some redistribution of all binding fractions but most marked in the non-binding fraction (0.05M NaCl) due to the dynamic binding equilibrium. Nevertheless, the binding profiles showed a clear shift to the right from the non-binding to high binding fractions. Interestingly, the high binding fraction has also shifted further to the right than the original binding profile, possibly due to the absence of competition from low affinity dp12. Therefore the initial subfractionation was considered adequate to compare structural characteristics of these S-domains relative to affinity for HEM and the ability of low binding species to rebind with higher affinity (although minimal at > 0.15M) was consistent with previous data.

With the exception of a minor proportion of [UA-GlcNS(6S)] in the medium affinity dp18 fraction, the trisulphated disaccharide [UA(2S)-GlcNS(6S)] provides the 6-O-sulphate in the binding S-domains and it is not possible to discern whether both the 2-O-sulphate and 6-O-sulphate present on this disaccharide are of equal importance. However, in contrast to the marked differences in 6-O-sulphate, there are similar (near maximal) 2-O-sulphate levels in all the dp12 fractions, and the low compared to medium and high affinity dp18 fractions, indicating a requirement for 6-O-sulphate to confer stronger binding.

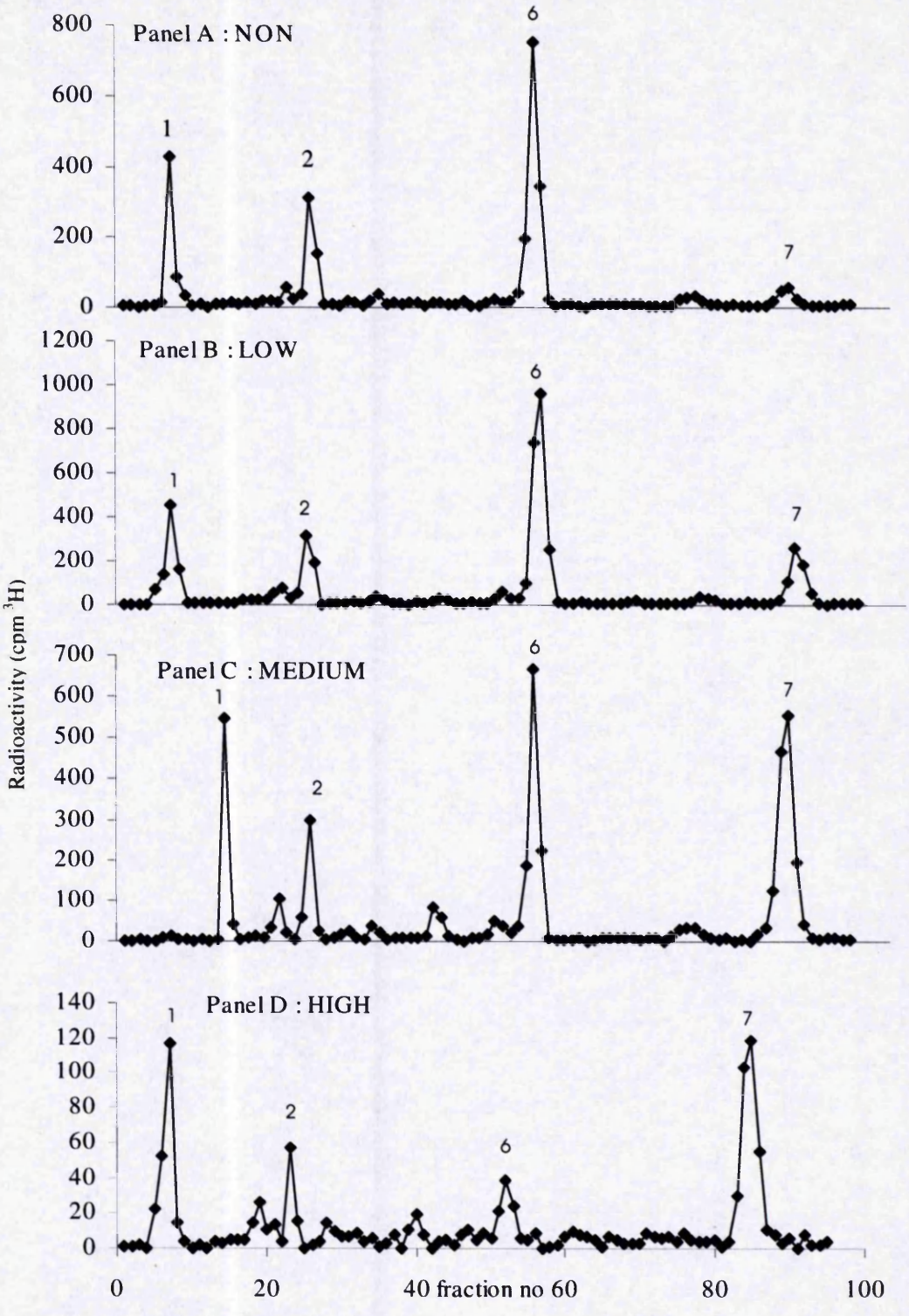

Figure 6.18 SAX-HPLC analysis of disaccharides comprising dp12 oligosaccharides fractionated by affinity for HEM. ~100K cpm ^{3}H-dp12 from 3T3 fibroblast HS were incubated with 40μM HEM in 0.05M NaCl, 10mM Tris, pH7.0, and bound ^{3}H-dp12 eluted with increasing 0.05M NaCl increments using the FBA. Pooled fractions were desalted, digested with heparinase I and II to disaccharides, then resolved on a Pro-Pac PA1 SAX-HPLC column eluted with a 0-1M NaCl, pH3.5 gradient over 45 minutes. Fractions collected (0.5ml) were monitored by scintillation counting. The numbered peaks correspond to the elution positions of known disaccharide standards as follows:- 1= UA-GlcNAc; 2=UA-GlcNS; 6=UA(2S)GlcNS; 7=UA(2S)GlcNS(6S). Panel A- nonbound dp12; Panel B – Low affinity dp12; Panel C – Medium affinity dp12, Panel D –high affinity dp12.

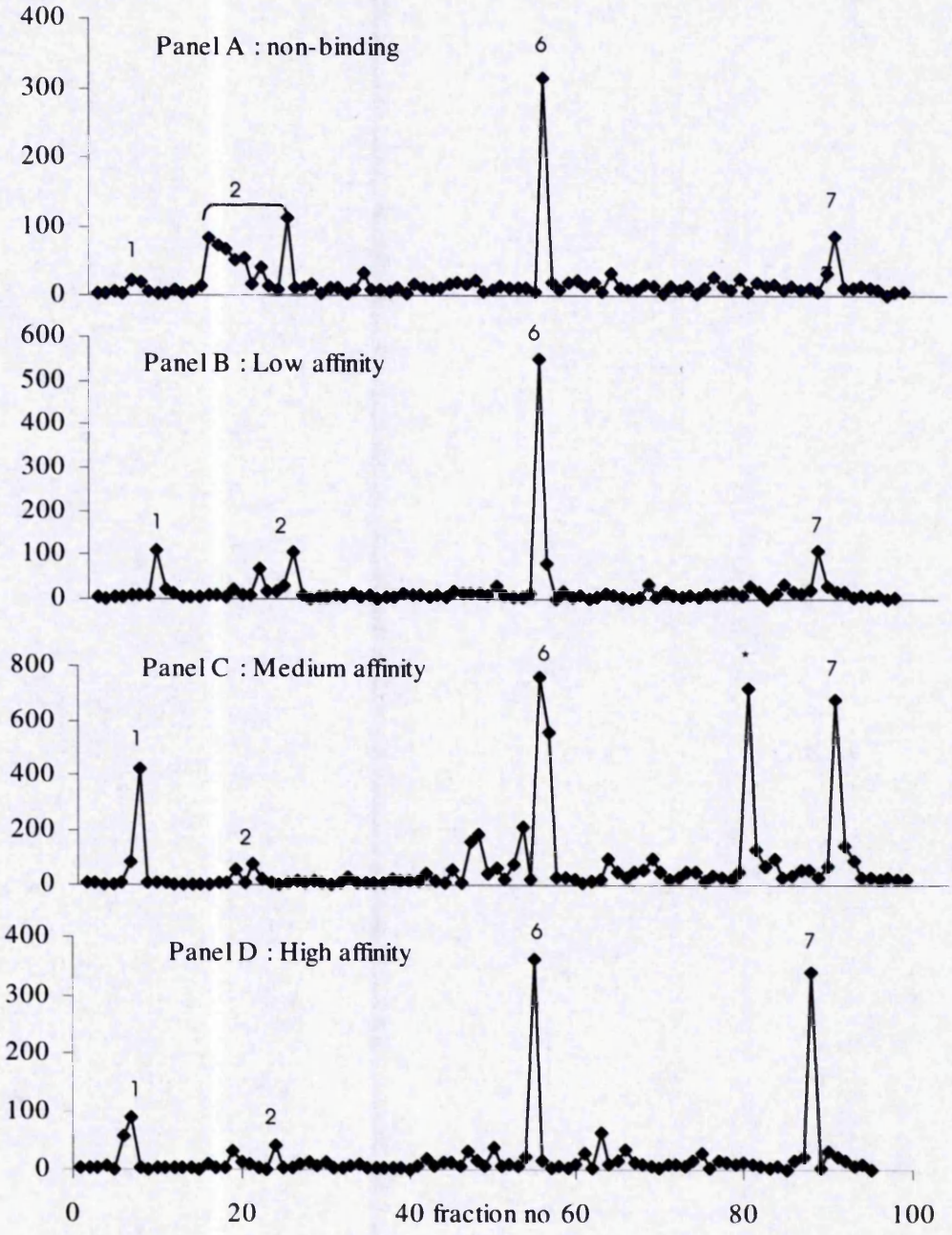

Figure 6.19 : SAX-HPLC analysis of disaccharides comprising dp18 oligosaccharides fractionated by affinity for HEM. ~100K cpm ^{3}H-dp18 from 3T3 fibroblast HS were incubated with 40μM HEM in 0.05M NaCl, 10mM Tris, pH7.0, and bound ^{3}H-dp18 eluted with increasing 0.05M NaCl increments using the FBA. Pooled fractions were desalted, digested with heparinase I and II to disaccharides, then resolved on a Pro-Pac PA1 SAX-HPLC column eluted with a 0-1M NaCl, pH3.5 gradient over 45 minutes. Fractions collected (0.5ml) were monitored by scintillation counting. The numbered peaks correspond to the elution positions of known disaccharide standards as follows:- 1= UA-GlcNAc; 2=UA-GlcNS; 6=UA(2S)GlcNS; 7=UA(2S)GlcNS(6S). Panel A- nonbound dp18; Panel B – Low affinity dp18; Panel C – Medium affinity dp18, Panel D –high affinity dp18. Panel C * denotes unidentified peak due to incomplete digest.

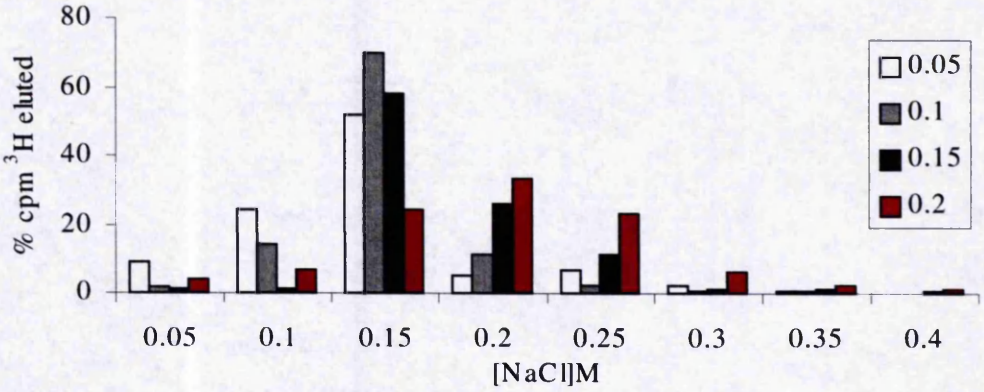

Figure 6.20 : Rebinding of dp12 S-domains. ~100K cpm 3H 3T3 fibroblast HS dp12 were fractionated according to affinity for HEM, recovered, desalted and aliquots rebound to . Bound ^{3}H-HS was determined by the FBA with 3 x 1 ml washes of increasing, 0.05M increments of NaCl. No binding was observed in negative controls substituting BSA for HEM and ^{3}H-HS retained on the filter was <0.1% (data not shown).

Panel A

DP12				
Disaccharide Species (%)	NON 0.05M NaCl	LOW 0.1M NaCl	MED 0.15M NaCl	HIGH 0.3M NaCl
UA-GlcNAc	22	20	17	30
UA-GlcNS	20	14	11	9
UA-GlcNAc(6S)				
UA(2S)-GlcNAc				
UA-GlcNS(6S)				
UA(2S)-GlcNS	54	51	32	13
UA(2S)-GlcNS(6S)	4	15	40	48
Sulphate distribution per S-domain				
Total Sulphate	8.4	9.7	11.7	10.74
Total N-sulphate	4.7	4.8	5.0	4.2
Total 2-O-sulphate	3.5	4.0	4.32	3.7
Total 6-O-sulphate	0.2	0.9	2.4	2.9

Panel B

DP18				
Disaccharide Species (%)	NON 0.05M NaCl	LOW 0.1M NaCl	MED 0.15M NaCl	HIGH 0.3M NaCl
UA-GlcNAc	37	13	17	17
UA-GlcNS	14	13	3	0
UA-GlcNAc(6S)				
UA(2S)-GlcNAc				
UA-GlcNS(6S)			7	
UA(2S)-GlcNS	36	61	43	42
UA(2S)-GlcNS(6S)	13	13	30	42
Sulphate distribution per S-domain				
Total Sulphate	11.25	15.7	17.4	18.9
Total N-sulphate	3.8	7.8	7.5	7.6
Total 2-O-sulphate	4.4	6.7	6.6	7.6
Total 6-O-sulphate	1.2	1.2	3.3	3.8

Table 6.3 : Disaccharide composition and sulphate distribution of affinity fractionated 3T3 dp12 (Panel A) and dp18 (Panel B) S-domains. The total ^{3}H cpm contributing to each peak in the disaccharide analysis was calculated as a percentage of the total ^{3}H of all peaks to obtain the disaccharide compositions. These proportions were used to estimate the sulphate contents for the oligosaccharides of given lengths.

6.7 The role of specific sulphate groups in the HEM binding domain of HS

Competition with chemically desulphated GAGs

As an approach to tease out the role of 6-O-sulphate compared to 2-O-sulphate in the HS recognition sequence for HEM, a range of chemically desulphated HS species, bovine lung heparin, CS and DS were used to compete with ^{3}H-HS (HMVEC and BAEC) for HEM in the FBA. As described in Methods, ~ 2K ^{3}H-HS and cold competitor (40 or 200μg/ml) were incubated together with 40 μM HEM in 0.13M NaCl, 10mM Tris, pH 7.0 for 2 hours. The proportions of unbound and bound ^{3}H-HS were determined by the FBA with 3 x 1 ml washes of 0.13M NaCl, 10mM Tris, pH 7.0, then 3 x 1ml washes of 1.0M NaCl, 10mM Tris, pH 7.0 respectively. The results are shown as the proportion of ^{3}H-HS bound compared to control samples (90-92% bound in the absence of competitor) in Figure 6.21.

The highly sulphated heparin was the best competitor and the desulphated HS species were poorer competitors than normal porcine mucosal HS. The loss of either 6-O-sulphate or N-sulphate from HS significantly impaired competition indicating that these are important modifications for binding of HS. The ability of 2-O-desulphated HS to compete was not impaired to the same extent. This is interesting given that the de 2-O-sulphated and de 6-O-sulphated HS share the same overall level of sulphation, and therefore charge (Table 6.4). In addition, the 6-O-desulphation is not complete, suggesting that the positions of these sulphate groups may also be critical. The reduced ability of the de-N-sulphated HS to compete may be a reflection of its lower charge density. Similarly, CS type C (from shark cartilage) and DS (CSB from bovine mucosa) both compete with ^{3}H-HS for HEM and it is difficult to discern the extent to which this reflects their relatively high charges. CS type C, characterised by disaccharides that lack iduronate and predominantly 6-O-sulphated hexosamine residues, was found to compete as well as porcine mucosal HS. DS contains iduronate rich domains of variable length, and is predominantly 4-O-sulphated with 2-O-sulphated iduronate and a minor proportion of 6-O-sulphate. Taken together, these results provide further support for 6-O-Sulphate as a more important determinant of affinity than 2-O-Sulphate.

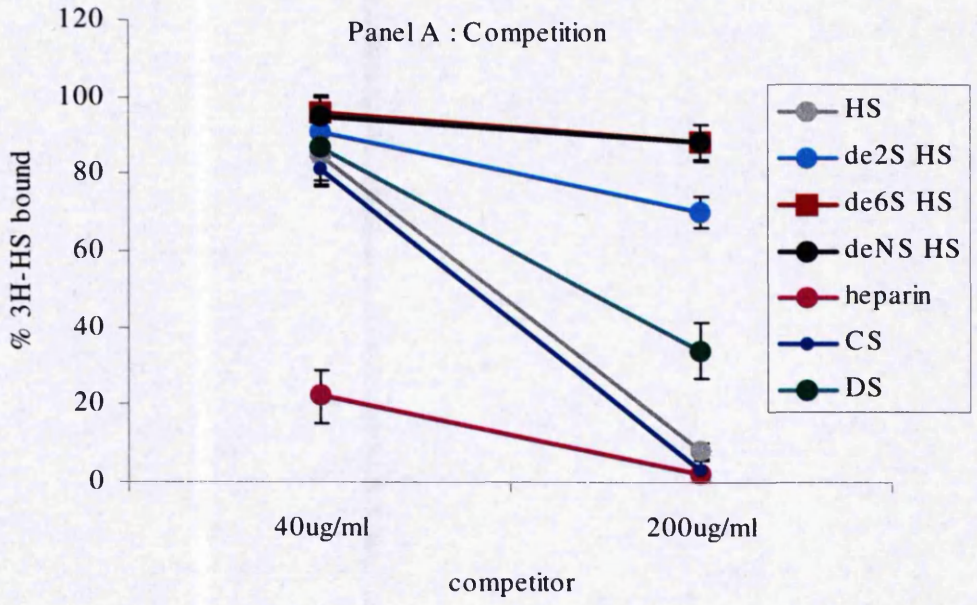

Figure 6.21 : The ability of non-labelled GAG species to compete with ^{3}H-HS for HEM. ~ 2K ^{3}H- HMVEC or BAEC HS was incubated in the presence of cold competitor and 40μM endostatin monomer (HEM) in 0.13M NaCl, 10mM Tris, pH7.0 for two hours. The proportions of unbound and bound ^{3}H-HS were determined by the FBA with 3 x 1 ml washes of 0.13M NaCl, 10mM Tris, pH7.0 then 3 x 1 ml washes of 1.0M NaCl, 10mM Tris, pH7.0 respectively. 1 ml washes were monitored for radioactivity by scintillation counting. Means + SD of % of ^{3}H-HS bound compared to control are shown, n=3. ^{3}H-HS retained on the filter was <0.1%. HS, porcine mucosal HS; CS, chondroitin sulphate; DS, dermatan sulphate; de2S, De-2-O-sulphated porcine mucosal HS; de6S, De-6-O-sulphated porcine mucosal HS; HS de NS, De-N-sulphated/re-N-acetylated porcine mucosal HS; heparin, bovine lung heparin.

HEPARIN/HS SPECIES	N-SULPHATES	2-O-SULPHATES	6-O-SULPHATES	TOTAL SULPHATE
	No. of sulphate groups per 100 disaccharides			
Bovine lung heparin	97.7	89.3	92.4	279
Porcine mucosal HS	43.4	19.9	21.9	85.2
HMVEC HS	38	14	10	62
BAEC HS	38	13	5.4	56
De-N-sulphated/re-N-acetylated porcine mucosal HS	3.6	19.9	22.7	47
De-6-O-sulphated porcine mucosal HS	41.5	18	9.8	68
De-2-O-sulphated porcine mucosal HS	41.5	3.3	21.4	68

Table 6.4 : Content and distribution of sulphate groups in native and selectively desulphated HS species. Table adapted from Lyon et al.,2000.

Direct binding with 2-O-desulphated ^{3}H-HS

The HS modifying enzyme 2-O-sulphotransferase (HS 2OST), has been cloned and is thus far, thought to be the product of a single gene that is not subject to alternate splicing (Bullock *et al.*, 1998). The HS 2OST knockout mouse (*Hs2st*$^{-/-}$) has a characteristic phenotype that includes renal agenesis (Bullock *et al.*, 1998) and it synthesises HS that is completely deficient in 2-O-sulphate groups (Merry *et al.*, 2001). To clarify whether 2-O-sulphate is essential for binding between HS and HEM, ^{3}H-HS from *Hs2st*$^{-/-}$ mouse fibroblasts was tested against wild type HS for affinity to HEM using the FBA as previously described (Figure 6.22, Panel A). These species of HS bound HEM with equivalent affinity (see Chapter 7 for detailed discussion). In contrast bFGF, that binds sequences enriched in 2-O-sulphate and does not require 6-O-sulphate (see Table 1.5), has reduced affinity for the 2OST mutant HS (Figure 6.22, Panel B).

6.8 Localisation of the HEM binding HS domain(s) within intact chains

The preceding experiments indicated several features of the HEM binding HS domain. Minimal hexasaccharide sequences with either a trisulphated disaccharide, or two disulphated disaccharides exhibited weak binding whereas stronger binding required a longer N-sulphated sequence of ~ dp10/12. Physiological binding species were generally characterised by increased charge density and the presence of one or more trisulphated disaccharides. In addition, 6-O-sulphate was emerging as a more important contributor to the binding domain than 2-O-sulphate.

The S-domains, due to the specificity of heparinase III, lack the transition zones that are believed to contain the 6-O-sulphated disaccharide [UA-GlcNAc(6S)] in mixed sequences of alternating GlcNAc/GlcNS containing disaccharides (Figure 1.2). We therefore tested the ability of oligosaccharides generated by the action of heparinase I to bind HEM since this enzyme cleaves within the S-domains, disrupting internal repeating sequences of IdoA(2S) containing disaccharides and preserves the transition zones (see Fig 1.3 for heparinase I specificity).

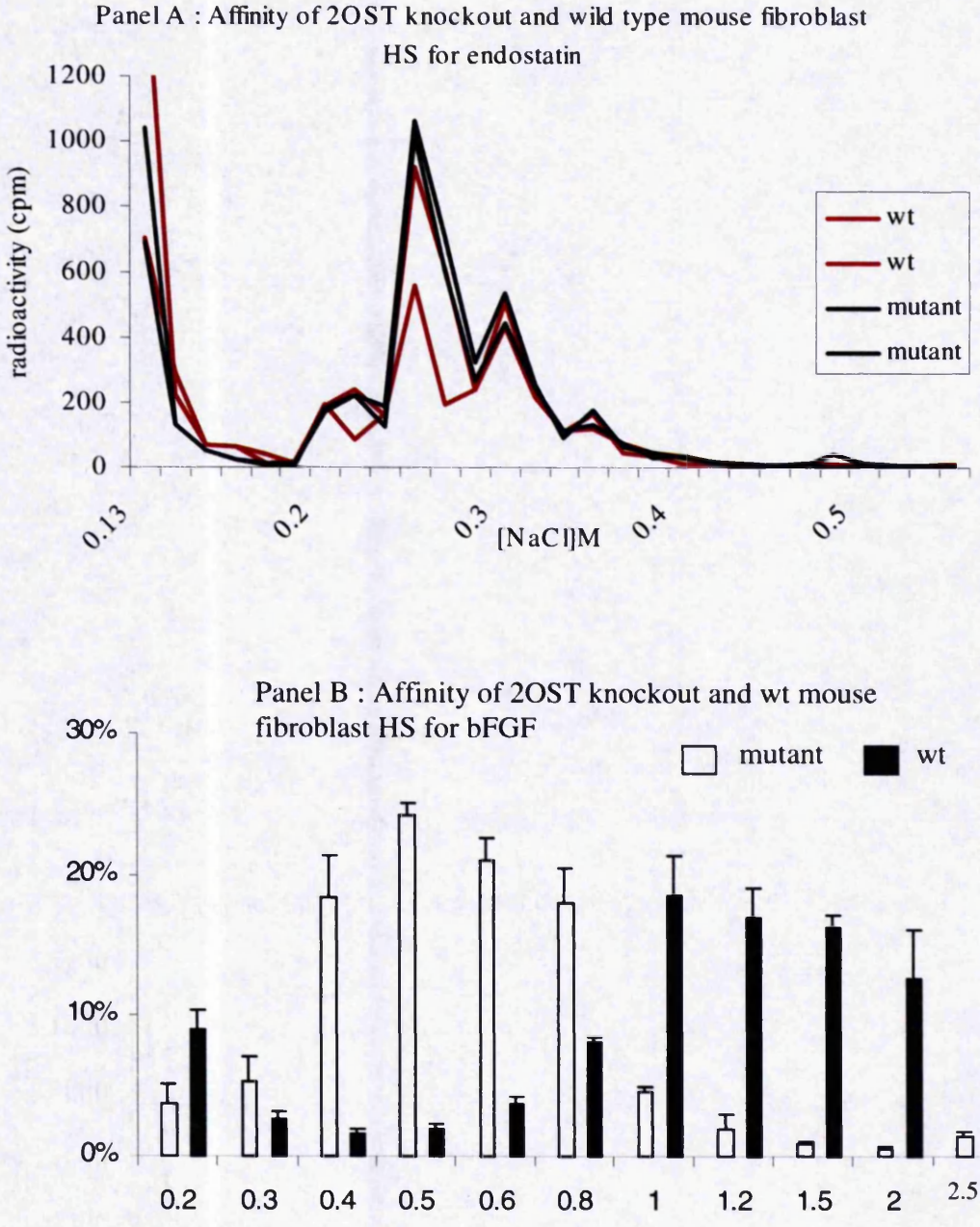

Figure 6.22 : Affinity of 2OST knockout and wild type mouse fibroblast HS for HEM. Panel A: ~10K ^{3}H- HS from wild type(wt) or 2OST mutant fibroblasts was incubated with 40µM HEM in 25 µl 0.13M NaCl, 10mM Tris, pH7.0. Bound ^{3}H-HS was determined by the FBA with 3 x 1 ml washes of increasing, 0.05M increments of NaCl. 1 ml washes were monitored for radioactivity by scintillation counting. ^{3}H-HS retained on the filter was <0.1%, experiments were performed in duplicate with identical results and no binding was observed in negative controls substituting BSA for HEM (data not shown). Panel B shows the relative affinities of these HS species to bFGF in the FBA, plotted as percent cpm ^{3}H radioactivity eluted, for comparison (obtained from C Merry, with kind permission).

Affinity of heparinase I generated oligosaccharides for HEM

HMVEC HS (~200K cpm ^{3}H) was treated with heparinase I and aliquots (~10K cpm ^{3}H) checked for complete digestion, demonstrated by a shift to ~9kDa, by Sepharose CL-6B chromatography (Figure 6.23, Panel A). Heparinase I was denatured by boiling for 10 minutes and the digest buffer adjusted to 0.05M NaCl, 10mM Tris, 10μM calcium acetate, 10mM sodium acetate, pH7.0 (as described for heparinase III, Section 6.3). An aliquot (~ 10K cpm ^{3}H-HS) of the digest was incubated with 40μMHEM in 0.05M NaCl, 10mM Tris, pH 7.0, alongside control samples containing either 10K cpm ^{3}H-HS intact HMVEC HS or heparinase III digested HMVEC HS. Bound ^{3}H-HS was eluted using the FBA with 3 x 1 ml washes of increasing 0.05M NaCl increments (0.1M NaCl after 0.2M) and the results are shown in Figure 6.23, Panel B. It can be seen that the intact HMVEC HS binds with highest affinity (~0.3-0.35M NaCl). The heparinase I treated HS also binds, with affinity approaching that of the intact chains, and with equivalent affinity to the heparinase III treated HS (~0.2-0.25M NaCl). Subsequent independent experiments revealed identical results with ~ 25 ± 5% (n= 4) of the heparinase I digested HS binding to HEM beyond 0.15M NaCl (Figure 6.23, Panel C). Bound heparinase I generated oligosaccharides were found to retain their elution positions upon rebinding (Figure 6.24) so further characterisation of binding species was performed after one FBA. These studies indicated the presence of a structural motif for HEM within the heparinase I resistant oligosaccharides.

Estimation of molecular weight and chain length of heparinase I generated oligosaccharides with affinity for HEM.

Heparinase I digested HMVEC HS, prepared as described above, was endostatin affinity fractionated using the FBA. A typical profile is shown in Figure 6.24, Panel A, from which heparinase I resistant oligosaccharides eluting with 0.05, 0.1, 0.15, 0.2 and 0.3M NaCl were pooled and de-salted as described previously. Aliquots (~ 2-3K cpm ^{3}H) from each pool were chromatographed on Sepharose CL-6B to determine their size. The profiles from the 0.05, 0.2 and 0.3M NaCl pools are shown with that of the total heparinase I digest for comparison and the results from all pools tabulated in Figure 6.25. Samples were chromatographed in random order on the same column with a Vt marker, to ensure that shifts in elution of peaks were not due to changes in column behaviour. Although the radioactive trace is at a low level, similar results were obtained from two independent experiments and the sizes of the

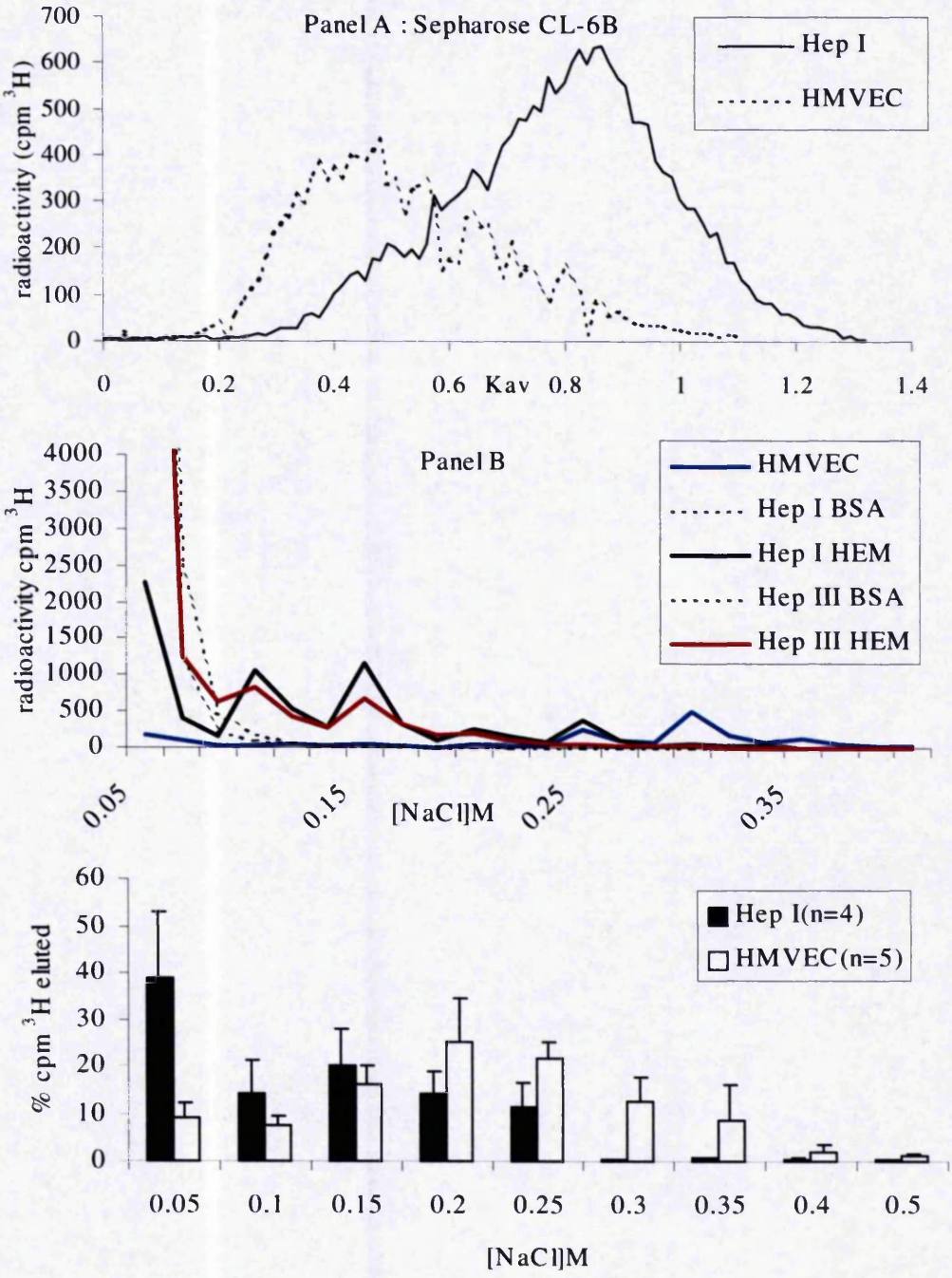

Figure 6.23 : Affinity of heparinase I digested HS for HEM. Panel A ~ 200K ^{3}H-HMVEC HS was digested with heparinase I and 10K ^{3}H –HS aliquots checked for complete digestion by CL-6B chromatography as previously described. Panel B ~ 10K ^{3}H –HS cpm aliquots of ^{3}H- HMVEC HS treated with either heparinase I, III or untreated were incubated with 40µM HEM in 25µl 0.05M NaCl, 10mM Tris, 10µM calcium acetate, 10mM sodium acetate, pH7.0, and bound ^{3}H-HS determined by the FBA with 3 x 1 ml washes of increasing, increments of NaCl. 1 ml washes were monitored for radioactivity by scintillation counting. Panel C. Bars show means + sd for heparinase I digested HMVEC HS (Hep I, n=4) compared to undigested HMVEC HS (HMVEC) binding to HEM in the FBA of cpm ^{3}H –HS eluted as a percent of total radioactivity of the sample.

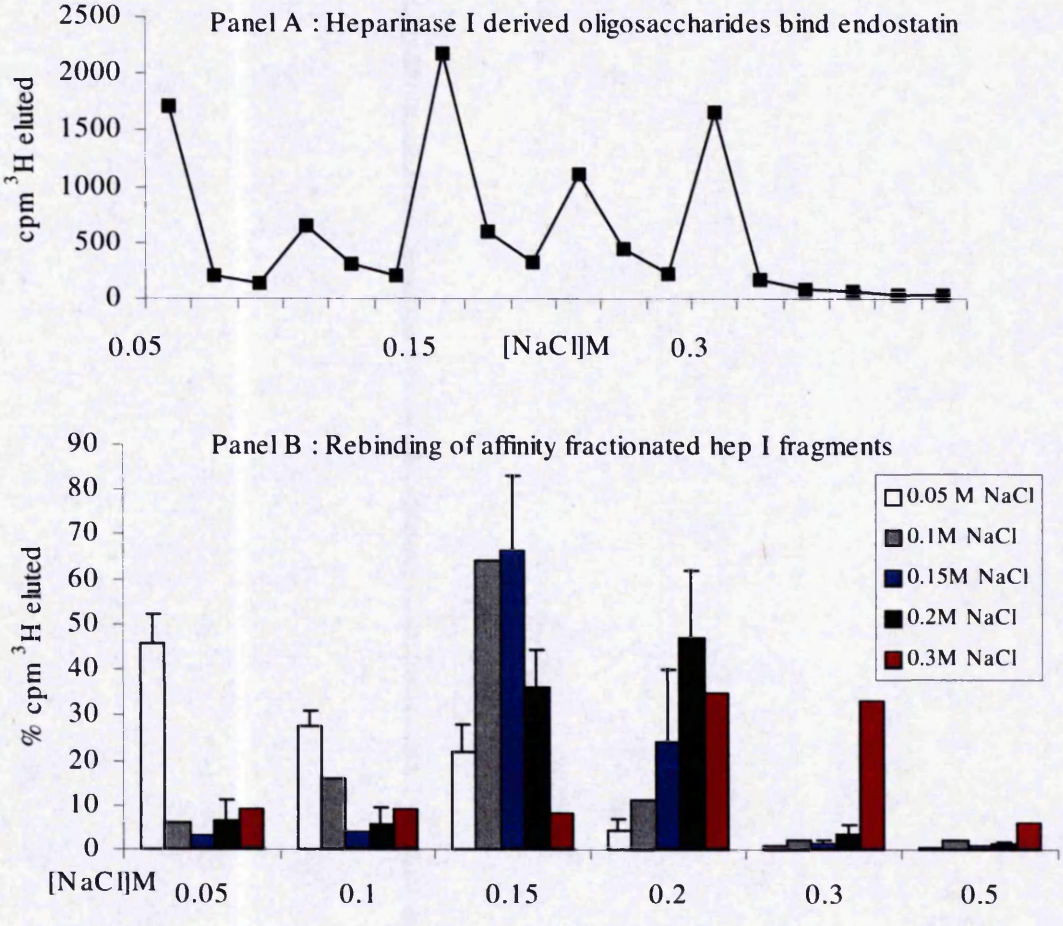

Figure 6.24 : Rebinding of fractionated heparinase I digested HS according to affinity for HEM. ~ 200K cpm ^{3}H-HMVEC HS were treated with heparinase I, incubated with 40μM HEM and eluted using the FBA as described. Small aliquots were taken for monitoring of radioactivity by scintillation counting and pools eluting with 0.05M, 0.1M, 0.15M, 0.2M and 0.3M NaCl recovered and desalted. A typical profile is shown in Panel A. An ~3K cpm ^{3}H-HS aliquot of each pool was rebound to HEM and eluted as above. The bars show means + SD, n=1-3 of cpm ^{3}H-HS eluted as a % of total radioactivity. No binding was observed in negative controls substituting BSA for HEM and ^{3}H-HS retained on the filter was <0.1% (data not shown).

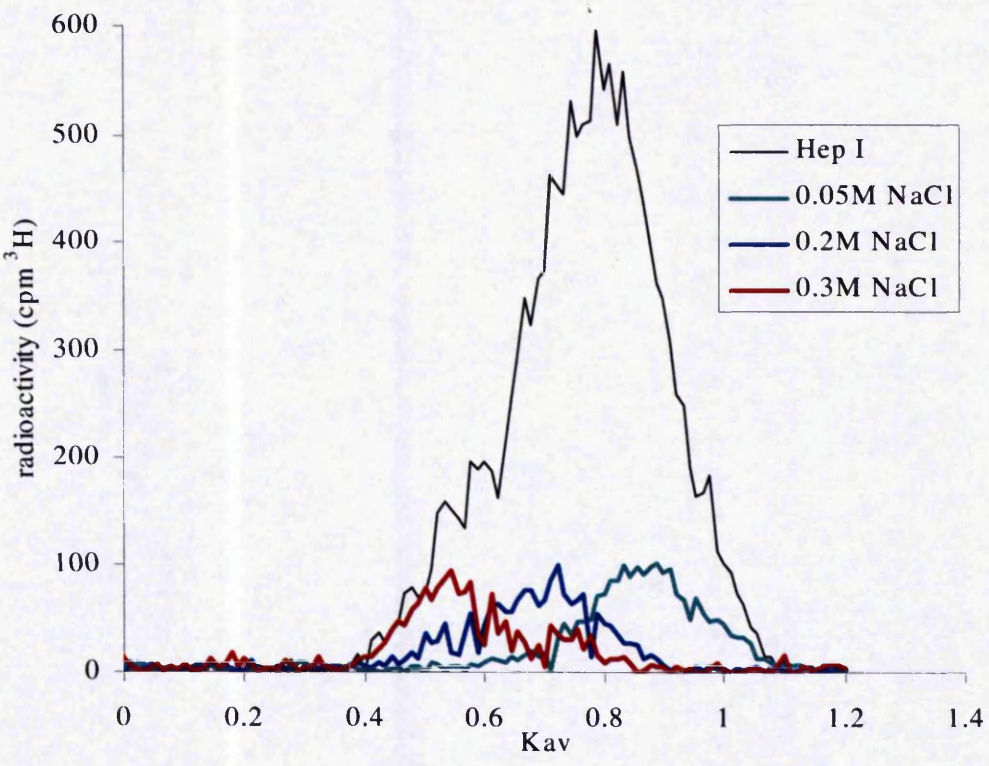

Table 6.5

[NaCl]M to dissociate HS from HEM	Kav	Mr	Average no disaccharides per heparinase I resistant oligosaccharide
0.05	0.9	Outside calibration	unknown
0.1	0.9	Outside calibration	unknown
0.15	0.9	Outside calibration	unknown
0.2	0.7	8000	~18
0.3	0.6	15000	~ 30

Figure 6.25 : CL-6B gel filtration of heparinase I resistant oligosaccharides Heparinase I resistant oligosaccharides were subfractionated by affinity for HEM using the FBA as previously described and ~ 2-3K cpm ^{3}H from each pool was loaded onto a CL-6B column, (1.5 x 66 cm) eluted in 0.2M ammonium hydrogen carbonate at a flow rate of 12ml per hour. 1 ml fractions were collected and monitored by scintillation counting. K_{av} was calculated from elution positions of sodium dichromate (V_t, K_{av} = 1.0) and dextran blue (V_o,K_{av} = 0) and the values are shown in table 6.5. The CL-6B profiles of the total heparinase I digest and the oligosaccharides that were eluted by 0.05M, 0.2M , and 0.3M NaCl are shown. Experiments were performed in duplicate with similar results.

oligosaccharides were calculated from the Kav values, as described in Chapter 4. The size of the heparinase I resistant oligosaccharides increased with higher affinity for HEM and the strongest binding fragments (eluted with 0.2 and 0.3M NaCl) ranged from ~ 18 to 30 disaccharides in length (Table 6.5).

Disaccharide composition of heparinase I resistant oligosaccharides with affinity for HEM

The disaccharide compositions of the heparinase I resistant oligosaccharides with the highest affinity, that eluted from HEM with 0.2M and 0.3M NaCl (Figure 6.22, Panel A), were obtained by sequential digestion of ~ 5K cpm ^{3}H-HS with heparinases II and III, then resolution by SAX-HPLC as previously described. Typical profiles are shown in Figure 6.26 and combined results of two independent experiments in Table 6.6. In contrast to the S-domain analyses and consistent with the specificity of heparinase I (Figure 1.3), the oligosaccharides comprise predominantly non-sulphated disaccharides and a low proportion of modified / sulphated disaccharides. There is a small proportion of 2-O-sulphated disaccharides, that would be expected to arise from the cleavage site of heparinase I. In addition, contiguously 2-O-sulphated oligosaccharides in S-domains of dp 6 may resist heparinase I (Rice & Linhardt,1989; Yamada *et al.*, 1994). Both the trisulphated disaccharide and [UA-GlcNAc (6S)], the latter thought to reside in the transition zones, are present at a low frequency.

The contributions of different disaccharides present in the oligosaccharides eluted by 0.2M NaCl, compared to 0.3M NaCl, are similar. This suggests that the chain lengths and/or sequences of the disaccharides confer the differences in affinity between these two pools. Due to the lengths of the heparinase I resistant oligosaccharides with highest affinity for HEM (~30 disaccharides) compared to the intact chains (~45 disaccharides) it was possible that these oligosaccharides were still intact chains. However, the disaccharide composition of the heaprinase I resistant oligosaccharides was distinct (compare to intact chains, Table 4.2a). There is a decrease in the trisulphated disaccharide which confirms that digestion has occurred and that heparinase I favours the linkages between the most sulphated disaccharides. Also, to further evaluate the composition of the heparinase I resistant oligosaccharides, aliquots were digested with heparinase III as previously described, then separated by Bio-Gel

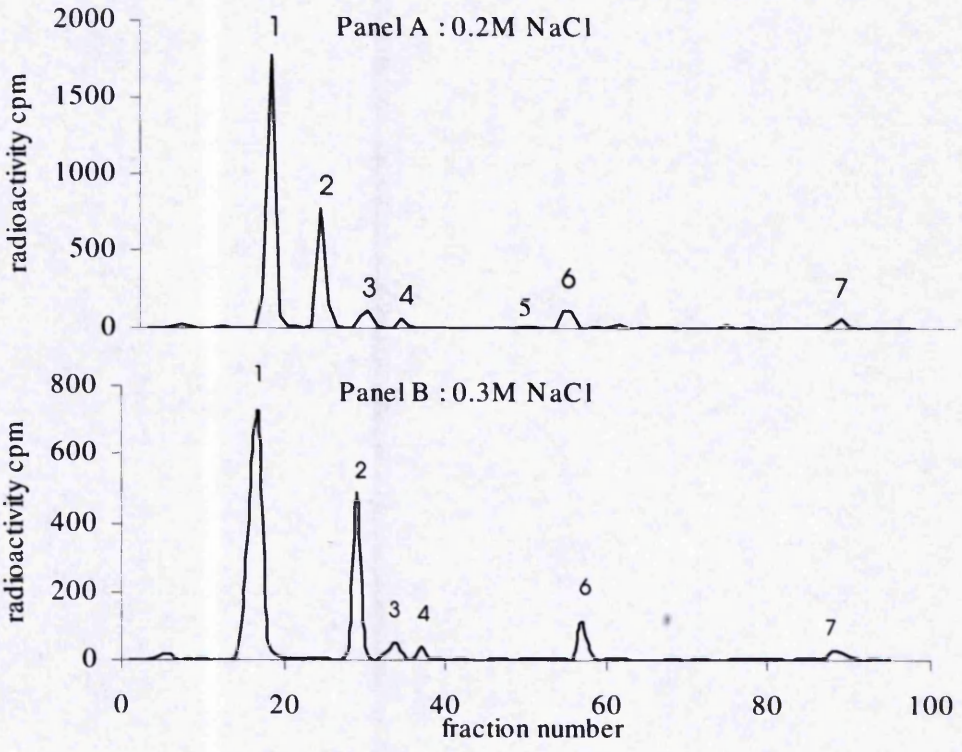

Figure 6.26 : SAX-HPLC analysis of disaccharides comprising heparinase I resistant oligosaccharides : ~ 3-5K cpm ^{3}H heparinase I resistant oligosaccharides that were dissociated from HEM in the FBA with 0.2M NaCl (Panel A) and 0.3M NaCl (Panel B) were digested to disaccharides with heparinases II and III then analysed by SAX-HPLC as previously described. The numbered peaks correspond to the elution positions of known disaccharide standards as follows:- 1= UA-GlcNAc; 2=UA-GlcNS; 3=UA-GlcNAc(6S); 4=UA(2S)-GlcNAc; 5=UA-GlcNS(6S); 6=UA(2S)GlcNS; 7=UA(2S)GlcNS(6S).

STANDARD PEAK NO. (in order of elution)	DISACCHARIDE STRUCTURE	TOTAL DISACCHARIDES (%) (MEANS ±SD)	
		0.2M NaCl	0.3M NaCl
1	**UA-GlcNAc**	58 ± 1	64±1
2	UA-GlcNS	26 ± 1.6	23±1
3	UA-GlcNAc(6S)	4.4 ± 0.6	3.2±0.2
4	UA(2S)-GlcNAc	1.8 ± 0	1.85±0.15
5	UA-GlcNS(6S)	0.35 ± 0.6	0±0
6	UA(2S)-GlcNS	6.2 ± 3	5.85±0.15
7	UA(2S)-GlcNS(6S)	2.35 ± 0	2.35±0.35

Table 6.6 : Disaccharide compositions of heparinase I resistant oligosaccharides with affinity for HEM in physiological conditions. The total ^{3}H cpm contributing to each peak in Figure 6.26 was calculated as a percentage of the total ^{3}H of the sum of all peaks to obtain the disaccharide compositions of the oligosaccharides as indicated and the data presented as means ± SD of two independent experiments.

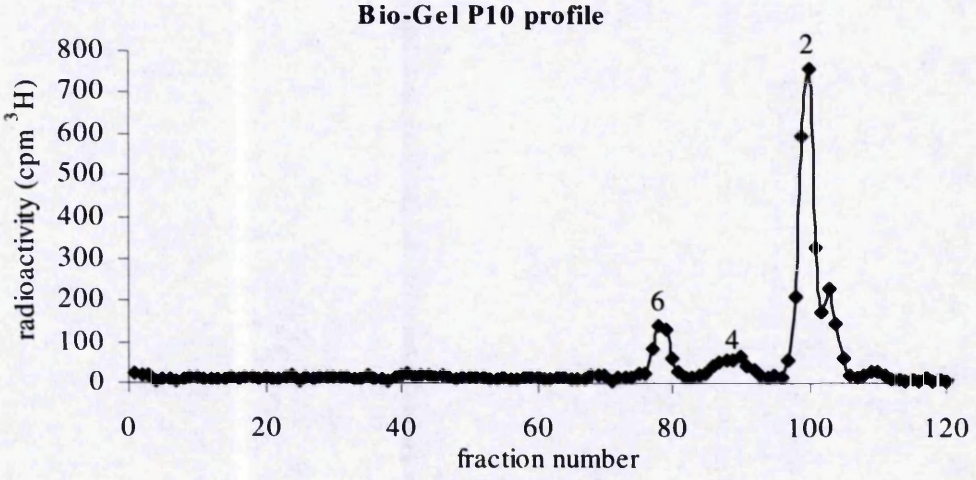

Figure 6.27 : Digestion of heparinase I resistant oligosaccharides with heparinase III ~ 3-5K cpm ^{3}H heparinase I resistant oligosaccharides that eluted with 0.3M NaCl were digested with heparinase III and the products separated by Bio-Gel P10 filtration as previously described. The peaks are numbered according to degree of polymerisation where dp2 = disaccharides etc. Identical profiles were obtained for heparinase I resistant oligosaccharides that dissociated from HEM with 0.2M NaCl.

P10 filtration. This revealed the presence of short heparinase III resistant regions (S-domains) of dp4 and dp6 (Figure 6.27), with no longer S-domains in contrast to heparinase III digested native HMVEC HS (Figure 4.10, Table 4.12). The majority of linkages were susceptible to heparinase III (87%±sd, n=3), indicated by an absolute yield of 78±5% dp2, 11±1.7% dp4 and 10.3±4% dp6. Furthermore, heparinase III digestion completely abolished binding of these oligosaccharides to HEM, as did nitrous acid digestion, confirming that repeating sequences of N-acetylated disaccharides (and their associated carboxyl groups) could not be the sole mediators of binding (data not shown).

In summary, the heparinase I resistant oligosaccharides contain short, sulphated heparinase III resistant domains but can bind with comparable affinity to the longest S-domains and intact HS. From the lengths and disaccharide compositions of these oligosaccharides we can predict that the most sulphated disaccharides occur with very low frequency, ~1-2 per chain, and therefore these must be sufficient to mediate binding. This is in contrast to short excised S-domains (Figure 6.9) and suggests that the [UA-GlcNAc] repeats (that may include occasional [UA-GlcNS] disaccharides) confer stability to the highly sulphated disaccharides within the short S-domains, possibly by optimising their conformation for binding. These findings provide further evidence that charge is not the sole mediator of binding and also suggest that the transition zones may play a role. Thus, the optimal HS recognition site for HEM in the parent chain may span an S-domain and transition zone. Alternatively, HEM may recognise a variety of structural motifs at different locations in the chain, eg within the most highly sulphated longer S-domains or at the transition zones. Further possible mechanisms to explain these data are discussed in Chapter 7.

6.9 The interaction between oligomerised HEM and HMVEC HS

An artificially constructed dimer of HEM (HED) was recently shown to mimic the promigratory activity of the type XVIII collagen NC1 domain in an *in vitro* morphogenesis assay (Kuo *et al.*,2001) but its interaction with HS has not been explored. HED was constructed on the basis of an endostatin crystal structure study that predicted a zinc dependent dimer in which glutamine-7 residues in adjacent subunits are in close proximity (Ding *et al.*, 1998). Mutation of the glutamine-7 residue in endostatin to cysteine fortuitously produces a novel intermolecular disulphide bond between adjacent endostatin molecules when expressed as an Fc fusion protein and HED (40kDa) is liberated by enterokinase cleavage of the recombinant Fc-ES(mutated Q-C) (Kuo *et al.*,2001).

The activity of HED *in vitro* is dependent on a matrigel substratum. This is a complex matrix produced by EHS tumour and rich in HSPG (perlecan) that induces a morphogenetic change in that ECs spontaneously form tube like structures. Kuo *et al.*,2001, demonstrated that HED prevented EC tube formation and induced migration of cells from established tubules. This activity was associated with activation of MAPK signalling and inhibited by preincubation with HEM suggesting a negative autoregulatory mechanism since NC1/HED is the precursor of HEM (Figure 1.12).

To determine whether these activities could also involve HS, we have performed preliminary investigations to determine the HS binding properties of HED (obtained from K Javaherian). The bioactivities of HED and HEM, as described by Kuo *et al.*,2001, in the matrigel tube formation/morphogenesis assay are shown in Figure 6.28. As described in methods, BAEC cells in complete medium were seeded at a density of $5x10^5$ cells into 24 well plates containing 250µl of matrigel. HED (50nM) and HEM (3000nM) were added with the cells at time 0 and their effects on the formation of tubules examined by light microscopy at 16 hours. As shown in Figure 6.28A, HEM did not affect tubule formation compared to the positive control with no added protein. In marked contrast, HED prevented tubule formation and the cells remained disaggregated and spread, as if plated on plastic. In Figure 6.28B, the effects of HEM and HED on preformed tubules (16 hours after plating cells on matrigel), were observed. Plates were observed at 24 hours, 8 hours after the addition of proteins to the preformed tubules . Again, no change in morphology was observed for cells treated

with HEM, but the appearance of the HED treated cells was very different, with evidence of migration and a 'spread' appearance. In Figure 6.28C, the effect of preincubation with HEM prior to HED is shown. When HEM (3000nM) was added to preformed tubules 30 minutes before addition of HED (50nM), no disaggregation of tubules was observed and the activity of HED was blocked (compare to 6.28C, panel II), confirming previous data describing distinct activites of the monomer and dimer, and the possibility of a negative autoregulatory mechanism (Kuo *et al.*,2001; Zatterstrom, 2000; Ackley *et al.*,2001).

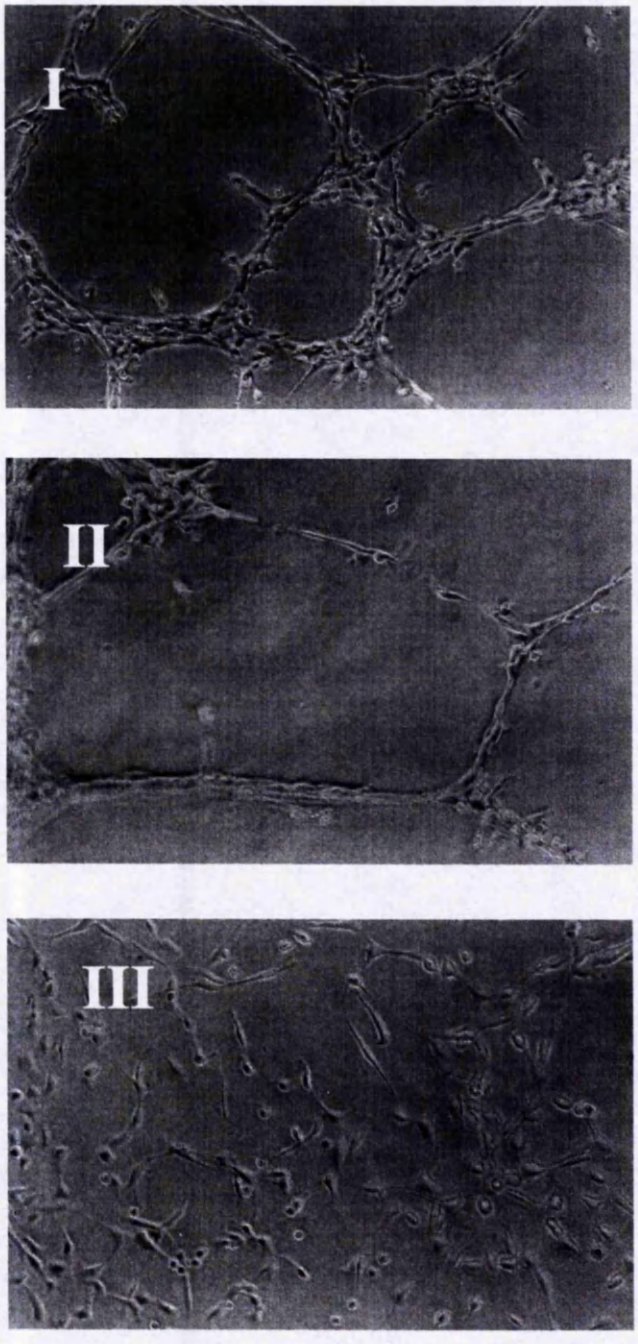

Figure 6.28A : The effect of HEM versus HED on endothelial cells in the matrigel tube formation/morphogenesis assay. BAEC were plated on matrigel at the same time as HEM (3000nM) or HED (50nM) and observed for tubule formation and endothelial cell morphology after 16 hours. The cells were photographed using phase contrast microscopy at x 100 magnification. I= positive control with no added protein, II= HEM; III=HED.

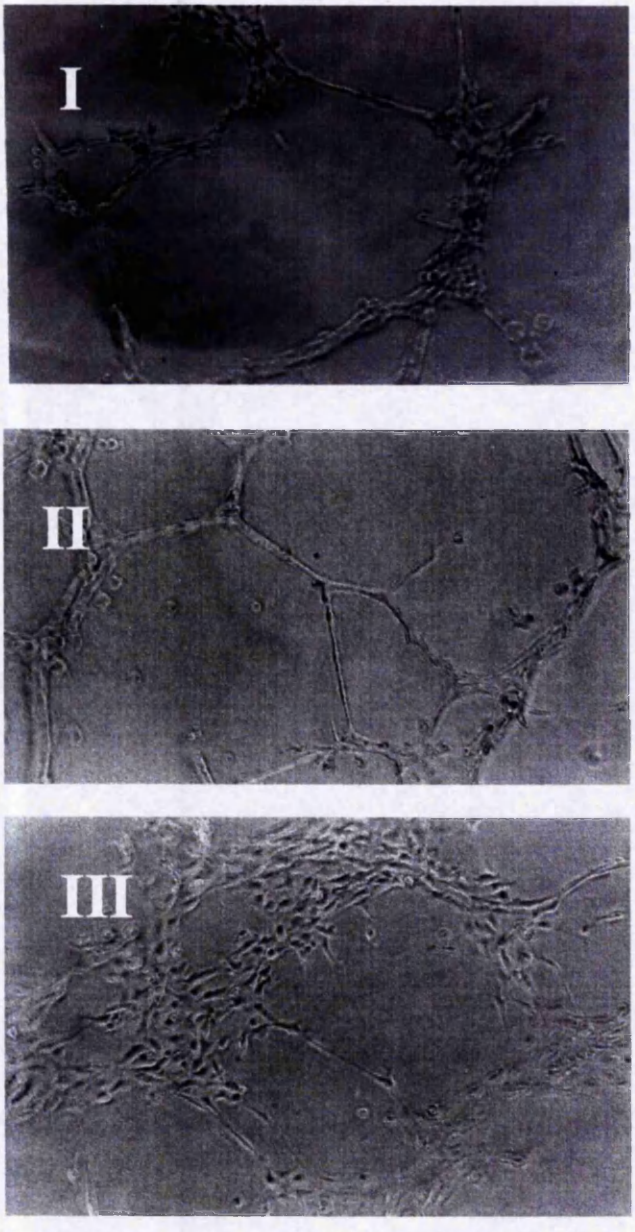

Figure 6.28B: The effect of HEM versus HED on established endothelial cell tubules in the matrigel tube formation/morphogenesis assay. BAEC were plated on matrigel and allowed to form tubules for 16 hours (Panel I) before addition of HEM (3000nM) or HED (50nM). Plates were observed for tubule formation and endothelial cell morphology after 24 hours (8 hours after addition of protein) and photographed using phase contrast microscopy at x 100 magnification. II= HEM, III=HED. The appearance of Panel I was identical at 24 hours (not shown).

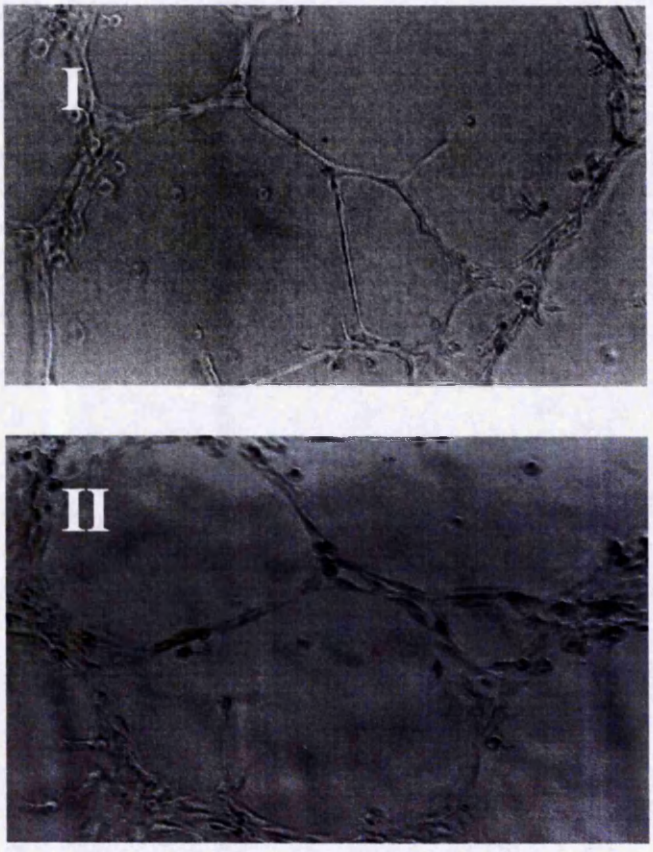

Figure 6.28C: The effect of preincubation with HEM on the activity of HED in the matrigel tube formation/morphogenesis assay. BAEC were plated on matrigel and allowed to form tubules for 16 hours before addition of HEM (3000nM) (both panels). HED (50nM) was added 30 minutes after addition of HEM (Panel II). Plates were observed for tubule formation and endothelial cell morphology at 24 hours (8 hours after addition of protein) and photographed using phase contrast microscopy at x 100 magnification.

Affinity of HED for HS

The conditions for the FBA were optimised as for HEM (Section 6.1). Binding of BAEC ^{3}H-HS to HED in 0.13M NaCl, 10mM Tris, pH 7.0, approached saturation (~80%HS bound) with protein concentrations ~5μM (Figure 6.29), an 8 fold lower concentration of HED compared to HEM. This suggested that HED had greater affinity for HMVEC HS consistent with previous reports (Sasaki *et al.*,2000). Using the FBA, elution profiles of HED-bound ^{3}H-HS derived from HMVEC and 3T3 fibroblast HS were indistinguishable from those obtained with HEM (not shown, see Figures from subsequent experiments). This confirmed affinity of the dimer for HS and suggested a similar interaction at the HED-HS interface to HEM-HS. The difference in affinity suggested by the binding curves, given the similar NaCl concentration to elute HEM compared to HED is intriguing. A higher NaCl concentration would usually be required to dissociate a stronger GAG-protein interaction (Conrad, 1998). Therefore one possibility is that the protein is sensitive to NaCl and undergoes a conformational change that dissociates the GAG (see discussion also).

The role of the primary heparin binding site in the affinity of HED for HS

As for HEM (Section 6.2, Figure 6.7) HED mutated to display alanine residues in place of R158,270 within each of its HEM subunits, was compared to native HED for affinity to HMVEC HS in 0.15M NaCl, 10mM Tris, pH 7.0 using the FBA as described. Figure 6.30 demonstrates that there is no measurable affinity of the R-A mutant HED to HMVEC HS at physiological ionic strength, consistent with the previous findings for the monomer and indicating that R158 and 270 also determine the affinity of the dimer to HS. Similarly, MAb 12C1 blocks binding of HED to HMVEC HS whereas there is no interaction between HS and 12C1 alone, or HED and the control mAb PDM (Figure 6.30). These observations suggest that R158/270 are also the essential determinants of affinity of HED to HS and that the conformations of the heparin binding domains within the HEM subunits are not signficantly altered by artificial dimerisation.

Specificity for particular sulphate groups

Chemically desulphated HS species were used to compete with ^{3}H-HMVEC HS for HED using the FBA as previously described for HEM (Section 6.7) and a similar result was obtained although 40μg/ml competitor (HS) resulted in greater inhibition

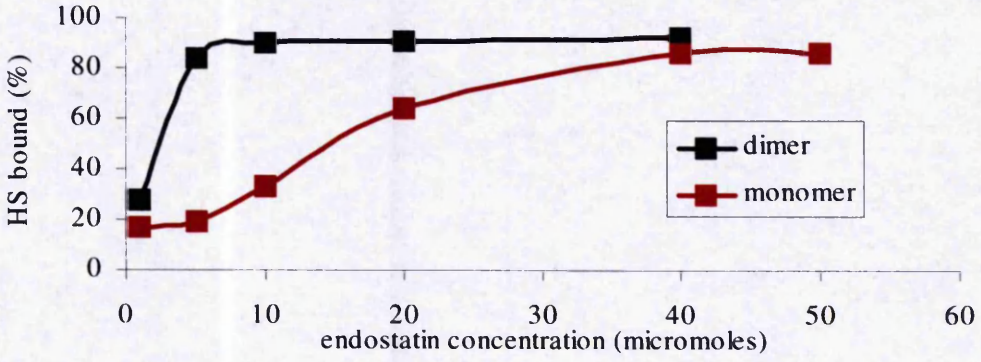

Figure 6.29 : Optimisation of protein concentration for HED in the filter binding assay. ~ 10K ^{3}H- HS from BAEC was incubated with HED and bound ^{3}H-HS determined by the FBA with 3 x 1 ml washes of 1.0M NaCl of varying concentrations of HED (0.5 to 40 µM) in 100µl 0.13M NaCl, 10mM Tris, pH7.0 for 2 hours. ^{3}H-HS retained on the filter was <0.1% (data not shown). Previous results obtained with HEM shown for comparison.

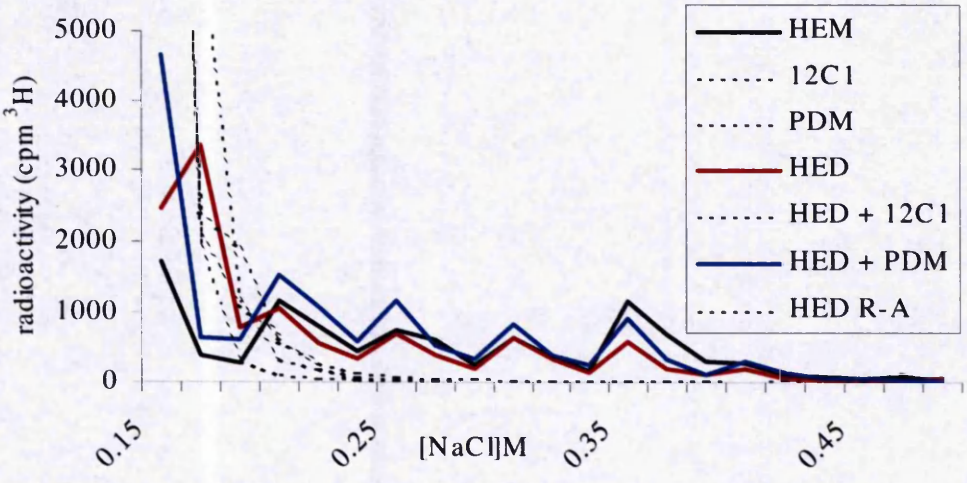

Figure 6.30 : Affinity of R-A mutant HED for HMVEC HS and Competition with neutralising mAb 12C1. ~ 10-20 K ^{3}H- HMVEC HS was incubated in 25 µl 0.15M NaCl, 10mM Tris, pH7.0 with 5µM R-A mutant HED or 5µM HED in the presence of 10µM neutralising mAb 12C1 or non-neutralising PDM. 12C1 and PDM were also incubated with HMVEC HS in the absence of HED. Previous results obtained with HEM are shown for comparison. Bound ^{3}H-HS was determined by the FBA with 3 x 1 ml washes of increasing, 0.05M increments of NaCl. 1 ml washes were monitored for radioactivity by scintillation counting. ^{3}H-HS retained on the filter was <0.1%. Experiments were performed in duplicate with identical results and no binding was observed in negative controls substituting BSA for HEM or HED (data not shown).

than observed for HEM, presumably due to the different concentrations of endostatin used in the assays. As for HEM, Figure 6.31 suggests that the loss of 2-O-sulphate has less impact on the competitive ability of HS than loss of 6-O-sulphate and N-sulphate groups. Also, Figure 6.32 shows that ^{3}H-HS from *HS2st*$^{-/-}$ mouse fibroblasts and wild type HS bind HED with equal affinity, confirming that 2-O-sulphate is not essential for the HED-HS interaction. This supports similar HS-binding epitopes in both HEM and HED. Also, 3T3 fibroblast derived S-domains (dp12 and dp18) and HMVEC HS derived heparinase I resistant oligosaccharides prepared as described in 'Methods' and sections 6.6 and 6.8 respectively, were incubated with either 5μM HED or 40μM HEM. The binding curves to these oligosaccharides for HEM and HED are identical as shown in Figure 6.33. A disaccharide analysis of the dp18 with highest affinity for HED was identical to that for HEM (not shown). Therefore, in these analyses there were no apparent differences in the behaviour of HEM compared to HED except for the significantly lower concentration of HED required in the aforementioned assays suggesting that the dimerisation confers a binding advantage.

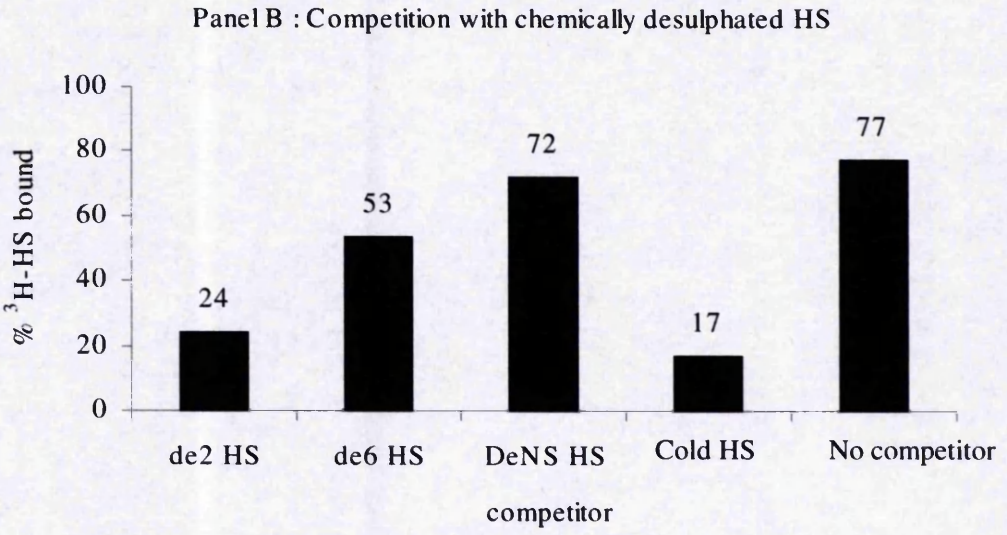

Figure 6.31 : The ability of unlabelled GAG species to compete for ^{3}H-HS with HED in the filter binding assay. ~ 2K ^{3}H- HMVEC HS was incubated in the presence of 1µg cold competitor and 5µM HED in 0.13M NaCl, 10mM Tris, pH7.0 for two hours. The proportions of unbound and bound ^{3}H-HS were determined by the FBA with 3 x 1 ml washes of 0.13M NaCl, 10mM Tris, pH7.0 then 3 x 1 ml washes of 1.0M NaCl, 10mM Tris, pH7.0 respectively. 1 ml washes were monitored for radioactivity by scintillation counting. (^{3}H-HS retained on the filter was <0.1%, data not shown).

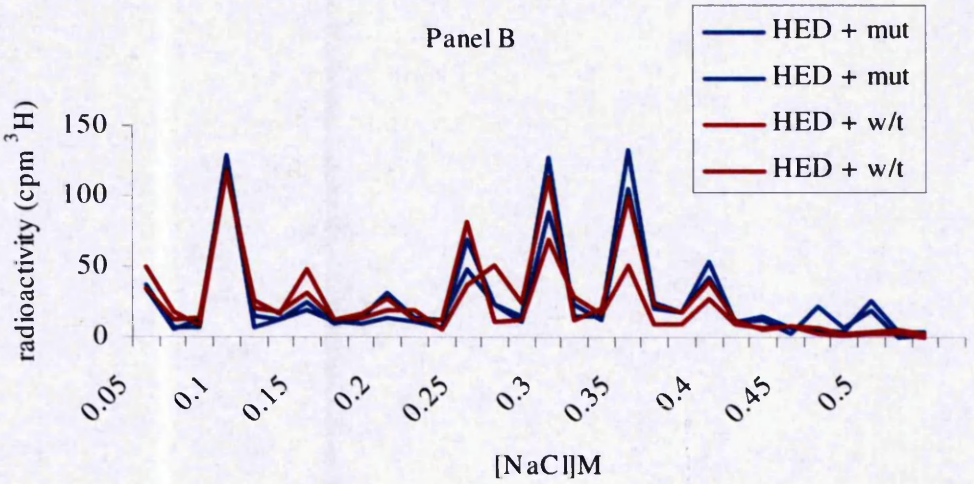

Figure 6.32 : Affinity of 2OST knockout and wild type mouse fibroblast HS for HED. ~10K ^{3}H- HS from wild type(wt) or 2OST mutant fibroblasts was incubated with 5µM HED in 25 µl 0.13M NaCl, 10mM Tris, pH7.0. Bound ^{3}H-HS was determined by the FBA with 3 x 1 ml washes of increasing, 0.05M increments of NaCl. 1 ml washes were monitored for radioactivity by scintillation counting (^{3}H-HS retained on the filter was <0.1%, data not shown).

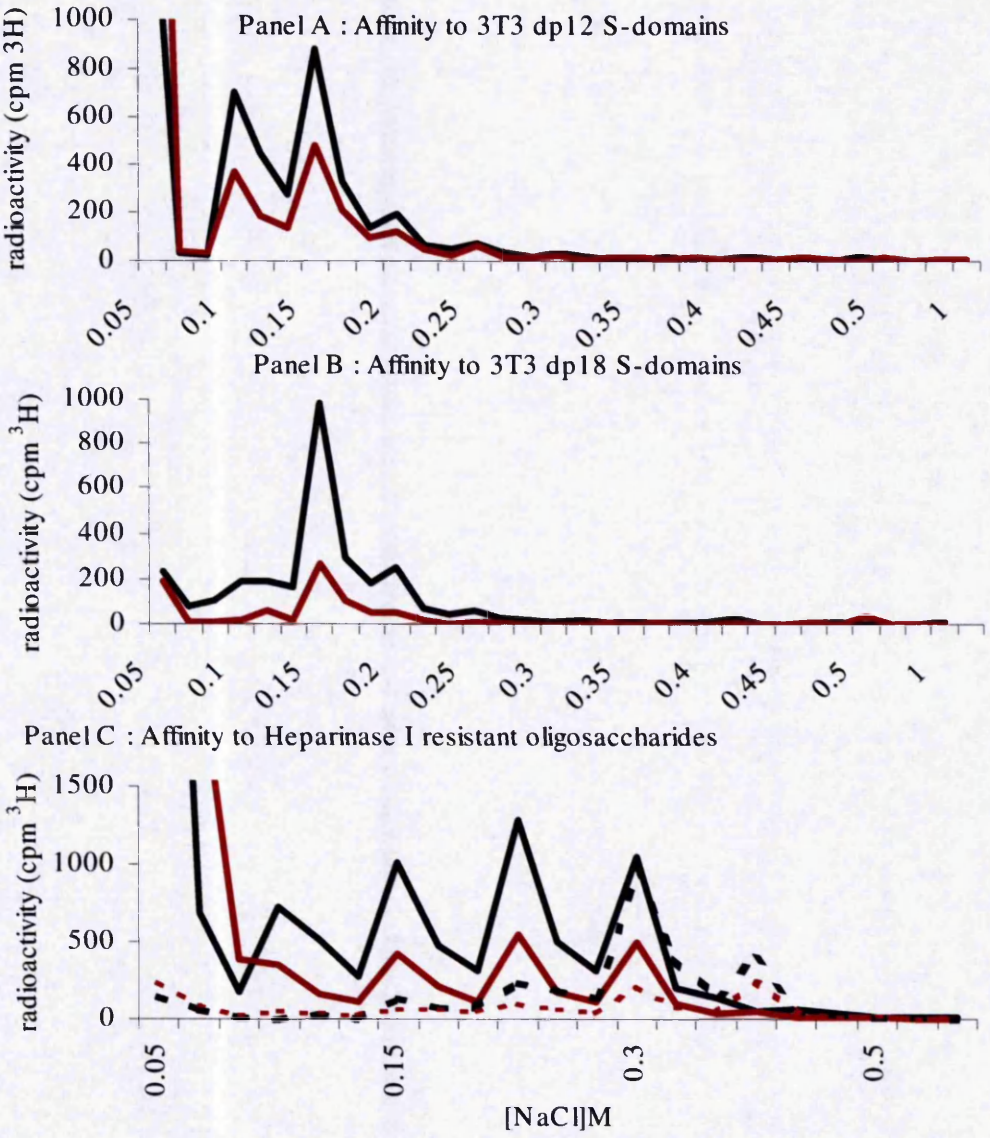

Figure 6.33 : Comparison between HEM and HED of affinity for selected S-domains and heparinase I resistant oligosaccharides. 5μM HED or 40μM HEM was incubated with ~10-20K cpm ^{3}H-HS S-domains of dp12 and dp18 purified by Bio-Gel P10 filtration of heparinase III digested ^{3}H-3T3 fibroblast HS (Panel A and B) or ~10-20K cpm ^{3}H-HS heparinase I digested HMVEC (Panel C) in 0.05 M NaCl, 10mM Tris, pH7.0, and bound ^{3}H-HS determined by the FBA with 3 x 1 ml washes of increasing 0.05M NaCl increments. 1 ml washes were monitored for radioactivity by scintillation counting. Binding to HEM = solid black line, HED = solid red line, hashed lines (Panel C) indicate HS binding to HEM (black) and HED (red), for comparison.

6.10 Zero length cross-linking of GAG to endostatin – a basis for investigation of structure – function relationships

To gain further insight into the GAG-protein interaction of HEM compared to HED the stoichiometry of binding was explored by using a two step zero length crosslinking technique (Grabarek & Gergely, 1990) that covalently couples protein to GAG. We were also interested in using this technique to generate conjugates with defined GAG structures to test for stability and activity in bioassays.

Analysis of products obtained from zero-length cross-linking of HEM and HED to heparin and heparin derived dodecasaccharides

Preliminary experiments were carried out to assess the type of conjugates formed. First, porcine intestinal mucosal (PIM) heparin (average Mr 7000) and dp12, the minimal fragment size required for physiological binding, subfractionated by gel filtration from heparin, partially-degraded with heparinase I, were crosslinked (CL) to HEM and HED. No spacer is introduced using this method, so crosslinking should only occur between the oligosaccharide and amino acid side chains within the HS binding site of the protein.

As described in Methods, the cross-linking process is a two-step procedure, initially involving a brief incubation of oligosaccharide with EDC in the presence of NHS in 0.1M MES, 0.1M NaCl, pH 6.0. This results in the conversion of some of the oligosaccharide carboxyls into succinimide esters. This oligosaccharide activation reaction is then terminated by gel filtration to separate activated oligosaccharides from crosslinkers on Sephadex-G50. The activated oligosaccharides are eluted in the void and added to either HED or HEM. Covalent cross-linking arises from the reaction of the succinimide esters with the lysine ε-amino groups of the protein. A two-step process has the advantage that only the oligosaccharide comes into contact with the active cross-linking reagents; hence, only oligosaccharide-protein crosslinks are formed (Figure 6.34). The following data is complicated to interpretate due to the number of different conjugates formed and the results obtained therefore a summary of the results is provided at the end of this section for clarification (Figure 6.41).

Zero-length crosslinking

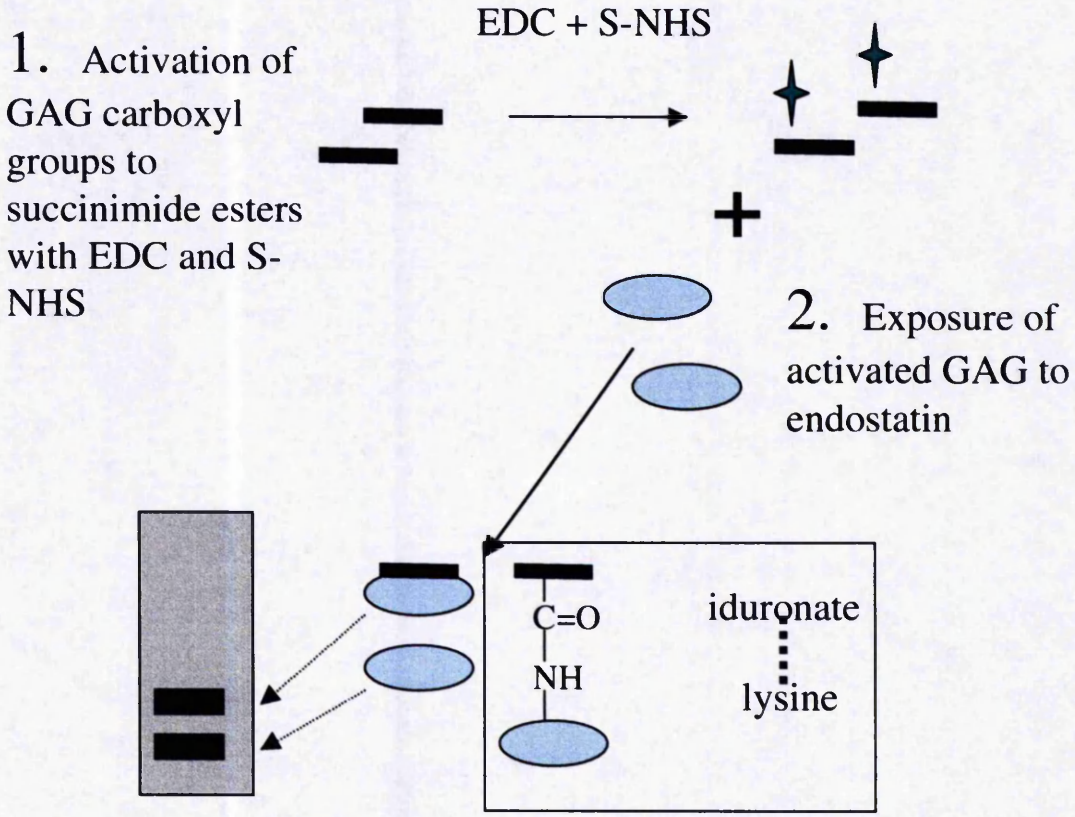

Figure 6.34 : The two step zero length crosslinking technique used to study the molecular association of heparin and endostatin.

Figure 6.35 shows an SDS-PAGE and ECL immunodetection analysis of native HEM (20KDa), native HED (40KDa) and the products obtained by crosslinking of heparin (Panel A) and dp12 oligosaccharides (Panel B). It can be seen that the crosslinking reaction is incomplete. Free uncrosslinked protein is present in all lanes, but higher molecular weight bands indicate crosslinked (CL) conjugates. In Panel A, the smears represent different sizes of conjugate due to the range of molecular masses of the heparin chains. The molecular masses of HEM crosslinked to heparin (CL-HEM-heparin, lanes 3-5), are between 43 and 68kDa. This is higher than would be anticipated for a 1:1 ratio of HEM (20kDa) to heparin (~7KDa) and indicates 'pseudo-dimerisation' of HEM ie. the GAG has acted as a template to approximate two HEM molecules. This assumes that there is not a protein-protein interface since endostatin monomer does not oligomerise when exposed to EGS crosslinking (Ackley *et al.*,2001) despite the crystal structure studies of Ding *et al.*,1998 in which zinc dependent endostatin dimers were observed. The molecular masses of HED crosslinked to heparin, (CL-HED-heparin, lanes 6 and 7) provide a useful internal control for the pseudo-dimerisation of HEM. In panel B, sharper bands indicating protein crosslinked to a single size of oligosaccharide (dp12) are present. The bands in lanes 3 and 4 running just behind free HEM at ~ 25 KDa, are consistent with a 1:1 ratio of HEM and dp12 (CL-HEM-dp12, ~ Mr 3000). A higher molecular weight band (~ 43 KDa) also indicates 2:1 conjugates of HEM:dp12 (CL-HEM(2)-dp12) indicating that these oligosaccharides may also induce dimerisation of HEM. Cross-linked-HED-dp12 is shown in lane 5. Two bands behind the free HED at ~43KDa and ~46KDa indicate that HED is crosslinked to either one (CL-HED-dp12), or two dp12 (CL-HED-dp12(2)) respectively. In addition, the band just visible at the top of the gel in lane 5 indicates multimerisation of HED by the GAG to a tetramer of Mr ~80KDa.

Confirmation of covalent coupling

Samples obtained as outlined above were subjected to reducing SDS-PAGE to confirm that covalent crosslinking was responsible for the observed products in Figure 6.35. This also provided a check to ensure that covalent protein-protein conjugates were not formed during the crosslinking of HEM to GAG. Also, the disulphide bonded dimer (HED) was reduced to its component monomers by β-mercaptoethanol and this allowed us to determine whether both subunits of HED were crosslinked to GAG (dp12, see below). Figure 6.36, Panel A shows free HEM, free HED, CL-HEM-heparin and CL-

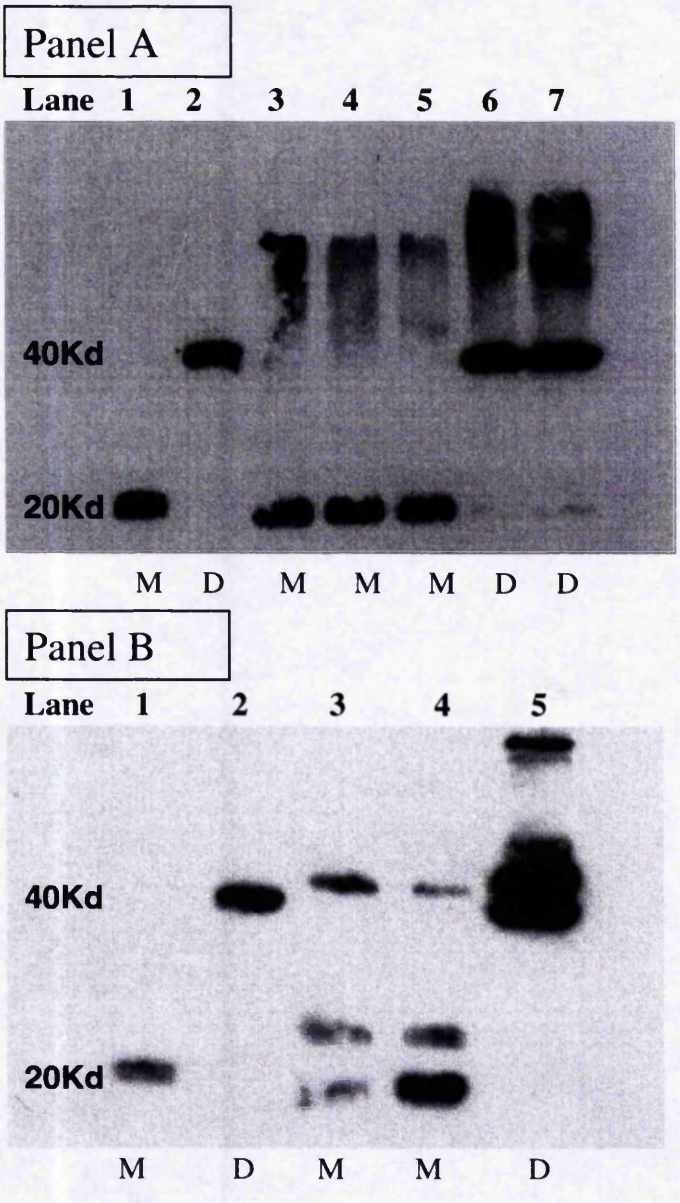

Figure 6.35 : Analysis of products obtained from the cross-linking of HEM and HED to heparin (Panel A) and heparin dp12 (Panel B). Heparin or dp12 oligosaccharides in 0.1M MES, 0.1M NaCl, pH6.0, were incubated for 15 minutes at 25°C with 23mM EDC and 25mM NHS. The activation of the GAG was then terminated by gel filtration on Sephadex G50 to elute GAG in the void and crosslinkers at Vt. Crosslinking was initiated by the addition of HEM (M) or HED (D) in a 10 fold molar excess of GAG. The reaction was allowed to proceed for 2 hours at 25°C and the reaction products analysed by SDS-PAGE, followed by Western blotting and ECL immunodetection as described in 'Methods'. Panel A: 200ng native HEM (*lane 1*), 200ng native HED (*lane 2*), 1µg CL-HEM-heparin (*lanes 3-5*), 1µg CL-HED-heparin (*lanes 6-7).* Panel B: 200ng native HEM (*lane 1*), 200ng native HED (*lane 2*), 1µg CL-HEM-dp12 (*lanes 3-4*), 1µg CL-HED-dp12 (*lane 5).* CL = crosslinked.

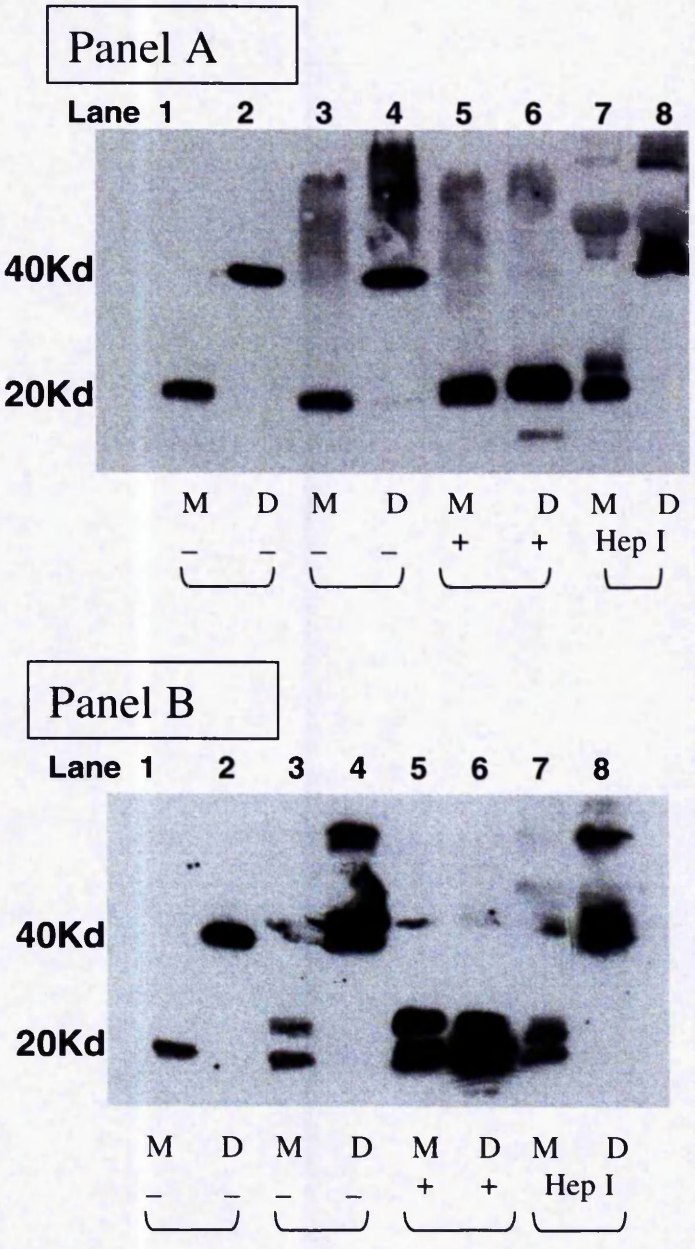

Figure 6.36 : Effect of reduction or heparinase I treatment on cross-linked HEM and HED to heparin (Panel A) and heparin dp12 (Panel B). Heparin or dp12 oligosaccharides were crosslinked to protein as previously described. Samples as indicated were analysed under reducing conditions (with β-mercaptoethanol) (+), non-reducing conditions (-), or treated with heparinase I (Hep I) for 18 hours in 10mM calcium acetate, sodium acetate at 37^0C and recovered by BSA/TCA precipitation. The reaction products were analysed by SDS-PAGE, followed by Western blotting and ECL immunodetection as described in 'Methods'. Panel A: 200ng native HEM (*lane 1*), 200ng native HED (*lane 2*), 1µg CL-HEM-heparin (*lane 3*), 1µg CL-HED-heparin (*lane 4*), 1µg CL-HEM-heparin (+) (*lane 5*), 1µg CL-HED-heparin (+) (*lane 6*), Hep I treated CL-HEM-heparin (*lane 7*), Hep I treated CL-HED-heparin (*lane 8*) Panel B: 200ng native HEM (*lane 1*), 200ng native HED (*lane 2*), 1µg CL-HEM-dp12 (*lanes 3*), 1µg CL-HED-dp12 (*lane 4*), 1µg CL-HEM-dp12 (+) (*lane 5*), 1µg CL-HED-dp12 (+)(*lane 6*), Hep I treated CL-HEM-dp12 (*lane 7*), Hep I treated CL-HED-dp12 (*lane 8*)

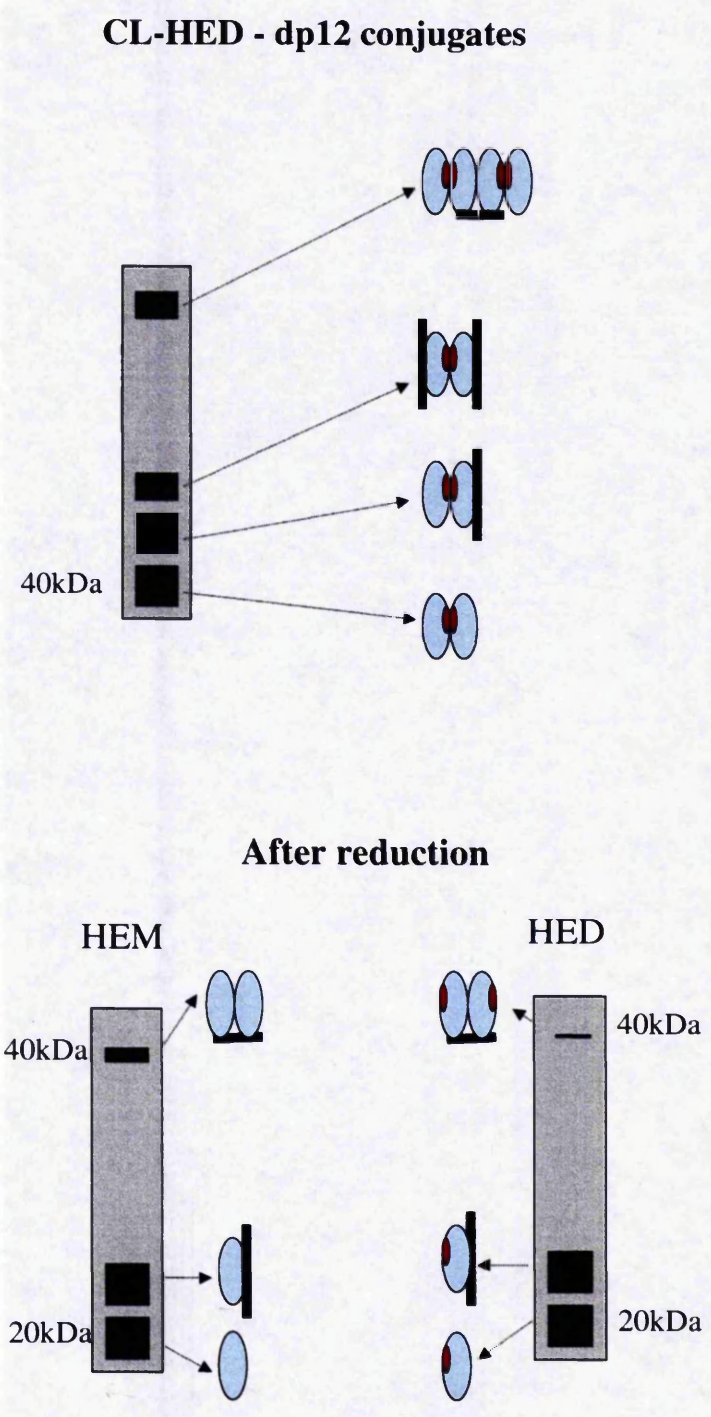

Figure 6.37 : Schematic representation of CL-HED-dp12 conjugates exposed to reducing and non-reducing SDS-PAGE. The CL-HED-dp12 conjugates shift in molecular weight following reduction to a pattern of bands that is identical to that of the CL-HEM-dp12 conjugates. This suggests that a heparin dodecasaccharide (dp12) can act as a template to 'dimerise' endostatin monomers in contrast to preformed dimer in which only one subunit appears to crosslink the saccharide. See Figure 6.36 for original result.

HED-heparin. In lane 5, it can be seen that reducing conditions have no effect on CL-HEM-heparin (compare to lane 3). In lane 6, reduction of CL-HED-heparin causes a shift in the free protein band to 20KDa, consistent with the size of each monomer subunit and higher molecular weight product also remains. These patterns confirm covalent crosslinking of both HEM and HED to heparin.

Figure 6.36, Panel B shows free HEM, free HED, CL-HEM-dp12 and CL-HED-dp12. There is no effect of reduction on CL-HEM-dp12 shown in lane 5, compared to lane 3 or Figure 6.35, Panel B, lanes 3 and 4. The 1:1 and 2:1 CL-HEM-dp12 conjugates have persisted, indicating covalent coupling for both stoichiometries. In marked contrast, reduction of CL-HED-dp12 produces a banding pattern that is indistinguishable from that of HEM-dp12 (Figure 6.36, Panel B, lane 6). The ~40KDa free HED has been reduced as expected from its disulphide bonded structure. Importantly, a ~25KDa band shows reduction of CL-HED-dp12 to the same position as CL-HEM-dp12. This indicates that dp12 is not covalently associated with both subunits of the dimer (HED) simultaneously. There is a faint band in the CL-HED-dp12 (1:1 ratio) position, that persists following reduction but the HED tetramer band is no longer present (~80kDa band in Figure 6.35B, lane 5, and 6.36B, lane 4). Possible binding conformations to explain these data are presented in Figure 6.37. It appears that dp12 can act as a template to induce dimerisation of two HEM molecules but preformed dimer (HED) cannot bind one dp12 to both subunits simultaneously suggesting that the dimerisation imposes a constraint on the conformations that the subunits can adopt.

Recovery of protein by digestion with heparinase I

To ensure that higher molecular weight bands contained GAG, samples were treated with heparinase I for 18 hours as described in 'Methods' and recovered by precipitation with BSA and TCA for SDS-PAGE and Western blotting. Figure 6.36, Panel A shows CL-HEM-heparin in lane 3 and CL-HED-heparin in lane 4. Treatment of these conjugates with heparinase I causes a change in the pattern of bands (lanes 7 and 8, respectively). Free protein is not recovered to its original size and the additional bands suggest that a short heparin fragment is protected from heparinase I digestion. In contrast CL-HEM-dp12 and CL-HED-dp12 are not affected by heparinase I (Figure 6.36, Panel B, lanes 7 and 8, respectively). Taken together, these experiments suggest that an oligosaccharide fragment of the order of a dp12 is protected from heparinase I

digestion due to its close association to the protein and this is in line with the optimal fragment size for binding in physiological conditions detected using the FBA (Figure 6.9).

Heparin affinity of cross linked GAG-protein conjugates.

To test the heparin affinity of crosslinked HEM and HED-GAG conjugates, samples were mixed with 30µl heparin-agarose beads in 0.1M MES, 0.1M NaCl, pH7.0, centrifuged for 10 minutes, the supernatant (unbound product) removed, and the remaining beads containing bound, heparin-binding product dissolved in sample buffer. Unbound and bound samples were then analysed by PAGE and Western blotting as described. The Western blot shown in Figure 6.38 confirms that the heparin binding ability of the monomer (HEM) is blocked by crosslinking to heparin and dp12. In contrast, Figure 6.39, indicates that crosslinking has not blocked the heparin affinity of any of the endostatin dimer conjugates (ie CL-HED-heparin or CL-HED-dp12). Again, this suggests a difference in the conformation of the dimer compared to the monomer.

Purification of crosslinked HEM-heparin and HEM-dp12

The previous result suggested that CL-HEM-heparin and CL-HEM-dp12 could be purified ie separated from free protein, by heparin affinity. Also, to optimise the yield of CL-HEM-heparin in larger scale preparations, two different concentrations and ratios of EDC:NHS were tested (6mM:15mM compared to 23mM:25mM) but there was no significant difference as shown in Figure 6.40, lanes 2 and 4. Note that the smears of CL-HEM-heparin are similar to those obtained previously with high molecular weight bands indicating pseudo-dimerisation of HEM but there are also more obvious lower molecular weight bands consistent with a 1:1 GAG:protein ratio. These conjugates were not consistent in proportion and indicate some variation in crosslinking efficiency that is one potential difficulty to overcome in preparation of samples in bulk for assays.

For purification of crosslinked conjugates from free protein on a larger scale, samples were applied in 0.1M MES, 0.1M NaCl, pH7.0 to a 0.5ml heparin-agarose affinity column and recirculated 5 times instead of using heparin-agarose beads as described above. The products collected in the void are shown in Figure 6.40. In lanes 3,5 and 7,

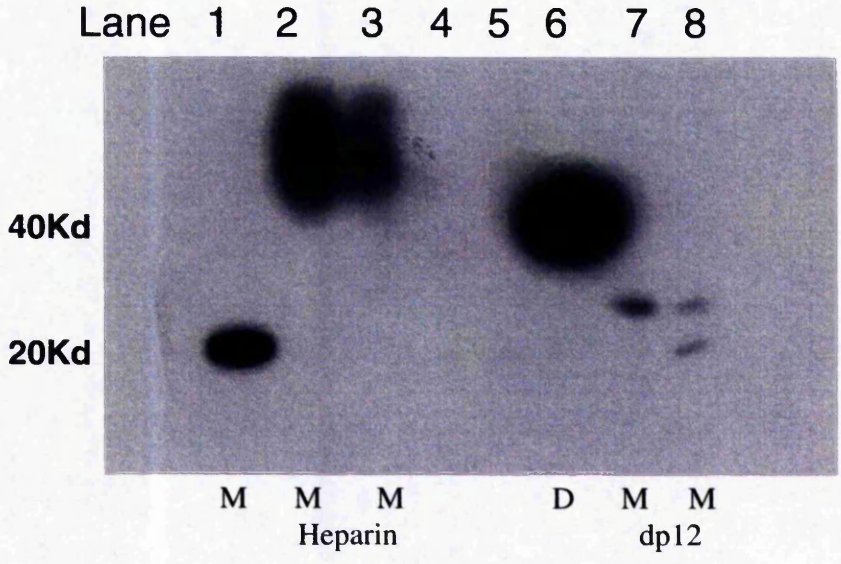

Figure 6.38 : Heparin affinity of cross linked GAG-HEM conjugates. Heparin or dp12 oligosaccharides were crosslinked to HEM (M) as previously described. Samples were mixed with 30µl heparin-agarose beads in 0.1M MES, 0.1M NaCl, pH7.0 and centrifuged to separate the supernatant (unbound conjugates). The beads (with bound conjugates) were dissolved in sample buffer. Samples were analysed by SDS-PAGE, followed by Western blotting and ECL immunodetection as described in 'Methods'. 200ng native HEM (*lane 1*), 1µg CL-HEM-heparin unbound (*lanes 2& 3*), 1µg CL-HEM-heparin bound (*lanes 4 and 5*). 200ng native HED (*lane 6*), 1µg CL-HEM-dp12 unbound (*lane 7*), 1µg HEM-dp12 bound (*lane 8*). CL = crosslinked.

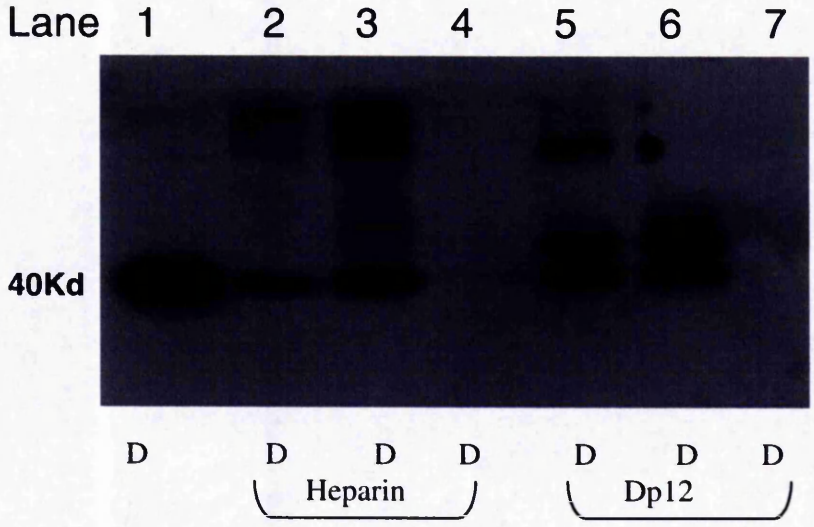

Figure 6.39 : Heparin affinity of cross linked GAG-HED conjugates. Heparin or dp12 oligosaccharides were crosslinked to HED (D) as previously described. Samples were mixed with 30µl heparin-agarose beads in 0.1M MES, 0.1M NaCl, pH7.0 and centrifuged to separate the supernatant (unbound conjugates). The beads (with bound conjugates) were dissolved in sample buffer. Samples were analysed by SDS-PAGE, followed by Western blotting and ECL immunodetection as described in 'Methods'. 200ng native HED (*lane 1*), 1µg CL-HED-heparin (*lane 2*), 1µg CL-HED-heparin bound (*lane 3),* 1µg CL-HED-heparin unbound (*lane 4*), 1µg CL-HED-dp12 (*lane 5),* 1µg CL-HED-dp12 bound (*lane 6*), 1µg CL-HED-dp12 unbound (*lane 7).*

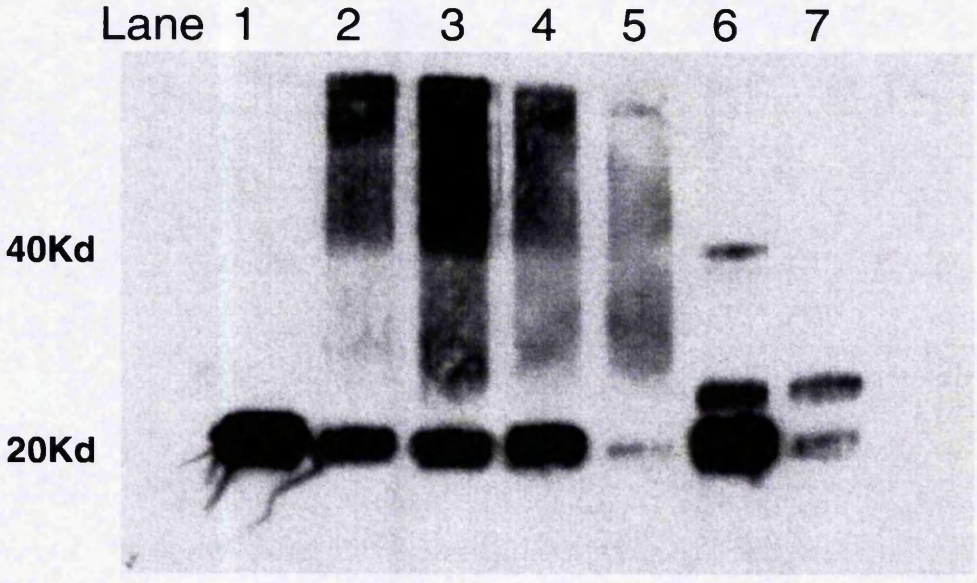

Figure 6.40 : Purification of GAG-HEM conjugates by heparin affinity. Heparin, activated using EDC:NHS in a ratio of 6mM:15mM *(lane 2 &4)* or 23mM:25mM *(lane3 &5)* and dp12 in a 5 molar excess to protein, were crosslinked to HEM as described. Samples were applied to a 0.5 ml heparin-agarose column, recirculated 5 times and eluted in 0.1M MES, 0.1M NaCl, pH7.0 for analysis by SDS-PAGE, followed by Western blotting and ECL immunodetection as described in 'Methods'. Panel A: 200ng native HEM (*lane 1*), 1µg CL-HEM-heparin (*lanes 2& 4*), 1µg CL-HEM-heparin eluted from heparin affinity column (void) (*lane 3 &5*), 1µg CL-HEM-dp12 (*lane 6*), 1µg CL-HEM-dp12 eluted from heparin affinity column (*lane 7*). CL = crosslinked.

there is still free HEM although there is evidence of depletion in lanes 5 and 7. The CL-HEM(2)-dp12 conjugates were not recovered suggesting that they may have been retained on the heparin affinity column. Therefore, additional strategies are required to optimise both the yield of HEM and HED-GAG conjugates and separation from uncrosslinked protein and free GAG. Nevertheless, these studies provide novel information about the molecular association between heparin, endostatin monomer and dimer that may have a bearing on their distinct activities (see Chapter 7). In addition, these data confirm the possibility of generating crosslinked conjugates to test in bioassays and the main findings are summarised in Figure 6.41.

Zero-length crosslinking - summary

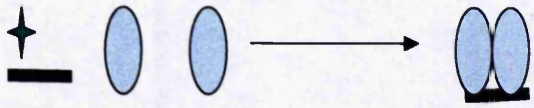

1. GAG acts as a template for 'pseudo-dimerisation' of HEM

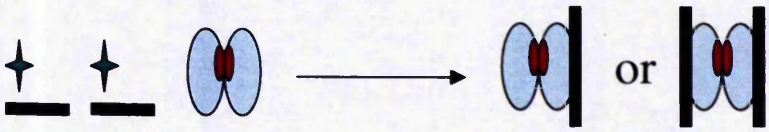

2. GAG does not bind both subunits of HED simultaneously

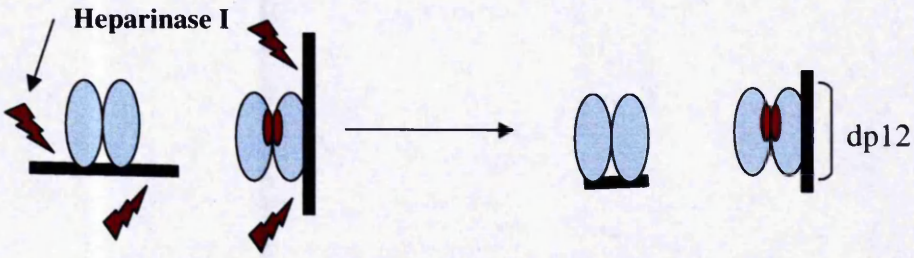

3. Heparin-endostatin conjugates protect a saccharide ~ dp12 from digestion by heparinase I

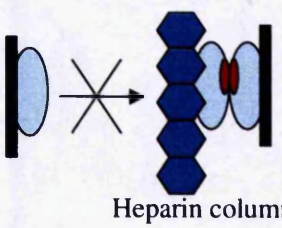

4. Heparin-HEM conjugates do not bind heparin in contrast to their dimeric counterparts that retain affinity after crosslinking

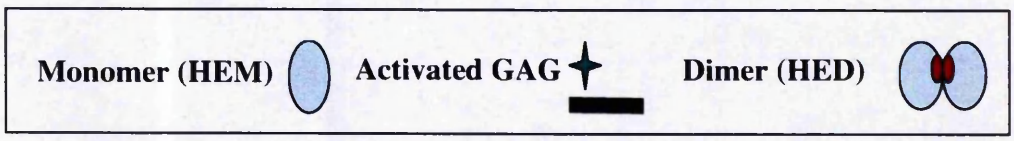

Figure 6.41 Summary of results of zero-length crosslinking studies. See text for definition of 'pseudo-dimerisation'.

7. DISCUSSION

PART 2 : THE INTERACTION OF HEPARAN SULPHATE WITH ENDOSTATIN

The interaction between the potent angiogenic inhibitor, endostatin, and naturally occuring EC HS has been examined using a sensitive filter binding assay and a zero-length covalent crosslinking strategy. Excised hexasaccharide sequences bind to endostatin with weak affinity but longer sequences (dp10/12) bind with affinity approaching that of the intact chains. Rather than an interaction with a unique binding sequence, endostatin binds to a variety of structural motifs that are characterised by the presence of 6-O-sulphation within the trisulphated disaccharide [UA(2S)-GlcNS(6S)]. Consistent with this specificity, loss of 6-O-sulphate groups markedly impairs the competitive ability of HS and using HS synthesised by an *Hs2st*$^{-/-}$ mutant, we have demonstrated that 2-O-sulphation is not critical for the interaction. Analysis of complexes formed by zero-length crosslinking revealed that a heparin dodecasaccharide can act as a template to 'dimerise' endostatin monomers in contrast to preformed dimer in which only one subunit appeared to crosslink the saccharide. These findings provide various possible models of the molecular assemblies that may form between HS and endostatin (monomer/dimer) in the pericellular environment and novel insight into the structural features within EC HS that determine binding to endostatin.

Endostatin was originally purified as a 20kDa protein from the culture media of EOMA cells by heparin affinity (O'Reilly *et al.*, 1997). Sequencing revealed homology to the C terminus of the NC1 domain of collagen XVIII, the primary structure was noted to contain a highly conserved, discontinuous sequence of 11 basic arginine residues, and the crystal structure confirmed that these were arranged in a cluster on the protein surface (Hohenester *et al.*, 1998). These findings provided initial clues to a heparin binding epitope and the proposal that HS is required for the biological activity of endostatin (Sasaki *et al.*, 1999). Although contentious, this theory was supported by studies in which mutation of critical arginine residues impaired heparin affinity and bioactivity (Dixelius *et al.*, 2000; Sasaki *et al.*, 1999).

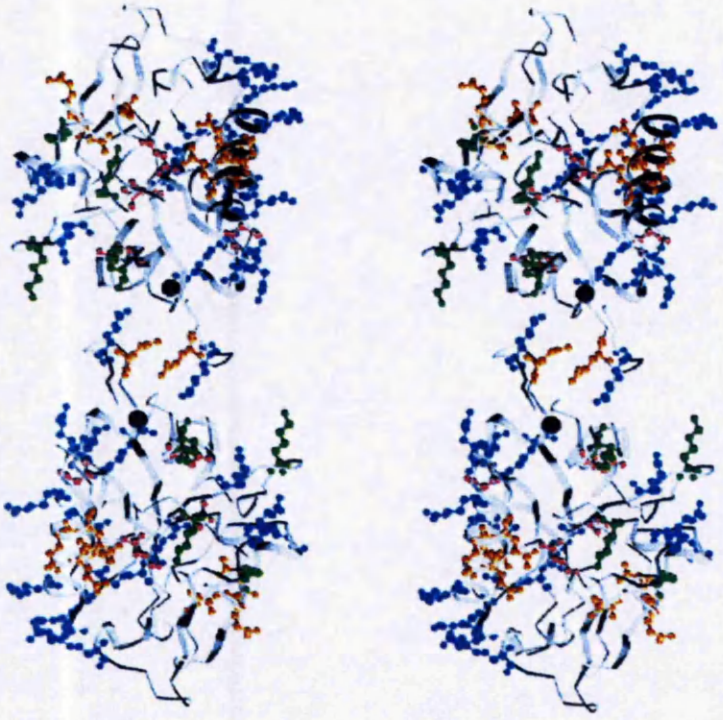

Figure 7.1 : Human endostatin dimer
A positively charged surface formed by arginines on the human endostatin dimer. Stereo diagram, surface glutamines (yellow), asparagines (cyan), lysines (green), and arginines (blue) are shown. (Ding et al.,1998)

Subsequently, the trimeric NC1 domain of type XVIII collagen, that is the physiological precursor of endostatin, was shown to have pleiotrophic, HGF-like promigratory/scatter factor activity (Kuo *et al.*, 2001, Ackley *et al.*,2001). It promotes neural cell migration in *C. elegans* (Ackley *et al.*, 2001) and an inherited mutation that causes truncation of the commonly occuring α1(XVIII)collagen short form, is believed to account for the phenotype of human Knobloch syndrome (Sertie *et al.*, 2000). This is an autosomal recessive disorder characterised by structural abnormalities in the retina and occipital encephalocele due to defective neural tube closure. The activity of NC1 is replicated *in vitro* by an artificial recombinant endostatin dimer (Kuo *et al.*,2001) that was modelled from studies of the crystal structure of endostatin (Ding *et al.*, 1998) (Figure 7.1). Endostatin monomer, antagonises the promigratory activity of the oligomeric forms of endostatin *in vitro* (Kuo *et al.*,2001) and in *C.elegans* (Ackley *et al.*,2001) whereas in the CAM assay of angiogenesis the α1(XVIII)collagen NC1 domain is inactive (Sasaki *et al.*,2000) and endostatin monomer is a potent angiogenic inhibitor (Sasaki *et al.*,1999; Sasaki *et al.*,2000).

These findings support the concept of a negative autoregulatory loop in which NC1 and endostatin are proteolytically cleaved from collagen XVIII and act locally to regulate its activities (Figure 1.12) (Zatterstrom *et al.*,2000, Ackley *et al.*,2001, Kuo *et al.*,2001). Significantly, the α1(XV) collagen homologue of the α1(XVIII) collagen NC1 domain does not bind heparin and is not promigratory (Kuo *et al.*, 2001) (Ackley *et al.*, 2001). This strengthens the potential importance of an interaction with HS for the α1(XVIII) collagen NC1 domain. Although restin, the non-heparin binding α1(XV)collagen homologue of endostatin, is antiangiogenic (Ramchandran *et al.*, 1999) it is possible that HS dependent and independent mechanisms of action exist for endostatin that would explain conflicting results obtained to date (Dixelius *et al.*, 2000; Sasaki *et al.*, 1999; Yamaguchi *et al.*, 1999).

We have used the filter binding assay (FBA) to examine the molecular interaction between EC HS and endostatin (monomer/dimer). This assay was initially developed to examine the interactions between GAGs and PF4, ATIII and fibronectin (Maccarana & Lindahl, 1993), and was modified for this investigation to enable examination of trace quantities of biologically relevant HS from human microvessel (neonatal dermal) endothelial cells (HMVEC). As presented previously, this HS is characterised by a

relatively short chain length (~45 disaccharides), a low sulphate content (~ 0.62 sulphates/disaccharide), and a typical domain structure with fine structural variation.

HS binds to monomeric and dimeric forms of endostatin

Endostatin monomer (HEM) and dimer (HED) have moderate apparent affinity for EC and 3T3 fibroblast HS indicated by the elution of all bound GAG from protein with ~ 0.35 M NaCl in the FBA. This is in agreement with Sasaki *et al.*, 1999 who also defined a Kd ~ 0.3μM for endostatin binding to heparin. In the first characterisation of endostatin, its antiproliferative effect was restricted to ECs but a broader tissue tropism is now evident (Ackley *et al.*, 2001; Kuo *et al.*, 2001) that concurs with the binding of endostatin to non EC HS in this, and previous reports (Karumanchi *et al.*, 2001; Sasaki *et al.*, 1999; Sasaki *et al.*, 2000). HED has enhanced affinity for HS, demonstrated by an 8 fold lower molar concentration of HED (5μM), compared to HEM (40 μM), for optimal binding to HS chains in the FBA. This suggests that the tertiary structures of the heparin binding epitopes are conserved in HED and the different bioactivities of HED and HEM could, in part, be explained by the higher apparent affinity of HED for HS. However, it is perplexing that equivalent concentrations of NaCl are required to dissociate HEM and HED from HS. This suggests that electrostatic interactions may not be the sole mediator of the HED-GAG interaction, and/or that the protein itself is sensitive to NaCl. In the latter case higher NaCl concentrations may alter the conformation of the protein enabling GAG to dissociate. Detailed studies of the association and dissociation rate constants using a biosensor would better define the binding kinetics of these proteins to GAGs. However, the strength of binding does not dictate the functional importance of GAG-protein interactions. The anti-angiogenic matrix protein, fibronectin, also binds HS with moderate to weak affinity (Kd 0.1-1μM) and membrane HSPGs are an essential co-receptor for this protein. The interaction of HS with the hep-2 domain of fibronectin promotes focal adhesion formation in cooperation with integrins and also induces cytoskeletal re-organisation in fibroblasts leading to formation of filopodia and lamellipodia (Woods *et al.*, 1998).

The first confirmation of a biological role for heparin/HS in the regulation of endostatin came from mutagenesis studies in which various arginine-alanine (R-A) mutations were introduced into recombinant murine endostatin (Sasaki *et al.*,1998). Two of eleven arginine residues (R158/270) were found to be the principal contributors of heparin

affinity, with 0.35M NaCl required to elute the native protein from heparin-Sepharose, reducing to 0.11M NaCl for the R158/270 mutant (Sasaki *et al.*, 1999; Yamaguchi *et al.*, 1999). The R158/270-A mutant was also inactive as an inhibitor in the CAM angiogenesis assay (Sasaki *et al.*,1998). However, mutation of two other arginines, R193/194, ~30 Å away from R158/270 also inactivated endostatin in the CAM assay, but heparin affinity was only slightly reduced (0.27M NaCl to elute). This led to the proposal of primary (centred around R158/270), and secondary (centred around R193/194) heparin binding sites (Sasaki *et al.*, 1999).

The consequences of these mutations in the dimeric form of endostatin have not been reported. Like HEM, R158/270-A mutated HED does not bind to HMVEC HS at physiological pH and ionic strength in the FBA. Notably, the promigratory activity of R-A mutant HED is significantly reduced compared to the wild type (K Javaherian, personal communication). An antibody (mAb 12C1) that recognises arginines within the primary heparin binding domain and neutralises HED activity *in vitro* (K Javaherian, in preparation) also blocked binding of HMVEC HS to both HEM and HED in the FBA (Figures 6.5 and 6.30). Taken together these observations indirectly support a role for heparin/HS in the regulation of both HEM and HED. In addition, they reinforce the view that the primary heparin binding epitope is the principal recognition site for HS in HEM (Sasaki *et al.*, 1999) and suggest that this is maintained for HED. Due to the strong affinity of mAb 12C1 for endostatin relative to that of HS, it has not been possible to determine whether it directly competes with HS or induces a conformational change that prevents association of HS. However, the possibility that mAb 12C1 inhibited binding of HS to endostatin by steric hindrance or due to non-specific recognition of a basic heparin-binding domain was excluded by the ability of HS to bind endostatin in the presence of a control Ab (PDM) and to bFGF in the presence of mAb 12C1, respectively.

HEM versus HED

The dose dependent antagonism of HED by HEM *in vitro* favours direct competition between these proteins for the same ligand (Kuo *et al.*, 2001). We have shown that both bind HS, but only oligomeric forms activate MAPK signalling pathways (Kuo *et al.*, 2001). One possibility is that an endostatin monomer may bind HS (either matrix or cell-surface) but an oligomer may be required to engage both HS and an additional

ligand in a signalling complex. Although a specific receptor for endostatin has not been identified, there are various candidates known to bind endostatin that could participate with HSPGs in a trimolecular signalling complex. In theory, the signalling protein could be a cell surface HSPG, such as glypican (Karumanchi *et al.*,2001) with a matrix protein co-factor such as laminin (Sasaki *et al.*, 1998) or, signalling could be mediated through a cell-surface adhesion molecule such as an integrin (Rehn *et al.*, 2001), with a matrix HSPG, for example, perlecan, or even collagen XVIII, as a co-factor (Zatterstrom *et al.*,2000).

An alternative possibility, that does not exclude the above, is that HS adopts a different conformation with HEM compared to HED. We examined products obtained by coupling GAGs to these proteins using a two step zero-length cross-linking technique (Grabarek & Gergely, 1990). This technique enables GAG-protein, but avoids protein-protein, coupling and has been used succesfully to examine minimal complexes of bFGF-GAG for bioactivity (Pye & Gallagher, 1999). Covalent crosslinking occurs through the ε-amino groups of lysines to the carboxyl groups of uronate residues. The GAG must be closely approximated to the protein for this to occur, so successful coupling in itself suggests a biologically signficant affinity. Although we have not examined endostatin-HS conjugates, the studies in this thesis of the HEM and HED-heparin and heparin dodecasaccharide (dp12) conjugates revealed distinctions that may have a bearing on their opposing mechanisms.

Both heparin and dp12 acted as a 'template' for creating pseudo-dimers (ie no protein-protein interface, Figure 6.35, 6.41). In contrast most HED-dp12 conjugates were reduced to monomeric forms by β-mercaptoethanol suggesting that the disulphide-bonded subunits of HED were not (or rarely) crosslinked to dp12 simultaneously (Figure 6.36, 6.37, 6.41). This suggests that the conformation of HED, compared to the conformations that two HEM molecules may adopt, imposes constraints on the GAG interaction. Also, the reason why heparin affinity persists in all the HED conjugates after crosslinking is unclear but may be explained by a conformational change.

An important factor when interprating crosslinking data is that the formation of these conjugates occurs through the activated carboxyl groups of the GAG and lysine residues as previously described. Therefore, the lysine residues must be in close proximity to

arginines in the heparin binding site. Without this, crosslinking either does not occur, or may occur suboptimally ie, with persistence of heparin affinity. Since the HEM conjugates demonstrate optimal crosslinking, ie heparin affinity is blocked, a conformational change imposed by dimerisation may have altered the relationship between lysine(s) and heparin-binding arginines. This would not be detected in direct binding studies of R-A mutated HED or in the presence of mAb 12C1. A combination of the above possibilities is that binding of the GAG to one subunit of HED may induce a conformational change in the other that enables it to engage an additional ligand, other than HS, such as a signalling receptor. Interestingly, GAG-endostatin co-crystal studies have been hampered by the ability of both GAG and protein to adopt multiple conformations in solution (Sasaki *et al.*, 1998) and the potential biological relevance of this warrants further investigation.

Size of the HEM binding site within HS

In contrast to the differences observed between HEM and HED in the crosslinking studies, the determinants of HS required for binding appeared similar although detailed investigations were only undertaken for HEM. From the crystal structure of endostatin it was predicted that a dp12 would be required to occupy both primary and secondary heparin binding domains; and heparin dodecasaccharides were found to bind maximally to endostatin by affinity chromatography and filter binding (Sasaki *et al.*, 1999). Our data strengthens these observations. Treatment of crosslinked HEM and HED conjugates with heparinase I did not restore the protein to its native size but indicated a residual fragment of the order of a dodecasaccharide by comparison to crosslinked conjugates (Figure 6.36). Using heparin derived oligosaccharides of defined length for competitive binding, octasaccharides (dp8) competed with HMVEC HS for HEM, but optimal competition was observed for deca- and dodecasaccharides (dp10/12). Correspondingly, HMVEC HS heparinase III resistant S-domains that bound HEM at physiological ionic strength and pH in the FBA were deca-dodecasaccharides (dp10/12).

Hexasaccharides are the smallest oligosaccharides with affinity for HEM

In agreement with other reports (Karumanchi *et al.*, 2001; Sasaki *et al.*, 1999), hexasaccharides were the smallest HS oligosaccharides to bind HEM measurably in this study, detected by size fractionation of bound S-domains on Bio-Gel P10 (Figure 6.8) and direct binding of size-defined S-domains (Figure 6.9). However, in contrast to

heparin hexasaccharides that bind endostatin at physiological ionic strength (Karumanchi *et al.*, 2001; Sasaki *et al.*, 1999), the affinity of HMVEC HS hexasaccharides was weak, indicated by elution from HEM with 0.1 M NaCl in the FBA.

These findings likely reflect the structural variation between heparin and HS. The differences in molecular design of these chemically related GAGs are well documented (Gallagher & Walker, 1985; Lindahl *et al.*, 1998; Lyon *et al.*, 2000), although functional distinctions are less clear. Heparin is of significantly greater overall sulphation compared to HS. In addition, it differs in the relative distribution of sulphate groups among different ring positions. There is near equivalence in the frequency of N-,2-O-, and 6-O-sulphates in bovine lung heparin, with ≥90% occupancy at each position. However, in mucosal HS, sulphate groups are localised mainly to the S-domains, in which N-sulphates constitute approximately half of the total, with the remainder split almost evenly between 2-O- and 6-O-sulphates (Lyon *et al.*, 2000).

Although Sasaki *et al.*,1999 did not characterise the sulphate content of binding hexasaccharides Karumanchi *et al.*, 2001 reported an almost fully modified sequence, with three 6-O-sulphate groups, lacking only 1 of three possible 2-O-sulphate groups on a reducing end glucuronate. This is substantially more sulphated than the four hexasaccharide structures detected in HMVEC HS (Figure 6.10, 6.11). Indeed, highly sulphated hexasaccharide S-domains are not characteristic of any HS species examined in this investigation but these hexasaccharide motifs may reside (rarely) within longer S-domains of at least dp 10/12. Interestingly, heparin-derived hexasaccharides did not compete with HMVEC HS in this study which implies that direct binding and competition studies are not necessarily comparable. Our data suggest that at least an octasaccharide is required to dissociate bound HMVEC HS from HEM in physiological conditions. Nevertheless, we demonstrated by zero length crosslinking, that a dodecasaccharide can bind two HEM molecules.

Structural analysis of HMVEC HS hexasaccharides demonstrated two binding species (the more highly sulphated dp6c and dp6d, Figure 6.12), with enrichment of the trisulphated disaccharide [UA(2S)-GlcNS(6S)] in the binding fraction. From the crystal structure and mutagenesis data, it was predicted that a highly sulphated tetra or

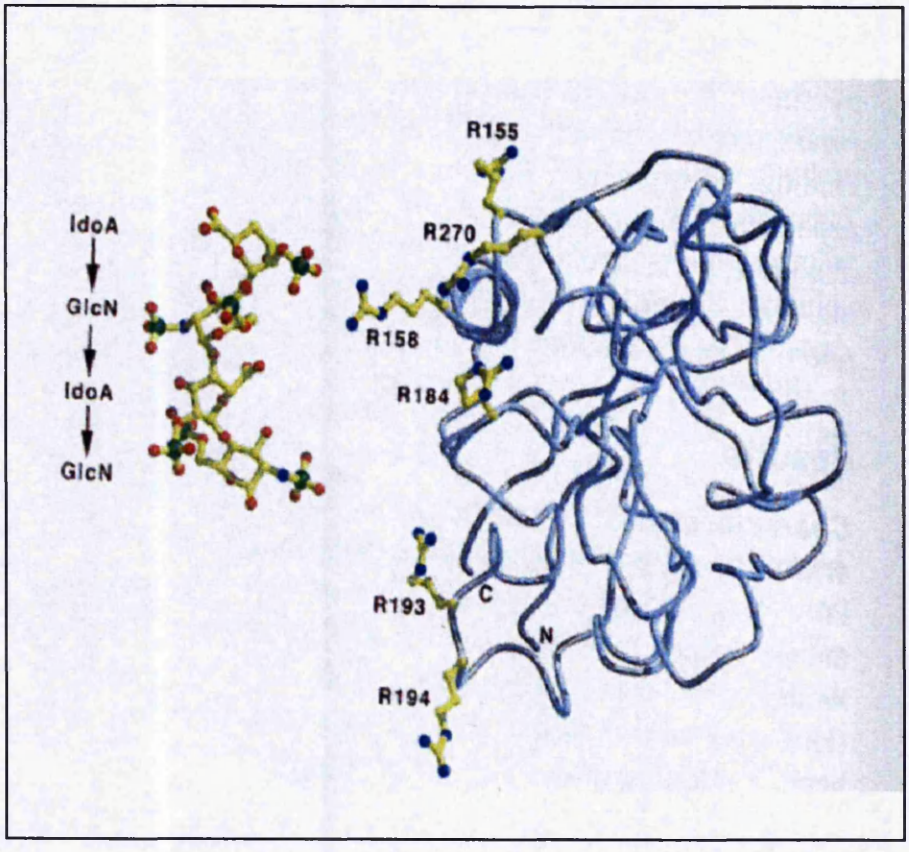

Figure 7.2 : The interaction between heparin and endostatin. The crystal structure of endostatin predicts that a heparin tetra-hexasaccharide can be accomodated in the primary heparin binding domain centred around R158/270. A dodecasaccharide would be required to extend to the secondary heparin binding domain (R193/R194). Sasaki *et al.*,1999.

hexasaccharide could be accommodated in the primary binding site but at least a dodecasaccharide would be required to simultaneously engage the secondary binding site (Sasaki *et al.*, 1999) (Figure 7.2).

The finding that mAb 12C1 blocked association of hexasaccharide dp6d to HEM is consistent with this. An interesting observation is that mutation of R193/194 to alanine in the secondary heparin binding site of endostatin was demonstrated to have greater impact on the affinity of HS (ie decreased affinity) compared to heparin (little change in affinity) (Sasaki *et al.*,1999). Perhaps HS must engage both sites for optimal affinity whereas heparin-binding may be preferentially mediated through the primary heparin binding site? If so, this reinforces the importance of examining HS in addition to heparin in these investigations.

Pinpointing the HS recognition domain for endostatin

Heparinase III generated S-domains (≥dp12), and heparinase I resistant oligosaccharides that are composed of the transition zones and predominantly N-acetylated disaccharides (Figure 1.3), both bind to endostatin with comparable affinity, approaching that of the intact chains. It has not been possible to define an exact sequence but structural analysis of these oligosaccharides reveal important clues to the GAG-endostatin interaction. Compositional analysis of binding S-domains from HMVEC, BAEC and 3T3 fibroblast HS showed a connection between increased sulphate content and stronger binding to endostatin for each size-defined class. Binding and non-binding subpopulations were predominantly non-overlapping in charge, and strongest binding to HEM was associated with the most modified sequences, that contained the highest proportion of 6-O-sulphate and the trisulphated disaccharide [UA(2S)-GlcNS(6S)].

The known mediation of binding by arginine residues rather than lysine (Hohenester *et al.*, 1998; Sasaki *et al.*, 1999), supports sulphates as the principal determinants of binding since the guanidinium groups are more effective in co-ordinating anions such as sulphate, rather than carboxyls (Lyon *et al.*, 2000). It was not possible to define the importance of position of N-sulphate groups since the S-domains, due to the specificity of heparinase III, were invariably fully N-sulphated with an N-acetylated disaccharide at the reducing end. Similarly, the trisulphated disaccharide [UA(2S)-GlcNS(6S)] was the main provider of 6-O-sulphate so the relative importance of 2-O-sulphate compared

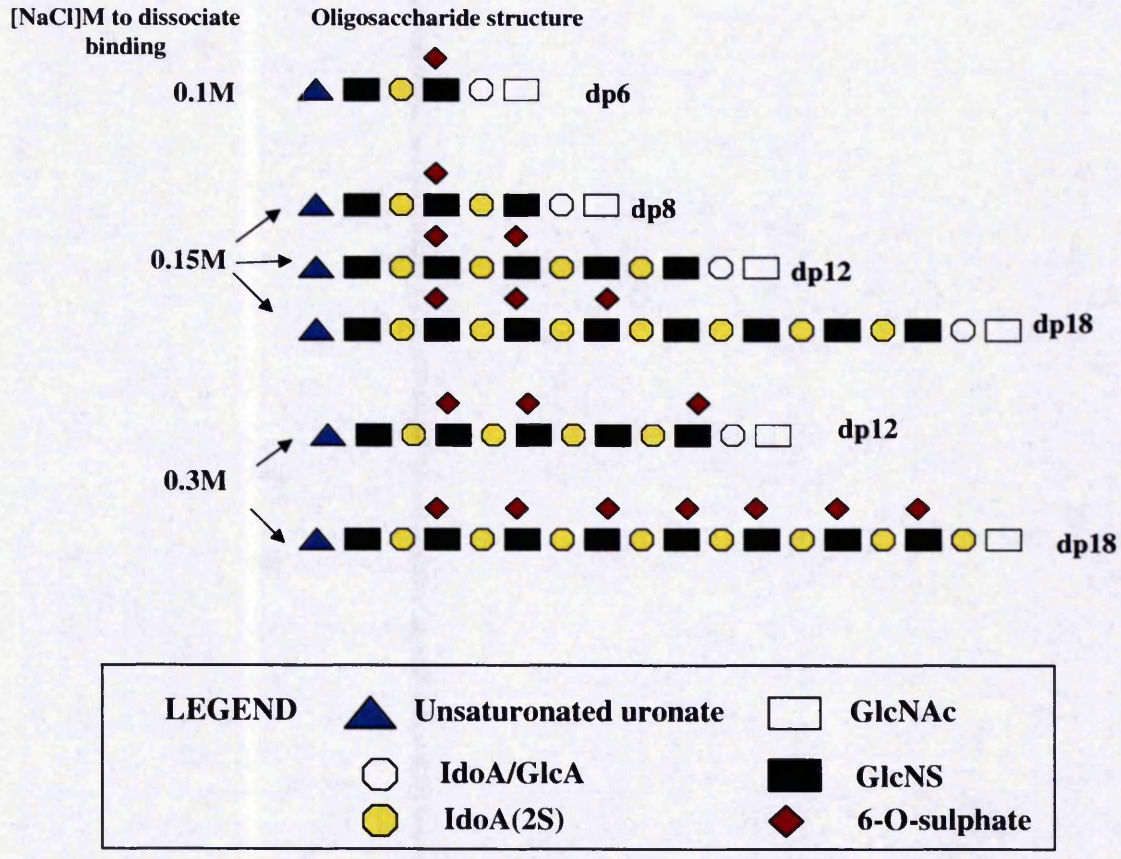

Figure 7.3 : Schematic representation of S-domains that bind to endostatin.
Theoretical structures of S-domains, modelled from disaccharide analyses have different affinities for HEM, indicated by the NaCl concentration to dissociate binding. A longer S-domain with an increased sulphate content does not automatically confer stronger binding. This suggests that the positions of sulphate groups, rather than the charge alone, are important for the HS-endostatin interaction.

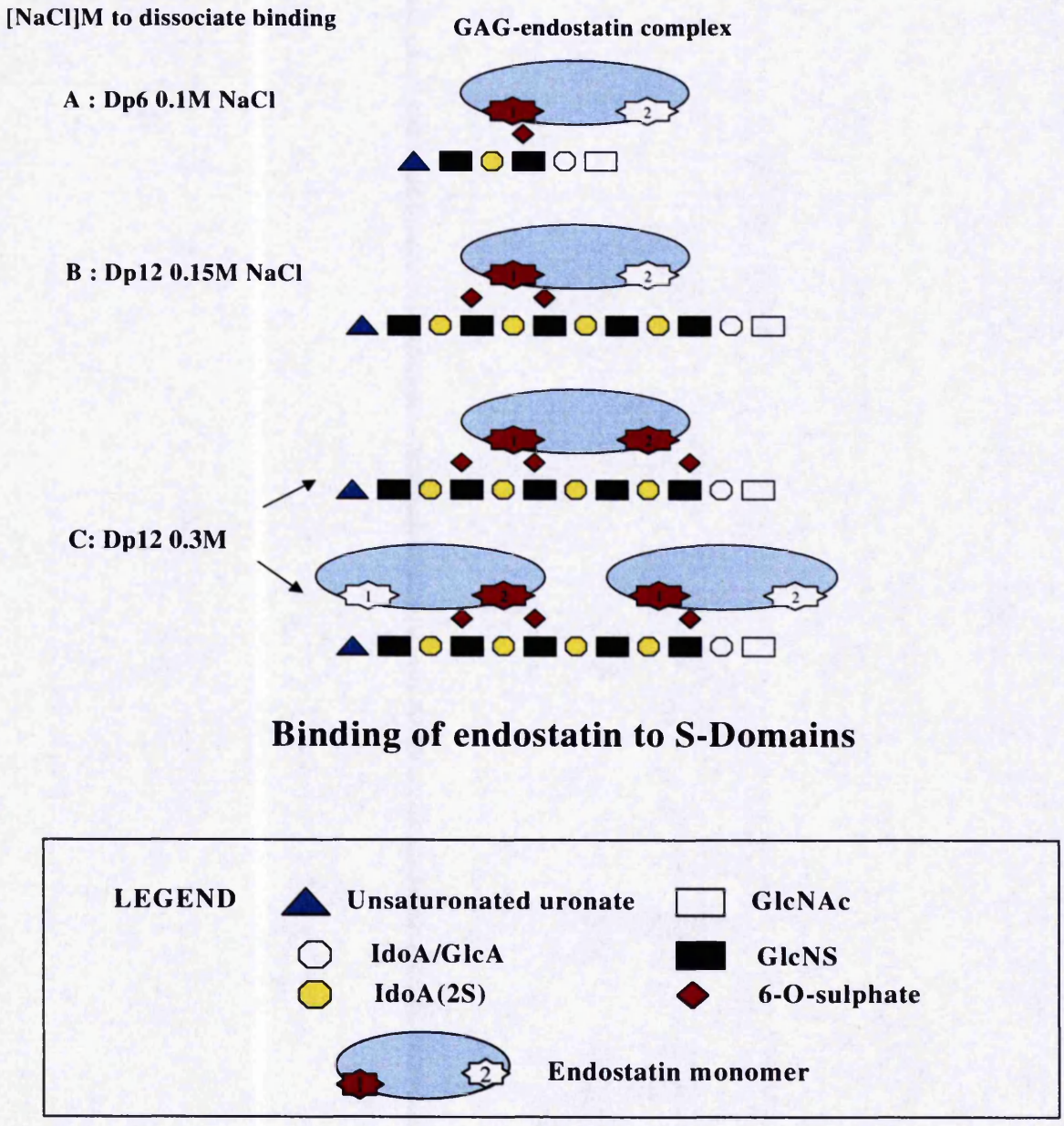

Figure 7.4: Models of S-domains (dp6 and dp12) that bind to endostatin. **A**: a hexasaccharide (dp6) is shown docking into the primary heparin binding site of endostatin but is too short to engage the secondary heparin binding site for maximal affinity. **B**: The weaker binding dp12 (eluted with 0.15M NaCl) has sulphate groups positioned to confer stronger binding than dp6 but lacks critical sulphate groups for maximal affinity. **C**: The dp12 with highest affinity (0.3M NaCl) can interact with both primary and secondary heparin binding domains or may dimerise HEM.

to 6-O-sulphate in this disaccharide is difficult to discern. This illustrates the difficulty in assigning minimal sequences and critical determinants for binding when reliant on naturally occuring oligosaccharides. However, there are indications of selectivity.

In S-domains of similar total sulphate content and charge, a relative increase in 6-O-sulphate correlated with stronger binding (compare BAEC 8c*, e and f*, Figure 6.16 and dp12 and 18, Table 6.3). Also, a higher charge density in a longer sequence does not appear to automatically confer stronger binding. This is illustrated in Figure 7.3 that compares the structures of model S-domains (based on the disaccharide compositions obtained in Table 6.1, 6.2, 6.3A) to their affinity (indicated by NaCl concentration) for endostatin. This suggests that there may be a requirement for sulphate groups in specific positions. As shown in Figure 7.4, the spacing of sulphate groups may be important to engage both primary and secondary heparin binding sites of a monomer, or enable two molecules to bind. Therefore, the most sulphated S-domains may bind with greater affinity because the probability of finding the correct arrangement of sulphate groups is higher.

Heparinase I resistant oligosaccharides bind to endostatin

The ability of heparinase I resistant oligosaccharides to bind HEM and HED strengthens our argument against a purely charge driven interaction. Heparinase I cleaves in the most sulphated regions of the chain so disrupts the longer S-domains but leaves the transition zones intact (Figure 1.3, 7.5). As shown by our disaccharide analyses the heparinase I resistant oligosaccharides that bind strongly to HEM are composed of a relatively low proportion of sulphate groups compared to the S-domains and are mainly composed of N-acetylated disaccharides. In addition, these saccharides contained heparinase III resistant, and therefore sulphated, tetra- and hexasaccharide sequences (Figure 6.27). When the heparinase I resistant oligosaccharides were treated with nitrous acid (that disrupts linkages joining N-sulphated disaccharides) they no longer bound HEM. Taken together, these findings suggest that in contrast to the weak affinity of hexasaccharide S-domains, short sulphated sequences that exist in heparinase I resistant oligosaccharides can mediate binding to endostatin in physiological conditions (ie >0.15m NaCl) provided that they are *in situ*, rather than excised from HS. It is not clear why this is the case but one possibility is that the less modified (N-acetylated) saccharides provide a conformational stability that presents the tetra- and

Heparinase I resistant oligosaccharides bind to endostatin

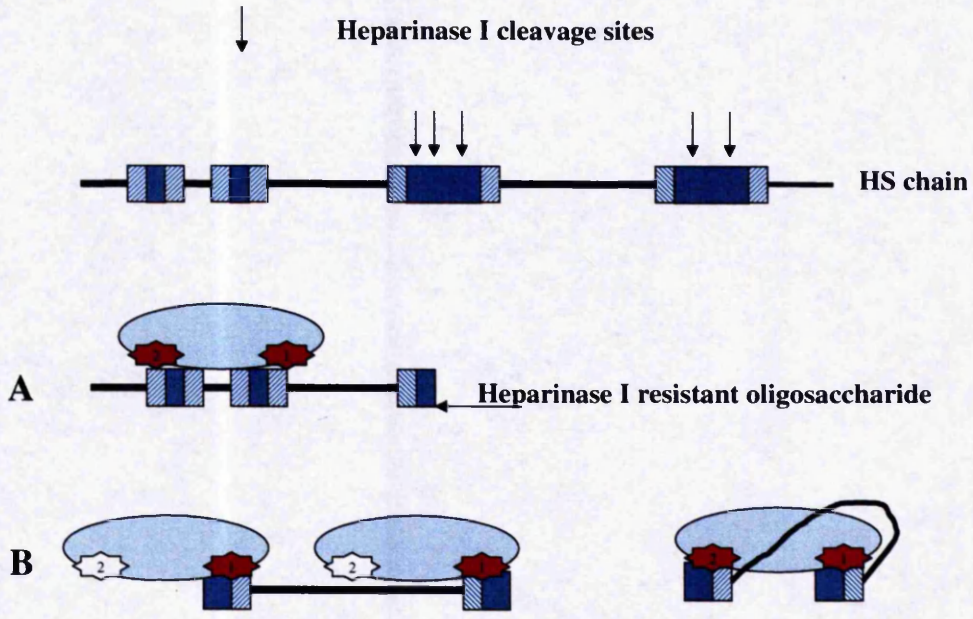

Figure 7.5 : Models of the interaction between endostatin and heparinase I resistant oligosaccharides. **A**, interaction of one endostatin molecule with a heparinase I resistant oligosaccharide in which short sulphated disaccharide sequences cluster to approximate a 'split' S-domain of dp10/12. **B** : Short sequences of sulphated disaccharides at both ends of the oligosaccahride may induce dimerisation of endostatin or wrap round one endostatin molecule, due to the flexibility conferred by the long N-acetylated region, to engage both binding sites. Solid blue rectangles = S-domains, hashed blue rectangles = transition zones.

hexasaccharides in the correct orientation for binding. Alternatively 6-O-sulphated GlcNAc in the transition zones may also play an important role in strengthening the HS-endostatin interaction.

An important factor in the interpretation of these data is the arrangement of the sulphated disaccharides within the heparinase I resistant oligosaccharides and work is in progress to obtain sufficient quantities of material for this analysis. There are at least two possibilities that are represented in Figure 7.5. First, the sulphated disaccharides may cluster in the oligosaccharide and approximate a sulphated domain of dp10/12 with a short central N-acetylated region. This type of oligosaccharide was proposed by Sasaki *et al.*,1998 as a candidate recognition sequence. Interestingly, short S-domains that were in close proximity (termed split S-domains), were observed at either end of 3T3 fibroblast HS oligosaccharides that bound to PF4 (Stringer & Gallagher, 1997b) (Table 1.5, Figure 1.6). Alternatively, the sulphated disaccharides may be located at both ends of the oligosaccharides. The allowed rotations about a glycosidic linkage are much more limited than the rotations that can occur at peptide linkages, *ie* the heparin chains are quite linear, with limited bending possible (Mulloy & Forster, 2000). Although the degree of bending of the chain is not easily deduced from contour plots it has been estimated that, in order to bend 180° and go back in the opposite direction, a heparin sequence must be more than 20 disaccharides long ie the bend at each glycosidic bond is less than 4-5°. Since greater degrees of rotational freedom are observed for the GlcA-containing disaccharides than for the Ido A- containing disaccharides, fewer GlcA-containing disaccharides may be required for a similar 180° bend (Conrad, 1998; Mulloy & Forster, 2000). The estimated length of ~ 30 disaccharides for the heparinase I resistant oligosaccharides with highest affinity for HEM may enable a conformation in which the oligosaccharide wraps around one or two endostatin molecules with each sulphated end engaging either a primary or secondary heparin binding domain on the protein (Figure 7.5).

Importantly, neither the S-domains, nor the heparinase I resistant fragments, exactly reproduce the affinity of the intact chains so it is possible that both provide a component of the optimal recognition site for endostatin. For example, the optimal site may involve the transition zone and extend into the S-domain. If so, both heparinase I and heparinse III would cut into the optimal binding site. In theory a 'protection' or

'fingerprinting' assay (Lortat-Jacob *et al.*, 1995; Stringer & Gallagher, 1997b) would be required to investigate this possibility but the significantly higher affinity of the bacterial heparinases for HS compared to endostatin has, so far, precluded this approach. Alternatively, as suggested by crosslinking studies, the relatively increased affinity of the intact chains may be due to increased probability of oligomerisation of HEM. In addition, excised HS oligosaccharides may adopt conformations that are less constrained, and therefore more easily dissociated from endostatin, compared to their *in situ* counterparts. An attractive approach would be to adapt the zero length crosslinking strategy to identify the optimal HS recognition sequence but there is currently no method to reverse the amide bond and recover crosslinked GAG from the protein for structural analysis.

Implications for the activity of mammalian heparanase

An important consideration from our data is that the mammalian heparanase enzyme is thought to cleave in the transition zone immediately preceding an S-domain, resulting in 7kDa fragments that have features in common with both the heparinase I, and heparinase III resistant oligosaccharides. The products generated by mammalian heparanase are not as well defined as those from the bacterial heparinases but are thought to comprise a non-reducing end S-domain linked to an intact transition zone then an N-acetylated sequence and finally a transition zone at the reducing end (Pikas *et al.*, 1998). As discussed previously, heparanase enzymes act in concert with proteases to degrade the ECM and in cancer, this is believed to facilitate angiogenesis, invasion and metastases (Vlodavsky *et al.*, 1999). There are an increasing number of reports that these proteases liberate cryptic antiangiogenic proteins. In addition to endostatin from collagen XVIII (O'Reilly *et al.*, 1997), restin is cleaved from collagen XV (Ramchandran *et al.*, 1999) and arresten from collagen IV (Colorado *et al.*, 2000). However, if the proteases and heparanases are proangiogenic, there must be a mechanism to suppress the activities of the antiangiogenic proteins that are released.

Although heparanase is believed to liberate heparin-binding growth factors and oligosaccharides that activate the stimulators of angiogenesis (Kato *et al.*, 1998) it is possible that antiangiogenic proteins with heparin binding ability, and particularly those with affinity for the transition zones, may be inactivated by heparanase. TSP-1 is thought to bind optimally to saccharides of dp12-14 predominantly as a function of

increased overall charge density and with a preference for 6-O-sulphate in the trisulphated disaccharide (Feitsma *et al.*, 2000). It is not known whether TSP-1 can also bind heparinase I resistant oligosaccharides. However, alternating GlcNAc-GlcNS containing disaccharides were noted in a proportion of long (dp12) S-domains derived from porcine aortic HS with affinity for TSP-1, suggesting that the transition zones may also play a role in the recognition of this angiogenic inhibitor. The recent cloning and availability of recombinant mammalian heparanase (Hulett *et al.*, 1999; McKenzie *et al.*, 2000; Vlodavsky *et al.*, 1999) combined with functional assays (discussed later) should now enable examination of the interaction between naturally occuring angiogenic regulators and biologically relevant oligosaccharides liberated from HS *in vivo*.

6-O-sulphate versus 2-O-sulphate ?

To unravel the role of 6-O-sulphate compared to 2-O-sulphate, a range of chemically desulphated heparin and HS species were tested for ability to compete with HMVEC and BAEC HS for HEM. The interpretation of this competition data is potentially complicated by several factors. Firstly, it is difficult to distinguish the effect of charge over specificity for a protein with moderate affinity for HS. In this study, the radiolabelled EC HS used was of significantly lower charge (~ 0.6 sulphates/disaccharide) than the bovine lung heparin, CS, DS, or mucosal HS used in competition assays (Table 6.4). Secondly, the chemical desulphations may be incomplete. For example, the 6-O-desulphated HS still retained approximately half of its 6-O-sulphate groups . Thirdly, the desulphation may not be specific. For example, loss of ~17% of the 6-O-sulphate groups has been reported in 2-O-desulphated heparin (Sasaki *et al.*, 1998) which may have a significant impact if the positions of sulphate groups, rather than absolute content, are important. In view of these limitations, and constraints in supply of materials, we did not perform extensive analyses with chemically modified heparin and HS species.

Competition with chemically modified HS

Nevertheless, our experiments suggested that all the sulphate groups, but particularly 6-O-sulphate, were important for binding. Loss of 6-O-sulphate dramatically reduced the competitive ability of this HS compared to unmodified porcine mucosal HS (Figure 6.21) and to 2-O-desulphated HS. The 2-O-desulphated and 6-O-desulphated HS used

in this investigation were of equivalent charge (both ~0.68 sulphates/disaccharide) to HMVEC ^{3}H-HS again suggesting that charge is not the sole determinant of binding between HS and endostatin. Furthermore, in the 6-O-desulphated HS ~ 45% of the 6-O-sulphate groups were still present, strengthening the potential importance of location, rather than the absolute number, of these groups within the binding site. The N-desulphated HS was also a poor competitor suggesting an integral role for this modification in addition to 6-O-sulphate. Although the 2-O-desulphated HS was a better competitor than the N-desulphated and 6-O-desulphated HS, it was inferior to the intact porcine mucosal HS suggesting that this modification also has a role (see below). The equivalent inhibition of binding by CS type C (enriched in 6-O-sulphates) is intriguing and may indicate a role for this GAG in the regulation of endostatin. Although the ability of CS to compete may be explained in part by charge, this is offset by the decreased competition of DS that has a similar charge, but is predominantly composed of IdoA(2S) and 4-O-sulphated disaccharides with a minor proportion of 6-O-sulphate. There are recent reports of biologically significant interactions between heparin binding proteins and GAGs other than HS. For example, an interaction between midkine and CS type E is important for neuronal cell adhesion *in vitro* (Ueoka *et al.*, 2000); and DS has affinity for HGF (Lyon *et al.*, 1998) and IL12 (Hasan *et al.*, 1999). Indeed, substitution of HS by other GAGs has been proposed to explain the functions of some heparin dependent ligands that are apparently unaffected in genetic mutants with defective HS synthesis (Selleck, 2001). For example, bFGF may exploit the 2-O-sulphated iduronates that reside in DS for some of its activites (Selleck, 2001). This may reflect an evolved back up mechanism to ensure alternative paths for heparin binding ligands in processes such as embryogenesis, development and morphogenesis.

Binding does not strictly require 2-O-sulphate groups

The cloning of HS biosynthetic enzymes has provided a molecular tool by which to overcome problems inherent with competition studies and chemical desulphation of GAGs. We observed identical affinity of HS derived from fibroblasts of 2-O-sulphotransferase knockout mice (Bullock *et al.*,1998), completely deficient in 2-O-sulphate groups (Merry *et al.*, 2001) for HEM and HED compared to the wild type. This provides direct evidence that binding between HS and HEM, unlike bFGF (Turnbull *et al.*,1992), does not strictly require 2-O-sulphate groups. Significantly, characterisation of the 2OST mutant fibroblast HS has revealed that compensatory

mechanisms for loss of 2-O-sulphation occur. There is an increase of 6-O-sulphation and N-sulphation, with longer S-domains compared to the wild type, and this maintains the overall charge density of the mutant HS (Merry *et al.*,submitted). Thus, the contribution of charge compared to specific sulphate groups for affinity to HEM and HED cannot be dissected using these HS species. However, it is GlcNS(6S) that is increased in the mutant HS and the level of GlcNAc(6S) in the transition zones is not affected. If this latter region is important for recognition of HEM then this may partly explain why the affinities were identical. It is not possible to selectively 6-O-desulphate GlcNS rather than GlcNAc containing disaccharides but characterisation of the substrate specificities of the 6OST isoenzymes should eventually enable selective modification of 6-O-sulphated disaccharides and aid identification of essential substitutions for protein recognition.

Our findings favour 6-O-sulphate and N-sulphate as more important binding determinants for endostatin than 2-O-sulphate. Sasaki *et al.*,1999, demonstrated a requirement for 6-O-sulphate groups in chemically-modified, heparin-derived dodecasaccharides using endostatin affinity chromatography and the affinity of chemically 2-O-desulphated dodecasaccharides was decreased to an equivalent degree. Again, this may reflect the structure of heparin rather than HS. Also, there was loss of a minor proportion (up to 30%) of either 2-O-sulphate or 6-O-sulphate groups, respectively, in addition to the selected modifications (Sasaki *et al.*, 1999) creating difficulties in interpretation as outlined above.

Endostatin was recently claimed to bind with significantly reduced affinity to HS synthesised by endothelial cells in which 2-O-sulphotransferase was inhibited by antisense (Karumanchi *et al.*, 2001). One caveat in the interpretation of these data is that the authors did not specify whether other HS modifications were affected, either by the 2OST antisense or by compensatory mechanisms of the other HS modifying enzymes. However, it could be argued that a critical level of sulphation may be necessary for binding that does not depend on particular functional groups. Specific groups such as the 6-O-sulphates may act to strengthen binding on a background of 'generic' sulphation. This has been noted for the interaction between the hep 2 domain of fibronectin and HS, where 2-O-sulphate groups appear more important than 6-O-sulphate groups provided that a critical threshold of sulphate groups (N, 2-O, and 6-O)

is exceeded (Lyon *et al.*,2000). Thus, loss of 2-O-sulphation by antisense may significantly reduce the overall charge of the HS, and compensatory mechanisms may not occur as observed in the *Hs2st*$^{-/-}$ mouse. Another theory is that the loss of 2-O-sulphate groups may alter the presentation of 6-O-sulphate groups for binding. This has been proposed as a role for 2-O-sulphation in the binding of HS to TSP1 (Feitsma *et al.*, 2000), is consistent with our competition data for de 2-O-sulphated HS, and may explain why additional 6-O-sulphate groups of the *Hs2st*$^{-/-}$ HS are unable to sustain stronger binding than the wild type. However, with the exception of de N-desulphated, N-reacetylated heparin, the solution conformations of chemically modified heparins are similar (Mulloy *et al.*, 1994), but this may not be the case for HS. In addition, small changes in conformation may have a greater impact at the GAG – protein interface in an interaction of moderate affinity.

Structure – activity relationships

The HS binding site for HEM involves a structural motif that does not appear to be confined to the longest S-domains unlike, for example, bFGF (Turnbull *et al.*, 1992), and fibronectin (Lyon *et al.*, 2000) nor dependent on the long composite domains that bind IL8 (Spillmann *et al.*, 1998), or PF4 (Stringer & Gallagher, 1997b). Significantly, 2-O-sulphate is not essential for binding arguing against direct competition between endostatin and bFGF for the same recognition sequence as a mechanism of action. Also, there are indications from the heparinase I resistant oligosaccharides, S-domain analyses and competition studies that the arrangement of sulphated disaccharides (substituted with 6-O-sulphate) may be more important than overall charge and the transition zones may provide an important structural motif. Finally, crosslinking studies suggest a role for heparin/HS in the 'pseudo-dimerisation' of HEM and that the interaction between HS and HED differs from that of its monomeric counterpart due to a conformational change.

Following the initial identification of a high affinity binding sequence for bFGF that lacked essential structural determinants for activation of signalling receptors, it is clear that affinity of a protein for a GAG does not imply activity (Pye *et al.*, 1998; Turnbull *et al.*, 1992). Also, for ATIII, the ability to test anticoagulant activity *in vitro* was vital to detect a highly specific but rare structural motif within heparin and HS (Conrad, 1998). The role of HS in the activity of endostatin remains uncertain and may differ for

oligomeric forms. In addition, there is some evidence that the HS chains of glypican (rather than syndecan) specifically mediate binding to endostatin (Karumanchi *et al.*, 2001). An early observation in our study was the ability of a subset of HS chains to bind endostatin with increased affinity (Figure 6.3). This may indicate a variation in fine structure of HS chains peculiar to one core protein although to date, there is little evidence that this occurs for any of the other heparin-binding proteins (Bernfield *et al.*, 1999). Indeed, it is only a minor proportion of HS or heparin chains that are anticoagulantly active due to the presence of the rare ATIII binding pentasaccharide but in a study of rat EC HS, the anticoagulantly active chains could not be ascribed to an individual core protein (Kojima *et al.*, 1992). It is therefore essential to develop approaches by which the functions of HSPGs, HS oligosaccharides and other GAGs such as CS, with affinity for endostatin, can be tested for function.

Future work

There are several problems to be overcome in the development of bioassays to test HS oligosaccharides for activity. For bFGF, the use of cells either denuded of surface HS by treatment with sodium chlorate, that prevents incorporation of sulphate into HS (Olwin & Rapraeger, 1992) or cells phenotypically deficient in HS, and transfected with FGFR (Pye *et al.*,1998) enabled saccharides of known structure and size to be characterised for activity. However, HEM inhibits bFGF induced endothelial cell proliferation, so any proliferative assay must enable a normal response to bFGF ie, have HS present. Also, ECs are often intolerant of chlorate treatment (P Hyde, personal communication), and sulphation may not be completely blocked by this method (Safaiyan *et al.*, 1999).

We have replicated the effects of HEM and HED in the *in vitro* morphogenesis assay of Kuo *et al.*,2001 that is currently the most promising bioassay to adopt. In this assay, the morphological effects of endostatin are observed in cells cultured on the complex substratum, matrigel (Figure 6.28). Matrigel is enriched in matrix proteins such as fibrin, collagen I, laminin, soluble growth factors and perlecan. The effects of the endostatin dimer do not occur on plastic so an important cofactor for HED is assumed to be present in matrigel although its identity remains elusive. So far, fibrin and collagen I have been excluded (Kuo *et al.*,2001) and through our collaboration with K Javaherian, we are testing perlecan. Studies have also been initiated to test the ability of

exogenously added heparin and HS to modulate the activity of HEM and HED in the morphogenesis assay. As a parallel strategy, we are examining the effect of HED on genetically modified Chinese hamster ovary (CHO) cells, plated on matrigel, that are either totally deficient in HS (CHO 745), or lack specific HS modifications compared to the wild type cells (CHOK-1) (Murphy-Ullrich *et al.*, 1988). Our preliminary observations have revealed a role for cell surface HS in the regulation of HED (see Appendix 2). In addition the activity of HED in the morphogenesis assay can be restored in CHO 745 cells by addition of low concentrations of exogenous heparin, whereas high concentrations of heparin inhibit the effects of HED on CHOK-1 and BAEC (data not shown). Further studies are underway to check the validity of these data.

The use of a zero length crosslinking technique has been succesful in demonstrating formation of covalent conjugates but difficulties in obtaining sufficient yields and purified conjugates for bioassays have to be addressed. Higher yields may be achieved by altering the GAG-protein ratios in the initial incubation. The issue of purification is more problematic. It is necessary to consider that the crosslinked proteins need to be separated from free GAG and protein. Potential strategies to improve purification include reverse phase HPLC, size exclusion HPLC, heparin affinity as reported here, DEAE-anion exchange chromatography and immunoprecipitation with mAb 12C1. Once these problems have been solved it will be particularly interesting to test the bioactivity of HED crosslinked to heparin/dp12, to determine whether a functionally important conformational change has occurred. An important consideration is that endostatin is currently undergoing evaluation for therapeutic use. At present, endostatin is administered by daily injection as a recombinant protein but strategies to prolong its activity and optimise its delivery are actively sought (Blezinger *et al.*, 1999; Chen *et al.*, 2000; Chen *et al.*, 1999; Ding *et al.*, 2001; Joki *et al.*, 2001). Heparin has been known to stabilise proteins such as bFGF for many years (Saksela *et al.*, 1988). Therefore, covalent crosslinking of GAG may protect endostatin from proteolytic degradation and provide a relatively cheap method to extend the bioavailability of this protein *in vivo*. Thus, the focus of future studies will be to explore the modulation of endostatin monomer and dimer by soluble and covalently complexed heparin/HS in bioassays that mimic different aspects of angiogenesis.

8. CONCLUSIONS

This thesis describes novel data on the structure of HS synthesised by human microvessel endothelial cells (HMVEC) and features that are important for binding to the potent angiogenic inhibitor, endostatin. The structure-function relationships between many proteins and HS have been viewed as relatively non-specific, with the GAGs likened to 'extracellular fly paper' attracting proteins by virtue of anionic charge (Perrimon & Bernfield, 2000). However, it is argued that HS-protein interactions are based on an evolutionarily conserved extracellular code (Woopark *et al.*,2000; Bernfield *et al*, 1999). This is consistent with the prevalence and diversity of proteins that bind heparin/HS, and the role of these proteins in fundamental processes such as morphogenesis, wound repair, host defense, and energy metabolism (Gerhart & Kirschner, 1997). In addition, biochemical and cell-culture evidence from several decades has indicated a specific role for HS/heparin in the functions of proteins. An early discovery was a requirement for a specific pentasaccharide sequence within heparin/HS for the activation of ATIII (Lindahl *et al.*, 1984). Cell culture studies at the beginning of the last decade then suggested an essential co-receptor function for HS in the activation of bFGF (Rapraeger *et al.*, 1991; Yayon *et al.*, 1991). More recently, genetic models bearing mutations in biosynthetic enzymes, have revealed dedicated functions for HSPGs in specific signalling pathways involved in cell differentiation and morphogenesis (Selleck, 2000).

HS is widely expressed in mammalian tissues. Although it is structurally heterogeneous, consistent but subtle variations in its design, depending on the cell or tissue type of origin, support a non-random element in its synthesis. This is substantiated by our analyses of EC HS. All exhibited the characteristic domain structure that distinguishes HS from heparin, with fine structural variation. The conservation of a proportion of S-domains has not been reported previously and is intriguing. Perhaps these conserved sequences are for a common function, or are 'universal' binding sequences with low specificity to concentrate, sequester and establish diffusion gradients of ligands. The variations unique to each HS form are generally believed to equip cells with the binding sequences necessary to regulate ligands. The heparin binding angiogenic regulators usually require oligosaccharides of >dp6 for optimal affinity or activity in addition to rarer modifications such as 6-O-

sulphation, and the most modified trisulphated disaccharide, [UA(2S)-GlcNS(6S)] (Table 1.5). The relatively low abundance of longer S-domains and sparing distribution of 6-O-sulphates in only a proportion of each size class of S-domain in EC HS may reflect tight regulation necessary to coordinate cellular responses, specifically within the vasculature, to pro- and anti-angiogenic proteins.

As is the case for other regulators of angiogenesis, binding of endostatin to HS does not appear to be mediated through unusual sequences such as the pentasaccharide that binds to ATIII, although functional studies may enable further refinement of the HS-recognition motif. Endostatin binds in physiological conditions to sequences of at least 5-6 repeating disaccharide units with a preference for 6-O-sulphation and the trisulphated disaccharide [UA(2S)-GlcNS(6S)]. In general, more highly sulphated S-domains bind with greater affinity but overall charge of these oligosaccharides does not appear to be the exclusive driving force. The ability of less sulphated heparinase I resistant fragments to bind strongly to endostatin suggests that there may be structurally redundant sulphate groups within the S-domains. Thus the more highly modified S-domains have a greater chance of containing sulphate groups in the correct positions. An alternative possibility is that endostatin recognises different motifs with variable affinity. This may be important at the level of the parent chains for the capture and docking of endostatin onto its favoured binding site. Of the HS modifications, 2-O-sulphation is not strictly essential but may contribute to a general charge based affinity, or to the correct conformation of the saccharide. In contrast 6-O-sulphation may confer specificity to the interaction and the contribution of the transition zones that contain [UA-GlcNAc(6S)] in the heparinase I resistant oligosaccharides requires further investigation.

The anti-angiogenic matrix proteins fibronectin and TSP-1 exhibit some similar HS binding characteristics to ES (discussed in chapter 7, and see Table 1.5). These proteins are believed to bind optimally to saccharides of dp12-14 predominantly as a function of increased overall charge density; 6-O-sulphate and the trisulphated disaccharide [UA(2S)-GlcNS(6S)] correlate with stronger binding (Feitsma *et al.*, 2000; Lyon *et al.*, 2000). However, there are distinctions in that 2-O-sulphate is more important than 6-O-sulphate for the affinity of fibronectin to HS (Lyon *et al.*,2000), whereas the converse is true for TSP-1 (Feitsma *et al.*,2000). As intimated by our data the bFGF and endostatin

binding epitopes within HS also appear to be distinct although endostatin may compete with the 6-O-sulphate(s) assumed to be required for formation of the FGF/FGFR trimolecular signalling assembly (Pye *et al.*, 1998).

In considering the coordination of angiogenesis by HS several questions arise. It is well known that HS can approximate one protein (ATIII) to another (thrombin) thereby achieving enhanced biological effect by greatly accelerating the rate of complex formation. However the possibility that several angiogenic regulators may bind a single HS chain simultaneously has received little attention. Also, PF4 binds directly to bFGF (Perollet *et al.*, 1998); and TSP-1 binds to HIV-TAT protein (Rusnati *et al.*, 2000) and bFGF (Taraboletti *et al.*, 1997). Although heparin can inhibit these protein-protein interactions *in vitro* it is not known whether HS modulates these associations *in vivo.* Although endostatin and bFGF have not been shown to bind each other directly, it is feasible, from their HS binding chracteristics, that they could bind to different sites in the same HS chain and it is not known what the net cellular effect of this would be. A further question is to what extent endothelial cells can modulate their HS structure, over what time scale, and in response to changes in environmental conditions? Several reports describe altered composition of HS during development (Nurcombe *et al.*, 1993), differentiation (Salmivirta *et al.*, 1998), transformation (Jayson *et al.*, 1998; Winterbourne & Mora, 1981), and ageing (Feyzi *et al.*, 1998). Thus, ECs recruited in new vessel formation may enhance modifications necessary for activation of angiogenic stimulators. Indeed, the relatively low level of sulphation present in the EC species examined in this study may in part reflect downregulation of structural motifs due to the abundant growth factors present in the culture medium.

Importantly, it remains unclear as to whether all proteins that interact with HS require an 'optimal' saccharide sequence. As illustrated by ATIII, and suggested by the phenotypes of genetic models with defective HS biosynthesis, there are clearly proteins with specific requirements (Conrad, 1998; Selleck, 2001; Stickens *et al.*, 2000). However other ligands may have less stringent requirements that are, nevertheless, equally essential for their biological roles. Endostatin, together with fibronectin and TSP-1, may fall into the latter category and studies to examine the structure-activity relationships are now mandatory to further define the GAG-endostatin interaction.

The HS 'code' has been likened to that for RNA in that it is degenerate, redundant, and sequence specific (WooPark *et al.*, 2000). In contrast to analysis of RNA, it is not possible to amplify HS oligosaccharides to obtain quantitative and qualitative differences in expression of bioactive sequences. However recent years have witnessed significant advances in techniques to study the structure-activity relationships of HSPGs that should increase momentum in defining their roles. Developmental genetic studies, and manipulation of genes encoding biosynthetic enzymes for HS have accelerated functional analysis of HSPGs. The availability of recombinant exoenzymes, used in the treatment of inherited mucopolysaccharidoses (Hopwood, 1989), has inspired various techniques sensitive enough to reveal the exact order and composition of monosaccharides within an HS sequence of interest akin to DNA or peptide sequencing (Merry *et al.*,1999; Turnbull *et al.*,1999; Vives *et al.*,1999). The application of phage display technology has generated new antibodies that may be capable of discriminating distinct HS epitopes, such as that for bFGF (van Kuppevelt *et al.*,1998) and novel functional assays are emerging to detect the ability of HSPGs to form signalling complexes *in situ* (Chang *et al.*, 2000). Finally, the long sought after heparanase enzymes have been cloned and assays for their activity are becoming available (Hulett *et al.*, 1999; McKenzie *et al.*, 2000; Vlodavsky *et al.*, 1999).

There is accumulating evidence that HSPGs play pivotal roles in angiogenesis, co-ordinating and directing appropriate responses to multiple angiogenic stimulators and inhibitors. The natural mechanisms regulating their activities in endothelial cells may be exploited by cancer cells that liberate varying cocktails of growth factors, cytokines, proteases and heparanase(s). The clinical success of heparin has prompted the development of HS and ectodomain 'mimics' to antagonise HB growth factors and heparanase(s) (Jayson *et al.*, 1997; Parish *et al.*, 1999). However, in view of the tissue specific and multifaceted interactions of HSPGs, caution is required to avoid promoting unwanted ligand interactions caused by HS(PG) mimics that lack sufficient specificity. In particular, the naturally occuring inhibitors of angiogenesis may be particularly vulnerable to antagonism due to their less stringent binding requirements.

The present challenge is to combine the recent advances in genetic, molecular, biochemical and immunological tools to unravel the HS code and identify novel targets for 'safe' therapeutic control. To this end, the detailed characterisation of HS

recognition sites for proteins is a prerequisite. Structural motifs within HS that bind endostatin are presented in this thesis that will provide a basis from which to address structure-activity relationships. As witnessed for other heparin-binding proteins such as ATIII and bFGF, it is likely that this, and future studies, will not only bring new insights for the control of endostatin, but also extend our understanding of the role HS plays in the regulation of angiogenesis.

Sequences from 3T3 Heparan Sulphate solved using step sequencing

ΔUA-GlcNS-IdoA(2S)-GlcNS-IdoA-GlcNAc	6A
ΔUA-GlcNS-IdoA(2S)-GlcNS-GlcA-GlcNAc	6B
ΔUA-GlcNS-IdoA(2S)-GlcNS-IdoA(2S)-GlcNAc	6C
ΔUA-GlcNS-IdoA(2S)-GlcNS(6S)-IdoA-GlcNAc	6D
ΔUA-GlcNS-IdoA(2S)-GlcNS-IdoA(2S)-GlcNS-IdoA-GlcNAc	8A
ΔUA-GlcNS-IdoA(2S)-GlcNS-IdoA(2S)-GlcNS-GlcA-GlcNAc	8B
ΔUA-GlcNS-IdoA(2S)-GlcNS-IdoA(2S)-GlcNS-IdoA(2S)-GlcNAc	8C
ΔUA-GlcNS-IdoA(2S)-GlcNS(6S)-IdoA(2S)-GlcNS-IdoA-GlcNAc	8D
ΔUA-GlcNS-IdoA(2S)-GlcNS(6S)-IdoA(2S)-GlcNS-GlcA-GlcNAc	8E
ΔUA-GlcNS-IdoA(2S)-GlcNS(6S)-IdoA(2S)-GlcNS-IdoA(2S)-GlcNAc	8F
ΔUA-GlcNS-IdoA(2S)-GlcNS-IdoA(2S)-GlcNS-IdoA(2S)-GlcNS-IdoA-GlcNAc	10A
ΔUA-GlcNS-IdoA(2S)-GlcNS-IdoA(2S)-GlcNS(6S)-IdoA(2S)-GlcNS-IdoA-GlcNAc	10C

Appendix 1: S-domains excised from 3T3 HS with heparinase III and sequenced using step sequencing (Merry et al., 1999). A proportion of these (6B, 8B and 8E) contain a GlcA residue as part of their reducing-end disaccharide. This demonstrates that heparinase III does not cleave all potential (GlcNAc/S ±6S-GlcA) digestion sites within the HS chain.

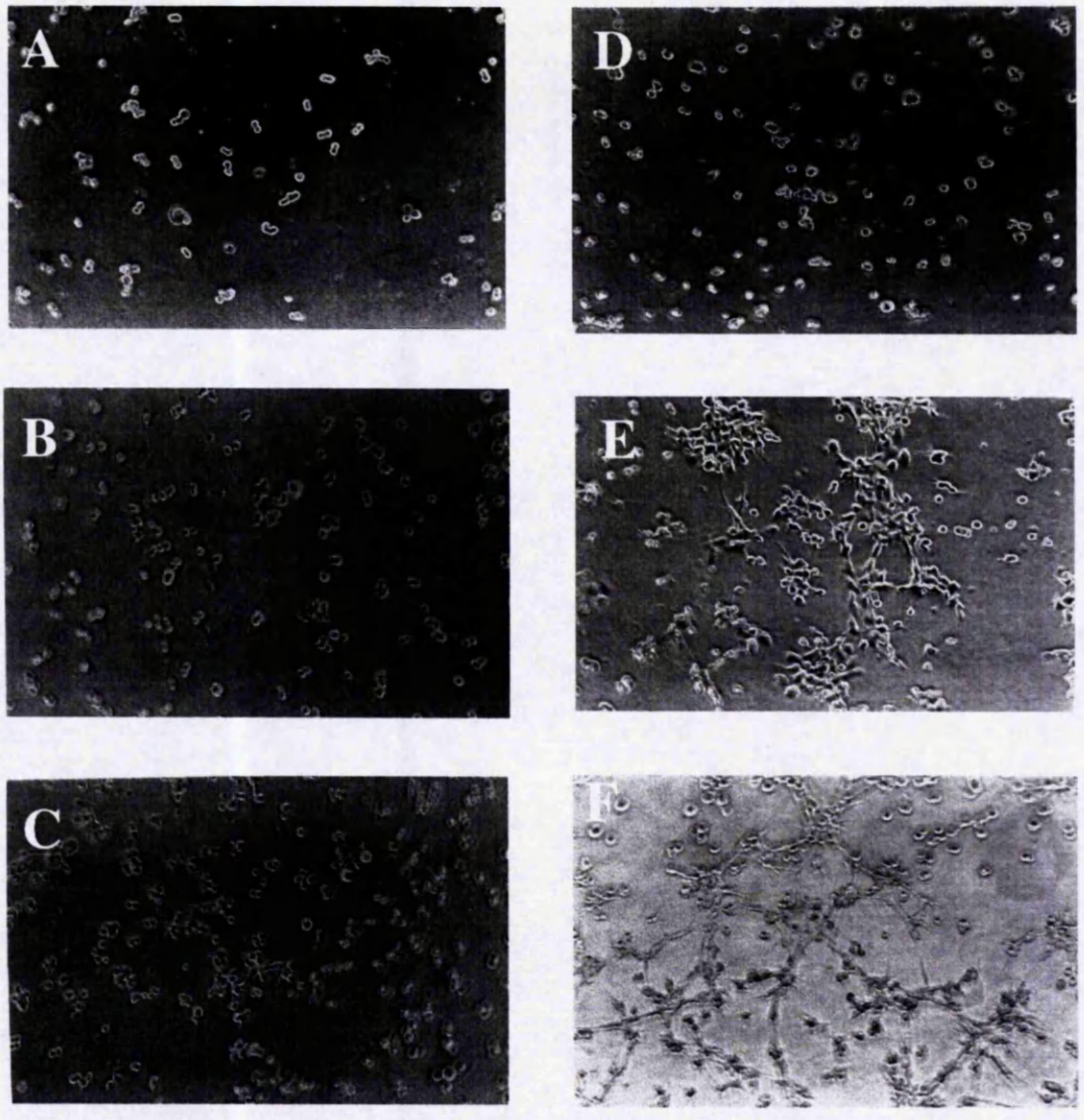

Appendix 2 : The role of cell surface HS in the modulation of endostatin dimer. Cells were plated on matrigel as described for the matrigel tube forming / morphogenesis assay. Panels A,B and C show CHO 745 cells that are deficient in GAGs and panels D,E and F show CHOK-1 (wild type cells). Panels A and D show positive controls with no added dimer, after 16 hours. Panels B and C, and E and F, show the cells at 16 hours and 24 hours, respectively after addition of dimer at the time of plating. Results from three independent experiments, each performed in triplicate are shown.

REFERENCES

Abe, N., Muragaki, Y., Yoshioka, H., Inoue, H. & Ninomiya, Y. (1993). Identification of a novel collagen chain represented by extensive interruptions in the triple-helical region. *Biochem Biophys Res Commun*, 196, 576-582.

Ackley, B.D., Crew, J.R., Elamaa, H., Pihlajaniemi, T., Kuo, C.J. & Kramer, J.M. (2001). The NC1/Endostatin Domain of Caenorhabditis elegans Type XVIII Collagen Affects Cell Migration and Axon Guidance. *J Cell Biol*, 152, 1219-1232.

Adiata, R., Albini, A., Carlone, S., Giunciuglio, D., Benelli, R., Santi, L. & Noonan, D. (1998). Suppression of invasive behaviour of melanoma cells by stable expression of anti-sense perlecan cDNA. *Ann Oncol*, 8, 1257-1261.

Aikawa, J.-i. & Esko, J.D. (1999). Molecular cloning and expression of a third member of the heparan sulfate/heparin GlcNAc N-Deacetylase/N-sulfotransferase family. *J Biol Chem*, 274, 2690-2695.

Albini, A., Benelli, R., Presta, M., Rusnati, M., Ziche, M., Rubartelli, A., Paglialunga, G., Bussolino, F. & Noonan, D. (1996). HIV-tat protein is a heparin-binding angiogenic growth factor. *Oncogene*, 12, 289-297.

Alexander, C., Reichsman, F., Hinkes, M., Lincecum, J., Becker, K., Cumberledge, S. & Bernfield, M. (2000). Syndecan-1 is required for Wnt-1 induced mammary tumorigenesis in mice. *Nat Genet*, 25, 329-332.

Algire, G. & Chalkley, H. (1945). Vascular reactions of normal and malignant tissues in vivo. I. Vascular reactions or mice to wounds and to normal and neoplastic transplants. *J Natl Cancer Inst, USA*, 6, 73-85.

Anderson, K.V. (1998). Pinning down positional information: Dorsal-ventral polarity in the *Drosophila* Embryo. *Cell*, 95, 439-442.

Andres, J., DeFalcis, D., Noda, M. & Massague, J. (1992). Binding of two growth factor families to separate domains of the proteoglycan betaglycan. *J Biol Chem*, 267, 5927-5930.

Aviezer, D., Hecht, D., Safran, M., Elsinger, M., David, G. & Yayon, A. (1994a). Perlecan, basal lamina proteoglycan, promotes basic fibroblast growth factor-receptor binding, mitogenesis, and angiogenesis. *Cell*, 79, 1005-1013.

Aviezer, D., Iozzo, R., Noonan, D. & Yayon, A. (1997). Suppression of autocrine and paracrine functions of basic fibroblast growth factor by stable expression of perlecan antisense cDNA. *Mol Cell Biol*, 17, 1938-1946.

Aviezer, D., Levy, E., Safran, M., Svahn, C., Buddecke, E., Scmidt, A., David, G., Vlodavsky, I. & Yayon, A. (1994b). Differential structural requirements of heparin and heparan sulphate proteoglycans that promote binding of basic fibroblast growth factor to its receptor. *J Biol Chem*, 269, 114-121.

Azizkhan, R., Azizkhan, J., Zetter, B. & Folkman, J. (1980). Mast cell heparin stimulates migration of capillary endothelial cells in vitro. *J Exp Med*, 152, 931-944.

Bame, K., Hassall, A., Sanderson, C., Venkatesan, I. & Sun, C. (1998). Partial purification of heparanse activities in chinese hamster ovary cells: evidence for multiple intracellular heparanases. *Biochem J*, 336, 191-200.

Bernfield, M., Gotte, M., Park, P., Reizes, O., Fitzgerald, M., Lincecum, J. & Zako, M. (1999). Functions of cell surface heparan sulfate proteoglycans. *Annu Rev Biochem*, 68, 729-777.

Bernfield, M., Kokenyesi, R., Kato, M., Hinkes, M., Spring, J., Gallo, R. & Lose, E. (1992). Biology of the syndecans: A family of transmembrane heparan sulphate proteoglycans. *Annu Rev Cell Biol*, 8, 365-393.

Bhanot, P., Brink, M., Samos, C., Hsieh, J., Wang, Y., Macke, J., Andrew, D., Nathans, J. & Nusse, R. (1996). A new member of the frizzled family from *Drosophila* functions as a Wingless receptor. *Nature*, 382, 225-230.

Bielicki, J., Hopwood, J., Wilson, P. & Anson, D. (1993). Recombinant human iduronate-2-sulphatase; correction of mucopolysaccharidosis-type II fibroblasts and characterization of the purified enzyme. *Biochem J*, 289, 241-246.

Bienkowski, M.J. & Conrad, H.E. (1985). Structural characterization of the oligosaccharides formed by depolymerisation of heparin with nitrous acid. *J Biol Chem*, 260, 356-365.

Binari, R.C., Staveley, B.E., Johnson, W.A., Godavarti, R., Sasisekharan, R. & Manoukian, A.S. (1997). Genetic evidence that heparin-like glycosaminoglycans are involved in *wingless* signaling. *Development*, 124, 2623-2632.

Blackhall, F., Merry, C., Davies, E. & Jayson, G. (2001). Heparan sulphate proteoglycans and cancer. *British Journal of Cancer*, In press.

Blezinger, P., Wang, J., Gondo, M., Quezada, A., Mehrens, D., French, M., Singhal, A., Sullivan, S., Rolland, A., Ralston, R. & Min, W. (1999). Systemic inhibition of tumor growth and tumor metastases by intramuscular administration of the endostatin gene. *Nat Biotechnol*, 17, 343-8.

Boehm, T., Folkman, J., Browder, T. & O'Reilly, M. (1997). Antiangiogenic therapy of experimental cancer does not induce acquired drug resistance. *Nature*, 390, 404-407.

Boehm, T., O'Reilly, M., Keough, K., Shiloach, J., Shapiro, R. & Folkman, J. (1998). Zinc-binding of endostatin is essential for its antiangiogenic activity. *Biochem Biophys Res Commun*, 252, 190-194.

Bonneh-Barkay, D., Shlissel, M., Berman, B., Shaoul, E., Admon, A., Vlodavsky, I., Carey, D., Asundi, V., Reich-Slotky, R. & Ron, D. (1997). Identification of glypican as a dual modulator of the biological activity of fibroblast growth factors. *J Biol Chem*, 272, 12415-12421.

Bullock, S.L., Fletcher, J.M., Beddington, R.S.P. & Wilson, V.A. (1998). Renal agenesis in mice homozygous for a gene trap mutation in the gene encoding heparan sulfate 2-sulfotransferase. *Genes & Development*, 12, 1894-1906.

Cano-Gauci, D.F., Song, H.H., Yang, H., McKerlie, C., Choo, B., Shi, W., Pullano, R., Piscione, T.D., Grisaru, S., Soon, S., Sedlackova, L., Tanswell, A.K., Mak, T.W., Yeger, H., Lockwood, G.A., Rosenblum, N.D. & Filmus, J. (1999). Glypican-3-deficient mice exhibit developmental overgrowth and some of the abnormalities typical of Simpson-Golabi-Behmel syndrome. *J Cell Biol*, 146, 255-264.

Carey, D. (1997). Syndecans:multifunctional cell-surface co-receptors. *Biochem J*, 327, 1-16.

Carmeliet, P. & Jain, R. (2000). Angiogenesis in cancer and other diseases. *Nature*, 407, 249-257.

Chan, S., Zheng, H., Su, M., Wilk, R., Killeen, M., Hedgecock, E. & Culotti, J. (1996). UNC-40, a C. elegans homolog of DCC (deleted in colorectal cancer), is required in motile cells responding to UNC-6 netrin cues. *Cell*, 87, 187-195.

Chang, Z., Choon, A. & Friedl, A. (1999). Endostatin binds to blood vessels in situ independent of heparan sulfate and does not compete for fibroblast growth factor-2 binding. *Am J Pathol*, 155, 71-76.

Chang, Z., Meyer, K., Rapraeger, A.C. & Friedl, A. (2000). Differential ability of heparan sulfate proteoglycans to assemble the fibroblast growth factor receptor complex in situ. *Faseb J*, 14, 137-144.

Chen, C., Parangi, S., Tolentino, M. & Folkman, J. (1995). A strategy to discover circulating angiogenesis inhibitors generated by human tumours. *Cancer Res*, 55, 4230-4233.

Chen, C.T., Lin, J., Li, Q., Phipps, S.S., Jakubczak, J.L., Stewart, D.A., Skripchenko, Y., Forry-Schaudies, S., Wood, J., Schnell, C. & Hallenbeck, P.L. (2000). Antiangiogenic gene therapy for cancer via systemic administration of adenoviral vectors expressing secretable endostatin. *Hum Gene Ther*, 11, 1983-96.

Chen, Q.R., Kumar, D., Stass, S.A. & Mixson, A.J. (1999). Liposomes complexed to plasmids encoding angiostatin and endostatin inhibit breast cancer in nude mice. *Cancer Res*, 59, 3308-12.

Colorado, P., Torre, A., Kamphaus, G., Maeshima, Y., Hopfer, H., Takahashi, K., Volk, R., Zamborsky, E., Herman, S., Sarkar, P., Ericksen, M., Dhanabal, M., Simons, M., Post, M., Kufe, D., Weichselbaum, R., Sukhatme, V. & Kalluri, R. (2000). Anti-angiogenic cues from vascular basement membrane collagen. *Cancer Res*, 60, 2520-2526.

Conrad, H. (1998). *Heparin-binding proteins*. Academic Press: San Diego.

Costell, M., Gustafsson, E., Aszodi, A., Morgelin, M., Bloch, W., Hunziker, E., Addicks, K., Timpl, R. & Fassler, R. (1999). Perlecan maintains the integrity of cartilage and some basement membranes. *J Cell Biol*, 147, 1109-1122.

Craig, L., Spelman, J., Strandberg, J. & Zink, M. (1998). Endothelial cells from diverse tissues exhibit differences in growth and morphology. *Microvasc Res*, 55, 65-76.

David, G., Bai, X.M., Van der Schueren, B., Marynen, P., Cassiman, J.-J. & Van den Berghe, H. (1993). Spatial and temporal changes in the expression of fibroglycan (syndecan-2) during mouse embryonic development. *Development*, 119, 841-854.

David, G., Lories, V., Decock, B., Marynen, P., Cassiman, J.J. & Van den Berghe, H. (1990). Molecular cloning of a phosphatidylinositol-anchored membrane heparan sulfate proteoglycan from human lung fibroblasts. *J Cell Biol*, 111, 3165-3176.

DeCat, B. & David, G. (2001). Developmental roles of the glypicans. *Seminars in Cell and Developmental Biology*, 12, 117-125.

Delaney, S.R. & Conrad, H.E. (1983). Changes in disaccharide composition of heparan sulphate fractions with increasing degrees of sulphation. *Biochem J*, 209, 315-322.

Delehedde, M., Steve, M., Sergeant, N., Wartelle, I., Lyon, M., Rudland, P. & Fernig, D. (2000). Fibroblast growth factor-2 stimulation of p42/44 MAPK phosphorylation and IκB degradation is regulated by heparan sulfate/heparin in rat mammary fibroblasts. *J Biol Chem*, 275, 33905-33910.

Deng, C., Wynthshaw-Boris, A., Zhou, F., Kuo, A. & Leder, P. (1996). Fibroblast growth factor receptor 3 is a negative regulator of bone growth. *Cell*, 84, 911-921.

Desai, U.R., Wang, H.M. & Linhardt, R.J. (1993). Specificity studies on the heparin lyases from Flavobacterium heparinum. *Biochemistry*, 32, 8140-8145.

Dhanabal, M., Ramchandran, R., Waterman, M.J., Lu, H., Knebelmann, B., Segal, M. & Sukhatme, V.P. (1999). Endostatin induces endothelial cell apoptosis. *J Biol Chem*, 274, 11721-11726.

Dhodapkar, M., Abe, E., Theus, A., Lacy, M., Langford, J., Barlogie, B. & Sanderson, R. (1998). Syndecan-1 is a multifunctional regulator of myeloma pathobiology: control of tumor cell survival, growth, and bone cell differentiation. *Blood*, 91, 2679-2688.

Ding, I., Sun, J.Z., Fenton, B., Liu, W.M., Kimsely, P., Okunieff, P. & Min, W. (2001). Intratumoral administration of endostatin plasmid inhibits vascular growth and perfusion in MCa-4 murine mammary carcinomas. *Cancer Res*, 61, 526-31.

Ding, Y., Javaherian, K., Lo, K., Chopra, R., Boehm, T., Lanciotti, J., Harris, B., Li, Y., Shapiro, R., Hohenester, E., Timpl, R., Folkman, J. & Wiley, D. (1998). Zinc-dependent dimers observed in crystals of human endostatin. *Proc Natl Acad Sci*, 95, 10443-19448.

Dixelius, J., Larsson, H., Sasaki, T., Holmqvist, K., Lu, L., Engstrom, A., Timpl, R., Welsh, M. & Claesson-Welsh, L. (2000). Endostatin-induced tyrosine kinase signaling through the Shb adaptor protein regulates endothelial cell apoptosis. *Blood*, 95, 3403-3411.

Echtermeyer, F., Streit, M., Wilcox-Adelman, S., Saoncella, S., Denhez, F., Detmar, M. & Goetinck, P. (2001). Delayed wound repair and impaired angiogenesis in mice lacking syndecan-4. *J Clin Invest*, 107, R9-R14.

Eklund, L., Piuhola, J., Komulainen, J., Sormunen, R., Ongvarrasopone, C., Fassler, R., Muona, A., Ilves, M., Ruskoaho, H., Takala, T.E. & Pihlajaniemi, T. (2001). Lack of type XV collagen causes a skeletal myopathy and cardiovascular defects in mice. *Proc Natl Acad Sci*, 98, 1194-1199.

Elenius, K., Vainio, S., Laato, M., Salmivirta, M., Theslaff, I. & Jalkanen, M. (1991). Induced expression of syndecan in healing wounds. *J Cell Biol*, 114, 585-595.

Erickson, A. & Couchman, J. (2000). Still more complexity in mammalian basement membranes. *J Histochem Cytochem*, 48, 1291-306.

Esko, J. & Zhang, L. (1996). Influence of core protein sequence on glycosaminoglycan assembly. *Curr Opin Cell Biol*, 6, 663-670.

Esko, J.D. (1991). Genetic analysis of proteoglycan structure, function and metabolism. *Curr Opin Cell Biol*, 3, 805-816.

Evans, D.L., Marshall, C.J., Christey, P.B. & Carrell, R.W. (1992). Heparin binding site, conformational change, and activation of antithrombin. *Biochemisty*, 31, 12629-12642.

Fahem, S., Hileman, R.E., Fromm, J.R., Linhardt, R.J. & Rees, D.C. (1996). Heparin structure and interactions with basic fibroblast growth factor. *Science*, 271, 1116-1120.

Fannon, M., Forsten, K.E. & Nugent, M.A. (2000). Potentiation and Inhibition of bFGF Binding by Heparin: A Model for Regulation of Cellular Response. *Biochemistry*, 39, 1434-1445.

Feitsma, K., Hausser, H., Robenek, H., Kresse, H. & Vischer, P. (2000). Interaction of thrombospondin-1 and heparan sulfate from endothelial cells. Structural requirements of heparan sulfate. *J Biol Chem*, 275, 9396-9402.

Felbor, U., Dreier, L., Bryant, R., Ploegh, H., Olsen, B. & Mothes, W. (2000). Secreted cathepsin L generates endostatin from collagen XVIII. *EMBO J*, 19, 1187-1194.

Feyzi, E., Saldeen, T., Larsson, E., Lindahl, U. & Salmivirta, M. (1998). Age-dependent modulation of heparan sulfate structure and function. *J Biol Chem*, 273, 13395-13398.

Feyzi, E., Trybala, E., Bergstrom, T., Lindahl, U. & Spillmann, D. (1997). Structural requirement of heparan sulfate for interaction with herpes simplex virus type 1 virions and isolated glycoprotein C. *J Biol Chem*, 272, 24850-24857.

Filmus, J. (2001). Glypicans in growth control and cancer. *Glycobiology*, 11, 19R-23R.

Filmus, J., Shi, W., Wong, Z.M. & Wong, M.J. (1995). Identification of a new membrane-bound heparan sulphate proteoglycan. *Biochem J*, 311, 561-565.

Folkman, J, (1995). Clinical Applications of Research on Angiogenesis. *New Eng J Med*, 333, 1757-1763.

Folkman, J. (1971). Tumor Angiogenesis: Therapeutic implications. *New Eng J Med*, 285, 1182-1186.

Folkman, J. & Haudenschild, C. (1980). Angiogenesis in vitro. *Nature*, 288, 551-556.

Folkman, J. & Klagsbrun, M. (1987). Angiogenic factors. *Science*, 235, 442-447.

Gallagher, J. & Lyon, M. (1989). . In *Heparin*, Lane, D. & Lindahl, U. (eds) pp. 135-158. Edward Arnold: London.

Gallagher, J. & Lyon, M. (2000). Heparan sulphate: Molecular structure and interactions with growth factors and morphogens. In *Proteoglycans: Structure, Biology and Molecular interactions*, Iozzo, R. (ed). Marcel Dekker: New York.

Gallagher, J.T., Turnbull, J.E. & Lyon, M. (1992). Patterns of sulphation in heparan sulphate: polymorphism based on a common structural theme. *Int J Biochem*, 24, 553-560.

Gallagher, J.T. & Walker, A. (1985). Molecular distinctions between heparan sulphate and heparin. Analysis of sulphation patterns indicates that heparan sulphate and heparin are separate families of N-sulphated polysaccharides. *Biochem J*, 230, 665-674.

Galliher, P.M., Cooney, C.L., Langer, R. & Linhardt, R.J. (1981). Heparinase production by *Flavobacterium heparinum. App Envir Microb*, 41, 360-365.

Gallo, R., Kim, C., Kokenyesi, R., Adzick, N. & Bernfield, M. (1996). Syndecans-1 and -4 are induced during wound repair of neonatal but not fetal skin. *J Invest Dermatol*, 107, 676-683.

Gasparini, G. (1999). The rationale and future potential of angiogenesis inhibitors in neoplasia. *Drugs*, 58, 17-38.

Gengrinovitch, S., Berman, B., David, G., Witte, L., Neufeld, G. & Ron, D. (1999). Glypican-1 is a VEGF165 binding proteoglycan that acts as an extracellular chaperone for VEGF165. *J Biol Chem*, 274, 10816-10822.

Gerhart, J. & Kirschner, M. (1997). *Cells, embryos and evolution.* Blackwell: MA.

Giancotti, F. & Ruoshlati, E. (1999). Integrin Signalling. *Science*, 285, 1028-1032.

Goldman, E. (1907). The growth of malignant disease in man and the lower animals with special reference to the vascular system. *Lancet*, 2, 1236-1240.

Gonzalez, A., Kaya, M., Shi, W., Song, H., Testa, J., Penn, L. & Filmus, J. (1998). OCI-5/GPC3, a glypican encoded by a gene that is mutated in the Simpson-Golabi-Behmel overgrowth syndrome, induces apoptosis in a cell line-specific manner. *J Cell Biol*, 141, 1407-1414.

Grabarek, Z. & Gergely, J. (1990). Zero-length crosslinking procedure with the use of active esters. *Anal Biochem*, 185, 131-135.

Grant, D., Lelkes, P., Fukuda, K. & Kleinman, H. (1991). Intracellular mechanisms involved in basement membrane induced blood vessel differentiation in vitro. *In vitro Cell Dev Biol*, 27A, 327-336.

Grootjans, J., Zimmermann, P., Reekmans, G., Smets, A., Deegest, G., Durr, J. & David, G. (1997). Syntenin, a PDZ protein that binds syndecan cytoplasmic domains. *Proc Natl Acad Sci*, 94, 13683-13688.

Guimond, S., Maccarana, M., Olwin, B.B., Lindahl, U. & Rapraeger, A.C. (1993). Activating and inhibitory heparin sequences for FGF-2 (basic FGF). Distinct requirements for FGF-1, FGF-2, and FGF-4. *J Biol Chem*, 268, 23906-23914.

Habuchi, H., Tanaka, M., Habuchi, O., Yoshida, K., Suzuki, H., Ban, K. & Kimata, K. (2000). The occurrence of three isoforms of heparan sulphate 6-O-sulphotransferase having different specificities for hexuronic acid adjacent to the targeted N-sulphoglucosamine. *J Biol Chem*, 275, 2859-2868.

Haerry, T.E., Heslip, T.R., Marsh, J.L. & O'Connor, M.B. (1997). Defects in glucuronate biosynthesis disrupt Wingless signaling in *Drosophila*. *Development*, 124, 3055-3064.

Hagg, P., Horelli-Kiutunen, N., Eklund, L., Palotie, A. & Pihlajaniemi, T. (1997). Cloning of mouse type XV collagen sequences and mapping of the corresponding gene to 4B1-3. *Genomics*, 45, 31-41.

Hagg, P., Muona, A., Lietard, J., Kivirikko, S. & Pihlajaniemi, T. (1998). Complete exon-intron organisation of the human gene for the a1 chain of type XV collagen (COL15A1) and comparison with the homologous Col18a1 gene. *J Biol Chem*, 273, 17824-17831.

Halfter, W., Dong, S., Schurer, B. & Cole, G. (1998). Collagen XVIII is a basement membrane heparan sulphate proteoglycan. *J Biol Chem*, 273, 25404-25412.

Hanahan, D. & Weinberg, R. (2000). The hallmarks of cancer. *Cell*, 100, 57-70.

Handler, M., Yurchenco, P. & Iozzo, R. (1997). Developmental expression of perlecan during murine embryogenesis. *Dev Dyn*, 210, 130-145.

Harris, A. (1997). Antiangiogenesis for cancer therapy. *Lancet*, 349, Supplement 13-15.

Hasan, M., Najjam, S., Gordon, M., Gibbs, R. & Rider, C. (1999). IL-12 is a heparin-binding cytokine. *J of Immunol*, 162, 1064-1070.

Hennekam, R. (1991). Hereditary Multiple exostosis. *J Med Genet*, 28, 262-266.

Herr, A., Ornitz, D., Sasisekharan, R., Venktaraman, G. & Waksman, G. (1997). Heparin-induced self-association of fibroblast growth factor-2: evidence for two oligomerization processes. *J Biol Chem*, 272, 16832-16839.

Hewett, P., Murray, E., Price, E., Watts, M. & Woodcock, M. (1993). Isolation and characterization of microvessel endothelial cells from human mammary adipose tissue. *In Vitro Cell Dev Biol Anim*, 29A, 325-331.

Hileman, R.E., Fromm, J.R., Weiler, J.M. & Linhardt, R.J. (1998). Glycosaminoglycan-protein interactions: definition of consensus sites in glycosaminoglycan binding proteins. *Bioessays*, 20, 156-167.

Hiscock, D.R., Canfield, A. & Gallagher, J.T. (1995). Molecular structure of heparan sulphate synthesised by bovine aortic endothelial cells. *Biochim Biophys Acta*, 1244, 104-112.

Hohenester, E., Sasaki, T., Olsen, B. & Timpl, R. (1998). Crystal structure of the angiogenesis inhibitor endostatin at 1.5 A resolution. *EMBO J*, 17, 1656-1664.

Horowitz, A. & Simons, M. (1998). Regulation of syndecan-4 phosphorylation in vivo. *J Biol Chem*, 273, 10914-10918.

Huebner, K., Cannizzaro, L., Jabs, E., Kivirikko, S., Manzone, H., Pihlajaniemi, T. & Myers, J. (1992). Chromosomal assignment of a gene encoding a new collagen type (COL15A1) to 9q21-q22. *Genomics*, 14, 220-224.

Hulett, M.D., Freeman, C., Hamdorf, B.J., Baker, R.T., Harris, M.J. & Parish, C.R. (1999). Cloning of mammalian heparanase, an important enzyme in tumor invasion and metastasis. *Nat Med*, 5, 803-809.

Humphries, D.E., Sullivan, B.M., Aleixo, M.D. & Stow, J.L. (1997). Localization of human heparan glucosaminyl N-deacetylase/N- sulphotransferase to the trans-Golgi network. *Biochem J*, 325, 351-357.

Hutter, H., Vogel, B., Plenefisch, J., Norris, C., Proenca, R., Spieth, J., Guo, C., Mastwal, S., Zhu, X., Scheel, J. & Hedgecock, E. (2000). Conservation and novelty in the evolution of cell adhesion and extracellular matrix genes. *Science*, 287, 989-994.

Inki, P. & Jalkanen, M. (1996). The role of syndecan-1 in malignancies. *Ann Med*, 28, 63-67.

Iozzo, R., Cohen, I., Grassel, S. & Murdoch, A. (1994). The biology of perlecan: the multifaceted heparan sulphate proteoglycan of basement membranes and pericellular matrices. *Biochem J*, 302, 625-639.

Ishihara, M., Guo, Y. & Swiedler, S.J. (1993). Selective impairment of the synthesis of basic fibroblast growth factor binding domains of heparan sulphate in a COS cell mutant defective in N- sulphotransferase. *Glycobiology*, 3, 83-88.

Itano, N., Oguri, K., Nagayasu, Y., YKusano, Nakanishi, H., David, G. & Okayama, M. (1996). Phosphorylation of a membrane-intercalated proteoglycan, syndecan-2, expressed in aq stroma-inducing clone from a Lewis mouse sarcoma. *Biochem J*, 315, 925-930.

Iwasaki, W., Nagata, K., Hatanaka, H., Inui, T., Kimura, T., Muramatsu, T., Yoshida, K., Tasumi, M. & Inagaki, F. (1997). Solution structure of midkine, a new heparin-binding growth factor. *EMBO J*, 16, 6936-6946.

Jackson, D., Bell, J., Dickson, R., Timans, J., Shields, J. & Whittle, N. (1995). Proteoglycan forms of lymphocyte homing receptor CD44 are alternatively spliced variants containing the V3 exon. *J Cell Biol*, 128, 673-685.

Jackson, S.M., Nakato, H., Sugiura, M., Jannuzi, A., Oakes, R., Kaluza, V., Golden, C. & Selleck, S.B. (1997). *dally*, a *Drosophila* glypican, controls cellular responses to the TGF-β-related morphogen, *Dpp*. *Development*, 124, 4113-4120.

Jayson, G.C. & Gallagher, J.T. (1997) Heparin oligosaccharides: inhibitors of the biological activity of bFGF on Caco-2 cells. *Br J Cancer* **75**:9-16.

Jayson, G.C., Lyon, M., Paraskeva, C., Turnbull, J.E., Deakin, J.A. & Gallagher, J.T. (1998). Heparan sulfate undergoes specific structural changes during the progression from human colon adenoma to carcinoma in vitro. *J Biol Chem*, 273, 51-57.

Joki, T., Machluf, M., Atala, A., Zhu, J., Seyfried, N.T., Dunn, I.F., Abe, T., Carroll, R.S. & Black, P.M. (2001). Continuous release of endostatin from microencapsulated engineered cells for tumor therapy. *Nat Biotechnol*, 19, 35-9.

Jorpes, J.E. & Gardell, N. (1948). On heparin monosulfuric acid. *J Biol Chem*, 176, 267-276.

Kainulainen, V., Wang, H., Schick, C. & Bernfield, M. (1998). Syndecans, heparan sulphate proteoglycans maintain the proteolytic balance of wound fluids. *J Biol Chem*, 273, 11563-11569.

Kan, M., Wang, F., Xu, J., Crabb, J.W., Hou, J. & McKeehan, W.L. (1993). An essential heparin-binding domain in the fibroblast growth factor receptor kinase. *Science*, 259, 1918-1921.

Kaneda, N., Talukder, A., Ishihara, M., Hara, S., Yoshida, K. & Muramatsu, T. (1996). Structural characteristics of heparin-like domain required for the interaction of midkine with embryonic neurons. *Biochem Biophys Res Commun*, 220, 108-112.

Karumanchi, S., Jha, V., Ramchandran, R., Karihaloo, A., Tsiokas, L., Chan, B., Dhanabal, M., Hanai, J., Venkataraman, G., Shriver, Z., Keiser, N., Kalluri, R., Zeng, H., Mukhopadhyay, D., Chen, R., Lander, A., Hagihara, K., Yamaguchi, Y., Sasisekharan, R., Cantley, L. & Sukhatme, V. (2001). Cell surface glypicans are low-affinity endostatin receptors. *Molecular Cell*, 7, 811-822.

Kato, M., Wang, H., Bernfield, M., Gallagher, J.T. & Turnbull, J.E. (1994). Cell surface syndecan-1 on distinct cell types differs in fine structure and ligand binding of its heparan sulfate chains. *J Biol Chem*, 269, 18881-18890.

Kato, M., Wang, H., Kainulainen, V., Fitzgerald, M.L., Ledbetter, S., Ornitz, D.M. & Bernfield, M. (1998). Physiological degradation converts the soluble syndecan-1 ectodomain from an inhibitor to a potent activator of FGF-2. *Nat Med*, 4, 691-7.

Keiser, N., Venkataraman, G., Shriver, Z. & Sasisekharan, R. (2001). Direct isolation and sequencing of specific protein-binding glycosaminoglycans. *Nat Med*, 7, 123-127.

Kerbel, R. (1997). A cancer therapy resistant to resistance. *Nature*, 390, 335-336.

Kim, C.W., Goldberger, O.A., Gallo, R.L. & Bernfield, M. (1994). Members of the syndecan family of heparan sulphate proteoglycans are expressed in distinct cell-, tissue-, and development-specific patterns. *Mol Biol Cell*, 5, 797-805.

Kinnunen, T., Kaksonen, M., Saarinen, J., Kalkkinen, N., Peng, H. & Rauvala, H. (1998). Cortactin/Src-kinase signaling pathway is involved in N-syndecan-dependent neurite outgrowth. *J Biol Chem*, 273, 10702-10708.

Kitagawa, H., Shimakawa, H. & Sugahara, K. (1999). The tumor suppressor EXT-like gene EXTL2 encodes an α1,4-N-acetylhexosaminyltransferase that transfers N-acetylgalactosamine and N-acetylglucosamine to the common

glycosaminoglycan-protein linkage region. the key enzyme for the chain initiation of heparan sulfate. *J Biol Chem*, 274, 13933-13937.

Kivirikko, S., Saarela, J., Myers, J., Autio-Harmainen, H. & Pihlajaniemi, T. (1995). Distribution of type XV collagen transcripts in human tissue and their production by muscle cells and fibroblasts. *Am J Pathol*, 147, 1500-1509.

Kjellen, L. & Lindahl, U. (1991). Proteoglycans: structures and interactions. *Annu Rev Biochem*, 60, 443-475.

Klass, C.M., Couchman, J.R. & Woods, A. (2000). Control of extracellular matrix assembly by syndecan-2 proteoglycan. *J Cell Sci*, 113, 493-506.

Kojima, T., Shworak, N. & Rosenberg, R. (1992). Molecular cloning and expression of two distinct cDNA-encoding heparan sulfate proteoglycan core proteins from a rat endothelial cell line. *J Biol Chem*, 267, 4870-4877.

Kramer, J. (1997). Extracellular matrix structure and function. In *The nematode C.elegans*, Riddle, D. (ed), Vol. 2. pp. 471-500. Cold Spring Harbor Laboratory Press: Cold Spring Harbor, New York.

Kreuger, J., Prydz, K., Pettersson, R.F., Lindahl, U. & Salmivirta, M. (1999). Characterization of fibroblast growth factor 1 binding heparan sulfate domain. *Glycobiology*, 9, 723-729.

Kuo, C.J., LaMontagne, K.R., Garcia-Cardena, G., Ackley, B.D., Kalman, D., Park, S., Christofferson, R., Kamihara, J., Ding, Y.H., Lo, K.M., Gillies, S., Folkman, J., Mulligan, R.C. & Javaherian, K. (2001). Oligomerization-dependent regulation of motility and morphogenesis by the collagen xviii nc1/endostatin domain. *J Cell Biol*, 152, 1233-1246.

Kuzu, I., Bicknell, R., Fletcher, C. & Gatter, K. (1993). Expression of adhesion molecules on the endothelium of normal tissue vessels and vascular tumours. *Lab Invest*, 69, 322-328.

Laemmli, U. (1970). Cleavage of structural proteins during the assembly of the head of bacteriophage T4. *Nature*, 227, 680-685.

Lander, A. (1998). Proteoglycans: Master Regulators of Molecular Encounter ? *Matrix Biology*, 17, 465-472.

Li, J., Hagner-McWhirter, A., Kjellen, L., Palgi, J., Jalkanen, M. & Lindahl, U. (1997). Biosynthesis of heparin/heparan sulfate. cDNA cloning and expression of D-glucuronyl C5-epimerase from bovine lung. *J Biol Chem*, 272, 28158-28163.

Lietard, J., Theret, N., Rehn, M., Musso, O., Dargere, D., Pihlajaniemi, T. & Clement, B. (2000). The promoter of the long variant of collagen XVIII, the precursor of endostatin, contains liver-specific regulatory elements. *Hepatology*, 32, 1377-1385.

Lin, X., Buff, E.M., Perrimon, N. & Michelson, A.M. (1999). Heparan sulfate proteoglycans are essential for FGF receptor signaling during *Drosophila* embryonic development. *Development*, 126, 3715-3723.

Lin, X. & Perrimon, N. (1999). *Dally* cooperates with *Drosophila Frizzled 2* to transduce *Wingless* signalling. *Nature*, 400, 281-284.

Lind, T., Tufaro, F., McCormick, C., Lindahl, U. & Lidholt, K. (1998). The putative tumor suppressors EXT1 and EXT2 are glycosyltransferases required for the biosynthesis of heparan sulfate. *J Biol Chem*, 273, 26265-26268.

Lindahl, U., Kusche-Gullberg, M. & Kjellen, L. (1998). Regulated diversity of heparan sulfate. *J Biol Chem*, 273, 24979-24982.

Lindahl, U., Thunberg, L., Backstrom, G., Riesenfeld, J., Nordling, K. & Bjork, I. (1984). Extension and structural variability of the antithrombin-binding sequence in heparin. *J Biol Chem*, 259, 12368-12376.

Lindblom, A. & Fransson, L.A. (1990). Endothelial heparan sulphate: compositional analysis and comparison of chains from different proteoglycan populations. *Glycoconj J*, 7, 545-562.

Linhardt, R., Rice, K., Kim, Y., Lohse, D., Wang, H.-M. & Loganathhan, D. (1988). Mapping and quantification of the major oligosaccharide components of heparin. *Biochem J*, 254, 781-787.

Linhardt, R.J., Turnbull, J.E., Wang, H.M., Loganathan, D. & Gallagher, J.T. (1990). Examination of the substrate specificity of heparin and heparan sulfate lyases. *Biochemistry*, 29, 2611-2617.

Linker, A. & Hovingh, P. (1972). Isolation and characterization of oligosaccharides obtained from heparin by action of heparinase. *Biochemistry*, 11, 563-568.

Lohse, D.L. & Linhardt, R.J. (1992). Purification and characterization of heparin lysases from *Flavobacterium heparinum*. *J Biol Chem*, 267, 24347-24355.

Lortat-Jacob, H., Turnbull, J.E. & Grimaud, J.A. (1995). Molecular organization of the interferon gamma-binding domain in heparan sulphate. *Biochem J*, 310, 497-505.

Lyon, M., Deakin, J., Rahmoune, H., Fernig, D., Nakamura, T. & Gallagher, J. (1998). Hepatocyte growth factor/scatter factor binds with high affinity to dermatan sulfate. *J Biol Chem*, 273, 271-278.

Lyon, M., Deakin, J.A. & Gallagher, J.T. (1994). Liver heparan sulfate structure. A novel molecular design. *J Biol Chem*, 269, 11208-11215.

Lyon, M. & Gallagher, J.T. (1994). Hepatocyte growth factor/scatter factor: a heparan sulphate-binding pleiotropic growth factor. *Biochem Soc Trans*, 22, 365-370.

Lyon, M. & Gallagher, J.T. (1998). Bio-specific sequences and domains in heparan sulphate and the regulation of cell growth and adhesion. *Matrix Biol*, 17, 485-493.

Lyon, M., Rushton, G., Askari, J., Humphries, M. & Gallagher, J. (2000). Elucidation of the structural features of heparan sulfate important for interaction with the hep-2 domain of fibronectin. *J Biol Chem*, 275, 4599-4606.

Lyon, M., Rushton, G. & Gallagher, J.T. (1997). The interaction of the transforming growth factor-betas with heparin/heparan sulfate is isoform-specific. *J Biol Chem*, 272, 18000-18006.

Maccarana, M., Casu, B. & Lindahl, U. (1993). Minimal sequence in heparin/heparan sulfate required for binding of basic fibroblast growth factor. *J Biol Chem*, 268, 23898-23905.

Maccarana, M. & Lindahl, U. (1993). Mode of interaction between platelet factor 4 and heparin. *Glycobiology*, 3, 271-277.

Maccarana, M., Sakura, Y., Tawada, A., Yoshida, K. & Lindahl, U. (1996). Domain structure of heparan sulfates from bovine organs. *J Biol Chem*, 271, 17804-17810.

Mali, M., Andtfolk, H., Miettinen, I. & Jalkanen, M. (1994). Suppression of tumor cell growth by syndecan-1 ectodomain. *J Biol Chem*, 269, 27795-27798.

Mani, K., Jonsson, M., Edgren, G., Belting, M. & Fransson, L.A. (2000). A novel role for nitric oxide in the endogenous degradation of heparan sulfate during recycling of glypican-1 in vascular endothelial cells. *Glycobiology*, 10, 577-586.

Marchetti, D. (1997). Specific Degradation of subendothelial matrix proteoglycans by brain-metastatic melanoma and brain endothelial cell heparanases. *J Cell Physiol*, 172, 334-342.

Marcum, J. & Rosenberg, R. (1989). The biochemistry, cell biology, and pathophysiology of anticoagulantly active heparin-like molecules of the vessel

wall. In *Heparin: Chemical and Biological Properties, Clinical Applications*, Lane, D. & Lindahl, U. (eds). CRC Press, Inc: Boca Raton, Florida.

Mathiak, M., Yenisey, C., Grant, D., Sharma, B. & Iozzo, R. (1997). A role for perlecan in the suppression of growth and invasion in fibrosarcoma cells. *Cancer Res*, 57, 2130-2136.

McCormick, C., Leduc, Y., Martindale, D., Mattison, K., Esford, L., Dyer, A. & Tufaro, F. (1998). The putative tumour suppressor EXT1 alters the expression of cell-surface heparan sulfate. *Nat Genet*, 19, 158-161.

McKenzie, E., Tyson, K., Stamps, A., Smith, P., Turner, P., Barry, R., Hircock, M., Patel, S., Barry, E., Stubberfield, C., Terrett, J. & Page, M. (2000). Cloning and expression profiling of Hpa2, a novel mammalian heparanase family member. *Biochem Biophys Res Commun*, 276, 1170-1177.

Merry, C., Bullock, S., Swan, D., Backen, A., Lyon, M., Beddington, R., Wilson, V. & Gallagher, J. (2001). The molecular phenotype of heparan sulfate in the *Hs2st*$^{-/-}$ mutant mouse. *submitted.*

Merry, C.L., Lyon, M., Deakin, J.A., Hopwood, J.J. & Gallagher, J.T. (1999). Highly sensitive sequencing of the sulfated domains of heparan sulfate. *J Biol Chem*, 274, 18455-18462.

Mikhailov, D., Young, H.C., Linhardt, R.J. & Mayo, K.H. (1999). Heparin dodecasaccharide binding to platelet factor-4 and growth related protein: induction of a partially folded state and implications for heparin-induced thrombocytopenia. *J Biol Chem*, 274, 25317-25329.

Moy, F., Safron, M., Seddon, A., Kitchen, D., Bohlen, P., Aviezer, D., Yayon, A. & Powers, R. (1997). Properly orientated heparin-decasaccharide-induced dimers are the biologically active form of basic fibroblast growth factor. *Biochemistry*, 36, 4782-4791.

Mulloy, B. & Forster, M. (2000). Conformation and dynamics of heparin and heparan sulfate. *Glycobiology*, 10, 1147-1156.

Mulloy, B., Forster, M., Jones, C., Drake, A., Johnson, E. & Davies, D. (1994). The effect of variation of substitution on the solution conformation of heparin : a spectroscopic and molecular modelling study. *Carbohydr Res*, 255, 1-26.

Muragaki, Y., Timmons, S., Griffith, C., Oh, S., Fadel, B., Quertermous, T. & Olsen, B. (1995). Mouse Col18a1 is expressed in a tissue-specific manner as three

alternative variants and is localised in basement membrane zones. *Proc Nat Acad Sci*, 92, 8763-8767.

Murphy-Ullrich, J., Westrick, L., Esko, J. & Mosher, D. (1988). Altered metabolism of thrombospondin by Chinese hamster ovary cells defective in glycosaminoglycan synthesis. *J Biol Chem*, 263, 6400-6406.

Musso, O., Rehn, M., Theret, N., Turlin, B., Bioulac-Sage, P., Lotrian, D., Campion, J., Pihlajaniemi, T. & Clement, B. (2001). Tumor progression is associated with a significant decrease in the expression of the endostatin precursor collagen XVIII in human hepatocellular carcinomas. *Cancer Res*, 61, 45-49.

Najjam, S., Mulloy, B., Theze, J., Gordon, M., Gibbs, R. & Rider, C. (1998). Further characterisation of the binding of human recombinant interleukin 2 to heparin and identification of putative binding sites. *Glycobiology*, 8, 509-516.

Nakato, H., Futch, T.A. & Selleck, S.B. (1995). The *division abnormally delayed (dally)* gene: a putative integral membrane proteoglycan required for cell division patterning during postembryonic development of the nervous system in *Drosophila. Development*, 121, 3687-3702.

Nicole, S. (2000). Perlecan, the major proteoglycan of basement membranes is altered in patients with Schwartz-Jampel syndrome (chondrodystrophic myotonia). *Nat Genet*, 26, 480-483.

Noonan, D.M., Fulle, A., Valente, P., Cai, S., Horigan, E., Sasaki, M., Yamada, Y. & Hassell, J.R. (1991). The complete sequence of perlecan, a basement membrane heparan sulfate proteoglycan, reveals extensive similarity with laminin A chain, low density lipoprotein-receptor, and the neural cell adhesion molecule. *J Biol Chem*, 266, 22939-22947.

Nurcombe, V., Ford, M.D., Wildschut, J.A. & Bartlett, P.F. (1993). Developmental regulation of neural response to FGF-1 and FGF-2 by heparan sulfate proteoglycan. *Science*, 260, 103-106.

Obeso, J., Weber, J. & Auerbach, R. (1990). A hemangioendothelioma cell line: its use as a model for the study of endothelial cell biology. *Laboratory Investigation*, 63, 259-269.

Oh, E., Woods, A. & Couchman, J. (1997). Syndecan-4 proteoglycan regulates the distribution and activity of protein kinase C. *J Biol Chem*, 272, 8133-8136.

Oh, E.S., Woods, A., Lim, S.T., Theibert, A.W. & Couchman, J.R. (1998). Syndecan-4 proteoglycan cytoplasmic domain and phosphatidylinositol 4,5- bisphosphate coordinately regulate protein kinase C activity. *J Biol Chem*, 273, 10624-10629.

Oh, S., Warman, M., Seldin, M., Cheng, S.-D., Knoll, J., Timmons, S. & Olsen, B. (1994b). Cloning of cDNA and genomic DNA encoding human type XVIII collagen and localisation of the alpha-1(XVIII) collagen gene to mouse chromosome 10 and human chromosome 21. *Genomics*, 19, 494-499.

Oh, S.K., Kamagata, Y., Muragaki, Y., Timmons, S., Ooshima, A. & Olsen, B.R. (1994). Isolation and sequencing of cDNAs for proteins with multiple domains of Gly-Xaa-Xaa repeats identify a distinct family of collagenous proteins. *Proc Natl Acad Sci*, 91, 4229-4233.

Olsen, B.R. (1999). Life without perlecan has its problems. *J Cell Biol*, 147, 909-912.

Olwin, B. & Rapraeger, A. (1992). Repression of myogenic differentiation by aFGF, bFGF, and K-FGF is dependent on cellular heparan sulfate. *J Cell Biol*, 118, 631-639.

Ono, K., Hattori, H., Takeshita, S., Kurita, A. & Ishihara, M. (1999). Structural features in heparin that interact with VEGF165 and modulate its biological activity. *Glycobiology*, 9, 705-711.

O'Reilly, M., Holmgren, L., Shing, Y., Chen, C., Rosenthal, R., Moses, M., Lane, W., Cao, Y., Sage, E. & Folkman, J. (1994). Angiostatin:A novel angiogenesis inhibitor that mediates the suppression of metastases by a Lewis lung carcinoma. *Cell*, 79, 315-328.

O'Reilly, M.S., Boehm, T., Shing, Y., Fukai, N., Vasios, G., Lane, W.S., Flynn, E., Birkhead, J.R., Olsen, B.R. & Folkman, J. (1997). Endostatin: an endogenous Inhibitor of Angiogenesis and Tumour Growth. *Cell*, 88, 277-285.

Ornitz, D.M. (2000). FGFs, heparan sulfate and FGFRs: complex interactions essential for development. *Bioessays*, 22, 108-112.

Ornitz, D.M., Yayon, A., Flanagan, J.G., Svahn, C.M., Levi, E. & Leder, P. (1992). Heparin is required for cell-free binding of basic fibroblast growth factor to a soluble receptor and for mitogenesis in whole cells. *Mol Cell Biol*, 12, 240-247.

Paine-Saunders, S., Viviano, B.L., Zupicich, J., Skarnes, W.C. & Saunders, S. (2000). Glypican-3 controls cellular responses to Bmp4 in limb patterning and skeletal development. *Dev Biol*, 225, 179-187.

Parish, C.R., Freeman, C., Brown, K.J., Francis, D.J. & Cowden W.B. (1999) Identification of sulfated oligosaccharide-based inhibitors of tumor growth and metastasis using novel *in vitro* assays for angiogenesis and heparanase activity. *Cancer Res* **59**:3433-3441.

Pellegrini, L., Burke, DF., von Delft, F., Mulloy, B & Blundell T. (2000). Crystal structure of fibroblast growth factor receptor ectodomain bound to ligand and heparin. *Nature*, 407, 1029-1034.

Perollet, C., Han, Z., Savona, C., Caen, J. & Bikfalvi, A. (1998). Platelet factor 4 modulates fibroblast growth factor 2 (FGF-2) activity and inhibits FGF-2 dimerization. *Blood*, 91, 3289-3299.

Perrimon, N. & Bernfield, M. (2000). Specificities of heparan sulphate proteoglycans in developmental processes. *Nature*, 404, 725-728.

Pihlajaniemi, T. & Rehn, M. (1995). Two new collagen subgroups; membrane associated collagens and types XV and XVII. *Prog Nucleic Acid Res Mol Biol*, 50, 225-262.

Pikas, D.S., Li, J.P., Vlodavsky, I. & Lindahl, U. (1998). Substrate specificity of heparanases from human hepatoma and platelets. *J Biol Chem*, 273, 18770-18777.

Pilia, G., Hughes-Benzie, R., Mackenzie, A., Baybayan, P., chen, E., Huber, R., Neri, G., Cao, A., Forabosco, A. & Schlessinger, D. (1996). Mutations in GPC3, a glypican gene, cause the Simpson-Golabi-Behmel overgrowth syndrome. *Nat Genet*, 12, 241-247.

Prockop, D. & Kivirikko, K. (1995). Collagens: molecular biology, diseases, and potentials for therapy. *Annu Rev Biochem*, 64, 403-434.

Pye, D. & Kumar, S. (1995). Molecular attributes of bovine aortic endothelial cell heparan sulfate. *Biochimica et Biophysica Acta*, 1266, 235-244.

Pye, D., Vives, R., Turnbull, J., Hyde, P. & Gallagher, J. (1998). Heparan sulfate oligosaccharides require 6-O-sulfation for promotion of basic fibroblast growth factor mitogenic activity. *J Biol Chem*, 273, 22936-22942.

Pye, D.A. & Gallagher, J.T. (1999). Monomer complexes of basic fibroblast growth factor and heparan sulfate oligosaccharides are the minimal functional unit for cell activation. *J Biol Chem*, 274, 13456-13461.

Pye, D.A. & Kumar, S. (1998). Endothelial and fibroblast cell-derived heparan sulphate bind with differing affinity to basic fibroblast growth factor. *Biochem Biophys Res Comm*, 248, 889-895.

Radoff, S. & Danishefsky, I. (1985). Distribution of glucuronic and iduronic acid units in heparin chains. *J Biol Chem*, 260, 15106-15111.

Rahmoune, H., Chen, H.L., Gallagher, J.T., Rudland, P.S. & Fernig, D.G. (1998). Interaction of heparan sulfate from mammary cells with acidic fibroblast growth factor (FGF) and basic FGF. Regulation of the activity of basic FGF by high and low affinity binding sites in heparan sulfate. *J Biol Chem*, 273, 7303-7310.

Ramchandran, R., Dhanabal, M., Volk, R., Waterman, M., Segal, M., Lu, H., Knebelmann, B. & Sukhatme, V. (1999). Antiangiogenic activity of restin, NC10 domain of human collagen XV: comparison to endostatin. *Biochem Biophys Res Commun*, 255, 735-739.

Rapraeger, A. (2001). Molecular interactions of syndecans during development. *Seminars in Cell and Developmental Biology*, 12, 107-116.

Rapraeger, A.C., Krufka, A. & Olwin, B.B. (1991). Requirement of heparan sulfate for bFGF-mediated fibroblast growth and myoblast differentiation. *Science*, 252, 1705-1708.

Rehn, M. & Pihlajaniemi, T. (1994). α1(XVIII), a collagen chain with frequent interruptions in the collagenous sequence, a distinct tissue distribution, and homology with type XV collagen. *Proc Natl Acad Sci*, 91, 4234-4238.

Rehn, M. & Pihlajaniemi, T. (1995). Identification of three N-terminal ends of type XVIII collagen and tissue specific differences in the expression of the corresponding transcripts. *J Biol Chem*, 270, 4705-4711.

Rehn, M., Veikkola, T., Kukk-Valdre, E., Nakamura, H., Ilmonen, M., Lombardo, C., Pihlajaniemi, T., Alitalo, K. & Vuori, K. (2001). Interaction of endostatin with integrins implicated in angiogenesis. *Proc Nat Acad Sci*, 98, 1024-1029.

Reichsman, F., Smith L & Cumberledge, S. (1996). Glycosaminoglycans can modulate extracellular localization of the wingless protein and promote signal transduction. *J Cell Biol*, 135, 819-827.

Rhomberg, A.J., Ernst, S., Sasisekharan, R. & Biemann, K. (1998). Mass spectrometric and capillary electrophoretic investigation of the enzymatic degradation of heparin-like glycosaminoglycans. *Proc Natl Acad Sci*, 95, 4176-4181.

Rice, K. & Linhardt R.J. (1989) Study of structurally defined oligosaccharide substrates of heparin and heparan monosulfate lyases. *Carbohydr Res*, 190, 219-233.

Ringvall, M., Ledin, J., Holmborn, K., van Kuppevelt, T., Ellin, F., Eriksson, I., Olofsson, A.M., Kjellen, L. & Forsberg, E. (2000). Defective Heparan Sulfate Biosynthesis and Neonatal Lethality in Mice Lacking N-Deacetylase/N-Sulfotransferase-1. *J Biol Chem*, 275, 25926-25930.

Roskams, T., Vos, R.D., David, G., Damme, B.V. & Desmet, V. (1998). Heparan sulphate proteoglycan expression in human primary liver tumours. *J Pathol*, 185, 290-297.

Rusnati, M., Taraboletti, G., Urbinati, C., Tulipano, G., Giuliani, R., Molinari-Tosatti, M., Sennino, B., Giacca, M., Tyagi, M., Albini, A., Noonan, D., Giavazzi, R. & Presta, M. (2000). Thrombospondin-1/HIV-1 tat protein interaction : modulation of the biological activity of extracellular Tat. *FASEB J*, 14, 1917-1930.

Saarela, J., Rehn, M., Oikarinen, A., Autio-Harmainen, H. & Pihlajaniemi, T. (1998b). The short and long forms of type XVIII collagen show clear tissue specificities in their expression and location in basement membrane zones in humans. *Am J Pathol*, 153, 611-626.

Saarela, J., Ylikarppa, R., Rehn, M., Purmonen, S. & Pihlajaniemi, T. (1998a). Complete primary structure of two variant forms of human type XVIII collagen and tissue-specific differences in the expression of the corresponding transcripts. *Matrix Biol*, 16, 319-328.

Sadir, R., Forest, E. & Lortat-Jacob, H. (1998). The heparan sulfate binding sequence of interferon-gamma increased the on rate of the interferon-gamma-interferon-gamma receptor complex formation. *J Biol Chem*, 273, 10919-25.

Safaiyan, F., Kolset, S., Prydz, K., Gottfridsson, E., Lindahl, U. & Salmivirta, M. (1999). Selective effects of sodium chlorate treatment on the sulfation of heparan sulfate. *J Biol Chem*, 274, 36267-36273.

Saksela, O., Moscatelli, D., Sommer, A. & Rifkin, D. (1988). Endothelial cell-derived heparan sulfate binds fibroblast growth factor and protects it from proteolytic degradation. *J Cell Biol*, 107, 743-751.

Salmivirta, M., Lidholt, K. & Lindahl, U. (1996). Heparan sulfate: a piece of information. *Faseb J*, 10, 1270-1279.

Salmivirta, M., Safaiyan, F., Prydz, K., Andresen, M.S., Aryan, M. & Kolset, S.O. (1998). Differentiation-associated modulation of heparan sulfate structure and function in CaCo-2 colon carcinoma cells. *Glycobiology*, 8, 1029-1036.

Sanderson, R. (2001). Heparan sulfate proteoglycans in invasion and metastasis. *Seminars in Cell and Developmental Biology*, 12, 89-98.

Sanderson, R.D., Turnbull, J.E., Gallagher, J.T. & Lander, A.D. (1994). Fine structure of heparan sulfate regulates syndecan-1 function and cell behavior. *J Biol Chem*, 269, 13100-13106.

Sasaki, T., Fukai, N., Mann, K., Gohring, W., Olsen, B. & Timpl, R. (1998). Structure, function and tissue forms of the C-terminal globular domain of collagen XVIII containing the angiogenesis inhibitor endostatin. *EMBO J*, 17, 4249-4256.

Sasaki, T., Larsson, H., Kreuger, J., Salmivirta, M., Claesson-Welsh, L., Lindahl, U., Hohenester, E. & Timpl, R. (1999). Structural basis and potential role of heparin/heparan sulfate binding to the angiogenesis inhibitor endostatin. *EMBO J*, 18, 6240-6248.

Sasaki, T., Larsson, H., Tisi, D., Claesson-Welsh, L., Hohenester, E. & Timpl, R. (2000). Endostatins derived from collagens XV and XVIII differ in structural and binding properties, tissue distribution and anti-angiogenic activity. *J Mol Biol*, 301, 1179-1190.

Sasisekharan, R., Moses, M., Nugent, M., Cooney, C. & Langer, R. (1994). Heparinase inhibits neovascularization. *Proc Natl Acad Sci*, 91, 1524-1528.

Schlessinger, J., Lax, I. & Lemmon, M. (1995). Regulation of growth factor activation by proteoglycans: What is the role of the low affinity receptors ? *Cell*, 83, 357-360.

Schlessinger, J., Plotnikov , A., Ibrahimi O., Eliseenkova, A., Yeh B., Yayon A., Linhardt R and Mohammed M. (2000). Crystal structure of a ternary FGF-FGFR-Heparin complex reveals a dual role for heparin in FGFR binding and dimerization. *Mol Cell*, 6, 743-750.

Schor, A. & Schor, S. (1983). Tumour angiogenesis. *J Pathol*, 141, 385-413.

Seidel, C., Sundan, A., Hjorth, M., Turesson, I., Dahl, I., Abildgaard, N., Waage, A. & Borset, M. (2000). Serum syndecan-1: a new independent prognostic marker in multiple myeloma. *Blood*, 95, 388-392.

Selleck, S. (2001). Genetic dissection of proteoglycan function in *Drosophila* and *C. elegans*. *Seminars in Cell and Developmental Biology*, 12, 127-134.

Selleck, S.B. (2000). Proteoglycans and pattern formation - sugar biochemistry meets developmental genetics. *Trends in Genetics*, 16, 206-212.

Sertie, A.L., Sossi, V., Camargo, A.A., Zatz, M., Brahe, C. & Passos-Bueno, M.R. (2000). Collagen XVIII, containing an endogenous inhibitor of angiogenesis and tumor growth, plays a critical role in the maintenance of retinal structure and in neural tube closure (Knobloch syndrome). *Hum Mol Genet*, 9, 2051-2058.

Sharma, B., Handler, M., Eichstetter, I., Whitelock, J., Nugent, M. & Iozzo, R. (1998). Antisense targeting of perlecan blocks tumour growth and angiogenesis in vivo. *J Clin Invest*, 102, 1599-1608.

Sharpe, R., Byers, H., Scott, C., Bauer, S. & Maione, T. (1990). Growth inhibition of murine melanoma and human colon carcinoma by recombinant human platelet factor 4. *J Natl Cancer Inst*, 82, 848-853.

Shing, Y., Folkman, J., Sullivan, R., Butterfield, C., Murray, J. & Klagsbrun, M. (1984). Heparin affinity: purification of a tumor-derived capillary endothelial cell growth factor. *Science*, 223, 1296-1299.

Shively, J. & Conrad, H. (1976). Formation of anhydrosugars in the chemical depolymerisation of heparin. *Biochemistry*, 15, 3932-3942.

Shworak, N.W., Liu, J., Petros, L.M., Zhang, L., Kobayashi, M., Copeland, N.G., Jenkins, N.A. & Rosenberg, R.D. (1999). Multiple isoforms of heparan sulfate D-glucosaminyl 3-O-sulfotransferase. Isolation, characterization, and expression of human cDNAs and identification of distinct genomic loci. *J Biol Chem*, 274, 5170-5184.

Soker, S., Takashima, S., Miao, H., Neufeld, G. & Klagsbrun, M. (1998). Neuropilin-1 is expressed by endothelial and tumor cells as an isoform-specific receptor for vascular endothelial growth factor. *Cell*, 92, 735-745.

Soncin, F., Strydom, D. & Shapiro, R. (1997). Interaction of Heparin with Human Angiogenin. *J Biol Chem*, 272, 9818-9824.

Soukka, T., Inki, P. & Happonen, R.-P. (1997). Syndecan-1 adhesion molecule is reduced during malignant progression of oral epithelium. In *Oral Oncology*, Varma, A. (ed), Vol. 5. pp. 571-574. New Delhi McMillan India Ltd: London.

Spillmann, D., Witt, D. & Lindahl, U. (1998). Defining the Interleukin-8-binding domain of heparan sulfate. *J Biol Chem*, 273, 15487-15493.

Stanley, M., Stanley, M., Sanderson, R. & Zera, R. (1999). Syndecan-1 expression is induced in the stroma of infiltrating breast carcinoma. *Am J Clin Pathol*, 112, 377-383.

Stickens, D., Brown, D. & Evans, G.A. (2000). EXT genes are differentially expressed in bone and cartilage during mouse embryogenesis. *Dev Dyn*, 218, 452-464.

Stringer, S.E. & Gallagher, J.T. (1997a). Heparan sulphate. *Int J Biochem Cell Biol*, 29, 709-714.

Stringer, S.E. & Gallagher, J.T. (1997b). Specific binding of the chemokine platelet factor 4 to heparan sulfate. *J Biol Chem*, 272, 20508-20514.

Taraboletti, G., Belotti, D., Borsotti, P., Vergani, V., Rusnati, M., Presta, M. & Giavazzi, R. (1997). The 140-kilodalton antiangiogenic fragment of thrombospondin-1 binds to basic fibroblast growth factor. *Cell Growth Differ*, 8, 471-479.

The, I., Bellaiche, Y. & Perrimon, N. (1999). *Hedgehog* movement is regulated through tout velu-dependent synthesis of a heparan sulfate proteoglycan. *Mol Cell*, 4, 633-639.

Timpl, R. & Brown, J. (1996). Supramolecular assembly of basement membranes. *Bioessays*, 18, 123-132.

Tsen, G., Halfter, W., Kroger, S. & Cole, G.J. (1995). Agrin is a heparan sulfate proteoglycan. *J Biol Chem*, 270, 3392-3399.

Turnbull, J., Powell, A. & Guimond, S. (2001). Heparan sulfate: decoding a dynamic multifunctional cell regulator. *Trends Cel Biol*, 11, 75-82.

Turnbull, J.E., Fernig, D.G., Ke, Y., Wilkinson, M.C. & Gallagher, J.T. (1992). Identification of the basic fibroblast growth factor binding sequence in fibroblast heparan sulfate. *J Biol Chem*, 267, 10337-10341.

Turnbull, J.E. & Gallagher, J.T. (1990). Molecular organization of heparan sulphate from human skin fibroblasts. *Biochem J*, 265, 715-724.

Turnbull, J.E., Hopwood, J.J. & Gallagher, J.T. (1999). A strategy for rapid sequencing of heparan sulfate and heparin saccharides. *Proc Natl Acad Sci*, 96, 2698-2703.

Ueoka, C., Kaneda, N., Okazaki, I., Nadanaka, S., Muramatsu, T. & Sugahara, K. (2000). Neuronal cell adhesion, mediated by the heparin-binding neuroregulatory factor midkine, is specifically inhibited by chondroitin sulfate E. Structural and functional implications of the over-sulfated chondroitin sulfate. *J Biol Chem*, 275, 37407-37413.

Unger, E., Durrant, J., Anson, D. & Hopwood, J. (1994). Recombinant alpha-L-iduronidase: characterization of the purified enzyme and correction of mucopolysaccharidosis type I fibroblasts. *Biochem J*, 304, 43-49.

Van Kuppevelt, T.H., Dennissen, M.A.B.A., van Venrooij, W.J., Hoet, R.M.A. & Veerkamp, J.H. (1998) Generation and application of type-specific anti-heparan sulfate antibodies using phage display technology *J Biol Chem* 273:12960-12966.

Veugelers, M., De Cat, B., Ceulemans, H., Bruystens, A.-M., Coomans, C., Dürr, J., Vermeesch, J., Marynen, P. & David, G. (1999). Glypican-6, a new member of the glypican family of cell surface heparan sulphate proteoglycans. *J Biol Chem*, 274, 26968-26977.

Vives, R., Goodger, S. & Pye, D. (2001). Combined strong anion-exchange HPLC and PAGE approach for the purification of heparan sulphate oligosaccharides. *Biochem J*, 354, 141-147.

Vives, R., Pye, D., Salmivirta, M., Hopwood, J., Lindahl, U. & Gallagher, J. (1999). Sequence analysis of heparan sulphate and heparin oligosaccharides. *Biochem J*, 339, 767-773.

Vlodavsky, I., Friedmann, Y., Elkin, M., Aingorn, H., Atzmon, R., Ishai-Michaeli, R., Bitan, M., Pappo, O., Peretz, T., Michal, I., Spector, L. & Pecker, I. (1999). Mammalian heparanase: gene cloning, expression and function in tumor progression and metastasis. *Nat Med*, 5, 793-802.

Wasteson, A. (1971). A method for the determination of the molecular weight and molecular weight distribution of chondroitin sulphate. *J Chromatog*, 59, 87-97.

Wen, W., Moses, M., Wiederschain, D., Arbiser, J. & Folkman, J. (1999). The generation of endostatin is mediated by elastase. *Cancer Res*, 59, 6052-6056.

Whitelock, J., Murdoch, A., Iozzo, R. & Underwood, P. (1996). The degradation of human endothelial cell-derived perlecan and release of bound basic fibroblast growth factor by stromelysin, collagenase, plasmin and heparanases. *J Biol Chem*, 271, 10079-10086.

Winterbourne, D.J. & Mora, P.T. (1981). Cells selected for high tumorigenicity or transformed by simian virus 40 synthesize heparan sulfate with reduced degree of sulfation. *J Biol Chem*, 256, 4310-4320.

Woods, A., Oh, E.-S. & Couchman, J. (1998). Syndecan proteoglycans and cell adhesion. *Matrix Biology*, 17, 477-483.

WooPark, P., Reizes, O. & Bernfield, M. (2000). Cell surface heparan sulfate proteoglycans: selective regulators of ligand-receptor encounters. *J Biol Chem*, 275, 29923-29926.

Yamada, S., Sakamoto, K., Tsuda, H., Yoshida, K., Sugahara, K., Khoo, K.-H., Morris, H.R. & Dell, A. (1994). Structural studies on the tri- and tetrasaccharides isolated from porcine intestinal heparin and characterization of heparinase/heparitinases using them as substrates. *Glycobiology*, 4, 69-78.

Yamaguchi, N., Anand-Apte, B., Lee, M., Sasaki, T., Fukai, N., Shapiro, R., Que, I., Lowik, C., Timpl, R. & Olsen, B. (1999). Endostatin inhibits VEGF-induced endothelial cell migration and tumor growth independently of zinc binding. *EMBO J*, 18, 4414-4423.

Yanagishita, M. & Hascall, V.C. (1992). Cell surface heparan sulfate proteoglycans. *J Biol Chem*, 267, 9451-9454.

Yang, V.C., Linhardt, R.J., Bernstein, H., Cooney, C.L. & Langer, R. (1985). Purification and characterization of heparinase from *Flavobacterium heparinum*. *J Biol Chem*, 260, 1849-1857.

Yayon, A., Klagsbrun, M., Esko, J.D., Leder, P. & Ornitz, D.M. (1991). Cell surface, heparin-like molecules are required for binding of basic fibroblast growth factor to its high affinity receptor. *Cell*, 64, 841-848.

Zatterstrom, U., Felbor, U., Fukai, N. & Olsen, B. (2000). Collagen XVIII/endostatin structure and functional role in angiogenesis. *Cell Structure and Function*, 25, 97-101.

Zhang, L., David, G. & Esko, J.D. (1995). Repetitive Ser-Gly sequences enhance heparan sulfate assembly in proteoglycans. *J Biol Chem*, 270, 27127-27135.

Zucker, M. & Katz, J. (1991). Platelet factor 4: production, structure, and physiologic and immunologic action. *Proc Soc Exp Biol Med*, 198, 693-702.